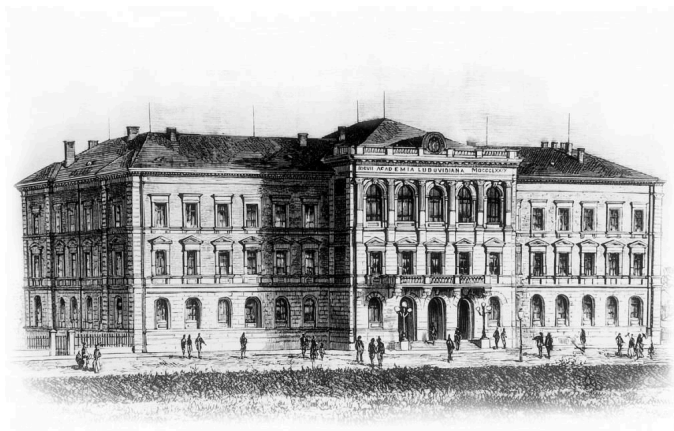




Justus-Liebig-Universität Gießen
Institut für Anorganische und
Analytische Chemie

Fachbereich
Biologie und
Chemie

Synthetic and Kinetic Investigations on Selective Oxidation of Aromatic and Aliphatic Hydrocarbons with Copper Complexes



**Inaugural-Dissertation zur Erlangung des
Doktorgrades der Naturwissenschaften**

vorgelegt von Jonathan Becker aus Wetzlar

Die vorliegende Arbeit wurde von März 2011 bis April 2015 am Institut für Anorganische und Analytische Chemie der Justus-Liebig-Universität Gießen unter der Betreuung von Prof. Dr. Siegfried Schindler durchgeführt.

Der Kernteil dieser Arbeit besteht aus zwei Kapiteln, die zur Publikation bereits angenommen oder in Vorbereitung zur Einreichung sind. Aus diesem Grund ist der wissenschaftliche Teil dieser Dissertation in englischer Sprache verfasst.

Erklärung

Ich habe die vorgelegte Dissertation selbständig und ohne unerlaubte fremde Hilfe und nur mit den Hilfen angefertigt, die ich in der Dissertation angegeben habe. Alle Textstellen, die wörtlich oder sinngemäß aus veröffentlichten Schriften entnommen sind, und alle Angaben, die auf mündlichen Auskünften beruhen, sind als solche kenntlich gemacht. Bei den von mir durchgeführten und in der Dissertation erwähnten Untersuchungen habe ich die Grundsätze guter wissenschaftlicher Praxis, wie sie in der „Satzung der Justus-Liebig-Universität Gießen zur Sicherung guter wissenschaftlicher Praxis“ niedergelegt sind, eingehalten.

Gießen, den 24.04.15

Jonathan Becker

Danksagung

Mein Dank gilt an erster Stelle Herrn Prof. Dr. Siegfried Schindler, für die Aufgabenstellung, die große Unterstützung, das entgegengebrachte Vertrauen und die Freiheiten, die ich bei der Durchführung dieser Arbeit hatte.

Der ganzen Arbeitsgruppe danke ich für die Zusammenarbeit und die schöne Zeit: Dr. Sabine Becker, Dr. Alexander Beitat, Cornelius Brombach, Tim Brückmann, Christopher Gawlig, Ursula Gorr, David Haas, Dr. Anja Henß, Tobias Hoppe, Melanie Jopp, Natascha Kempf, Dr. Sandra Kisslinger, Markus Lerch, Jolanthe Lintl, Frank Mehlich, Andreas Miska, Dr. Jörg Müller, Dr. Thomas Nebe, Florian Ritz, Dr. Sabrina Schäfer, Stefan Schaub, Pascal Specht, Dr. Manfred Steinbach, Dr. Lars Valentin, Miriam Wern, Janine Will und Dr. Christian Würtele.

Dr. Christian Würtele gilt mein besonderer Dank für die Einführung in die Kristallographie und Pascal Specht für seine große Hilfe bei der Untersuchung des Liganden DPDen. Weiterhin bedanke ich mich bei Prof. Andrey Fokin, PhD für die große Hilfe bei der Arbeit mit Adamantan und Diamantan. Für die große Hilfe in vielen Dingen möchte ich mich bei den Mitarbeitern des Fachbereiches 08 bedanken, im Besonderen bei den Mitarbeitern des Gerätezentrums OC-Analytik. Danke auch an alle meine ehemaligen Kommilitonen für eine schöne Zeit während des Studiums. Nicht zuletzt danke ich meiner Frau Sabine und meiner ganzen Familie, ihr wart mir eine wertvolle Unterstützung!

Für meine Familie.

*Für Sabine,
die mir immer beigestanden, mich ermutigt und bestärkt hat.*

Contents

1	Introduction	9
1.1	Copper	9
1.2	Copper Containing Metalloproteins	10
1.2.1	Types of Copper Proteins	10
1.2.2	Roles of Copper Proteins	13
1.3	Hydroxylation of Organic Substrates with Copper and Dioxygen	22
1.3.1	Aromatic Hydroxylation	22
1.3.2	Aliphatic Hydroxylation	25
1.4	Aims of the Research	27
2	Selective Aromatic Hydroxylation	29
2.1	Selective Aromatic Hydroxylation with Dioxygen and Simple Copper Imine Complexes	31
2.1.1	Introduction	31
2.1.2	Results and Discussion	32
2.1.3	Conclusions	44
2.1.4	Experimental Section	45
2.1.5	Acknowledgements	53
2.2	Selected Supporting Information and Unpublished Results . .	53
2.2.1	Crystallization of Copper(I) Complexes	53
2.2.2	Crystallization of $[\text{Cu}(\text{H}_2\text{BDED})\text{Cl}_2]$	55
2.2.3	Formation of $[\text{Cu}_2(\text{BDED})(\mu\text{-OH})(\mu\text{-}o\text{-O-BDED})]^{2+}$.	56
2.2.4	Additional Experiments for Characterization	57
2.2.5	Additional Variation of the Reactions with BDED . .	59
3	Selective Aliphatic Hydroxylation	63
3.1	Selective Aliphatic Hydroxylation with Dioxygen Using a Sim- ple Copper Imine Complex System	65
3.1.1	Introduction	65
3.1.2	Results and Discussion	66
3.1.3	Conclusions	75
3.1.4	Experimental Section	76
3.2	Selected Supporting Information	81
3.2.1	Formation of $[\text{Cu}_2(\text{DPDen})(\mu\text{-OH})(\mu\text{-}o\text{-O-DPDen})]^{2+}$	81

3.2.2	Selective Hydroxylation of Ketones	83
3.2.3	Additional Results for the Synthesis of Adamantanyl- methylidene-diethylaminomethylamine.	84
3.2.4	Cyclisation of 3-Hydroxy-2,2-dimethylpropionaldehyde.	85
4	Supporting Information	87
4.1	Supporting Information for Chapter 2	89
4.1.1	NMR Data	89
4.1.2	Crystallographic Data	105
4.1.3	Computational Details	117
4.2	Supporting Information for Chapter 3	184
4.2.1	Kinetic Rate Constants	184
4.2.2	NMR Data	185
4.2.3	Mass Spectra	203
4.2.4	IR Spectra	205
4.2.5	Crystallographic Data	206
5	Summary/Zusammenfassung	221
5.1	Summary	221
5.1.1	Selective Aromatic Hydroxylations	221
5.1.2	Selective Aliphatic Hydroxylations	223
5.2	Zusammenfassung	225
5.2.1	Selektive aromatische Hydroxylierungen	226
5.2.2	Selektive aliphatische Hydroxylierungen	228
6	Bibliography	231
7	List of Figures	243
8	List of Tables	249
9	Publications	253
9.1	Full Papers	253
9.2	Oral Presentations	254
9.3	Poster Presentations	254
10	Curriculum Vitae	255

Table of Abbreviations

BLYP-D(2/3)	dispersion corrected density functional
BuLi	butyllithium
COSMO	continuum solvation model
CSC	center for scientific computing
Cys	cysteine
D β H	dopamine beta-monooxygenase
DFT	density functional theory
DMSO	dimethyl sulfoxide
ECP	effective core potential
en	ethylenediamine
Et	ethyl
EPR	electron paramagnetic resonance
GC/MS	gas chromatography with mass spectrometry
Gly	glycine
His	histidine
IE	ionization energy
IR	infrared
Me	methyl
Met	methionine
NMR	nuclear magnetic resonance

Table of Abbreviations

ORTEP	Oak Ridge thermal ellipsoid plot (program)
p. a.	pro analysis
PAM	peptidylglycine α -amidating monooxygenase
PCC	pyridinium chlorochromate
pMMO	particulate methane monooxygenase
ppm	parts per million
PPO	polyphenol oxidase
RKS	restricted Kohn-Sham
sMMO	soluble methane monooxygenase
SOD	Cu,Zn superoxide dismutase
TFA	trifluoroacetic acid
THF	tetrahydrofurane
TS	transition state
TZVP	triple- ζ basis set
UKS	unrestricted Kohn-Sham
UVB	ultraviolet B (315 - 280 nm)
UV-vis	ultraviolet and visible (light)

Table of Ligands

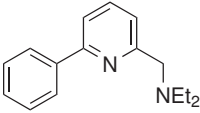
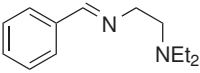
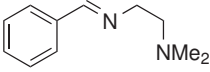
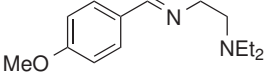
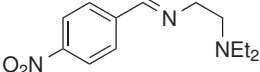
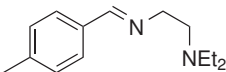
	2-(diethylaminoethyl)-6-phenylpyridine (PPN)	$C_{16}H_{20}N_2$ 240.34 g/mol
	<i>N'</i> -benzylidene- <i>N,N</i> -diethylethylenediamine (BDED)	$C_{13}H_{20}N_2$ 204.31 g/mol
	<i>N'</i> -Benzylidene- <i>N,N</i> -dimethyl-ethylenediamine	$C_{11}H_{16}N_2$ 176.26 g/mol
	2-(diethylamino)ethyl(4-methoxy-phenyl)methylideneamine	$C_{14}H_{22}N_2O$ 234.34 g/mol
	2-(diethylamino)ethyl(4-nitrophenyl)methylideneamine	$C_{13}H_{19}N_3O_2$ 249.31 g/mol
	2-(diethylamino)ethyl(4-methyl-phenyl)methylideneamine	$C_{14}H_{22}N_2$ 218.34 g/mol

Table of Ligands

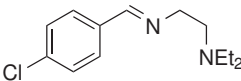
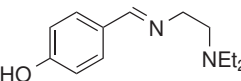
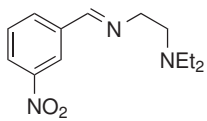
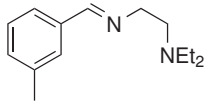
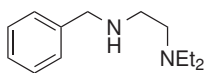
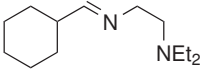
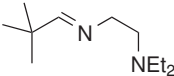
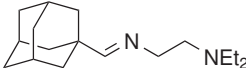
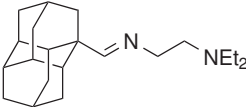
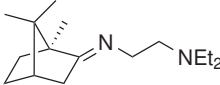
	2-(diethylamino)ethyl(4-chloro-phenyl)methylideneamine	$C_{13}H_{19}ClN_2$ 238.76 g/mol
	2-(diethylamino)ethyl(4-hydroxy-phenyl)methylideneamine	$C_{13}H_{20}N_2O$ 220.31 g/mol
	2-(diethylamino)ethyl(3-nitrophenyl)methylideneamine	$C_{13}H_{19}N_3O_2$ 249.31 g/mol
	2-(diethylamino)ethyl(3-methyl-phenyl)methylideneamine	$C_{14}H_{22}N_2$ 218.34 g/mol
	<i>N'</i> -Benzyl- <i>N,N</i> -diethylethane-1,2-diamine (H ₂ BDED)	$C_{13}H_{22}N_2$ 206.33 g/mol

Table of Ligands

	<i>N'</i> -Cyclohexylmethylene- <i>N,N</i> -diethyl-ethane-1,2-diamine	$C_{13}H_{26}N_2$ 210.36 g/mol
	<i>N'</i> -(2,2-dimethylpropylidene)- <i>N,N</i> -diethyl-ethylendiamine (DPDen)	$C_{11}H_{24}N_2$ 184.32 g/mol
	Adamantanylmethylidene-diethylaminomethylamine	$C_{17}H_{30}N_2$ 262.43 g/mol
	Diamantylmethylidene-diethylaminomethylamine	$C_{21}H_{34}N_2$ 314.51 g/mol
	<i>N,N</i> -Diethyl- <i>N'</i> -(1,7,7-trimethyl-bicyclo[2.2.1]hept-2-ylidene)-ethane-1,2-diamine	$C_{16}H_{30}N_2$ 250.42 g/mol

1 Introduction

1.1 Copper

Copper is the 25th most abundant element in the solar system, it is part of the Earth's crustal with 50 ppm and thus omnipresent for humans (Figure 1.1). For about 11,000 years the element is known to mankind and it has been used for thousands of years. Tools and weapons made of copper metal were an important progress in the development of mankind: copper together with tin as alloy shaped a whole era, known as the Bronze Age. Since then copper gained importance and prevalence. Today we are surrounded by copper in our daily life. It is used for power distribution, telecommunications, electronics and much more.

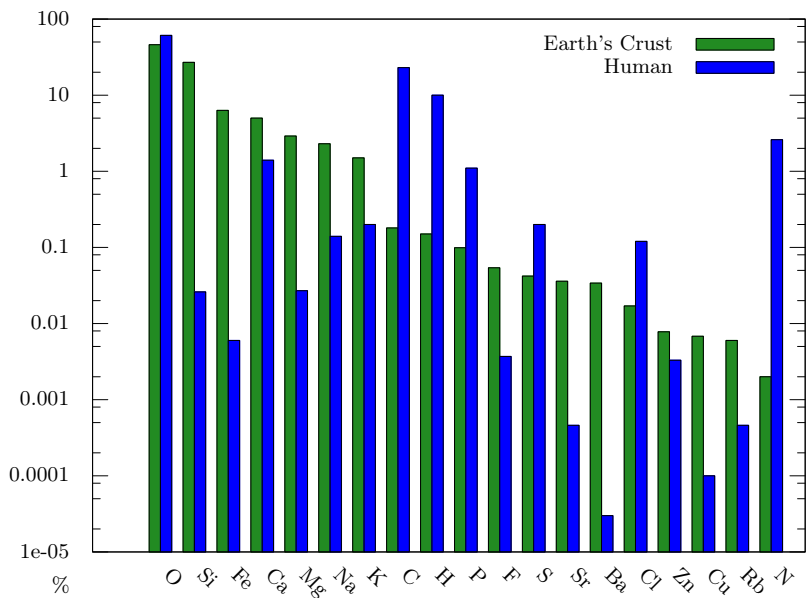


Figure 1.1: Abundance of selected elements in Earth's crust and humans.

Copper is also omnipresent for us in a non obvious way. The human body of an adult contains about 150 mg copper which is essential for life [1]-[4].

1.2 Copper Containing Metalloproteins

Copper is observed in the active site of various metalloproteins in humans, animals, microorganisms and plants. As a redox active element it takes part in outer-sphere electron transfer and interacts with molecular oxygen, superoxide, nitrite or nitrous oxide. Typical copper sites are divided into three types, although there are several copper centers known not to fit into this classification [5]-[8].

1.2.1 Types of Copper Proteins

The classification of copper proteins is based on spectroscopic properties of the d^9 configuration of copper(II) at the active site. Cysteine as ligand exhibits a strong absorption band at 600 or also 460 nm with a sulfur to copper charge transfer.

Such proteins were classified as type I copper proteins, often they are called "blue copper proteins" because of their intense color owed to the strong absorption band. Examples for proteins with type I copper centers are azurins (Figure 1.2) and plastocyanins, where the active site provides an intermolecular electron transfer. Furthermore ascorbate oxidase and laccases are important examples. Here the type I center ensures an intramolecular electron transfer for the multicopper enzymes [9],[10]. The inherent part of such type I centers are two histidines and a cysteinate, forming a trigonal planar geometry with the copper ion. An additional weak ligand, in most cases methionine, completes the resulting approximate trigonal pyramidal geometry. Figure 1.2 shows the binding site for copper in azurin II [11].

Among these enzymes, there are exceptions as azurin for example, indeed. Here there is an additional weak bond to an oxygen of the peptide framework, resulting in a trigonal bipyramidal geometry. This geometry is a trade-off between the tetrahedral coordination of copper(I) (d^{10}) and the square planar or pyramidal coordination of copper(II) (d^9), which leads to faster electron transfer.

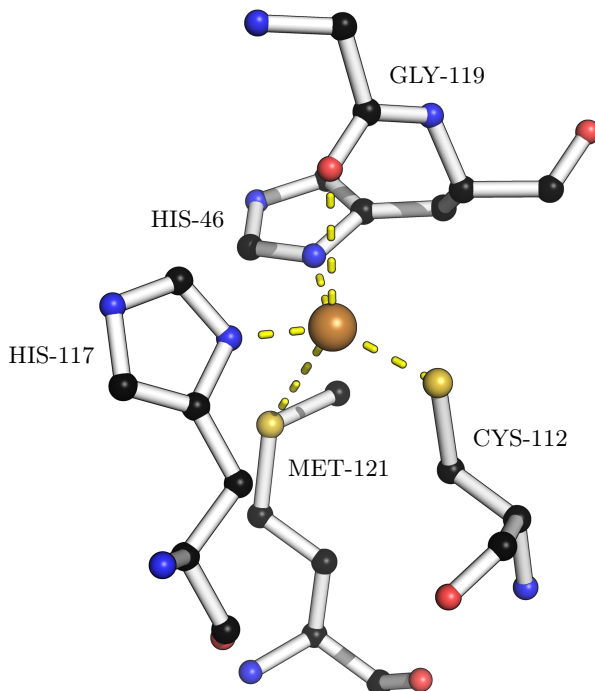


Figure 1.2: Type I binding site for copper in azurin II.

Active sites with one copper ion but without sulfur ligands are categorized as type II. Here histidine mostly binds to copper(II) ions, thus only $d \rightarrow d$ transitions with very weak absorptions above 500 nm are observed. As a result of this weak absorption proteins containing only type II copper centers are nearly colorless. This resembles "normal" copper(II) complexes which have similar properties. These active centers exhibit square planar or distorted tetrahedral coordination with vacant coordination sites, where substrates can be bound. Examples for proteins with type II copper centers are Cu/Zn superoxide dismutase (Figure 1.3), galactose oxidase, peptidylglycine α -amidating monooxygenase (PAM) and dopamine β -hydroxylase (D β H).

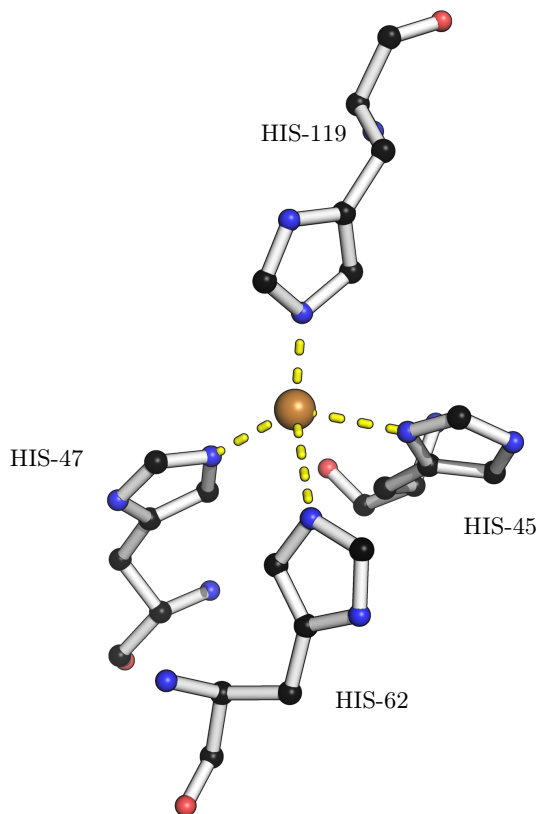


Figure 1.3: Type II binding site for copper in Hydra Cu-Zn superoxide dismutase [12].

Type III centers are very similar to type II: they are characterized by two of the described histidine coordinated copper centers, which are less than 6 \AA apart (Figure 1.4). Both, PAM and D β H, have neighboring copper centers, however the distance exceeds 6 \AA and thus both enzymes belong to type II as already named above. EPR spectroscopy can be used to differentiate between type II and III, because for distances shorter than 6 \AA the $S=1/2$ magnetic dipoles couple, resulting in a broadened or splitted copper(II) EPR signal; however due to binding of substrates the proteins can be EPR-silent, e.g. oxyhemocyanin. Proteins with typical type III center are hemocyanin,

catechol oxidase and tyrosinase. Furthermore there are several examples of slightly different active sites and a diversity of combination of two or more copper centers in proteins [13]; however they are not discussed in more detail here.

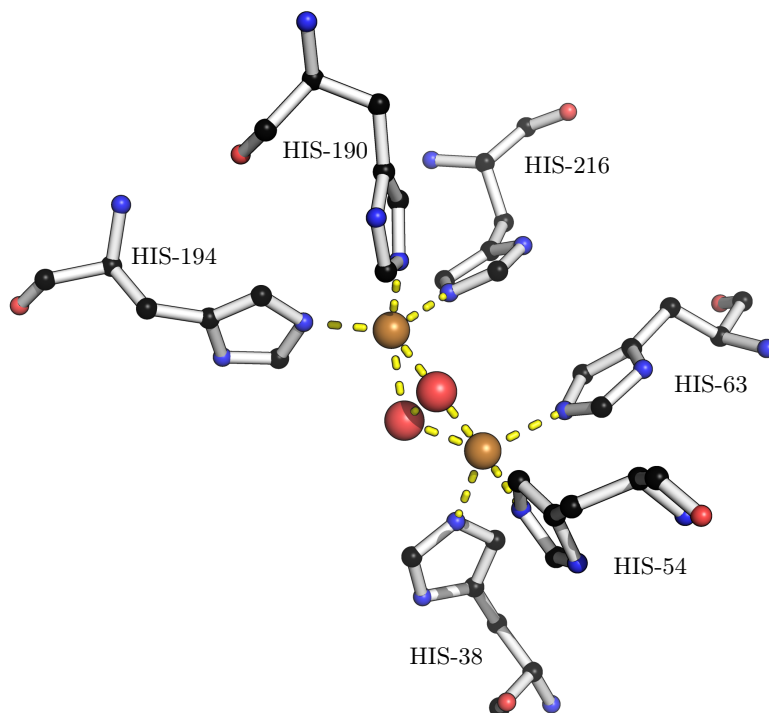


Figure 1.4: Active site of tyrosinase with a coordinated peroxide ion as an example for type III copper proteins [14].

1.2.2 Roles of Copper Proteins

The functions of copper containing proteins are very versatile and thus their reactivity differs a lot depending on the characteristics of their active sites. Figure 1.5 gives an overview of several copper containing proteins and their functions.

Type I active sites contribute to redox reactions by conducting one-electron

1 Introduction

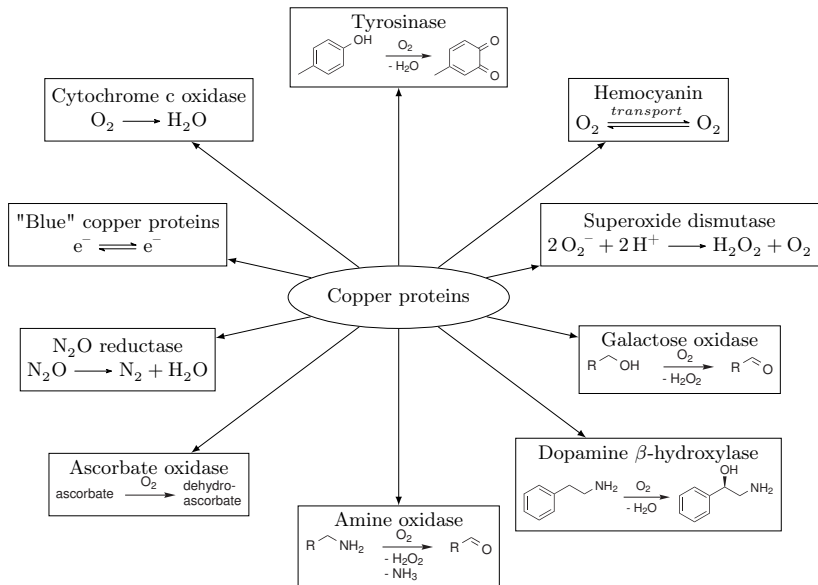


Figure 1.5: Overview over several functions performed by proteins containing copper [15].

transfer. Throughout this process copper(I) is oxidized to copper(II) which changes the coordination geometry of the copper active site [16],[17]. The redox potentials of type I active sites cover a wide range which can be explained by the contribution of several effects such as ionization energy of the copper center or the solvation contribution of the reorganization of the coordination geometry during the electron transfer process. Equation 1.1 summarizes these effects with IE as ionization energy, U as the term for the reorganization and the constant to correct the potential to the normal hydrogen electrode (-4.5 eV).

$$E_0(V) = IE - 4.5 \text{ eV} + U \quad (1.1)$$

Because of these effects the redox potential of type I copper proteins is significantly higher than the standard potential E_0 for the transition of $Cu^{2+} + e^- \rightleftharpoons Cu^+$ with 160 mV. Depending on the more or less constrained coordination geometry, such copper centers vary up to 500mV [18],[19]. Azurin as mentioned above, an example for a type I copper site has a potential of about 250 mV. Regarding the speed of such electron transfer reactions, the

"blue copper proteins" show very fast electron exchange. Rate constants are in the range of $10^4 - 10^6 \text{ M}^{-1}\text{s}^{-1}$ [20]. These electrons can be transferred several Å through the protein by tunneling, for instance in cytochrome *c* oxidase about 19 Å from the Cu_A site to the heme *a* center [21]. The simplest type I copper proteins are the cupredoxins, named after the iron-containing ferredoxins with similar function. Important examples are plastocyanin, azurin, amicyanin and sulfocyanin. As already mentioned there exists a variety of multinuclear copper proteins containing a type I center as well. Examples for these enzymes are nitrite reductases, laccases or ceruplasmin with two, three and six copper domains [22]. Another class, the so called phytocyanins differ from plastocyanins in additional, distinct sequence motifs [23].

Due to the rigid conformation of type I copper sites, synthesis of model systems is challenging. One problem is the tendency of small thiolates to form disulphides; nevertheless it was possible to obtain some copper(II)-thiolate complexes. Another problem is the difficulty to assign the spectroscopic properties and reduction potentials completely, representing the specific nature of type I active sites [24]. Figure 1.6 shows one of the first stable copper (II) aliphatic thiolate complexes [25].

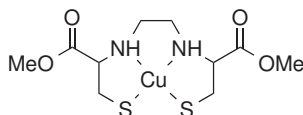
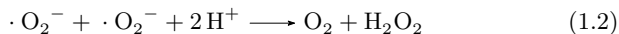


Figure 1.6: Model system for type I copper proteins.

Although all type II copper proteins share a similar coordination geometry of copper, their reactivity differs. They catalyze a wide range of reactions. One of the most extensively studied type II enzyme is the Cu, Zn superoxide dismutase (SOD). It catalyzes the extreme fast dismutation of superoxide to dioxygen and hydrogen peroxide (equation 1.2).



In the proposed mechanism copper acts as a redox catalyst and activates the O–O bond. As a first step the copper(II) ion oxidizes superoxide to dioxygen, the resulting copper(I) ion then binds another superoxide and hydrogen peroxide is formed. Besides the copper center SOD contains a zinc ion as well; however the zinc(II) has only a structural role and is probably not catalytically active itself [26],[27]. Whilst SOD binds superoxide, many type II active

1 Introduction

sites bind and activate dioxygen. An important example is the dopamine β -monooxygenase (D β M). This enzyme catalyzes the hydroxylation of dopamine with dioxygen in the formation process of norepinephrine, important hormones and neurotransmitters. There are several possibilities how dioxygen can be bound: mononuclear copper complexes with dioxygen react to an η^1 -superoxido, an η^2 -superoxido or the corresponding η^2 -peroxido complex (Figure 1.7) [28].



Figure 1.7: Binding of dioxygen as 1:1 copper adduct complexes (charges are omitted).

In the case of D β M the η^1 -superoxido complex reacts by hydrogen transfer to the corresponding η^1 -hydroperoxido complex. In a proposed radical mechanism hydrogen is abstracted from dopamine by the "oxygen adduct", water is formed and the remaining oxygen and dopamine radicals recombine [29],[30]. The peptidylglycine α -amidating monooxygenase (PAM) shows very similar reactivity, but has two active domains. During the catalytic cycle copper(II) is reduced by the co-reagent ascorbate. Other examples for type II active sites containing copper proteins are the dioxygenase quercetinase, which catalyzes the cleavage of *O*-heterocyclic rings in flavones, and the galactose oxidase [31]. For modelling type II copper proteins, the formation of 1:1 dioxygen adducts is the most challenging part. In 1994 and 2006 it was possible for the first time to crystallize these side-on and end-on copper-"dioxygen adducts" of artificial model complexes [32],[33]. For the synthesis of these complexes sterically demanding ligands (shown in Figure 1.8) were used to avoid dimerization.

Catalytically active type II model systems are known for example of the galactose oxidase [34]. These model systems utilize dioxygen to oxidize alcohols to aldehydes and generate hydrogen peroxide. The ligand shown in Figure 1.9 was used to imitate the structure of the active site and showed oxidase activity in a mechanism similar to galactose oxidase for the first time. The design of the ligand was chosen to withstand this oxidative reaction conditions [35].

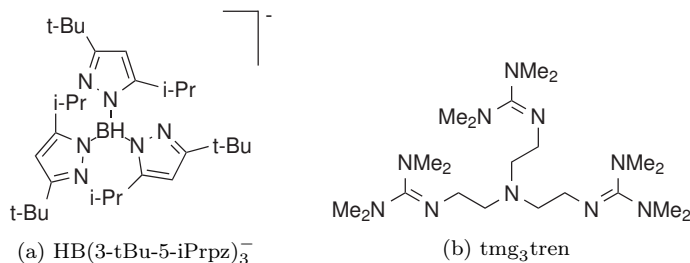


Figure 1.8: Ligands used for the first crystallization of η^2 (a) and η^1 (b) Cu/O_2 adducts.

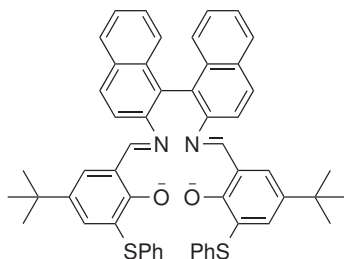


Figure 1.9: Ligand of the catalytically active model system of galactose oxidase.

In the following examples for copper proteins containing a type III active site are discussed. The dinuclear copper center allows binding of dioxygen in between of the two copper ions. Thus dinuclear copper complexes can also bind dioxygen in varying types. Figure 1.10 shows the three most important cases: The trans- μ -1,2-peroxido (a), the μ - $\eta^2:\eta^2$ -peroxido (b) and the bis(μ -oxido) (c) copper complex.

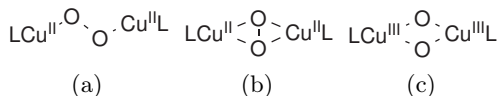


Figure 1.10: Binding of dioxygen as 2:1 copper adduct complexes (charges are omitted).

1 Introduction

One important example for a copper protein containing a type III active site is hemocyanin. This protein is responsible for the oxygen transport in the blood of Mollusca and Arthropoda similar to the transport function of the iron based hemoglobin. The oxygen transport is enabled by the reversible binding of oxygen by the type III center. Unlike the well known "red blood", the oxygenated form of hemocyanin exhibits a blue color. The intense color originates from oxygen to copper charge transfer transitions with intense optical absorption bands. Many of the copper "dioxygen adducts" exhibit such intense absorptions, leading to deeply colored complexes. The maxima of these absorption bands depend on the ligand, yet they are a characteristic feature of most copper proteins of type III. Table 1.1 shows approximate UV-vis absorption maxima of different Cu/O₂ binding motifs [36]. The blue color from the oxygenated form of hemocyanin indicates a $\mu\text{-}\eta^2\text{:}\eta^2\text{-peroxido}$ adduct at the active site which is supported by other spectroscopic features and crystal structure analyses [37], [38].

Table 1.1: Approximate UV-vis absorption of some Cu/O₂ adducts.

species	λ , nm (ϵ , nM ⁻¹ cm ⁻¹)
$\eta^1\text{-superoxido}$	410 (4), 585 (1)
trans- $\mu\text{-1,2-peroxido}$	530 (10), 600 (7)
$\mu\text{-}\eta^2\text{:}\eta^2\text{-peroxido}$	360 (24), 520 (1)
bis($\mu\text{-oxido}$)	300 (20), 400 (24)

Type III active sites are not only limited to reversible dioxygen binding, in fact even hemocyanin exhibits small oxidase activity [39]. Other proteins with the type III motif are cresolase, catechol oxidases/polyphenol oxidase (PPO), tyrosinases or tyrosinase-related proteins. All these proteins show very similar aromatic oxidase activity. Whilst catechol oxidase only catalyzes the oxidation of *o*-diphenols to the *o*-quinones with molecular oxygen, tyrosinase also catalyzes the *o*-hydroxylation of monophenols (Figure 1.11). Both enzymes are important in the synthesis of melanin, responsible for browning of fruits and vegetables or also important as protection against UVB-radiation damage of the skin.

Figure 1.11: *o*-hydroxylation of tyrosine by tyrosinase.

The *o*-hydroxylation activity of tyrosinase probably occurs by binding and activating dioxygen as $\mu\text{-}\eta^2\text{:}\eta^2$ -peroxido copper complex, coordinating phenolate at one copper center followed by aromatic hydroxylation reaction [40]-[42]. This is often described as electrophilic substitution mechanism but radical pathways were also proposed [43]. Several attempts were made in modeling the *o*-hydroxylation with dinuclear type III-like copper complexes. Figure 1.12 shows two examples of ligands used for intramolecular ligand hydroxylation. These ligands form dinuclear copper complexes and activate dioxygen as $\mu\text{-}\eta^2\text{:}\eta^2$ -peroxido complex (Figure 1.13 for the DAPA ligand) [44],[45].

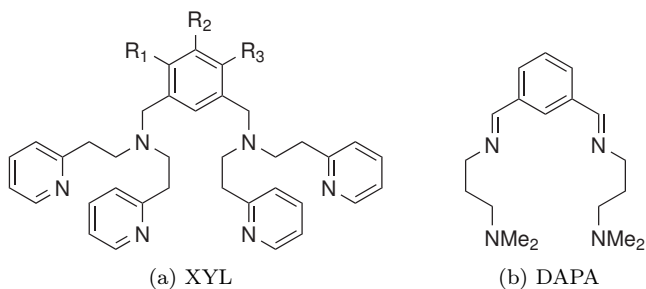


Figure 1.12: Ligands used for dinuclear complexes capable of tyrosinase-like, intramolecular hydroxylation reactions.

For some time only dinuclear copper complexes were discussed regarding aromatic hydroxylation. A different approach for modelling the tyrosinase-like activity is the use of two separate mononuclear complexes, forming the "dioxygen adduct" with a self organized dimer. This approach was used to hydroxylate the external substrate di-*t*-butylphenol (see Figure 1.14 (a)) [46]. An catalytic activity could be demonstrated by the use of (b) (Figure 1.14) [47],[48].

A proposed mechanism for the catalytic activity towards the external substrate di-*t*-butylphenol (DTBP-H) is shown in Figure 1.15. Further devel-

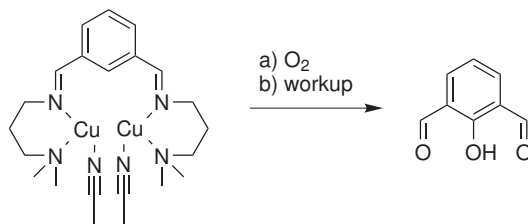


Figure 1.13: Intramolecular aromatic hydroxylation of the $[\text{Cu}_2\text{DAPA}]^{2+}$ complex with dioxygen.

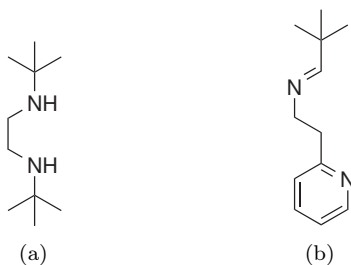


Figure 1.14: Ligands used for mononuclear complexes with tyrosinase-like activity towards external substrates as oxygen binding dimer.

opment led to a fast catalytic model with a wider scope of substrates. The use of mononuclear copper complexes seems to be a good alternative to the more complex ligands used for the preparation of dinuclear complexes [49]. Another outstanding copper protein is the particulate methane monooxygenase (pMMO). This integral membrane protein catalyzes the oxidation of methane to methanol. There are two types of methane monooxygenase and only pMMO contains copper whereas the soluble form (sMMO) in contrast contains iron. These enzymes are capable of activating the methane C–H bond, which is the strongest C–H bond and thus the interest in this reaction is very high; however, little is known about the reaction itself. The first crystal structure of the protein provided some insight, but a lot of questions concerning the bonded metal ions and their reactivity remained [50]. Probably there is a dinuclear and a mononuclear copper active site. In addition there are hints for another trinuclear site as well [51]. Computational studies were carried out in order to gain more insight concerning the reactivity of

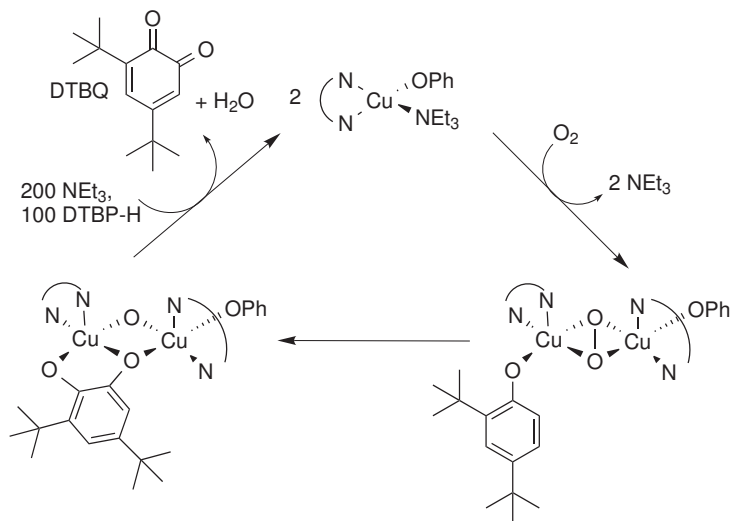


Figure 1.15: Proposed mechanistic cycle of the tyrosinase-like activity of mononuclear complexes [48].

1 Introduction

the individual copper sites. They showed that quite certain the dinuclear [52] and/or trinuclear sites [53] are active in the methane hydroxylation of pMMO. It is quite certain that the mononuclear site itself is not responsible for methane activation. In particular the postulated trinuclear copper cluster is of high interest and poorly understood. A model system for the trinuclear copper site is shown in Figure 1.16

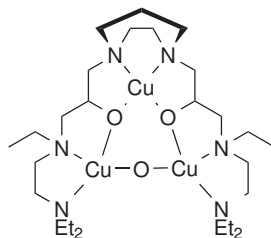


Figure 1.16: Model complex for the trinuclear copper site in pMMO.

1.3 Hydroxylation of Organic Substrates with Copper and Dioxxygen

Model systems should not only structurally resemble the active sites, but more important they should show the same catalytic reactivity. Synthetically available compounds could already be used for selective hydroxylations of substrates following the reactivity of their natural occurring counterparts. There are two possible ways, intra- and intermolecular hydroxylation. Although intramolecular reactions usually exhibit a great selectivity, their practical use or even a catalytic application is difficult or impossible. In contrast intermolecular hydroxylations can be catalytically performed. In some cases large turnovers were observed; however the reactions often lack selectivity.

1.3.1 Aromatic Hydroxylation

The allylic C–H bond dissociation energy with 372 kJ/mol (89 kcal/mol) is weaker than aliphatic equivalents [55]. These bonds are activated by tyrosinase in nature as already described above. In this context some model systems that exhibit similar reactivity were also presented.

For analyzing the intramolecular hydroxylation process dinuclear complexes with *m*-xylyl linker or similar ligands were used commonly. Using ¹⁸O₂ it was proved that the hydroxylation in fact directly occurs by activated dioxxygen.

The complex geometry allows side-on dioxygen complexes and it is almost certain that the $\mu\text{-}\eta^2\text{:}\eta^2$ -peroxido is the active species here. Only traces of a bis(μ -oxido) complex were found [56]. Among the mechanisms proposed, the most likely one explains the reaction as an electrophilic attack at the aromatic π -system. The final product is then formed by proton transfer and rearomatization. This mechanism is supported by several studies: The electrophilic attack was found to be the rate-determining step because no kinetic isotope effect was observed when the hydrogen at the hydroxylation position is substituted with deuterium [57]. Furthermore the change in rate constants with different aromatic substituents, although the effect is smaller than with typical aromatic substitutions, speaks for this mechanism proposed. These kinetic results object a possible alternative radical reaction pathway. Additionally radical traps had no influence on the hydroxylation process [58],[59]. The exact position of the $\mu\text{-}\eta^2\text{:}\eta^2$ -peroxido which undergoes only minimal geometrical change during the reaction, is a crucial feature for the reactivity [60],[61]. If a methylated aromatic system is used, the hydroxylation still occurs at the same position by forming a carbocation, followed by a 1,2-methyl migration [44],[62]. A comparable reaction with a similar 1,2-shift was also observed with a mononuclear η^2 -peroxido copper(III) complex (Figure 1.17) [63].

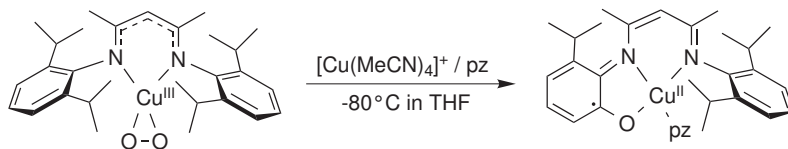


Figure 1.17: Intramolecular hydroxylation of mononuclear η^2 -peroxido copper(III) complex, charges are omitted.

η^1 -hydroperoxido copper "oxygen adduct" complexes, though not directly derived from dioxygen, are also capable of arene hydroxylations. Here it was proposed that O—O bond cleavage leads to a reactive copper-oxido species [64].

Concerning the side-on dinuclear copper "dioxygen adducts" there are also the bis(μ -oxido) complexes. Their capability of intramolecular aromatic hydroxylation was in question for some time but it could finally be demonstrated that it is possible with the ligand 2-(diethylaminomethyl)-6-phenylpyridine (PPN, Figure 1.18). Studies of the kinetic isotope effect when hydrogen was substituted with deuterium at the hydroxylation position argue for an electrophilic aromatic substitution pathway, similar to XYL-ligand based

1 Introduction

$\mu\text{-}\eta^2\text{:}\eta^2$ -peroxido complexes, as no such kinetic effect was observed. In addition the yield of the hydroxylation was correlated with substitutions at the aromatic ring [65].

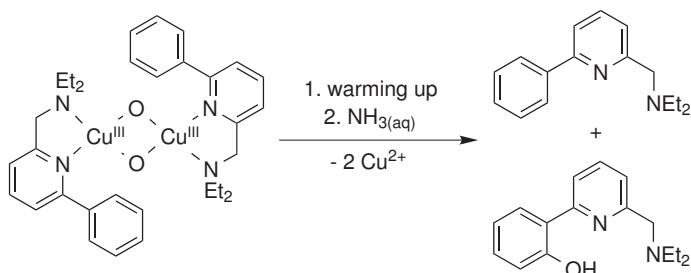


Figure 1.18: Intramolecular hydroxylation with a bis(μ -oxido) copper(III) complex, charges are omitted.

Some examples for the hydroxylation of external substrates - in most cases phenols or phenolates - were already described in section 1.2.2. Similar reactions with $\mu\text{-}\eta^2\text{:}\eta^2$ copper peroxido complexes were observed and described with other ligand systems, mononuclear or dinuclear, as well [66]. Surprisingly some XYL-based ligands also exhibit reactivity towards external substrates as $\mu\text{-}\eta^2\text{:}\eta^2$ -peroxido complex [67]. Similar ligands were found to be reactive as trans- μ -1,2-peroxido or bis(μ -oxido) complexes [68]-[70]. This demonstrates that a minimal change in the ligand system does not only effect the formation of different "oxygen adduct" complexes, but also effects the hydroxylation reactivity. The latter is in accordance with the results concerning the geometrical changes while reacting. Bis(μ -oxido) complexes based on mononuclear complexes with smaller ligands show reactivity towards external phenols and phenolates as well [71],[72]. Furthermore mononuclear copper "dioxygen adducts" are capable of aromatic hydroxylations. An η^1 -superoxido complex with a tridentate ligand was found to oxygenate phenols [73],[74].

With a bond dissociation energy of 377 kJ/mol (90 kcal/mol) the benzylic C—H position is comparable to the aromatic positions and should be discussed here as well. An intramolecular benzylic hydroxylation was observed by $\mu\text{-}\eta^2\text{:}\eta^2$ -peroxido [75] and bis(μ -oxido) intermediates [76]. Figure 1.19 shows an example for the hydroxylation with a bis(μ -oxido) copper complex.

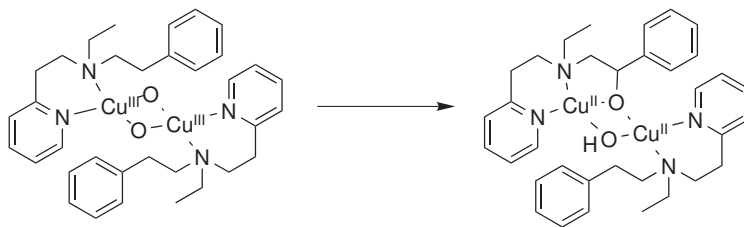


Figure 1.19: Intramolecular benzylic hydroxylation, charges are omitted.

The mechanism of these reactions is a topic of great interest, because of their resemblance to the dopamine β -monooxygenase catalyzed hydroxylation. Although a concerted mechanism similar to the aromatic substitutions was proposed [77], there are a number of arguments speaking for a radical mechanism [78],[79]. The oxygenation of external substrates at benzylic positions was also demonstrated using tripodal ligands in an $\mu\text{-}\eta^2\text{:}\eta^2$ -peroxido complex [80],[81].

1.3.2 Aliphatic Hydroxylation

Non-activated hydrocarbons have a bond dissociation energy approximately of 404 kJ/mol (97 kcal/mol) for the tertiary C–H bond and 439 kJ/mol for the methyl C–H bond (105 kcal/mol). This is significantly higher than bond dissociation energies for benzylic or allylic C–H bonds. The importance of metal complexes in activating these bonds is reflected by the fact that there are only very few known C–H bond activating enzymes without a metal ion in the active site [82]. Laboratory systems for direct hydroxylation without the use of metals are indeed possible and mostly based on oxygen centered radicals often derived from peroxides [83]. In comparison a lot more reactions involving metal ions are known. For most of them a radical mechanism is assumed [84]. Copper "oxygen adduct" complexes exhibit intramolecular hydroxylation activity towards non-activated C–H bonds in some cases [85]–[87]. Figure 1.20 shows an additional example for these hydroxylation reactions.

In this example a formation of a bis(μ -oxido) intermediate could be detected at -90°C . A crystal structure of a dinuclear copper complex with two ligands that were both hydroxylated at one of the isobutyl groups was obtained [88]. This product occurred probably by reorganization of ligands after a intramolecular hydroxylation, because redox and atom balance only allow one ligand to be oxidized directly.

1 Introduction

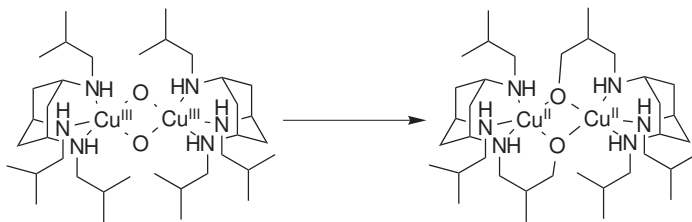


Figure 1.20: Intramolecular aliphatic ligand hydroxylation, charges are omitted.

Using steroid based ligand systems it was possible to demonstrate the regio- and stereoselectivity of aliphatic hydroxylation reactions with copper "dioxygen adducts" [89]-[92]. Figure 1.21 shows the amine ligand where a steroid is coupled and the reaction product of the intramolecular hydroxylation. The copper(II) complex with $\text{Cu}(\text{CF}_3\text{SO}_3)_2$ was reduced with benzoin and reacted with dioxygen. After work up yields of 12-26% of enantiopure products were obtained (example in Figure: 26%). It was shown that yield and stereoselectivity strongly depended on small changes in the ligand system as already mentioned above.

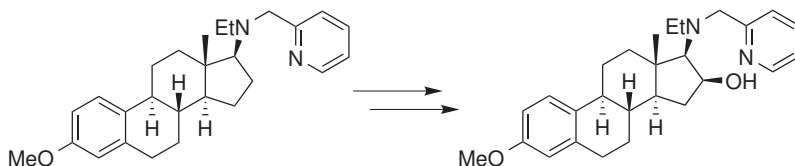


Figure 1.21: Stereo-selective β -hydroxylation of a steroid amine ligand with copper dioxygen complexes.

In accordance with the finding is the fact that using an imine instead of the amine ligand results in a complete different regioselectivity under the same reaction conditions. The ligand and the hydroxylation product for this reaction are shown in Figure 1.22. A bis(μ -oxido) intermediate was proposed as active species in this process.

These reactions gave further insight into reactions of the copper "oxygen adduct" intermediates and furthermore demonstrated that not only the activation of dioxygen is important for the attack of a C–H bond, but that

the exact geometrical positioning seems equally important for the reactivity.

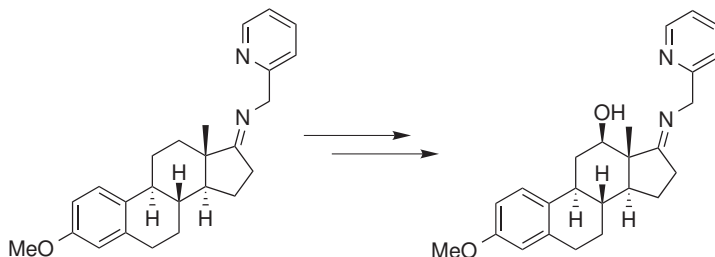


Figure 1.22: Stereo-selective γ -hydroxylation of a steroid imine ligand with copper dioxygen complexes.

1.4 Aims of the Research

As discussed above both, μ - η^2 : η^2 -peroxido and bis(μ -oxido) complexes, can play an important role in intramolecular and intermolecular hydroxylation reactions. Their formation and reactivity strongly depends on the ligands used. There are two fundamental challenges regarding these reactions:

1. The mechanism of the hydroxylation reactions is not yet understood in full detail; however, it is important for the design and optimization of oxidation reactions and for a better understanding of enzymatic processes. The short lifetime of the "oxygen adduct" intermediates in the reactions are experimentally very challenging and require special techniques and the results should be supported by DFT calculations.
2. Although hydroxylation reactions of dinuclear copper complexes are extremely common in nature, there is a lack of synthetic applications. Only some examples suggest a very specialized synthetic use such as the work of Schönecker et al. [89]–[92]. The rare use for synthetic applications is very unsatisfying, because great selectivity and mild conditions are promising and should be available to a broader spectrum of reactions.

In the scope of this work these two challenges should be addressed. Holland et al. suggested the use of small ligands for self-assembled dinuclear copper "oxygen adduct" complexes [65]. Their ligand system can be used as model for aromatic hydroxylations with a bis(μ -oxido) complex. Following up on

1 Introduction

this strategy there are two major research goals in this work: first mechanistic investigations on such systems and second the establishment of alternatives and synthetic applications with similar reactivity. For clarity these results are divided in two parts:

Selective Aromatic Hydroxylation

In the first part the reaction mechanism of the intramolecular ligand hydroxylation of the ligand PPN is investigated (Figure 1.18) and a synthetically easier available alternative (BDED, Figure 1.23) is introduced. The different ligand systems should be compared concerning their mechanism and reactivity.

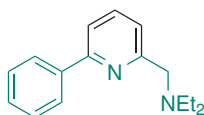


Figure 1.23: BDED (colored) is quite similar to PPN

Selective Aliphatic Hydroxylation

In the second part the idea of the intramolecular ligand hydroxylations should be expanded towards aliphatic hydroxylations. Mechanistic investigations and different substrates should be used to gain insight into the activation of aliphatic C-H bonds. The synthetic potential of intramolecular ligand hydroxylations with copper "oxygen adduct" complexes even for non activated aliphatic compounds should be investigated.

2 Selective Aromatic Hydroxylation

The main results described in this chapter have been accepted for publication in the journal "*Chemistry - A European Journal*" with the following authors: Jonathan Becker, Puneet Gupta, Friedrich Angersbach, Felix Tuzcek, Christian Näther, Max C. Holthausen and Siegfried Schindler. The DFT calculations were performed by Puneet Gupta and Max C. Holthausen. Furthermore selected parts of the supporting information and results that are not yet going to be published are presented. Spectroscopic, crystallographic and other supporting data are reported in chapter 4.1.

2.1 Selective Aromatic Hydroxylation with Dioxygen and Simple Copper Imine Complexes

2.1.1 Introduction

Tyrosinase, a copper enzyme, is an important monooxygenase responsible for the *o*-hydroxylation of the amino acid tyrosine [8],[14],[93]-[96]. Aiming at the transfer of its function to synthetic applications, enormous research efforts over the past decades have led to the development of a vast number of bioinorganic model systems (for selected references see [36],[41],[44],[45],[58],[60],[66],[70],[89],[96]-[104]). So far, however, only a few copper complexes have been identified that are actually able to hydroxylate organic substrates in a catalytic fashion, similar to the enzyme [43],[47],[49],[105]-[107]. In mechanistic considerations a bimetallic, side-on peroxido dicopper complex has been accepted as the catalytically active species for a long time, until later findings in a bioinorganic model system provided evidence for a rapid peroxido/bis- μ -oxido equilibrium in solution, with a subtle influence of the particular supporting ligand environment, the solvent, and counter ions on the relative thermodynamic stabilities of the individual isomers [46],[71],[108]-[111]. With this equilibrium representing a low-barrier initial O–O bond breaking step along the hydroxylation pathway, Tolman and coworkers suggested the involvement of a bis(μ -oxido) intermediate as the effective hydroxylating species in the course of aromatic C–H bond-activation processes taking place in enzymes or synthetic models. To investigate this question further, Holland et al. devised a bioinorganic model based on the ligand 2-(diethylaminoethyl)-6-phenylpyridine (PPN, Figure 2.1) [65]. Reacting the PPN copper(I) complex with O₂ at low temperatures they observed initial formation of a bis(μ -oxido)dicopper complex followed by the subsequent hydroxylation of the pendant phenyl group even at low temperatures.

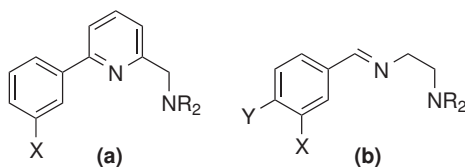


Figure 2.1: The ligands PPN (a: R=Et, X=H) and BDED (b: R=Et, X=Y=H).

Here we reinvestigated this system by means of fast stopped-flow techniques

at low temperatures to establish a clearer picture of the formation of the bis(μ -oxido)dicopper intermediate and its reactivity. While this system is interesting in terms of mechanistic insight the prospects of its use for synthetic applications appear very limited. To further investigate the transferability of the structure/reactivity relationship, we devised a related system based on the supporting ligand *N*'-benzylidene-*N,N*-diethylethylenediamine (BDED, Figure 2.1), which exhibits the same basic structural features but is synthetically more readily accessible. The reactivity of the copper complex formed with this ligand against dioxygen is studied and possible synthetic application in stoichiometric selective oxidations is reported herein. Furthermore, we unveiled the underlying mechanistic scenario for both systems by quantum chemical means.

2.1.2 Results and Discussion

Because 2-(chloromethyl)-6-phenylpyridine, the starting material used by Holland et al. for the synthesis of the PPN ligand, was no longer commercially available we established a slightly different synthetic route to this ligand according to literature procedures (Figure 2.2) [65],[112]-[114].

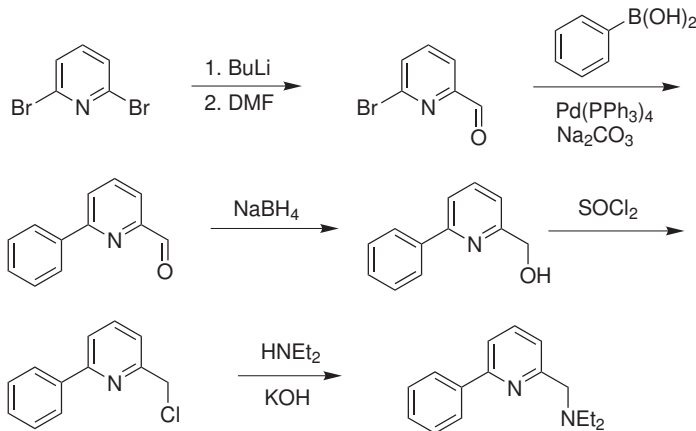


Figure 2.2: Synthesis of PPN.

The structure of the complex $[\text{Cu}(\text{PPN})\text{CH}_3\text{CN}]\text{SbF}_6$ was previously characterized by Holland et al. and exhibits an unusual T-shaped coordination geometry about a three-coordinate copper ion in the solid state [65]. For

reasons detailed below we prepared this complex in situ in acetone by mixing a solution of $[\text{Cu}(\text{CH}_3\text{CN})_4]\text{CF}_3\text{SO}_3$ under argon with a PPN solution saturated with dioxygen. Figure 2.3 displays the evolving time-resolved UV-vis spectra recorded in a stopped-flow measurement at -90.8°C , which indicate that the Cu(I) complex reacts quite slowly, over a period of 900 seconds, to a bis(μ -oxido) dicopper complex. Except an initial lagging period associated with complex formation, the spectral changes are identical to those reported previously by Holland et al. [65]. After about 30 seconds, the features of complex formation visible at the beginning of the reaction disappear and an exponential increase in absorbance sets in. No indications for other intermediates such as e.g. superoxido or peroxido complexes were observed.

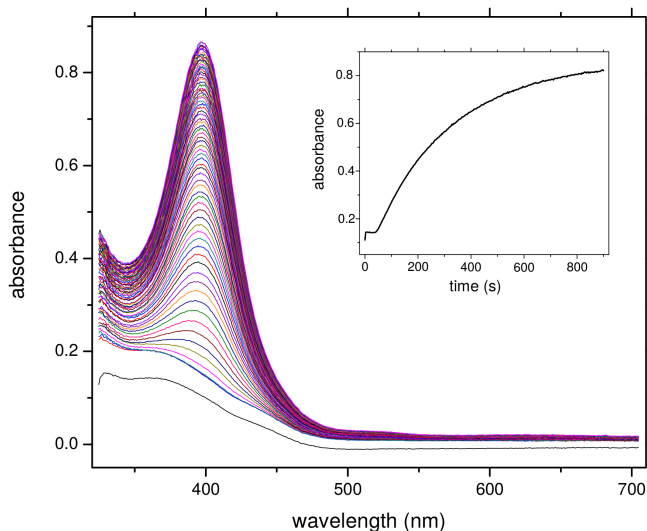


Figure 2.3: Time resolved UV-vis spectra of the reaction of $[\text{Cu}(\text{PPN})]\text{CF}_3\text{SO}_3$ (2.5×10^{-4} mol/L) with dioxygen (5.1×10^{-3} mol/L) in acetone at -91°C over 900 s. The inset shows increase of absorbance at 400 nm over time (first order rate constant $k_{\text{obs}} = 2.6 \times 10^{-3} \text{ s}^{-1}$; fit after the initial lag time).

2 Selective Aromatic Hydroxylation

Clouding of the solutions over time has precluded further detailed kinetic analysis. Due to the quite fast consecutive hydroxylation reaction even at low temperatures it was not possible to isolate and structurally characterize the bis(μ -oxido) dicopper intermediate complex. The first-order "decomposition" reaction (formation of the phenolate-bridged complex, Scheme 2) had been investigated by Holland et al. [65], who reported a rate constant of $k = 6 \times 10^{-4} \text{ s}^{-1}$ in acetone at -70°C . $^1\text{H-NMR}$ -spectroscopy and GC/MS revealed partial hydroxylation of the ligand after decomposition of the product complex. The postulated mechanism is presented in Figure 2.4 [65].

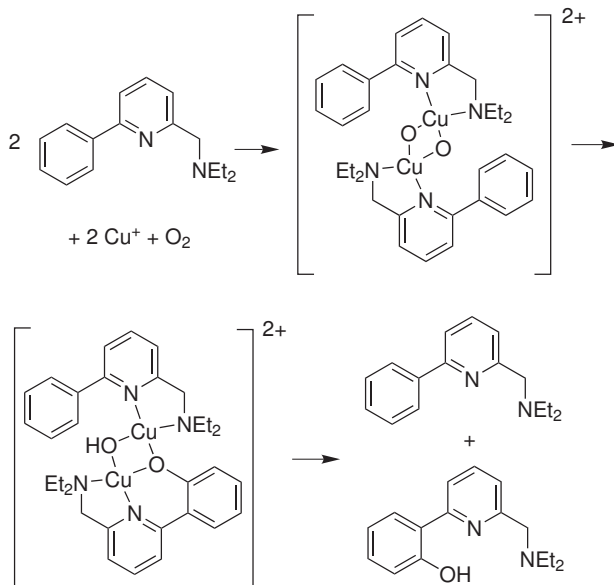


Figure 2.4: Oxidation of $[\text{Cu}(\text{PPN})\text{CH}_3\text{CN}]\text{SbF}_6$ with dioxxygen (scheme redrawn from reference [65])

We studied the underlying reaction mechanism at the BLYP-D/TZVP (COSMO) level of density functional theory (DFT; see the Computational Details section below for details), employing a slightly truncated PPN model ligand **L1** (Figure 2.1a: $\text{R}=\text{Me}$, $\text{X}=\text{H}$). All energies reported below refer to Gibbs energies in kcal mol^{-1} relative to the bis(μ -oxido)dicopper(III) complex (**2** in Figure 2.5) at -70°C . Akin to earlier mechanistic studies on aromatic hydroxylation reactions [45],[46],[74],[115]-[117], we assume initial formation

2.1 Selective Aromatic Hydroxylation with Dioxygen and Copper Complexes

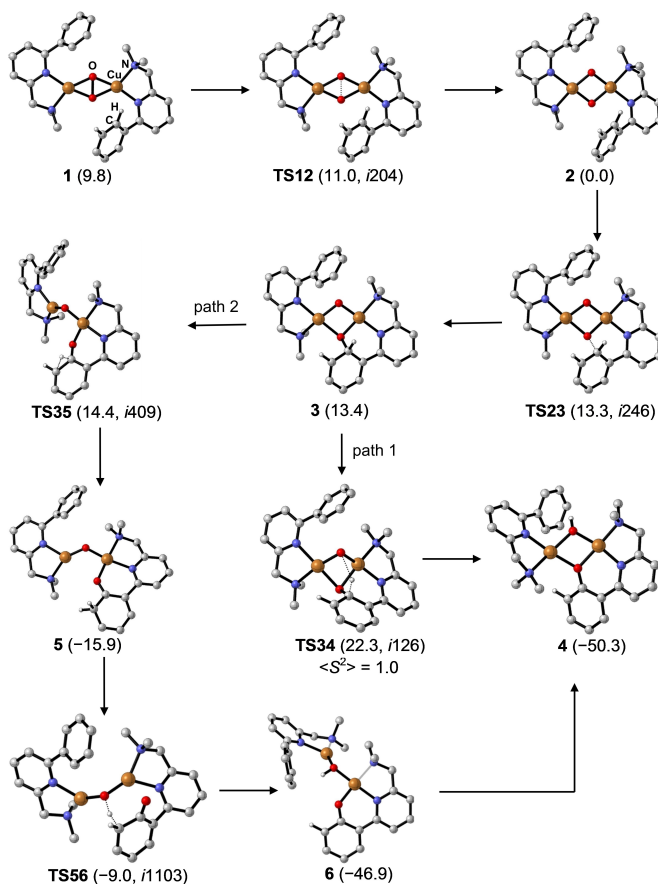


Figure 2.5: Computed reaction pathways for the intramolecular aromatic hydroxylation reaction of the PPN ligand starting from 1. Gibbs energies relative to 2 in kcal mol⁻¹ (BLYP-D/TZVP(COSMO) results, -70 °C, solvent acetone) are given in parentheses together with the characteristic imaginary wave numbers of transition states. For all stationary points reported, closed-shell singlet wavefunctions resulted in the computations, except **TS34**, for which a broken-symmetry wavefunction was obtained. Irrelevant H atoms not shown.

of the (μ - η^2 : η^2 -peroxido)dicopper(II) complex and we chose **1** as starting point for the exploration of reaction pathways (Figure 2.5). We find that **1** is less stable than the bis(μ -oxido) isomer **2** by 10 kcal mol⁻¹ and the core-isomerization process via **TS12** is connected with a minute activation barrier of merely 1 kcal mol⁻¹. Thus, fully in line with experimental observation, we conclude that isomer **2** represents the dominant species in the initial phase of the reaction. One of the μ -O atoms in the dicopper core of **2** is already located in close proximity (2.86 Å) to one of the *ortho*-carbon atoms of the phenyl group, which predetermines the position of the subsequent regioselective ligand hydroxylation commencing with the C–O bond formation via **TS23** (ΔG^\ddagger =13 kcal mol⁻¹). The resulting σ -complex **3** is thermodynamically unstable and two pathways branch off at this point. Along path 1, **3** directly transforms into complex **4** via proton transfer onto the second μ -O atom. This highly exergonic step results in the formation of a (μ -OH)(μ -O)-dicopper complex, which represents the final product of the reaction sequence studied here (in our experiments, liberation of the hydroxylated ligand is accomplished through warming the reaction mixture to room temperature and aqueous workup, in line with the reported procedure of Holland et al. [65]). However, with **TS34** giving rise to an effective activation barrier of ΔG^\ddagger =22 kcal mol⁻¹ for the process leading from **2** to **4**, path 1 cannot kinetically compete with path 2: The latter involves exergonic decay of **3** to the intermediate dienone **5** and subsequent proton abstraction via **TS56** followed by a conformational transition leads to **4**. With an effective activation barrier of ΔG^\ddagger =14 kcal mol⁻¹ associated with **TS35**, the sequence **2** \rightarrow **5** \rightarrow **4** represents the preferred route to product formation and the emergence of a dienone intermediate is coherent with the mechanistic picture suggested in earlier work [45]. However, the low barrier of merely 6 kcal mol⁻¹ computed for the strongly exergonic decay of the dienone intermediate to form **6**, and subsequently **4**, implies that this species will most likely escape any attempts for an experimental characterization.

For further comparison with the experimental results of Holland et al., we also investigated the influence of activating and deactivating substituents X introduced *para* to the activation position in the phenyl ring [65]. The activation barriers resulting for the substituted systems compiled in Table 2.1 were computed as the Gibbs-energy difference at -70 °C between **2-X** and **TS35-X** assuming that the nature of the overall rate-limiting step in the course of the hydroxylation reaction (i.e., the 1,2-H shift for the dienone formation) remains unaltered upon substitution. The resulting differences in computed barrier heights clearly follow the expected trend for substituent effects in electrophilic aromatic substitution reactions, which validates the view that the bis(μ -oxido)dicopper core acts as an electrophile [65]. The high activation barrier obtained for the complex with the strongly deactivating

2.1 Selective Aromatic Hydroxylation with Dioxygen and Copper Complexes

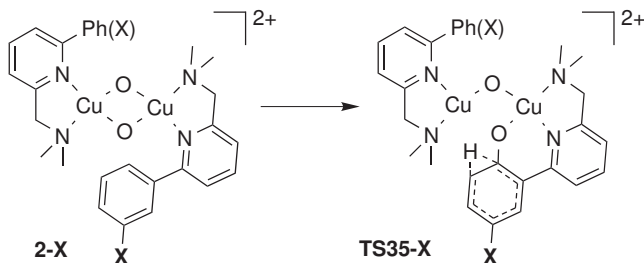


Table 2.1: Substituent effects on the overall rate-limiting step of the hydroxylation reaction.

X	ΔG^\ddagger (kcal mol ⁻¹)	Effect of X
OCH ₃	9.8	Strongly activating
OH	11.2	
CH ₃	12.7	
CH=CH ₂	13.6	Weakly activating
H	14.4	
F	15.5	Weakly deactivating
CHO	18.7	
NO ₂	20.0	Strongly deactivating
CF ₃	20.5	

NO₂ substituent (20 kcal mol⁻¹) is in line with the fact that Holland et al. did not observe formation of the hydroxylated PPN(NO₂) product in their low-temperature experiments [65].

Our efforts to isolate the supposed primary product of this reaction, the (μ-O)(μ-OH)dicopper complex (cf. Figure 2.4) remained unsuccessful. Yet, during workup of one reaction batch we were able to isolate the copper(II) complex with PPN where the two copper(II) ions are bridged by two hydroxide groups. According to the reaction mechanism detailed above (Figure 2.4) only one of the two ligands constituting the dinuclear complex is hydroxylated, i.e., the maximum product yield is 50%. The remaining unreacted ligand equivalents form the bis(μ-hydroxido) complex [Cu₂(PPN)₂(OH)₂](CF₃SO₃)₂, which crystallized when the solution was left on the bench after oxidation. A similar observation and crystal structure for a steroid system had been described by Schönecker et al. previously [89] and by Herres et al. for a

related bisguanidine copper complex system [118]. The molecular structure of the cation of this binuclear complex is shown in Figure 2.6. Crystallographic data are provided as Supporting Information.

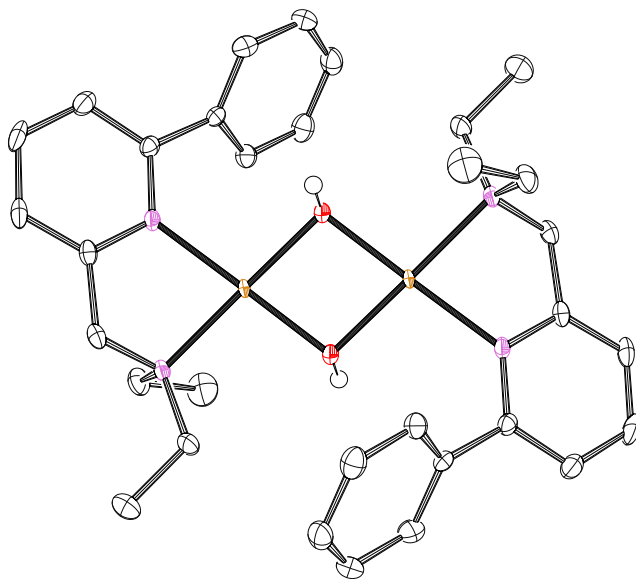


Figure 2.6: Molecular Structure (ORTEP plot, ellipsoids are drawn at 50% probability) of the cation of $[\text{Cu}_2(\text{PPN})_2(\text{OH})_2] (\text{CF}_3\text{SO}_3)_2$.

In contrast to the preparatively rather demanding synthesis of PPN, efficient synthetic access to the BDED ligand is readily achieved in a simple Schiff-base reaction from benzaldehyde and *N,N*-diethylethylenediamine according to the literature [119]. To the best of our knowledge BDED was not used as supporting ligand for metal ions thus far. We were able to crystallize the Cu(I) complex $[\text{Cu}(\text{BDED})_2]\text{CF}_3\text{SO}_3$ and its molecular structure as derived by X-ray crystallography is shown in Figure 2.7. Crystallographic data for this and the corresponding complex with an SbF_6^- anion are provided as Supporting Information.

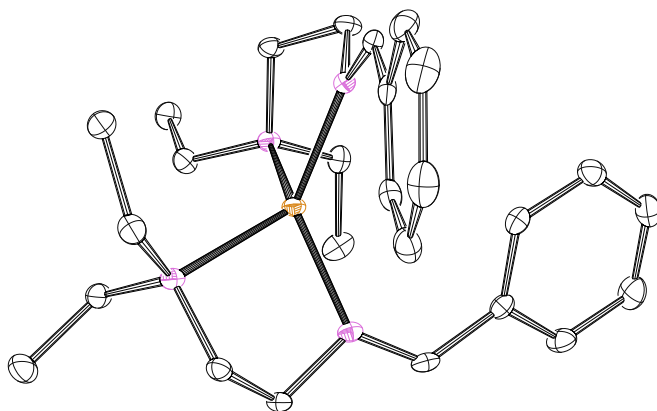


Figure 2.7: ORTEP plot of the molecular structure of $[\text{Cu}(\text{BDED})_2]^+$. Anion and hydrogen atoms are omitted for clarity; ellipsoids are drawn at 50% probability.

It is interesting to note that the PPN-supported copper(I) complex forms with a 1:1 ligand to Cu(I) ratio (together with a coordinated acetonitrile molecule) [65] whereas we find a 2:1 stoichiometry in the crystal structure reported above. To avoid potential problems in our kinetic studies with the formation of this complex we decided to devise an in situ formation of the Cu(I)/BDED complex in a 1:1 stoichiometry by mixing the acetone solution of the copper(I) salt under argon and the O_2 -saturated acetone solution of the ligand within the stopped-flow unit. The same procedure was used in our mechanistic study on the Cu(I)/PPN system described above and thus equivalent reaction conditions were established in both experiments.

Figure 2.8 shows time resolved UV-vis spectra obtained from a stopped-flow measurement at -90.0°C . The optical feature evolving at $\lambda_{\text{max}} = 400\text{ nm}$ is consistent with the formation of a bis(μ -oxido) complex for the Cu(I)/BDED system as well. As before facile kinetic fitting was not possible, however, the Cu(I)/BDED complex clearly reacted faster than the Cu(I)/PPN complex. We performed the same reaction also in a bench-top experiment. After workup of the product solution according to Figure 2.9 we identified the product salicylaldehyde by NMR and GC/MS. It is formed in high yields (getting

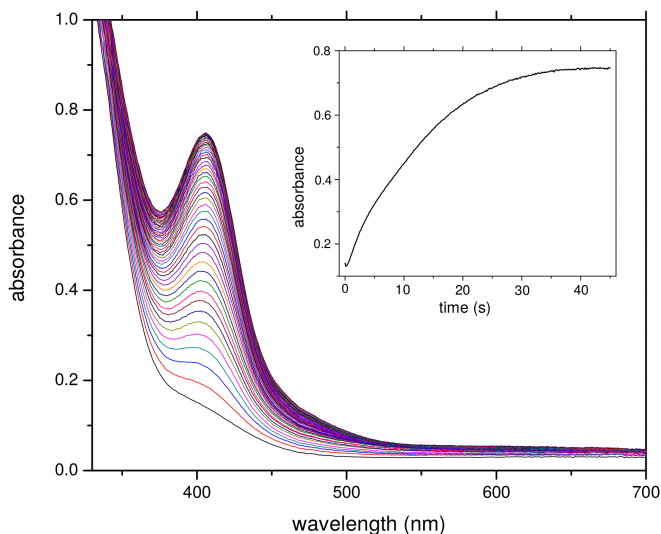


Figure 2.8: Time resolved UV-vis spectra of the reaction of $[\text{Cu}(\text{BDED})]\text{CF}_3\text{SO}_3$ (5.0×10^{-4} mol/L) with dioxygen (5.1×10^{-3} mol/L) in acetone at -90.0°C over 200 s. The inset shows increase of absorbance at 400 nm over time (first order rate constant $k_{\text{obs}} = 5.65 \times 10^{-2} \text{ s}^{-1}$).

close to maximum 50 %), which clearly demonstrates that selective aromatic hydroxylation can be achieved efficiently also by application of simple imine ligands (Figure 2.9). This opens encouraging perspectives for synthetic applications of related ligands. The importance of *ortho*-hydroxylation of arenes has been discussed previously [120],[121]. For copper chemistry on biomimetic hydroxylation reactions early work by Réglier and co-workers should be pointed out [87],[122],[123] and more recently, especially Schönecker et al. have demonstrated the potential of such reactions in organic synthesis using steroids [89]-[92].

In order to evaluate the influence of the supporting ligand environment on the energetics of the hydroxylation reaction we performed additional DFT calculations for the BDED supported complexes. As before we employed in

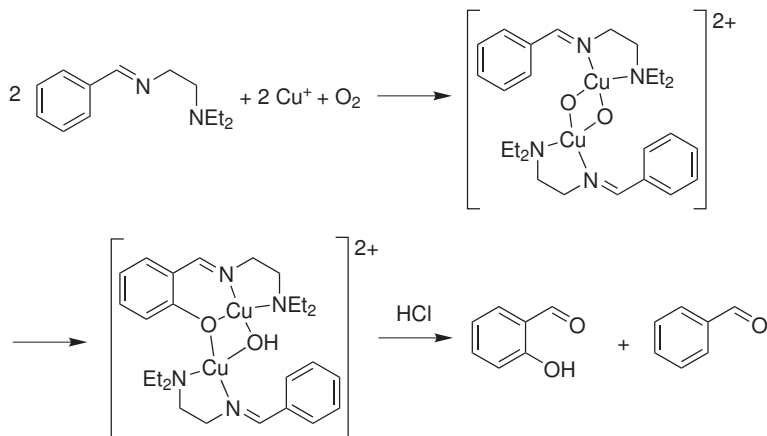


Figure 2.9: Oxidation of [Cu(I)BDED] with dioxygen.

these calculations a slightly truncated molecular model, in which we replaced the ethyl groups at the amine donor by methyl groups. We optimized a number of minima as well as two transition structures that characterize the hydroxylation pathways identified for the PPN-based system (Figure 2.10). Comparison with the results for the both systems reveals largely identical structural features and we found no indication of variations as to the reaction pathways and the nature of the rate limiting steps. Based on these results we estimate a slightly lower overall activation barrier for the hydroxylation (via **TS34'**: 13.6 kcal mol⁻¹ vs. **TS34**: 14.4 kcal mol⁻¹), which is perfectly in line with the observation that hydroxylation in the BDED system occurs at higher rates in the experiments.

To assess substituent effects we synthesized a series of BDED derivatives (Figure 2.1b: R=Et with Y(X=H)=Me, OMe, Cl, NO₂ and X(Y=H)=Me, NO₂). We prepared the corresponding copper(I) complexes and reacted them with dioxygen in the same way as described before for the parent BDED system. Only negligible effects were observed for ligands with a methyl or a methoxy group. The hydroxylated product still forms in high yields and for the methyl-substituted BDED ligand (Figure 2.1b, R=Et, Y=H, X=Me) hydroxylation occurs in *ortho* and *para* position of the methyl group, as expected. In contrast, hydroxylation yields were low for the chloro-substituted ligand (Y=Cl) and hydroxylation did not occur for nitro-substituted ligands. The latter finding is in accord with the report of Holland et al. for the nitro

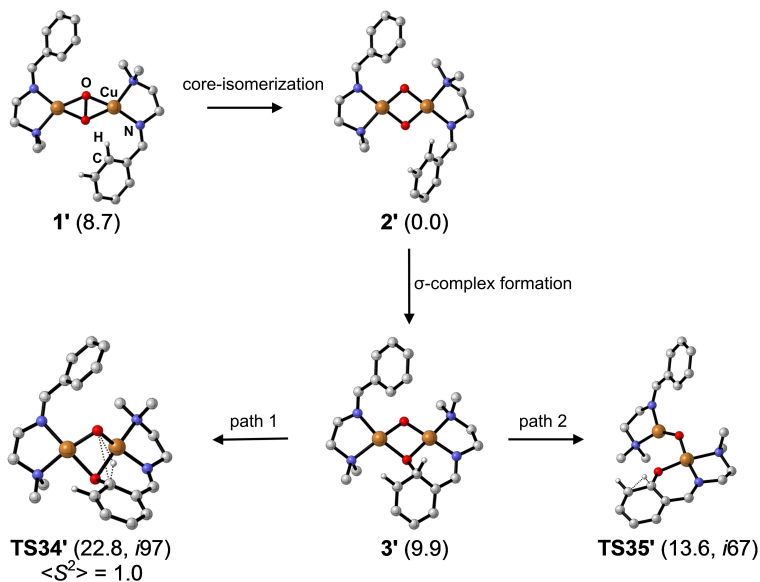


Figure 2.10: Selected reaction steps computed for the intramolecular aromatic hydroxylation reaction for the BDDE ligand starting from **1'**. Gibbs energies relative to **2** in kcal mol^{-1} (BLYP-D/TZVP(COSMO) results, -70°C , solvent acetone) are given in parentheses together with the characteristic imaginary wave numbers of transition states. For all stationary points reported, closed-shell singlet wavefunctions resulted in the computations, except **TS34'**, for which a broken-symmetry wavefunction was obtained. Irrelevant H atoms not shown.

analogue of PPN [65] and with the results of our model calculations on substituent effects on the effective barrier heights presented above. We also tested a BDED derivative, in which we replaced the ethyl groups at the amine donor by methyl groups (Figure 2.1b: R=Me, X=Y= H) and we observed only insignificant differences in terms of reactivity, but a slightly smaller yield of the hydroxylated product was obtained.

Furthermore, although obviously less attractive in terms of potential synthetic applications, we tested if the reduced form of the BDED ligand would also support ligand hydroxylation reaction. The corresponding H₂BDED ligand was obtained by treatment of BDED with sodium borohydride (Figure 2.11).

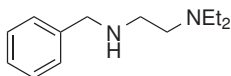


Figure 2.11: The ligand H₂BDED.

However, owing to problems with disproportionation reactions it was impossible to obtain and characterize the copper(I) complex of this ligand in the solid state. Oxidation experiments conducted in the same way as described for the imine complex did not lead to ligand hydroxylation. Yet, a copper(II) complex with this ligand was obtained by reacting CuCl₂ with H₂BDED. The molecular structure of [Cu(H₂BDED)Cl₂] and crystallographic data are presented in the Supporting Information.

Finally it is important to note that the BDED system can be quite sensitive with respect to particular conditions employed in the synthetic procedures. E.g., when a solution of [Cu(CH₃CN)]CF₃SO₃ with BDED in dichloromethane was reacted at -80 °C with dioxygen, and kept at this temperature for more than half an hour, no hydroxylation was observed. Instead, after evaporation of the solvent, crystals of a dinuclear bis-hydroxido bridged copper(II) complex with a *N,N*-diethyl-ethylenediamine ligand was obtained. The molecular structure of this complex (Figure 2.12, see the Supporting Information for crystallographic data. A crystal structure of this complex with a different anion has been reported previously [124].) reveals that the imine bond in the BDED ligand was cleaved - one could even smell the free benzaldehyde from the solution.

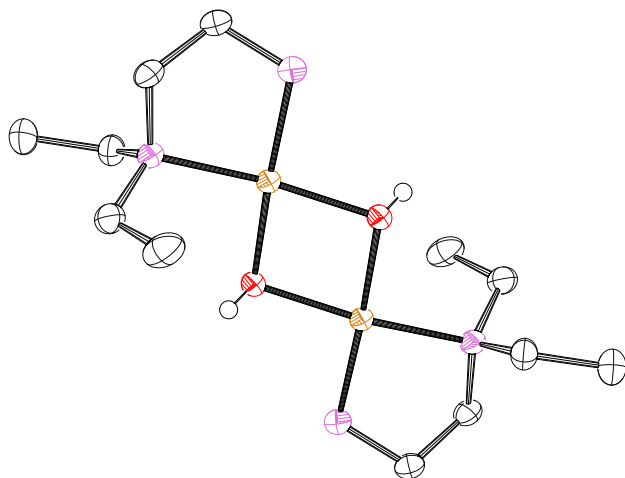


Figure 2.12: Molecular structure (ORTEP plot, ellipsoids are drawn at 50% probability) of the cation of $[\text{Cu}_2(\text{Et}_2\text{en})(\text{OH})_2](\text{CF}_3\text{SO}_3)_2$.

2.1.3 Conclusions

In the present contribution we have reinvestigated the aromatic hydroxylation in a dinuclear Cu_2O_2 complex supported by PPN ligands, which has been studied earlier by Holland et al. [65]. Stopped-flow measurements at low temperatures revealed the quite fast formation of a bis(μ -oxido)dicopper complex, however, no further intermediates such as a superoxido complex could be detected. We have elucidated the underlying reaction mechanism by DFT calculations. Fully in line with the interpretation of experimentally observed UV-vis signatures, the quantum-chemical results reveal the bis(μ -oxido) dinuclear complex as the dominant intermediate present in the initial phase of the reaction; the corresponding side-on peroxido complex is less stable by 10 kcal mol^{-1} . The hydroxylation sequence commences with an attack of one of the μ -O atoms of the bis(μ -oxido) complex on the phenyl group of the PPN ligand, which results in the formation of a thermodynamically and kinetically unstable σ -complex. Along the favored reaction path, this complex decays via a 1,2-H shift to form a dienone species, from which the

product species is formed in subsequent steps. The bis(μ -oxido)complex and the 1,2-H shift transition-state represent the rate-determining states [125] of the reaction sequence studied here, which is characterized by an effective largest barrier of 14 kcal mol^{-1} . Substituent effects on this barrier height are consistent with the characterization of the bis(μ -oxido) complex as an electrophile in this reaction.

We have further demonstrated experimentally as well as theoretically that the same facile selective hydroxylation of aromatic aldehydes can also be achieved using the related supporting imine ligand BDED, which is synthetically much easier to access than the PPN ligand. It is interesting to note at this point that while here, experimentally and from the calculations, a peroxido complex can be excluded, that has been the opposite for a quite related binuclear copper complex investigated previously by some of us [45]. While an intramolecular *o*-hydroxylation was observed as well, the active complex was characterized as a peroxido complex and no bis(μ -oxido)complex could be detected. Complexes of this type have already been used in synthetic applications [126], however these are limited for this kind of system.

We could clearly demonstrate that the possibility of preparing complexes of this type in situ and using dioxygen as an oxidant makes the whole setup promising for quite a number of preparative applications in the future. Herewith we provide a new synthetic approach in regard to the importance of *ortho*-hydroxylation of arenes [120],[121] discussed above.

2.1.4 Experimental Section

Materials and Methods

Solvents and reagents used were of commercially available reagent quality. $[\text{Cu}(\text{CH}_3\text{CN})_4]\text{CF}_3\text{SO}_3$ and $[\text{Cu}(\text{CH}_3\text{CN})_4]\text{SbF}_6$ were synthesized according to literature procedures [127]. ^1H -NMR and ^{13}C -NMR spectra were measured on a Bruker AV 400 and BRUKER AV 200 spectrometer. GC/MS spectra were recorded on a HP GL 6890 chromatograph with a HP 5973 mass detector.

Low Temperature Stopped-flow Measurements

Low temperature stopped-flow experiments were performed using a commercial HI-TECH SF-61SX2 instrument (TgK Scientific, Bratford-on-Avon, UK). Solvents used for stopped-flow measurements and experiments under inert conditions were obtained as already pure chemicals and distilled under argon atmosphere prior to transferring them into a glove box (MBraun, Garching, Germany). For the reaction of $[\text{Cu}(\text{PPN})]^+$ with dioxygen, a $5 \times 10^{-4} \text{ mol/L}$ solution of PPN and a $5 \times 10^{-4} \text{ mol/L}$ solution of $[\text{Cu}(\text{CH}_3\text{CN})_4]\text{CF}_3\text{SO}_3$ in acetone were prepared under inert conditions within the glove box. For the

corresponding reaction of $[\text{Cu}(\text{BDED})]^+$ with dioxygen, a 1×10^{-3} mol/L solution of BDED and a 1×10^{-3} mol/L solution of $[\text{Cu}(\text{CH}_3\text{CN})_4]\text{CF}_3\text{SO}_3$ in acetone were prepared under the same conditions. The solutions were transferred separately with gastight syringes to the stopped-flow instrument. The ligand solution was saturated with dioxygen (5.0) by bubbling a gas stream through the liquid for 10 min (10.2×10^{-3} mol/L) [128].

Single-Crystal X-ray Structure Determinations

For $[\text{Cu}_2(\text{PPN})_2(\text{OH})_2](\text{CF}_3\text{SO}_3)_2$ data collection was performed using a STOE Imaging Plate Diffraction System (IPDS-1) with MoK_α radiation. The structure was solved with direct methods using SHELXS-97 and refinement was performed against F^2 using SHELXL-97 [129]. All non-hydrogen atoms were refined anisotropic. The C–H H atoms were positioned with idealized geometry and refined isotropic with $U_{\text{iso}}(\text{H})=1.2 U_{\text{eq}}(\text{C})$ using a riding model. The O–H H atom was located in difference map, its bond lengths set to ideal values and finally it was refined isotropic using a riding model. For $[\text{Cu}(\text{BDED})_2]\text{CF}_3\text{SO}_3$ data collection a BRUKER D8 Venture system equipped with dual $I\mu\text{S}$ microfocus sources, a PHOTON100 detector and an OXFORD CRYOSYSTEMS 700 low temperature system was used. Data collection was performed using Mo-K_α radiation with wavelength 0.71073 \AA and a collimating Quazar multilayer mirror. Semi-empirical absorption correction from equivalents was applied using SADABS-2014/4 and the structure was solved by intrinsic phasing using SHELXT2014 [130]. Refinement was performed against F^2 using SHELXL-2014/7 [129]. All non-hydrogen atoms were refined anisotropically and hydrogen atoms were positioned geometrically. The X-ray crystallographic data for $[\text{Cu}_2(N,N\text{-(Et)}_2\text{en)}_2\text{OH}_2](\text{CF}_3\text{SO}_3)_2$ were collected using a BRUKER/NONIUS KappaCCD detector with a BRUKER/NONIUS FR591 rotating anode radiation source and an OXFORD CRYOSYSTEMS 600 low temperature system. Mo-K_α radiation with wavelength 0.71073 \AA and a graphite monochromator were used. The PLATON [131] MULABS semi-empirical absorption correction using multiple scanned reflection was applied on the data and the structure was solved by intrinsic phasing using SHELXT2014 [130] and refined with SHELXL2014/6 [129]. All non-hydrogen atoms were refined anisotropically, C-H and N-H hydrogen atoms were positioned geometrically and OH hydrogen atoms were located in difference map and refined isotropically.

Crystallographic data for the structures have been deposited with the Cambridge Crystallographic Data Centre as CCDC No. 1047585, 1047583 and 1032911.

Computational Details

Geometry optimizations and harmonic frequency calculations were performed with the Gaussian09 program [132] employing the dispersion corrected [133]-[135] BLYP-D2 density functional in combination with a triple- ζ basis-set/effective core potential (ECP) one-particle description (the def2-TZVP [136],[137] basis set was used for C, H, N and O atoms, and the quasi-relativistic SDD-type [138] ECP together with the corresponding triple- ζ basis set [138] was used for Cu; this combination is denoted def2-TZVP(SDD)). For improved computational efficiency the density-fitting approximation was used and the corresponding density-fitting basis set was generated automatically by routines implemented in the Gaussian09 program ("auto" keyword) [139],[140]. Default integration grids and convergence criteria have been used throughout. All structure optimizations were initially performed employing restricted Kohn-Sham (RKS) singlet wavefunctions. Subsequently we searched for energetically low lying unrestricted Kohn-Sham (UKS) wavefunctions with broken spin and spatial symmetry ("broken-symmetry" wavefunctions) using the "guess=mix" keyword. In all cases but two, the UKS wavefunctions collapsed during the self-consistent field optimization and closed-shell singlet wavefunctions resulted. For the two transition states **TS34** and **TS34'** broken-symmetry wavefunctions were obtained with lower energies than the RKS singlet wavefunctions; the former were used for geometry optimizations and harmonic frequency calculations on these two species. All stationary points have been characterized as minima or first order saddle points by eigenvalue analysis of the diagonalized Hessians. The connection of transition states and related minima was established by employing small geometry displacements along both directions of the imaginary vibrational mode resulting from the vibrational frequency calculations on the transition structures, followed by unconstrained geometry optimizations. XYZ coordinates of optimized minima and transition states are provided in the Supporting Information.

Based on these optimized geometries, subsequent single-point energy calculations were performed at the BLYP-D3 [133],[134],[141] /def2-TZVP(SDD) level including the COSMO continuum solvation model [142] implemented in the ORCA 2.9 program (solvent acetone) [143]. The resolution-of-identity (RI) [144]-[146] approximation for the BLYP functional was used employing the auxiliary def2-TZVP/J basis set [147]. For **TS34** and **TS34'**, broken-symmetry singlet energies (E_{BS}) were obtained applying the formalism of Yamaguchi [148],[149] as implemented in the ORCA program. All energies obtained were corrected to obtain Gibbs energies at 203 K by adding the corresponding thermal and entropic increments derived from the Hessian calculations with the Gaussian program (the "freqchk" utility program of

Gaussian09 was used for this purpose). Total electronic energies and Gibbs energies at 203 K for all stationary points reported are provided in the Supporting Information. Figures of the molecular structures were produced by means of the CYLview program [150].

Synthesis of 2-(diethylaminomethyl)-6-phenylpyridine (PPN)

The ligand was synthesized following slightly modified literature procedures [112]-[114] and only the last step was performed according to the publication by Holland et al. [65] because the starting material was no longer commercially available.

2-Bromo-6-formylpyridine

Following the literature procedure [112] 11.8 g (50.0 mmol) 2,6-dibromopyridine was dissolved in dry diethyl ether (150 mL) under argon atmosphere and cooled to -80°C . With vigorous stirring a solution of BuLi in hexane (2.50 mol/L, 20.0 mL, 50.0 mmol) was added slowly. After 30 minutes dimethylformamide (4.5 mL, 60.0 mmol) was added dropwise and the temperature was held for another 20 minutes. Then the solution was slowly heated to 0°C . Hydrochloric acid (1 mol/L) was added until an acidic pH was reached and the mixture was neutralized with an aqueous solution of NaHCO_3 . After workup with ethyl acetate and water the combined organic layers were dried over Na_2SO_4 and kept in a refrigerator overnight. White-yellow crystals precipitated and were washed with pentane (3.72 g, 40.0% yield). $^1\text{H-NMR}$ (400 MHz, CDCl_3): δ = 10.01 (s, 1H), 7.93 (d, 1H, $J=6.6$ Hz), 7.75 (m, 2H, $J=7.8$ Hz) ppm; $^{13}\text{C-NMR}$ (100 MHz, CDCl_3): δ = 191.7, 153.5, 142.6, 139.4, 132.7, 120.4 ppm.

6-Phenyl-2-pyridinecarbaldehyde

This reaction was performed according to the procedure described by Lin Chuang et al. [113]. Under inert conditions $\text{Pd(PPh}_3)_4$ (0.37 g, 0.30 mmol) was dispersed in dry toluene and added to a solution of 2-bromo-6-formylpyridine (2.0 g, 11 mmol) in toluene. A solution of Na_2CO_3 (2 mol/L) was degassed with argon for two hours and 11 mL were added to the reaction mixture. The solution was heated for 16 hours to 90°C . After cooling to room temperature CH_2Cl_2 (80 mL) and an aqueous solution of Na_2SO_4 (2 mol/L, 40 mL) was added. The organic layer was washed with brine and dried over Na_2SO_4 . It was concentrated under reduced pressure and kept in the refrigerator. Grey-white crystals precipitated and were washed with pentane (1.4 g, 69.9%). $^1\text{H-NMR}$ (400 MHz, CDCl_3): δ = 10.03 (s, 1H), 7.95 (d, 2H, $J=8.0$ Hz), 7.75 (m, 3H, $J=2.9$ Hz), 7.36 (m, 3H, $J=7.5$ Hz) ppm;

^{13}C -NMR (100 MHz, CDCl_3): δ = 194.0, 157.9, 152.8, 137.78, 129.7, 129.1, 129.0, 128.3, 127.1, 125.4, 124.5 ppm.

6-Phenyl-2-pyridinemethanol

A solution of NaBH_4 (0.380 g, 10.0 mmol) in water (10 mL) was added to a solution of 6-phenyl-2-pyridinecarbaldehyde (1.38 g, 7.57 mmol) in methanol (30 mL). After stirring at room temperature for 30 minutes the mixture was heated to boiling point and kept under reflux for 50 minutes. When the mixture was cooled to room temperature, the methanol was removed under reduced pressure and to the remaining solution hydrochloric acid (1 mol/L) was added to reach an acidic pH. Then the pH was raised to 12 with sodium hydroxide (1 mol/L). The solution was washed three times with CH_2Cl_2 and the combined organic layers were dried over Na_2SO_4 . The solvent was removed under reduced pressure. A yellow, partly crystallized oil was obtained (1.0 g, 72.3%). ^1H -NMR (400 MHz, CDCl_3): δ = 7.98 (d, 2H, J =7.1 Hz), 7.67 (t, 1H, J =7.4 Hz), 7.57 (d, 1H, J =7.4 Hz), 7.41 (m, 3H, J =7.8 Hz), 7.13 (d, 1H, J =8.0 Hz), 4.78 (s, 2H), 4.34 (s, 1H) ppm; ^{13}C -NMR (100 MHz, CDCl_3): δ = 137.5, 129.2, 128.8, 127.0, 127.0, 119.0, 118.8, 64.0 ppm.

2-(Chloromethyl)-6-phenylpyridine hydrochloride

Following the literature procedure of Makowska-Grzyska et al. [114] thionyl chloride (6 mL) was added dropwise to 6-phenyl-2-pyridinemethanol (1.00 g, 5.40 mmol) under inert conditions while being cooled with an ice bath. At the end of the reaction, the mixture was heated under reflux for two hours. The remaining thionyl chloride was removed under reduced pressure and the residue was washed several times with CH_2Cl_2 . A white solid was obtained (1.06 g, 95.6%). ^1H -NMR (400 MHz, CDCl_3): δ = 8.31 (t, 2H, J =8.2 Hz), 8.18 (d, 1H, J =7.3 Hz), 7.92 (dd, 2H, 4.3 Hz), 7.61 (m, 2H, J =3.9 Hz), 7.27 (s, 1H), 5.49 (s, 2H) ppm; ^{13}C -NMR (100 MHz, CDCl_3): δ = 155.0, 154.3, 144.1, 132.3, 129.5, 129.1, 124.0, 41.3 ppm.

2-(Diethylaminomethyl)-6-phenylpyridine

The ligand was synthesized according to the literature [65]. A mixture of 2-(chloromethyl)-6-phenylpyridine hydrochloride (0.60 g, 3.0 mmol) and diethylamine (4.5 mL) in dry THF (40 mL) with powdered KOH (1.5 g) was heated under inert conditions to reflux for 22 hours. The solvent was removed under reduced pressure and water (5 mL) and brine (5 mL) were added to the residue. The mixture was washed with diethyl ether several times and the combined organic layers were dried over Na_2SO_4 . After removing the solvent under reduced pressure the remaining oil was purified using a Kugelrohr

2 Selective Aromatic Hydroxylation

distillation. A yellow oil was obtained (0.44 g, 61.4%). $^1\text{H-NMR}$ (400 MHz, CDCl_3): δ = 7.92 (d, 2H, $J=7.1$ Hz), 7.62 (t, 1H, $J=7.6$ Hz), 7.49 (d, 1H, $J=8.0$ Hz), 7.36 (m, 4H, $J=3.9$ Hz), 3.76 (s, 2H), 2.55 (q, 4H, $J=7.0$ Hz), 1.02 (t, 6H, $J=7.3$ Hz) ppm; $^{13}\text{C-NMR}$ (100 MHz, CDCl_3): δ = 139.7, 136.9, 128.7, 127.0, 121.1, 118.4, 59.5, 47.4, 12.1 ppm.

***N'*-Benzylidene-*N,N*-diethyl-ethylendiamine (BDED)**

A solution of benzaldehyde (7.96 g, 75.0 mmol) in diethyl ether (200 mL) was stirred for one hour over MgSO_4 at room temperature. Then the mixture was heated for another hour under reflux. The solvent was removed under reduced pressure after filtration. A yellow oil was obtained (13.2 g, 86.5%). $^1\text{H-NMR}$ (400 MHz, CDCl_3): δ = 8.21 (s, 1H), 7.64 (m, 2H, $J=2.4$ Hz), 7.31 (t, 2H, $J=2.8$ Hz), 3.64 (t, 2H, $J=7.1$ Hz), 2.70 (t, 2H, $J=7.5$ Hz), 2.53 (q, 4H, $J=7.3$ Hz), 0.97 (t, 6H, $J=7.2$ Hz) ppm; $^{13}\text{C-NMR}$ (100 MHz, CDCl_3): δ = 161.7, 136.3, 130.5, 128.6, 128.0, 60.0, 53.5, 47.6, 12.0 ppm.

$[\text{Cu}^{\text{I}}(\text{BDED})_2]\text{CF}_3\text{SO}_3$

82 mg (0.2 mmol) BDED and 38 mg (0.1 mmol) $[\text{Cu}(\text{CH}_3\text{CN})_4]\text{CF}_3\text{SO}_3$ were dissolved in 2 mL dry acetone in a glove box under argon atmosphere. Orange crystals were obtained by slow ether diffusion over four weeks at -40°C .

***N'*-Benzyl-*N,N*-diethyl-ethane-1,2-diamine (H_2BDED)**

To a solution of 5.55 g (27.0 mmol) BDED in 50 mL methanol a solution of 0.80 g sodium borohydride in about 50 mL methanol was added slowly. After stirring for 30 minutes, the reaction mixture was heated under reflux for another 2 hours. The mixture was washed three times with diethyl ether after aqueous workup. It was dried over Na_2SO_4 and the solvent was removed under vacuum. 4.88 g (23.7 mmol, 87.6%) of a yellow oil were obtained. $^1\text{H-NMR}$ (400 MHz, CDCl_3): δ = 7.30 (m, 2H), 7.22 (m, 3H), 3.78 (s, 2H), 2.67 (t, 2H, $J=5.6$ Hz), 2.56 (t, 2H, $J=5.6$ Hz), 2.49 (q, 4H, $J=7.1$ Hz), 1.94 (s, 1H), 0.99 (t, 6H, $J=7.1$ Hz) ppm; $^{13}\text{C-NMR}$ (100 MHz, CDCl_3): δ = 140.6, 128.3, 128.1, 126.8, 54.1, 52.7, 47.0, 46.9, 11.8 ppm.

Synthetic Hydroxylations

A solution of 9.4 g $[\text{Cu}(\text{CH}_3\text{CN})_4]\text{CF}_3\text{SO}_3$ in 70 mL acetone was prepared under inert conditions and a solution of 5.1 g BDED in 20 mL acetone was added at room temperature. Dioxide was passed through the mixture for 45 minutes. After one hour, 40 mL of 1 mol/L hydrochloric acid were added. The mixture was stirred for one hour and then heated to its boiling point.

Most of the acetone was removed under reduced pressure, 2 g CuCl_2 were added and the mixture was washed with CH_2Cl_2 . The combined organic phases were stirred over Na_2SO_4 and the solvent was removed under reduced pressure. The remaining oil was purified with flash chromatography over alox with CH_2Cl_2 . Pure salicylaldehyde was obtained (0.24 g, 8%).

Variation of the BDED Ligand

For the synthesis of 2-(diethylamino)ethyl(4-methoxy-phenyl)methylideneamine ($\text{X}=\text{H}$, $\text{Y}=\text{OMe}$) 1.36 g 4-methoxybenzaldehyde were dissolved in 300 mL diethyl ether. While stirring over Na_2SO_4 , 1.16 g *N,N*-diethylethylenediamine were added. After reflux for 24 hours the solvent was removed under reduced pressure and a slightly yellow oil was obtained (2.14 g, 95%). ^1H -NMR (400 MHz, CDCl_3): δ = 8.23 (s, 1H), 7.66 (d, 2H, $J=8.7$ Hz), 6.91 (d, 2H, $J=8.7$ Hz), 3.83 (s, 3H), 3.69 (t, 2H, $J=7.5$ Hz), 2.77 (t, 2H, $J=7.5$ Hz), 2.61 (q, 4H, $J=7.2$ Hz), 1.06 (t, 6H, $J=7.2$ Hz) ppm; ^{13}C -NMR (100 MHz, CDCl_3): δ = 161.5, 161.1, 129.6, 129.3, 113.9, 59.8, 55.3, 53.6, 47.6, 11.9 ppm.

2-(diethylamino)ethyl(4-nitrophenyl)methylideneamine ($\text{X}=\text{H}$, $\text{Y}=\text{NO}_2$) was synthesized by adding 1.16 g *N,N*-diethylethylenediamine to a solution of 1.51 g *p*-nitrobenzaldehyde in 300 mL diethyl ether stirred over Na_2SO_4 . After 24 hours the solvent was removed under reduced pressure and a viscous, red oil was obtained (2.07 g, 83%). ^1H -NMR (400 MHz, CDCl_3): δ = 8.39 (s, 1H), 8.26 (d, 2H, $J=8.7$ Hz), 7.90 (d, 2H, $J=8.7$ Hz), 3.79 (t, 2H, $J=6.9$ Hz), 2.81 (t, 2H, $J=6.9$ Hz), 2.61 (q, 4H, $J=7.1$ Hz) 1.05 (t, 6H, $J=7.1$ Hz) ppm; ^{13}C -NMR (100 MHz, CDCl_3): δ = 159.4, 148.9, 141.8, 128.7, 123.8, 60.1, 53.2, 47.6, 11.9 ppm.

For the synthesis of 2-(diethylamino)ethyl(4-methyl-phenyl)methylideneamine ($\text{X}=\text{H}$, $\text{Y}=\text{Me}$) 0.60 g 4-methylbenzaldehyde and 0.58 g *N,N*-diethylethylenediamine were dissolved in about 50 mL diethyl ether and stirred for one hour over Na_2SO_4 and then heated under reflux for another hour. After filtration the solvent and remaining starting material were removed under reduced pressure and a yellow oil was obtained (0.79 g, 73%). ^1H -NMR (400 MHz, CDCl_3): δ = 8.26 (s, 1H), 7.60 (m, 2H), 7.22 (m, 2H), 3.71 (t, 2H, $J=7.2$ Hz), 2.78 (t, 2H, $J=7.2$ Hz), 2.61 (q, 4H, $J=7.2$ Hz), 2.38 (s, 3H), 1.06 (t, 6H, $J=7.2$ Hz) ppm; ^{13}C -NMR (100 MHz, CDCl_3): δ = 161.7, 140.8, 133.7, 129.3, 128.0, 59.9, 53.5, 47.6, 21.5, 12.0 ppm.

2-(diethylamino)ethyl(4-chloro-phenyl)methylideneamine ($\text{X}=\text{H}$, $\text{Y}=\text{Cl}$) was prepared by adding 1.16 g *N,N*-diethylethylenediamine to a solution of 1.41 g 4-chlorobenzaldehyde in 60 mL diethyl ether. It was stirred over Na_2SO_4 for one hour and heated under reflux for one hour. The solvent and remaining starting material were removed under reduced pressure after filtration and a

slightly yellow oil was obtained (2.04 g, 86%). $^1\text{H-NMR}$ (200 MHz, CDCl_3): δ = 8.25 (s, 1H), 7.63 (m, 2H), 7.39 (m, 2H), 3.71 (t, 2H, $J=7.2$ Hz), 2.78 (t, 2H, $J=7.2$ Hz), 2.59 (q, 4H, $J=7.2$ Hz) 1.05 (t, 6H, $J=7.2$ Hz) ppm; $^{13}\text{C-NMR}$ (50 MHz, CDCl_3): δ = 160.3, 136.4, 134.7, 129.2, 128.8, 59.9, 53.4, 47.6, 11.9 ppm.

For the synthesis of 2-(diethylamino)ethyl(3-nitrophenyl)methylideneamine ($\text{X}=\text{NO}_2$, $\text{Y}=\text{H}$) 7.56 g *m*-nitrobenzaldehyde were dissolved in 150 mL diethyl ether and 5.81 g *N,N*-diethylethyldiamine were added. It was stirred over Na_2SO_4 and heated under reflux for 16 hours. The mixture was filtrated and the solvent was removed under reduced pressure, a yellow oil was obtained (12.02 g, 96%). $^1\text{H-NMR}$ (400 MHz, CDCl_3): δ = 8.56 (s, 1H), 8.37 (s, 1H), 8.24 (d, 1H, $J=7.9$ Hz), 8.07 (d, 1H, $J=7.9$ Hz), 7.59 (t, 1H, $J=7.9$ Hz), 3.77 (t, 2H, $J=7.0$ Hz), 2.81 (t, 2H, $J=7.0$ Hz), 2.62 (q, 4H, $J=7.1$ Hz), 1.05 (t, 6H, $J=7.1$ Hz) ppm; $^{13}\text{C-NMR}$ (100 MHz, CDCl_3): δ = 159.0, 148.5, 138.0, 133.5, 129.5, 124.8, 122.5, 59.8, 53.3, 47.6, 12.0 ppm.

2-(diethylamino)ethyl(3-methyl-phenyl)methylideneamine ($\text{X}=\text{Me}$, $\text{Y}=\text{H}$) was synthesized by adding 0.59 g *N,N*-diethylethyldiamine to a solution of 0.60 g 3-methylbenzaldehyde in 50 mL diethyl ether. It was stirred for one hour over Na_2SO_4 and heated under reflux for another hour. After filtration and removing the solvent under reduced pressure, a slightly yellow oil was obtained (1.00 g, 92%). $^1\text{H-NMR}$ (400 MHz, CDCl_3): δ = 8.28 (s, 1H), 7.46 (m, 2H), 7.23 (m, 2H), 3.72 (t, 2H, $J=7.2$ Hz), 2.78 (t, 2H, $J=7.2$ Hz), 2.61 (q, 4H, $J=7.2$ Hz), 2.38 (s, 3H), 1.06 (t, 6H, $J=7.2$ Hz) ppm; $^{13}\text{C-NMR}$ (100 MHz, CDCl_3): δ = 162.0, 138.3, 136.3, 131.4, 128.9, 128.5, 125.6, 59.9, 53.6, 47.6, 21.3, 12.0 ppm.

N'-Benzylidene-*N,N*-dimethyl-ethylendiamine ($\text{R}=\text{Me}$) was prepared by dissolving 5.31 g benzaldehyde and 4.41 g *N,N*-dimethylethyldiamine in 200 mL diethyl ether. The reaction mixture was stirred over Na_2SO_4 for one hour and heated under reflux for one hour. It was filtrated, the solvent was removed under reduced pressure and a slightly yellow oil was obtained (7.87 g, 89%). $^1\text{H-NMR}$ (400 MHz, CDCl_3): δ = 8.31 (s, 1H), 7.73 (m, 2H), 7.40 (m, 3H), 3.75 (t, 2H, $J=7.1$ Hz), 2.66 (t, 2H, $J=7.1$ Hz), 2.32 (s, 6H) ppm; $^{13}\text{C-NMR}$ (100 MHz, CDCl_3): δ = 161.8, 136.2, 130.6, 128.5, 128.1, 60.1, 59.9, 45.9 ppm.

Aromatic Hydroxylation with BDED Variations

For each of the modified BDED-ligands 2-(diethylamino)ethyl(4-methoxyphenyl)methylideneamine, 2-(diethylamino)ethyl(4-nitrophenyl)methylideneamine and 2-(diethylamino)ethyl(3-nitrophenyl)methylideneamine 5 mmol were dissolved in 10 mL acetone under inert conditions. 8.3 mL of 0.6 mol/L $[\text{Cu}(\text{CH}_3\text{CN})_4]\text{CF}_3\text{SO}_3$ solution in acetone was added and dioxygen was

passed through the solution for 30 minutes. For the other derivatives 2-(diethylamino)ethyl(4-methyl-phenyl)methylideneamine, 2-(diethylamino)-ethyl(4-chloro-phenyl)methylideneamine and 2-(diethylamino)ethyl(3-methyl-phenyl)methylideneamine, 1 mmol was dissolved in 10 mL of dry acetone and a solution of 377 mg $[\text{Cu}(\text{CH}_3\text{CN})_4]\text{CF}_3\text{SO}_3$ (1 mmol) in 10 mL dry acetone was added. Dioxygen was also passed through these complex solutions. For *N'*-benzylidene-*N,N*-dimethyl-ethylendiamine 1.76 g (10 mmol) ligand and 3.76 g $[\text{Cu}(\text{CH}_3\text{CN})_4]\text{CF}_3\text{SO}_3$ (10 mmol) in 40 mL dry acetone were used in similar way. The mixture was left overnight in the refrigerator. 20 mL 1 mol/L hydrochloric acid were added and the solution was heated up to 70 °C for 30 minutes. Most of the acetone was removed under reduced pressure and the remaining solution was washed with CH_2Cl_2 several times. The combined organic phases were dried over Na_2SO_4 , the solvent was removed and a "pre"-purification was done over silica. The remaining oil was analyzed using GC/MS.

2.1.5 Acknowledgements

Pascal Specht is acknowledged for his assistance with some of the experiments performed during his Bachelor research project (JLU, Gießen). P. G. gratefully acknowledges a PhD grant provided by the Beilstein-Institut, Frankfurt am Main (Germany) within the research collaboration NanoBiC. Quantum-chemical calculations have been performed at the Center for Scientific Computing (CSC) Frankfurt on the Fuchs and LOEWE-CSC high-performance computer clusters.

2.2 Selected Supporting Information and Unpublished Results

2.2.1 Crystallization of Copper(I) Complexes

The ORTEP plots of the molecular structures of the cations of $[\text{Cu}^{\text{I}}(\text{BDED})_2]\text{SbF}_6$ and $[\text{Cu}^{\text{I}}(\text{m-Me-BDED})_2]\text{CF}_3\text{SO}_3$ are shown in Figure 2.13 and 2.14. Both structures exhibit typical distorted tetrahedral coordination of copper(I) by the two ligands. One of the ligands of the structure of $[\text{Cu}^{\text{I}}(\text{m-Me-BDED})_2]\text{CF}_3\text{SO}_3$ is disordered at the methyl position and also the anion is completely disordered. In the intramolecular hydroxylation process the two possible methyl positions lead to two different products.

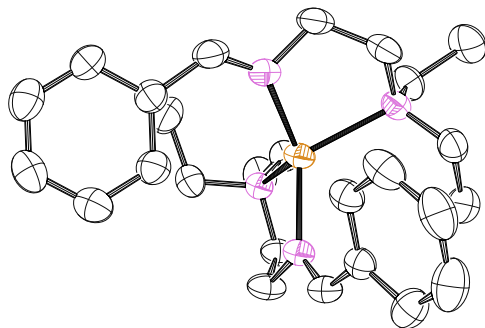


Figure 2.13: ORTEP plot of the molecular structure of [Cu(BDED)₂]⁺. Anion and hydrogen atoms are omitted for clarity, ellipsoids are drawn at 50% probability.

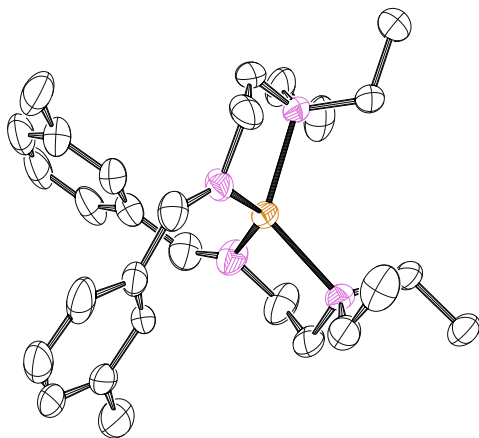


Figure 2.14: ORTEP plot of the molecular structure of [Cu(m-Me-BDED)₂]⁺. Anion and hydrogen atoms are omitted for clarity, ellipsoids are drawn at 50% probability.

Experimental Details

The X-ray crystallographic data of $[\text{Cu}(\text{BDED})_2]\text{SbF}_6$ were collected using a BRUKER/ NONIUS KappaCCD detector with a BRUKER/NONIUS FR591 rotating anode radiation source and an OXFORD CRYOSYSTEMS 600 low temperature system. Mo- K_α radiation with wavelength 0.71073 Å and a graphite monochromator were used. The PLATON [131] MULABS semi-empirical absorption correction using multiple scanned reflection was applied on the data and the structure was solved by direct methods using SHELXS97 and refined with SHELXL2014/6 [129]. All non-hydrogen atoms were refined anisotropically and hydrogen atoms were positioned geometrically. For data collection of $[\text{Cu}(\text{m-Me-BDED})_2]\text{CF}_3\text{SO}_3$ a BRUKER D8 Venture system with dual $\text{I}\mu\text{S}$ microfocus sources, a PHOTON100 detector and an OXFORD CRYOSYSTEMS 700 low temperature system was used. Data collection was performed using Mo- K_α radiation with wavelength 0.71073 Å and a collimating Quazar multilayer mirror. Semi-empirical absorption correction from equivalents was applied using SADABS-2014/4 and the structure was solved by intrinsic phasing using SHELXT2014 [130]. Refinement was performed against F^2 using SHELXL-2014/7 [129]. All non-hydrogen atoms were refined anisotropically and hydrogen atoms were positioned geometrically. Crystallographic data for the structures have been deposited with the Cambridge Crystallographic Data Centre as CCDC No. 1047584 and 1047582.

$[\text{Cu}^{\text{I}}(\text{m-Me-BDED})_2]\text{CF}_3\text{SO}_3$

87 mg (0.2 mmol) 2-(diethylamino)ethyl(3-methyl)methylideneamine and 38 mg (0.1 mmol) $[\text{Cu}(\text{CH}_3\text{CN})_4]\text{CF}_3\text{SO}_3$ were dissolved in 2 mL dry acetone in a glove box under argon atmosphere. Orange crystals were obtained by slow ether diffusion over four weeks at -40 °C.

$[\text{Cu}^{\text{I}}(\text{BDED})_2]\text{SbF}_6$

41 mg (0.2 mmol) BDED and 93 mg $[\text{Cu}(\text{CH}_3\text{CN})_4]\text{SbF}_6$ (0.2 mmol) were dissolved in 1 mL dry THF under inert conditions. Orange crystals were obtained with ether diffusion at -40 °C over one week.

2.2.2 Crystallization of $[\text{Cu}(\text{H}_2\text{BDED})\text{Cl}_2]$

Figure 2.15 shows the molecular structure of $[\text{Cu}(\text{H}_2\text{BDED})\text{Cl}_2]$.

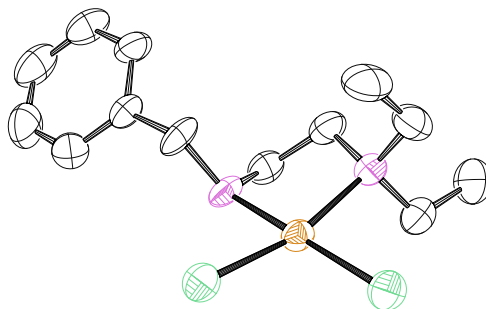


Figure 2.15: Molecular Structure (ORTEP plot, ellipsoids are drawn at 50% probability) of $[\text{Cu}(\text{H}_2\text{BDED})\text{Cl}_2]$.

Experimental Details

The X-ray crystallographic data for $[\text{Cu}(\text{H}_2\text{BDED})\text{Cl}_2]$ was collected using a STOE IPDS diffractometer using Mo-K_α radiation with wavelength 0.71073 Å and a graphite monochromator. No absorption corrections were applied. The structure was solved by intrinsic phasing using SHELXT2014 [130] and refined with SHELXL2014/6 [129]. All non-hydrogen atoms were refined anisotropically and hydrogen atoms were positioned geometrically. Crystallographic data for the structure have been deposited with the Cambridge Crystallographic Data Centre as CCDC No. 1047585.

$[\text{Cu}^{\text{II}}(\text{H}_2\text{BDED})\text{Cl}_2]$

0.83 g copper(II) chloride was dried with heating under vacuum and dissolved in a few mL acetone. 1.00 g H_2BDED were added dropwise and the complex solution was divided in several samples and crystallized at -30°C . Green crystals were obtained.

2.2.3 Formation of $[\text{Cu}_2(\text{BDED})(\mu\text{-OH})(\mu\text{-}o\text{-O-BDED})]^{2+}$

For reasons of comparison to the formation of the bis(μ -oxido) adduct, the final hydroxylation product was analyzed also by UV-vis spectroscopy. Figure 2.16 shows the absorbance of the $[\text{CuBDED}]^+$ complex before and after the addition of molecular dioxygen. The analogous to PPN proposed complex $[\text{Cu}_2(\text{BDED})(\mu\text{-OH})(\mu\text{-}o\text{-O-BDED})]^{2+}$ after hydroxylation exhibits a strong

absorbance with $\lambda_{\text{max}} = 360 \text{ nm}$ which is typically for similar phenolate complexes (e.g. [151]).

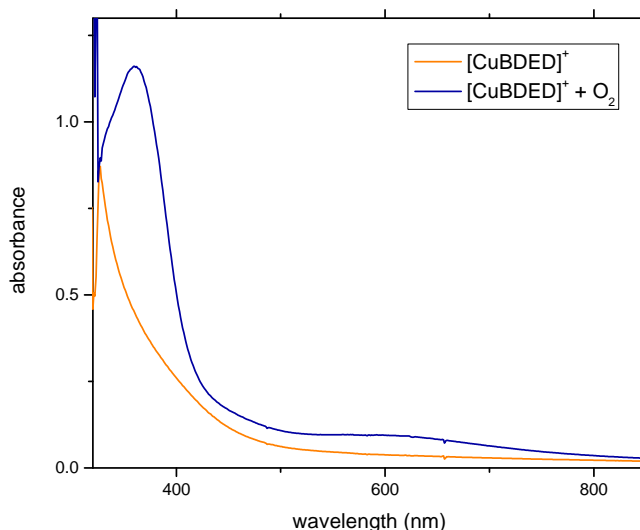


Figure 2.16: UV/vis of $[\text{CuBDED}]^+$ complex without and with O_2 ($\lambda_{\text{max}} = 360 \text{ nm}$, 0.5 mmol/L , acetone)

Experimental Details

37.6 mg (0.1 mmol) $[\text{Cu}(\text{CH}_3\text{CN})_4]\text{CF}_3\text{SO}_3$ and 20.4 mg BDED (0.1 mmol) were dissolved in 100 mL dry acetone in a glove box. For a 0.5 mmol/L complex solution 10 mL were diluted with 10 mL dry acetone. The oxygen free complex was analyzed by UV-vis using a Schlenk cuvette. Dry dioxygen was passed through the solution for 5 minutes and UV-vis spectra were recorded.

2.2.4 Additional Experiments for Characterization

For possible detection of reaction intermediates a low temperature IR measurement was performed. A 5% solution of the $[\text{CuBDED}]^+$ complex with

triflate anion in CH_2Cl_2 was mixed with molecular oxygen at -65°C . The solution was analyzed using a low temperature IR add-on device with potassium chloride windows. The recorded spectra are shown in Figure 2.17. No significant change can be observed, in accordance with the stopped-flow measurements showing the only very short life time of the oxygen adduct intermediate. Additionally the absorption of the windows and the solvent limit the detection range.

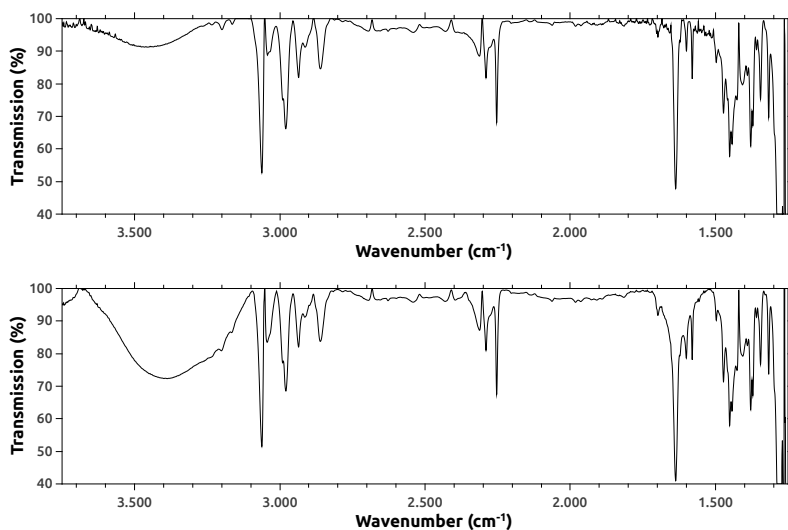


Figure 2.17: IR of $[\text{CuBDED}]\text{CF}_3\text{SO}_3$ complex solution in CH_2Cl_2 (5%) without (top) and with O_2 (bottom)

$[\text{CuBDED}]\text{CF}_3\text{SO}_3$ Complex Solution

For a $\sim 5\%$ complex solution 1.2 g BDED (6 mmol) and 2.6 g $[\text{Cu}(\text{CH}_3\text{CN})_4]\text{CF}_3\text{SO}_3$ (6 mmol) were dissolved in 50 mL CH_2Cl_2 . An ethanol/liquid nitrogen cooling bath was used for cooling the solution while analysis took place. IR (film): 2670-310 $\nu(\text{OH})$ (condensed water); 3090-3020 $\nu(\text{Ar-H})$; 3010-2850 $\nu(\text{C-H})$, $\nu(\text{CH}_2)$ and $\nu(\text{CH}_3)$; 2250 $\nu(\text{C}\equiv\text{N})$ (acetonitrile); 1635 $\nu(\text{C}=\text{N})$; 1600-1475 aromatic $\nu(\text{C}=\text{C})$; 1450 $\delta_s(\text{CH}_2)$; 1443 $\delta_{\text{as}}(\text{CH}_3)$; 1378 $\delta_s(\text{CH}_3)$ cm^{-1} .

2.2.5 Additional Variation of the Reactions with BDED

In addition to the ligand variations of BDED discussed above, the ligand 2-(diethylamino)ethyl(4-hydroxy-phenyl)methylideneamine ($X=H$, $Y=OH$) was synthesized. Contrary to the activating effect of the OH group in theory no aromatic hydroxylation occurred. This could be caused by different coordination of copper with this ligand or by side reactions caused by the protic ligand system.

Because acetone was not suitable for all analytical methods and further experiments, the hydroxylation of the ligand BDED was also tested in CH_2Cl_2 . No differences in the reaction behavior and yield could be observed. Regarding the similarity of the BDED ligand system with the work of Schönecker et al. [89]-[92] their approach for yields higher than 50% was tested for BDED. Starting with a copper(II) complex they reduced it with benzoin in the presence of triethylamine for oxidation of both ligands with molecular oxygen. As experiments have shown that BDED copper(II) complexes tend to decompose, the reaction was started as copper(I) complex and reacted in solution with benzoin and triethylamine with molecular oxygen. In contrast to the work of Schönecker et al. no hydroxylation was found at all.

Because of the great success with the activation of molecular oxygen, the activation of the next element in the chalcogens was tried. Using solid sulfur led to no detectable formation of any C–S bonds at the ligand. As there are already examples mentioned above for the sensitivity of the reaction towards small changes this is no surprise.

2-(diethylamino)ethyl(4-hydroxy-phenyl)methylideneamine

For the synthesis of 2-(diethylamino)ethyl(4-hydroxy-phenyl)methylideneamine ($X=H$, $Y=OH$) 2.44 g 4-hydroxybenzaldehyde (20 mmol) were dissolved in 200 mL methanol. While stirring over Na_2SO_4 , 2.32 g *N,N*-diethylethylendiamine (20 mmol) were added. After reflux for 4 hours the solvent was removed under reduced pressure and a red-brown oil was obtained (4.1 g, 93%). 1H -NMR (400 MHz, $CDCl_3$): δ = 8.14 (s, 1H), 7.50 (d, 2H, $J=8.6$ Hz), 6.74 (d, 2H, $J=8.6$ Hz), 3.70 (t, 2H, $J=7.3$ Hz), 2.81 (t, 2H, $J=7.2$ Hz), 2.66 (q, 4H, $J=7.1$ Hz), 1.06 (t, 6H, $J=7.1$ Hz) ppm; ^{13}C -NMR (100 MHz, $CDCl_3$): δ = 162.9, 160.7, 130.2, 126.7, 116.2, 58.2, 53.0, 47.0, 11.0 ppm.

Attempt for Synthetic Hydroxylation of

2-(diethylamino)ethyl(4-hydroxy-phenyl)methylideneamine

5 mmol 2-(diethylamino)ethyl(4-hydroxy-phenyl)methylideneamine were dissolved in 10 mL acetone under inert conditions. 8.3 mL of 0.6 mol/L tetrakis acetonitrile copper(I) triflate solution in acetone was added and dioxygen was

2 Selective Aromatic Hydroxylation

passed through the solution for 30 minutes. The mixture was left overnight in the refrigerator. 15 mL 1 mol/L hydrochloric acid were added and the solution was heated up to 70 °C for 30 minutes. Most of the acetone was removed under reduced pressure and the remaining solution was washed with CH_2Cl_2 several times. The combined organic phases were dried over Na_2SO_4 , the solvent was removed and a "pre"-purification was done over silica. The remaining oil was analyzed using GC/MS leading to no detectable amount of the desired product.

Hydroxylation of BDED in CH_2Cl_2

A solution of 376 mg $[\text{Cu}(\text{CH}_3\text{CN})_4]\text{CF}_3\text{SO}_3$ (1 mmol) and 204 mg BDED (1 mmol) in 40 mL CH_2Cl_2 was prepared under inert conditions. Dioxygen was passed through the mixture for 30 minutes at room temperature. After 16 hours 10 mL of 1 mol/L hydrochloric acid was added. The mixture was stirred for one hour and then heated to its boiling point. The mixture was washed with CH_2Cl_2 . The combined organic phases were stirred over Na_2SO_4 and the solvent was removed under reduced pressure. The remaining oil was pre-purified over silica and analyzed using GC/MS indicating a yield of about 40-45 %.

Reduction with Benzoin

Under inert conditions 204 mg BDED (2 mmol) and 753 mg $[\text{Cu}(\text{CH}_3\text{CN})_4]\text{CF}_3\text{SO}_3$ (2 mmol) were dissolved in 20 mL CH_2Cl_2 . A solution of 850 mg benzoin (4 mmol) and 405 mg triethylamine (4 mmol) in 10 mL CH_2Cl_2 was added. Dry oxygen was passed through the solution for 30 minutes and the reaction mixture was stirred under the oxygen atmosphere for one day. 20 mL hydrochloric acid (1 mol/L) was added and the mixture was heated under reflux for one hour. It was washed with CH_2Cl_2 two times and the combined organic layers were dried over Na_2SO_4 . After evaporation of the solvent, the remaining oil was analyzed using GC/MS leading to no yield of the desired product.

Attempted Activation of Sulfur

A $[\text{CuBDED}]\text{CF}_3\text{SO}_3$ complex solution was prepared by mixing 1.88 g $[\text{Cu}(\text{CH}_3\text{CN})_4]\text{CF}_3\text{SO}_3$ (5 mmol) with 1.02 g BDED (0.5 mmol) in 40 mL acetone. The solution was stirred over sulfur under inert conditions for 16 hours. The solvent was removed under reduced pressure, 15 mL hydrochloric acid (1 mol/L) and 20 mL CH_2Cl_2 were added. The mixture was stirred for one hour and heated under reflux for another. It was washed three times with CH_2Cl_2 , the combined organic layers were dried over Na_2SO_4 and the solvent

2.2 Selected Supporting Information and Unpublished Results

was partly removed under reduced pressure. The remaining solution was analyzed using GC/MS. No 2-mercapto benzaldehyde could be detected.

3 Selective Aliphatic Hydroxylation

The results described and discussed in this chapter are in preparation for submission as publication. The work on the adamantane- and diamantane-compounds was done in cooperation with Andrey A. Fokin and coworkers. Selected parts of the supporting information and results that are not yet going to be published are also presented. Further spectroscopic, crystallographic and other supporting data can be found in chapter 4.2.

3.1 Selective Aliphatic Hydroxylation with Dioxygen Using a Simple Copper Imine Complex System

3.1.1 Introduction

Selective oxidations are important in organic chemistry. Replacing toxic and often nonselective oxidants such as Cr(VI) compounds or OsO₄ with dioxygen/air would be highly desirable [152]-[155]. In nature metalloenzymes clearly demonstrate that this is possible [156]. Thus an enzyme such as tyrosinase, a copper based monooxygenase, is capable to selectively catalyze an *o*-hydroxylation of an aromatic system [95],[107],[157]. In regard to this a large number of low molecular weight copper complexes have been developed in an effort to model the function of this enzyme [158]. More recently the importance of finding new ways for selective *o*-hydroxylation has been documented in the literature. Following up on earlier work by the groups of Réglér [87] and Schönecker [89]-[92] we recently demonstrated that by using a very simple copper imine complex system facile stoichiometric *o*-hydroxylation reactions of aromatic aldehydes in good yields could be performed (Figure 3.1; due to the formation of a dinuclear complex only half of the aldehyde can be hydroxylated, leading to a maximum yield of 50 %) [118].

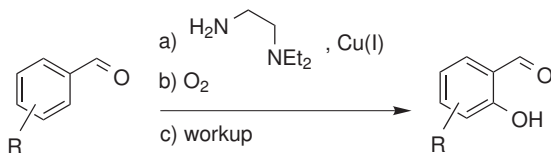


Figure 3.1: Selective *o*-hydroxylation using a simple Cu(I) complex and O₂.

To test the synthetic application further we became interested in aliphatic hydroxylation reactions. Methane monooxygenase (iron or copper based) is capable to oxidize methane to methanol with air under ambient conditions [50],[52],[159],[160]. While not applicable directly for our system we chose different aliphatic aldehydes to test the synthetic potential of our system. Here we describe our results on selective hydroxylation reaction of trimethyl-acetaldehyde, cyclohexanecarbaldehyde, adamantane-1-carbaldehyde and diamantane-1-carbaldehyde.

3.1.2 Results and Discussion

As a simple system to start with we chose the ligand based on trimethylacetaldehyde as a basic model for the intramolecular aliphatic ligand hydroxylation analogous to our previous work with aromatic systems described above. The imine ligand (DPDen, Figure 3.2) was obtained in a facile synthesis as a slightly yellow oil and no additional purification was necessary. The according copper(I) complex was prepared in situ simply by mixing a copper(I) salt with the ligand in a 1:1 stoichiometric ratio in dry acetone. Passing dioxygen through the solution led to hydroxylation of one ligand molecule in the dinuclear copper complex according to the reaction mechanism shown in Scheme 1. The near completeness of the hydroxylation reaction was confirmed after workup of the complex leading to about a 50 % yield of 3-hydroxy-2,2-dimethyl-propionaldehyde. However, separation of the product from the starting material on a synthetic scale turned out to be difficult.

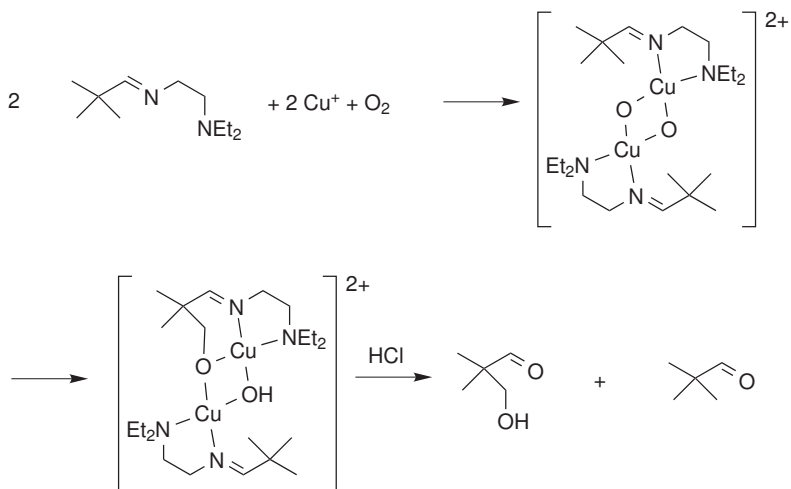


Figure 3.2: Oxidation of the [Cu^IDPDen]⁺ complex with dioxygen.

While performing the analytics on the product we obtained from one sample (8 mg in CHCl₃) left on the bench for several months in a NMR tube crystals that turned out to be 3-hydroxy-2,2-dimethyl-propionic acid. The molecular structure of this acid is presented in Figure 3.3 (crystallographic data are reported in the Supporting Information).

The molecular structure of the acid was the final proof that oxidation had

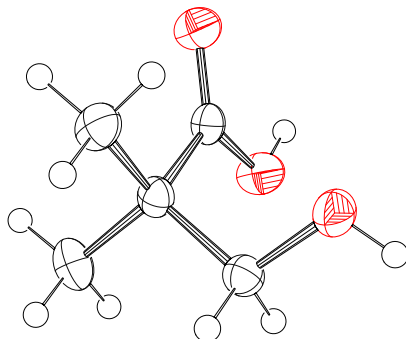


Figure 3.3: ORTEP plot of the molecular structure of 3-hydroxy-2,2-dimethylpropionic acid; ellipsoids are drawn at 50 % probability.

occurred and that the imine copper system was capable of ligand hydroxylation not only for aromatic ligands but for aliphatic aldehydes as well. That the carboxylic acid was obtained is a consequence that the aldehyde can be relatively easily oxidized over time to the corresponding acid after it had been separated from the reaction mixture.

From our previous mechanistic study on the ligand hydroxylation with the copper-BDED complex (chapter 2, [161]) we expected here as well the occurrence of a bis(μ -oxido) compound as a reactive intermediate. To confirm this, low temperature stopped-flow measurements were performed on the oxidation/hydroxylation reaction of the in-situ generated copper(I) complex of DPDen. So far efforts to prepare and structurally characterize the copper(I) complex failed, however as described previously, it is not really necessary to isolate this complex prior to the reaction. Time resolved UV-vis spectra of the reaction of the copper(I) complex with dioxygen in acetone obtained at -90.4°C are shown in Figure 3.4.

The optical feature evolving at $\lambda_{\text{max}} = 405\text{ nm}$ again is consistent with the formation of a bis(μ -oxido) complex [36]. The reaction is quite fast and about the same rate compared with previously reported aromatic hydroxylations. The absorbance over reaction time could be fitted perfectly well with one exponential function, which indicates a first order reaction in complex concentration with dioxygen in excess. Thus, as for the copper-BDED system reported previously, the formation of a 1:1 Cu:O₂ intermediate, a superoxido

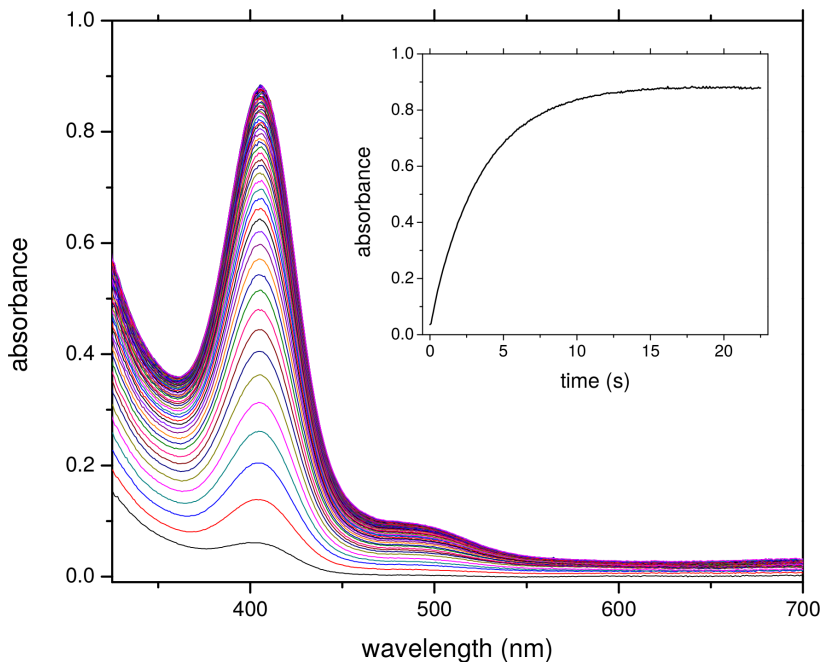


Figure 3.4: Time resolved UV-vis spectra of the reaction of $[\text{Cu}(\text{DPDen})]\text{CF}_3\text{SO}_3$ (2×10^{-4} mol/L) with dioxygen (5.1×10^{-3} mol/L) in acetone at -90.4°C over 22.5 s. The inset shows increase of absorbance at 405 nm over time.

complex must be the overall rate-determine step. Using excess of dioxygen leads to the simplified rate law $v = k_{\text{obs}} \times c([\text{CuDPDen}]^+)$ with $k_{\text{obs}} = k \times [\text{O}_2]$. It was possible to repeat the measurement several times in the temperature range -63.6 to -80.9°C . The obtained k_{obs} values were plotted as $\ln(k_{\text{obs}}T^{-1})$ (Figure 3.5) against T^{-1} according to the linearized form of the Eyring-Polanyi equation (3.1):

$$\ln \frac{k}{T} = \frac{-\Delta H^\ddagger}{R} \cdot \frac{1}{T} + \ln \frac{k_B}{h} + \frac{\Delta S^\ddagger}{R} \quad (3.1)$$

The activation enthalpy calculated from the slope of the linear fit shown in Figure 3.5 is $\Delta H^\ddagger = 20 \text{ kJ/mol}$ while the activation entropy calculated from the intercept is about 30 J/molK . Considering the extrapolation done here,

the activation entropy is near to 0 J/molK. This could indicate a possible interchange mechanism of dioxygen with previous coordinated solvent.

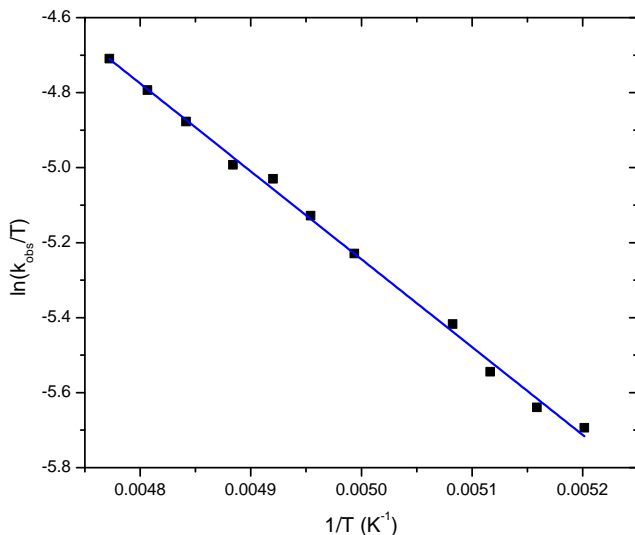


Figure 3.5: Plot $\ln(k_{\text{obs}}/T)$ versus $1/T$ according to the Eyring-Polanyi equation for k_{obs} in the temperature range -80.9 to -63.6 °C for the formation of the bis(μ -oxido) complex with linear fit (slope = -2342.5, intercept = 6.5).

This fits very well to known activation enthalpies for the formation of a bis(μ -oxido) complex of pseudo-second order from literature: $\Delta H^\ddagger = 25$ kJ/mol for a bidentate ligand system [76] and $\Delta H^\ddagger = 44$ kJ/mol for a tridentate ligand system [162].

Using the low temperature "stopped-flow" technique it was also possible to analyze the decay of the bis(μ -oxido) complex as a first-order reaction. Varying the temperature between -89.0 and -35.0 °C gave rate constants k for the decay. Figure 3.6 shows the plot of $\ln(k/T)$ versus $1/T$ according to the Eyring-Polanyi equation for these rate constants.

There is an obvious linear connection; however, the data is separated in

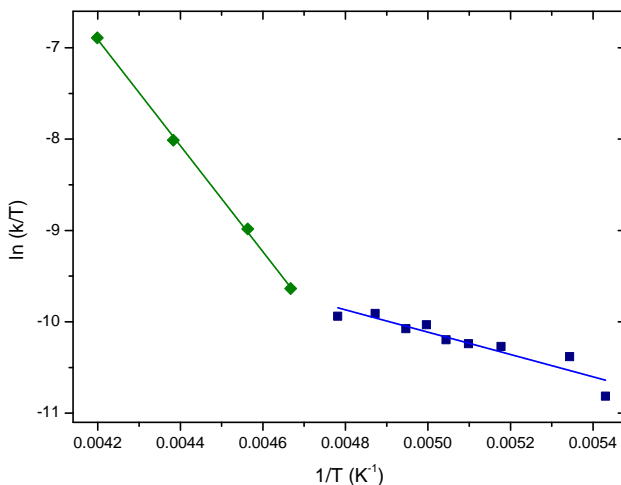


Figure 3.6: Plot $\ln(k_{\text{obs}}/T)$ versus $1/T$ according to the Eyring-Polanyi equation for k in the temperature range -89.0 to -35.0 °C for the decay of the bis(μ -oxido) complex with linear fits.

two parts with different fits. There seems to be a transition from one mechanism to another one at about -63 °C. For the temperature range -89 to -63 °C the activation enthalpy fitted is $\Delta H^\ddagger = 10$ kJ/mol, the activation entropy is $\Delta S^\ddagger = -60$ J/molK and for the temperature range -63 to -35 °C it is $\Delta H^\ddagger = 50$ kJ/mol and $\Delta S^\ddagger = 120$ J/molK for the activation entropy. Whilst the activation entropy at the lower temperature could indicate an interchange or associative mechanism, it probably indicates a dissociative mechanism at the higher temperature range. Thus the observed activation at lower temperature could be the intramolecular hydroxylation and at higher temperatures a complex dissociation step.

In direct comparison to previous work with benzaldehyde, we used cyclohexanecarbaldehyde for ligand synthesis and hydroxylation. The synthesized ligand *N'*-cyclohexylmethylene-*N,N*-diethyl-ethane-1,2-diamine has also the feature of an hydrogen atom at the α -position which allows further insight into the reactivity in comparison to DPDen (Figure 3.7).

In accordance with the reactivity of the ligand DPDen and also the previous

3.1 Selective Aliphatic Hydroxylation with Dioxygen and Copper Complexes

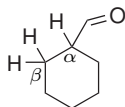


Figure 3.7: α and β positions for the hydroxylation of cyclohexanecarbaldehyde.

work regarding aromatic hydroxylation, we found only the β -position hydroxylated (Figure 3.8); however, only a hydroxylation yield of about 15% could be observed using GC/MS. Further optimization of the reaction is needed here.

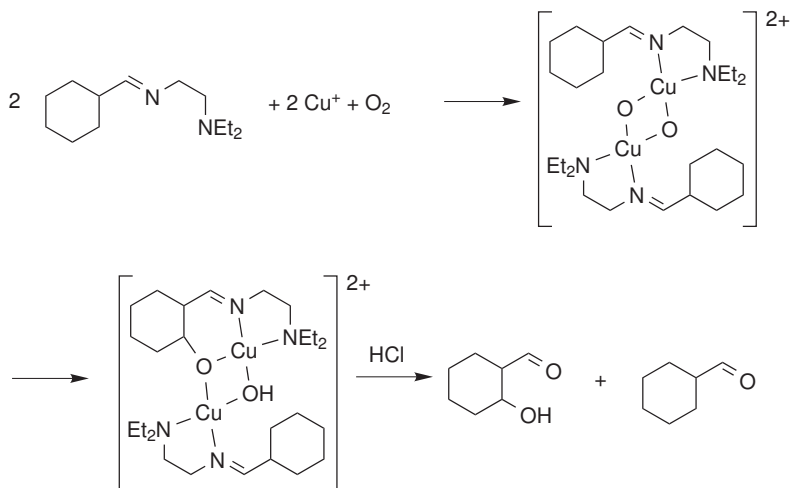


Figure 3.8: Oxidation of the copper(I) complex of *N'*-cyclohexylmethylenedipropylamine with dioxygen.

To test if our simple system would also be able to hydroxylate a carbon atom that is much less accessible to oxidation we decided to test an adamantane derivative, adamantane-1-carbaldehyde [163]. However, it turned out to be a bit of a synthetic challenge to prepare this compound. The synthetic route according to literature is displayed in Figure 3.9 and was performed by Prof. A. Fokin and coworkers in a cooperation.

Starting from adamantane itself the carboxylic acid was prepared according

3 Selective Aliphatic Hydroxylation

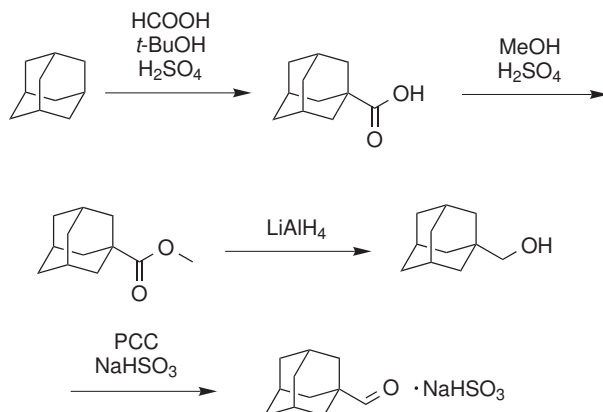


Figure 3.9: Synthetic route for adamantane-1-carbaldehyde.

to a literature procedure reported earlier [164]. A crystal structure of this compound has been described previously [165]. From the acid the methyl ester was prepared and crystallization from CH_2Cl_2 allowed to obtain crystals of adamantane-1-carboxylic acid methylester. The molecular structure of this compound is shown in Figure 3.10 (crystallographic data are reported in the Supporting Information).

Reduction of the ester with LiAlH_4 led to the formation of the according alcohol 1-hydroxymethyladamantane. Again it was possible to crystallize this compound and its molecular structure is shown in Figure 3.11.

Oxidation of the alcohol with PCC led to the final product, adamantane-1-carbaldehyde. However, it turned out that this aldehyde unfortunately is extremely unstable towards oxidation back to the carboxylic acid. Thus it had to be obtained as a hydrogensulfite adduct and was liberated using hydrochloric acid immediately prior to further use. The free aldehyde was characterized by NMR; however the decay to the carboxylic acid was so fast that it could already be observed in the short measurement period. Therefore, it was rather difficult to perform the imine reaction in time, to add the copper(I) salt and to oxidize the according copper(I) complex. Still it was possible, after several attempts, to perform the oxidation in the planned way. Workup of the product solution in the same way as discussed above for the ligand derived from trimethylacetaldehyde the hydroxylated adamantane-1-carbaldehyde was obtained again in a high yield close to the expected 50 % yield. The compound could be fully characterized by NMR analysis. Efforts

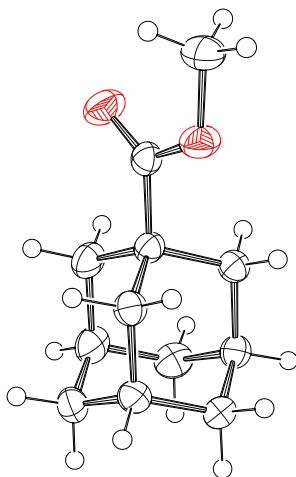


Figure 3.10: ORTEP plot of the molecular structure of adamantane-1-carboxylic acid methylester; ellipsoids are drawn at 50 % probability.

to obtain crystals of the hydroxylated product or the starting material were not successful. Furthermore, as with the starting material fast oxidation of the hydroxylated aldehyde to the according carboxylic acid was observed. However, again it was not possible to crystallize the hydroxylated carboxylic acid. Therefore, for further clarification we decided to stabilize the unstable hydroxylated aldehyde with pentafluorophenylhydrazine and we were able to isolate crystals of pentafluorophenylhydrazin-1-ylidenemethyladamantan-2-ol. The molecular structure of this compound is presented in Figure 3.12.

The crystal structure together with the NMR data clearly demonstrates that the adamantane-1-carbaldehyde is selectively hydroxylated in the bridging position. By choosing adamantane-1-carbaldehyde as starting material for our ligand synthesis, we introduced a very specific probe for selectivity. Because of the extreme instability of the compound itself a synthetic application is unlikely, but the differences in reactivity of the secondary and tertiary carbons are extreme. Oxidations with adamantane so far showed high selectivity for the reactive tertiary position or oxidations of both positions. Assuming a

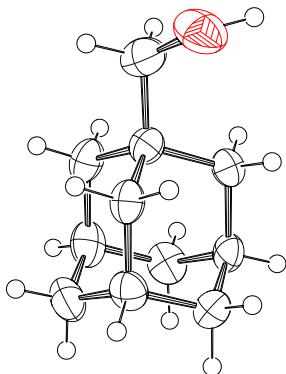


Figure 3.11: ORTEP plot of the molecular structure of 1-hydroxymethyladamantane; ellipsoids are drawn at 50 % probability.

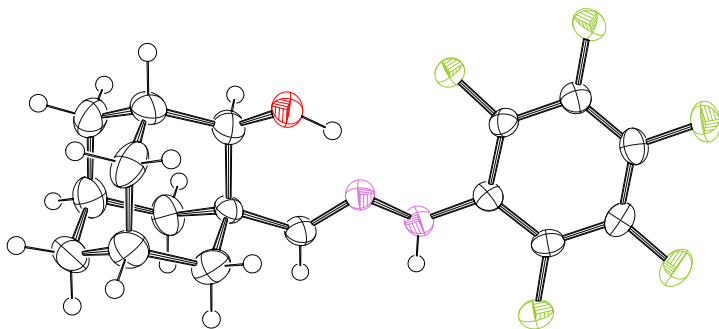


Figure 3.12: ORTEP plot of the molecular structure of pentafluorophenylhydrazin-1-ylidenemethyladamantan-2-ol; ellipsoids are drawn at 50 % probability.

radical intermediate, the tertiary position should be favored. The observed unlikely oxidation of the secondary carbon can be explained by a concerted mechanism, described for example by Spuhler et al. [77].

Whilst adamantane aldehyde is perfect as mechanistic “sensor”, we wanted to show the usage of this method for synthesis and thus switched to diamantane-1-carbaldehyde as substrate. Diamantane-1-carbaldehyde was prepared according to the following scheme:

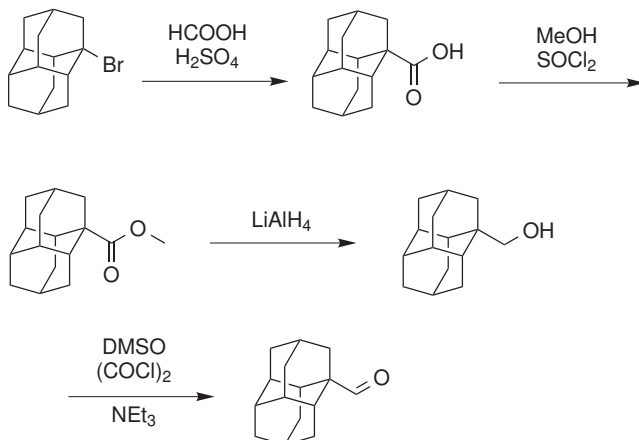


Figure 3.13: Synthetic route for diadamantane-1-carbaldehyde.

Diamantane-1-carbaldehyde, in contrast to adamantane-1-carbaldehyde, is a quite stable substrate. With this advantage synthetic hydroxylation with the described method was straight forward and again gave yields near the maximum of 50%. Separation of starting material and product was done by column chromatography and the remaining starting material could be reused. Unfortunately so far it was not possible to structurally characterize the product, however it could be easily identified by NMR analysis.

3.1.3 Conclusions

The results in this chapter presented demonstrate that following to previous work regarding aromatic hydroxylation the aliphatic hydroxylation occurs by very similar kinetics and reactivity. The synthetically easy accessible ligand DPDen has proven to be an ideal model for the aliphatic hydroxylation. Activation at a primary carbon is also very close to modeling pMMO like

reactivity. The kinetic activation parameters obtained for formation and decay of the bis(μ -oxido) complex contribute to a better understanding of the activation and the hydroxylation mechanism. These rapid processes could be analyzed with "stopped-flow" techniques at low temperatures, which has proven to be an efficient method here. Further understanding of the hydroxylation of aliphatic hydrocarbons was gained by the selective hydroxylation of adamantane. With the reported reactivity it is extremely unlikely that it occurs by radical mechanism and indicates the existence of a non radical hydroxylation mechanism of hydrocarbons. The presented synthetic applications are good examples for the variety of the possible substrates. The selectivity and ability for the activation of hard to activating C–H bonds offer opportunities for many synthetic applications.

3.1.4 Experimental Section

Materials and Methods

Solvents and reagents used were obtained as described in section 2.1.4 and NMR and GC/MS spectroscopic data were also obtained as described in section 2.1.4. IR measurements were performed on a Jasco FT/IR 4100 with samples prepared as KBr-pellets.

Low Temperature Stopped-flow Measurements

Low temperature "stopped-flow" experiments were performed as described in section 2.1.4. For the reaction of $[\text{Cu}(\text{DPDen})]^+$ with dioxygen, a 4×10^{-4} mol/L solution of $[\text{Cu}(\text{DPDen})]\text{CF}_3\text{SO}_3$ in acetone was prepared under inert conditions within the glove box from DPDen and $[\text{Cu}(\text{CH}_3\text{CN})_4]\text{CF}_3\text{SO}_3$ directly. The solution was transferred with a gastight syringe to the stopped-flow instrument. A saturated dioxygen (5.0) solution in acetone was prepared by bubbling a gas stream through the liquid for 10 min (10.2×10^{-3} mol/L) [128].

Single-Crystal X-ray Structure Determinations

The X-ray crystallographic data for 1-hydroxymethyladamantane, adamantane-1-carboxylic acid methylester, 3-hydroxy-2,2-dimethyl-propionic acid and pentafluorophenylhydrazin-1-ylidenemethyladamantan-2-ol were collected using a BRUKER/NONIUS KappaCCD detector with a BRUKER/NONIUS FR591 rotating anode radiation source and an OXFORD CRYOSYS-TEMS 600 low temperature system. Mo- $\text{K}\alpha$ radiation with wavelength 0.71073 Å and a graphite monochromator were used. The PLATON MULABS semi-empirical absorption correction using multiple scanned

reflection was applied on the data. The structure was solved by direct methods using SHELXS97 and refined with SHELXL2014 [129]. All non-hydrogen atoms were refined anisotropically. C-H hydrogen atoms were positioned geometrically for pentafluorophenylhydrazin-1-ylidenemethyladamantan-2-ol and located in difference map and refined isotropically for 1-hydroxymethyladamantane, adamantane-1-carboxylic acid methylester and 3-hydroxy-2,2-dimethyl-propionic acid. Non C-H H-atoms were located in difference map and refined isotropically.

Crystallographic data for the structures have been deposited with the Cambridge Crystallographic Data Centre as CCDC No. 1059672, 1059670, 1059671 and 1059674.

***N'*-(2,2-Dimethylpropylidene)-*N,N*-diethyl-ethylendiamine (DPDen)**

1.72 g trimethylacetaldehyde (20.0 mmol) were dissolved in 150 mL diethyl ether and 2.32 g *N,N*-diethylethylendiamine (20.0 mmol) were added. The reaction mixture was stirred over Na₂SO₄ for 1 hour and then heated under reflux for 2 hours. The solvent was removed after filtration and the remaining slightly yellow oil was dried in vacuum (3.14 g, 85 % yield). ¹H-NMR (400 MHz, CDCl₃): δ = 7.52 (s, 1H), 3.48 (t, 2H, J=7.1 Hz), 2.63 (m, 2H), 2.56 (m, 4H), 1.04 (m, 15H) ppm; ¹³C-NMR (100 MHz, CDCl₃): δ = 172.8, 59.5, 53.6, 47.4, 36.0, 26.9, 11.9 ppm.

Hydroxylation of *N'*-(2,2-Dimethylpropylidene)-*N,N*-diethyl-ethylendiamine (DPDen)

0.92 g *N'*-(2,2-dimethylpropylidene)-*N,N*-diethyl-ethylendiamine (DPDen, 5.0 mmol) were dissolved in 10 mL acetone in a glove box. A solution of 2.3 g [Cu(CH₃CN)₄]CF₃SO₃ (5.0 mmol) in 15 mL acetone was added. Dry oxygen was passed through the solution for 45 minutes and the mixture was left in the fridge for 20 hours. The solvent was removed, 20 mL 1 mol/L hydrochloric acid and 20 mL CH₂Cl₂ were added, stirred for two hours and then heated under reflux for another hour. It was washed three times with CH₂Cl₂ and the combined organic layers were dried over Na₂SO₄. The solvent was removed and the remaining brown oil was analyzed by GC/MS. For a small sample of the crude reaction product a purification was performed using semi-preparative GC. The colorless liquid (8 mg) was solved in chloroform and crystals of 3-hydroxy-2,2-dimethyl-propionic acid were obtained by very slow evaporation of the solvent and further oxidation of the aldehyde at aerobic conditions over several months.

***N'*-Cyclohexylmethylene-*N,N*-diethyl-ethane-1,2-diamine**

1.12 cyclohexanecarbaldehyde (10 mmol) and 1.16 g *N,N*-diethylethylenediamine (10 mmol) were dissolved in 100 mL diethyl ether and stirred for one hour over Na_2SO_4 and then heated under reflux for another hour. After filtration the solvent was removed under reduced pressure and the product was dried in vacuum (1.95 g, 93 %). $^1\text{H-NMR}$ (400 MHz, CDCl_3): δ = 7.52 (d, 1H, $J=5.1$ Hz), 3.45 (t, 2H, $J=7.3$ Hz), 2.60 (m, 6H), 1.75 (m, 5H), 1.26 (m, 6H), 1.03 (t, 6H, $J=7.1$ Hz) ppm; $^{13}\text{C-NMR}$ (100 MHz, CDCl_3): δ = 169.8, 59.5, 53.6, 47.4, 43.5, 29.7, 26.0, 25.5, 11.8 ppm.

Synthetic Hydroxylation of

***N'*-Cyclohexylmethylene-*N,N*-diethyl-ethane-1,2-diamine**

A solution of the complex was prepared directly by dissolving 210 mg *N'*-cyclohexylmethylene-*N,N*-diethyl-ethane-1,2-diamine (1 mmol) and 377 mg $[\text{Cu}(\text{CH}_3\text{CN})_4]\text{CF}_3\text{SO}_3$ (1 mmol) in 20 mL acetone in a glove box. Dry dioxygen was passed through the solution for 15 minutes and left in the fridge for 24 hours. 20 mL hydrochloric acid (1 mol/L) was added and it was stirred at room temperature for one hour. Then the mixture was heated to boiling point for a few minutes. Most of the acetone was removed under reduced pressure and the mixture was washed three times with CH_2Cl_2 . The combined organic layers were dried over Na_2SO_4 , the solvent was removed and the remaining oil was analyzed using GC/MS.

Adamantanylmethylidene-diethylaminomethylamine

268 mg of the adamantane-1-carbaldehyde- NaHSO_3 (1.0 mmol) complex were powdered and solved in about 20 mL water and washed with diethyl ether. Hydrochloric acid was added until pH 2 was reached. The solution was washed three times using diethyl ether and the combined organic layers were dried over Na_2SO_4 . To the crude product 180 mg *N,N*-diethylethylenediamine (1.5 mmol) was directly added under an argon atmosphere. After stirring for one hour, the solution was heated under reflux for 3 hours until GC/MS showed nearly complete conversion. The solvent was removed under reduced pressure and a colorless oil was purified by removing remaining amine with vacuum (215 mg, 82 % yield). $^1\text{H-NMR}$ (400 MHz, CDCl_3): δ = 7.29 (s, 1H), 3.38 (t, 2H, $J=7.1$ Hz), 2.50 (m, 7H), 1.64 (m, 12H), 0.95 (m, 8H) ppm; $^{13}\text{C-NMR}$ (100 MHz, CDCl_3): δ = 173.2, 59.0, 53.0, 47.0, 46.7, 39.4, 37.9, 36.7, 28.0, 11.8 ppm.

Synthetic Hydroxylation of

Adamantanylmethylidene-diethylaminomethylamine

0.25 g adamantanylmethylidene-diethylaminomethylamine (1 mmol) were solved in 180 mL CH_2Cl_2 in a glove box. A solution of 0.38 g $[\text{Cu}(\text{CH}_3\text{CN})_4]\text{CF}_3\text{SO}_3$ (1 mmol) in 20 mL CH_2Cl_2 was added slowly. Dry oxygen was passed through the complex solution for 40 minutes. After 18 hours in the fridge 20 mL 1 mol/L hydrochloric acid was added. The mixture was stirred for 30 minutes and then heated under argon for 30 minutes. The reaction mixture was washed with CH_2Cl_2 three times; the combined organic layers were washed with brine and dried over Na_2SO_4 . The solvent was removed and the obtained hydroxylated and non hydroxylated adamantane-1-carbaldehydes were separated by flash chromatography over silica (pentane/diethyl ether 10:1 for adamantane-1-carbaldehyde and 1:1 for 2-hydroxyadamantane-1-carbaldehyde, best fraction: 50 mg, 0.3 mmol, 28 %). $^1\text{H-NMR}$ (400 MHz, CDCl_3): δ = 9.29 (s, 1H), 4.00 (d, 1H, $J=2.34$ Hz), 3.40 (m, 5H), 1.14 (m, 11H) ppm; $^{13}\text{C-NMR}$ (100 MHz, CDCl_3): δ = 205.9, 71.8, 64.9, 49.4, 36.4, 35.6, 33.7, 30.3, 29.8, 26.6, 15.2 ppm. IR (KBr): 3482-3270 $\nu(\text{OH})$, 2950-2890 $\nu_{\text{as}}(\text{CH}_2)$, 2850 $\nu_{\text{s}}(\text{CH}_2)$, 1696 $\nu(\text{C}=\text{O})$, 1453 $\delta(\text{CHO})$, 1084 $\nu(\text{C-O}) \text{ cm}^{-1}$.

Pentafluorophenylhydrazin-1-ylidenemethyladamantan-2-ol

50 mg purified 2-hydroxyadamantane-1-carbaldehyde (0.3 mmol) was solved in 7 mL dry acetonitrile under argon. Some MgSO_4 , 1.2 eq pentafluorophenylhydrazine (120 mg) and a solution of 0.3 eq. TFA in acetonitrile (5 %) was added. After 15 minutes the solvent was removed under reduced pressure and the crude product was purified by flash chromatography (pentane/diethyl ether 10:1, then 1:1 for product and then pure ether, best fraction 15 mg, 0.04 mmol, 15 %). $^1\text{H-NMR}$ (600 MHz, CDCl_3): δ = 7.19 (s, 1H), 6.86 (s, 1H), 3.92 (d, 1H, $J = 3.07$ Hz), 1.70 (m, 13H) ppm; $^{13}\text{C-NMR}$ (150 MHz, CDCl_3): δ = 153.6, 74.5, 41.5, 39.4, 36.5, 35.9, 34.2, 33.6, 30.4, 27.3 ppm.

Diamantane-1-carboxylic acid

1-bromodiamantane (3.75 g, 14.03 mmol) was added to a mixture of 88 mL H_2SO_4 (99 %, 1.65 mol) and 7.00 mL formic acid (185 mmol). During one hour additional 10.0 mL formic acid (265 mmol) was added and the mixture was stirred for two hours at 10 °C and for another hour at room temperature. The solution was poured onto 300 g of ice and the precipitate was filtered and solved in CHCl_3 . It was washed with water and brine, dried over Na_2SO_4 and the solvent was removed under reduced pressure. 3.03 g colorless crystals were obtained (13.0 mmol, 93 %). $^1\text{H-NMR}$ (200 MHz, CDCl_3): δ = 11.90 (s, 1H), 2.14 (s, 2H), 1.93-1.90 (m, 2H), 1.88-1.84 (m, 3H), 1.81-1.79 (m,

3 Selective Aliphatic Hydroxylation

2H), 1.75-1.67 (m, 8H), 1.63-1.59 (m, 1H), 1.57-1.53 (m, 1H); ^{13}C -NMR (50 MHz, CDCl_3): δ = 183.2, 47.0, 41.6, 37.8, 37.4, 37.3, 37.0, 36.6, 35.2, 26.2, 25.1 ppm.

Diamantane-1-carboxylic acid methylester

Diamantane-1-carboxylic acid (2.05 g, 8.82 mmol) and 7.70 mL SOCl_2 (106.1 mmol) were heated under reflux for 3 hours. 6.60 mL dry CH_2Cl_2 and 4.0 mL dry methanol were added. It was stirred over night and then the solvent was removed under reduced pressure. Pure diamantane-1-carboxylic acid methylester was obtained by column chromatography on silica gel with diethyl ether/n-hexane 1:40 (1.65 g colorless crystals, 6.7 mmol, 75.9%). ^1H -NMR (200 MHz, CDCl_3): δ = 3.67 (s, 3H), 2.17-2.13 (m, 2H), 1.82-1.86 (m, 2H), 1.75-1.69 (m, 10H), 1.68-1.64 (m, 3H), 1.61-1.58 (m, 1H), 1.56-1.50 (m, 1H); ^{13}C -NMR (50 MHz, CDCl_3): δ = 177.81, 51.34, 47.22, 41.83, 37.92, 37.49, 37.46, 37.26, 36.68, 35.27, 26.29, 25.29 ppm.

1-Hydroxymethyldiamantane

To a suspension of 0.70 g LiAlH_4 (18.4 mmol) in 10 mL anhydrous THF a solution of 1.00 g diamantane-1-carboxylic acid methylester (4.06 mmol) in 4 mL anhydrous THF was added under an argon atmosphere at 0 °C. The stirred mixture was then heated under reflux for 1.5 hours. Water was added at 0 °C and the suspension was filtered through SiO_2 and extracted with CH_2Cl_2 . The organic layer was dried over Na_2SO_4 and the solvent was removed under reduced pressure. 0.84 g of a white solid was obtained (3.86 mmol, 95 %). ^1H -NMR (200 MHz, CDCl_3): δ = 3.60 (s, 2H), 2.04 (s, 1H), 1.97-1.89 (m, 2H), 1.81-1.74 (m, 4H), 1.70-1.67 (m, 6H), 1.60 (s, 2H), 1.55 (d, 2H, $J=3.1$ Hz), 1.48 (s, 1H), 1.41 (s, 1H), 1.26 (s, 1H); ^{13}C -NMR (50 MHz, CDCl_3): δ = 68.5, 40.1, 38.9, 38.2, 38.1, 38.1, 37.2, 32.8, 27.3, 25.8 ppm.

Diamantane-1-carbaldehyde

A mixture of 8.00 mL dry CH_2Cl_2 and 0.71 mL DMSO was cooled to -78 °C under argon atmosphere. Oxalyl chloride (0.580 mL, 6.76 mmol) was added slowly, the resulting mixture was stirred for 15 minutes. 1-hydroxymethyldiamantane (0.950 g, 4.35 mmol) in dry CH_2Cl_2 (5.00 mL) was added drop-wise and the solution was stirred for 1 hour at -78 °C. Triethylamine (2.78 mL, 37.9 mmol) was added slowly, the mixture was stirred for 30 minutes at -78 °C and warmed to room temperature. Cold 20 % aqueous solution of KH_2PO_4 (2.00 mL) and cold water (13.0 mL) were added and the mixture was stirred for 15 minutes. The product was extracted with diethyl ether,

the organic layer was washed with cold 10 % KH_2PO_4 (20 mL) and brine (20 mL). Column chromatography on silica gel with hexane/diethyl ether (1:1) as eluent gave 650 mg (3.00 mmol, 69 % yield) of a white solid. $^1\text{H-NMR}$ (400 MHz, CDCl_3): δ = 9.29 (s, 1H), 1.97 (s, 2H), 1.89 (m, 1H), 1.79 (m, 2H), 1.67 (m, 8H), 1.59 (m, 2H), 1.52 (m, 2H), 1.41 (d, 2H, J = 3.1 Hz); $^{13}\text{C-NMR}$ (100 MHz, CDCl_3): δ = 207.0, 37.6, 37.3, 37.3, 37.2, 37.1, 36.2, 34.6, 25.6, 25.3 ppm.

Diamantylmethylidene-diethylaminomethylamine

109 mg diamantane-1-carbaldehyde (0.5 mmol) and 75 mg *N,N*-diethylethylenediamine (0.65 mmol) were solved in 30 mL diethyl ether and heated under reflux for 20 hours. The solvent was removed under reduced pressure and a colorless micro-crystalline compound was obtained by removing remaining amine via evaporation in vacuum (156 mg, 99 % yield). $^1\text{H-NMR}$ (400 MHz, CDCl_3): δ = 7.39 (s, 1H), 3.49 (t, 2H, J =7.49 Hz), 2.64 (t, 2H, J =7.49 Hz), 2.57 (q, 4H, J =7.10), 1.70 (m, 19H), 1.03 (t, 6H, J =7.10 Hz) ppm; $^{13}\text{C-NMR}$ (100 MHz, CDCl_3): δ = 172.9, 59.9, 53.7, 47.3, 42.8, 41.7, 38.6, 37.7, 37.5, 34.0, 26.6, 25.7, 11.8 ppm. MS/MS: 314.269.

Synthetic Hydroxylation of diamantylmethylidene-diethylaminomethylamine

156 mg diamantylmethylidene-diethylaminomethylamine (0.5 mmol) were solved in 100 mL CH_2Cl_2 in a glove box. A solution of 188 mg $[\text{Cu}(\text{CH}_3\text{CN})_4]\text{CF}_3\text{SO}_3$ (0.5 mmol) in 20 mL CH_2Cl_2 was added. Dry oxygen was passed through the solution for 40 minutes and it was then left in the fridge over night. 10 mL 1 mol/L hydrochloric acid was added and the mixture was stirred for 20 minutes and then heated for one hour under argon atmosphere. It was washed three times with CH_2Cl_2 and dried over Na_2SO_4 . The solvent was removed under reduced pressure and the product was isolated by flash chromatography over silica (petrol ether / ether 2:1, then ether, yield 50 mg, 0.2 mmol, 43 %). $^1\text{H-NMR}$ (400 MHz, CDCl_3): δ = 9.38 (s, 1H), 2.74 (s, 1H), 2.00 (m, 7H), 1.60 (m, 9H), 1.34 (m, 2H) ppm; $^{13}\text{C-NMR}$ (100 MHz, CDCl_3): δ = 208.8, 71.2, 53.7, 42.8, 42.7, 38.9, 37.1, 36.8, 34.7, 32.2, 31.7, 29.8, 25.0 ppm.

3.2 Selected Supporting Information

3.2.1 Formation of $[\text{Cu}_2(\text{DPDen})(\mu\text{-OH})(\mu\text{-}o\text{-O-DPDen})]^{2+}$

To compare with the bis(μ -oxido) complex, the hydroxylation product of the reaction of $[\text{CuBDED}]^+$ with O_2 was analyzed by UV-vis spectroscopy. Figure

3.14 shows the complex before and after reaction with dioxygen. The probably occurring $[\text{Cu}_2(\text{DPDen})(\mu\text{-OH})(\mu\text{-}o\text{-O-DPDen})]^{2+}$ complex exhibits absorption at about 350 nm which is typical for similar alkoxide complexes.

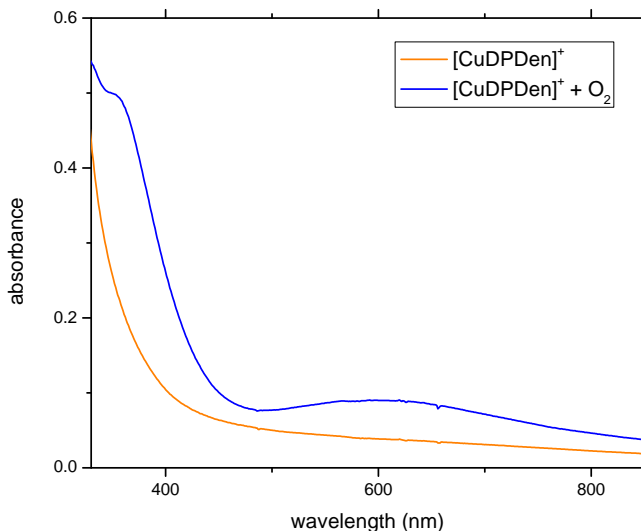


Figure 3.14: UV/vis of $[\text{CuDPDen}]^+$ complex without and with O_2 ($\lambda_{\text{max}} = 350$ nm, 0.4 mmol/L, acetone)

Experimental Details.

A 4×10^{-4} mol/L solution of $[\text{Cu}(\text{DPDen})]\text{CF}_3\text{SO}_3$ in acetone was prepared under inert conditions within the glove box from DPDen and $[\text{Cu}(\text{CH}_3\text{CN})_4]\text{CF}_3\text{SO}_3$ directly in a dilution series. The complex solution was analyzed by UV-vis spectroscopy, dry O_2 was passed through the solution for 10 minutes at room temperature and the solution was analyzed again.

3.2.2 Selective Hydroxylation of Ketones

Previously discussed are only selective hydroxylations of aldehydes. In the work of Schönecker et al. [89]-[92] mostly ketones were used. To test if selective hydroxylations with the ligands used in this work would also be possible with ketones, the ligand *N,N*-Diethyl-*N'*-(1,7,7-trimethyl-bicyclo[2.2.1]hept-2-ylidene)-ethane-1,2-diamine was synthesized and analyzed as copper(I) complex regarding reactivity towards dioxygen.

Whilst reacting with dioxygen, an intense coloring could be observed, but no hydroxylation product was found after workup. This again reflects the sensibility of the reaction towards minimal changes in the system.

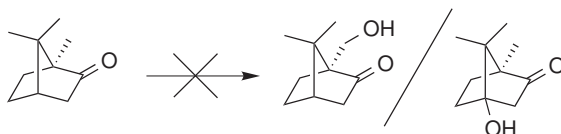


Figure 3.15: No hydroxylation of ketones such as camphor was observed.

N,N-Diethyl-*N'*-(1,7,7-trimethyl-bicyclo[2.2.1]hept-2-ylidene)-ethane-1,2-diamine.

7.61 g camphor (50 mmol) and 5.81 g *N,N*-diethylethylenediamine (50 mmol) were dissolved in about 200 mL toluene. A spatula tip's worth of *p*-toluenesulfonic acid was added and the reaction mixture was heated under reflux for 7 days with a Soxhlet apparatus filled with molecular sieve (4 Å). After removing the solvent a brown oil was obtained and purified by Kugelrohr distillation. A yellow oil was obtained (9.31 g, 37 mmol, 74 %). $^1\text{H-NMR}$ (400 MHz, CDCl_3): δ = 3.33 (m, 2H), 2.66 (t, 2H, $J=7.3$ Hz), 2.57 (q, 4H, $J=7.3$ Hz), 1.93 (t, 2H, $J=4.5$ Hz), 1.85 (m, 2H), 1.65 (m, 1H), 1.35 (m, 1H), 1.20 (m, 1H), 1.04 (t, 6H, $J=7.2$ Hz), 0.96 (s, 3H), 0.92 (s, 3H), 0.76 (s, 3H) ppm; $^{13}\text{C-NMR}$ (100 MHz, CDCl_3): δ = 182.4, 53.5, 53.4, 50.9, 47.4, 46.9, 43.8, 35.5, 32.1, 27.5, 19.6, 19.0, 11.9, 11.4 ppm.

Hydroxylation Attempt of *N,N*-Diethyl-*N'*-(1,7,7-trimethyl-bicyclo[2.2.1]hept-2-ylidene)-ethane-1,2-diamine.

0.50 g *N,N*-Diethyl-*N'*-(1,7,7-trimethyl-bicyclo[2.2.1]hept-2-ylidene)-ethane-1,2-diamine (2 mmol) and 0.75 g $[\text{Cu}(\text{CH}_3\text{CN})_4]\text{CF}_3\text{SO}_3$ were dissolved in a glove box in 50 mL dry CH_2Cl_2 . Dry dioxygen was passed through the

solution for 30 minutes and the reaction mixture was left in the fridge for 16 hours. 15 mL hydrochloric acid (1 mol/L) was added. The mixture was stirred for 30 minutes and heated under reflux for 3 hours. It was washed three times with CH_2Cl_2 and the combined organic layers were dried over Na_2SO_4 . The crude product was analyzed using GC/MS. Additionally the reaction was repeated using acetone as solvent.

3.2.3 Additional Results for the Synthesis of Adamantanylmethylidene-diethylaminomethylamine.

A lot of attempts were made in the synthesis and hydroxylation of Adamantanylmethylidene-diethylaminomethylamine. Figure 3.16 shows the molecular structure of the often obtained 2-diethylamino-ethyl-ammonium adamantancarboxylate. This compound occurs by oxidation of the aldehyde by air and demonstrates the sensibility of the adamantane carbaldehyde towards oxygen.

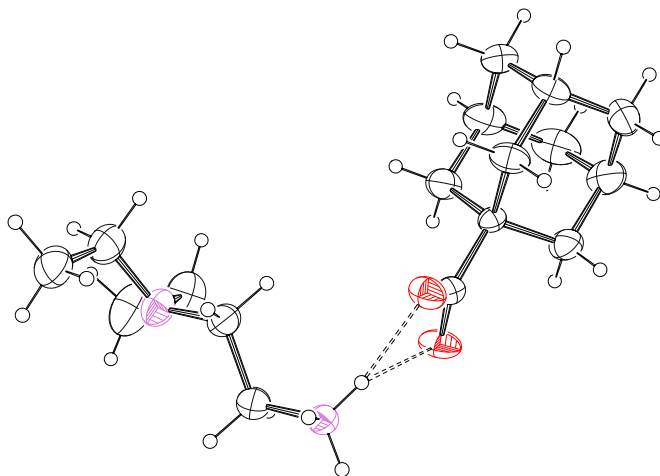


Figure 3.16: ORTEP plot of the molecular structure of 2-diethylamino-ethyl-ammonium adamantancarboxylate, ellipsoids are drawn at 30% probability.

To avoid the toxic PCC, an alternative oxidation reaction was tested. The adamantane-1-carbaldehyde could also be obtained by a Swern oxidation [166], but was not stabilized as when the reaction was done with PCC. This led to immediately further oxidation to the carboxylic acid. Thus this method was not used for the further synthesis.

Single-Crystal X-ray Structure Determination.

The X-ray crystallographic data for 2-diethylamino-ethyl-ammonium adamantancarboxylate were collected using a BRUKER/NONIUS KappaCCD detector with a BRUKER/NONIUS FR591 rotating anode radiation source and an OXFORD CRYOSYSTEMS 600 low temperature system. Mo-K α radiation with wavelength 0.71073 Å and a graphite monochromator were used. The PLATON [131] MULABS semi-empirical absorption correction using multiple scanned reflection was applied on the data. The structure was solved by direct methods using SHELXS97 and refined with SHELXL2014 [129]. All non-hydrogen atoms were refined anisotropically and hydrogen atoms were positioned geometrically. The absolute structure could not be determined. Crystallographic data for the structure have been deposited with the Cambridge Crystallographic Data Centre as CCDC No. 1059673.

Adamantane-1-carbaldehyde via Swern Oxidation.

To a solution of 4.6 g oxalyl chloride (36 mmol) in 75 mL dry CH₂Cl₂ at -90 °C 4.7 mL dry DMSO (66 mmol) were added drop wise under an argon atmosphere. After 15 minutes a solution of 5.0 g 1-hydroxymethyladamantane (30 mmol) in dry CH₂Cl₂ was added drop wise. After waiting for another 30 minutes 15.2 g triethylamine (151 mmol) was added. The reaction mixture was slowly warmed up to room temperature and stirred until GC/MS showed full conversion of the alcohol. Water was added slowly and the organic layer was separated and the water layer was washed with CH₂Cl₂. The combined organic layers were dried over Na₂SO₄.

3.2.4 Cyclisation of 3-Hydroxy-2,2-dimethylpropionaldehyde.

3-hydroxy-2,2-dimethylpropionaldehyde was synthesized according to literature [167] to compare the chromatographic retention factor to the product of the selective hydroxylation of trimethylacetaldehyde. Crystals were obtained from the colorless liquid in a closed flask. The molecular structure shows a cyclized dimer of 3-hydroxy-2,2-dimethylpropionaldehyde (Figure 3.17).

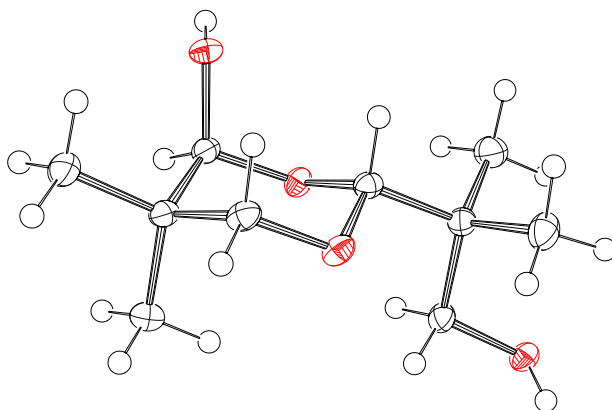


Figure 3.17: ORTEP plot of the molecular structure of 2-*tert*-butyl-5,5-dimethyl-[1,3]dioxan-4-ol, ellipsoids are drawn at 50% probability.

Single-Crystal X-ray Structure Determination.

The data for 2-*tert*-butyl-5,5-dimethyl-[1,3]dioxan-4-ol were obtained using a BRUKER D8 Venture system with dual I μ S microfocus sources, a PHOTON100 detector and an OXFORD CRYOSYSTEMS 700 low temperature system was used. Data collection was performed using Mo-Cu α radiation with wavelength 1.54178 Å and a collimating Quazar multilayer mirror. Semi-empirical absorption correction from equivalents was applied using SADABS-2014/4 and the structure was solved by intrinsic phasing using SHELXT2014 [130]. Refinement was performed against F² using SHELXL-2014/7 [129]. All non-hydrogen atoms were refined anisotropically, C-H hydrogen atoms were positioned geometrically and O-H hydrogen atoms were located in difference map and refined isotropically. Crystallographic data for the structure have been deposited with the Cambridge Crystallographic Data Centre as CCDC No. 1059669.

4 Supporting Information

This chapter assembles supporting information for the chapters 2 and 3. The data is arranged by the two chapters and herein by type and appearance. Interpretation and experimental details can be found in the corresponding chapters. For coordination compounds selected crystallographic bond lengths and angles are given, for organic compounds the full crystallographic bond lengths and angles (except for hydrogen atoms) are shown.

4.1 Supporting Information for Chapter 2

4.1.1 NMR Data

2-Bromo-6-formylpyridine

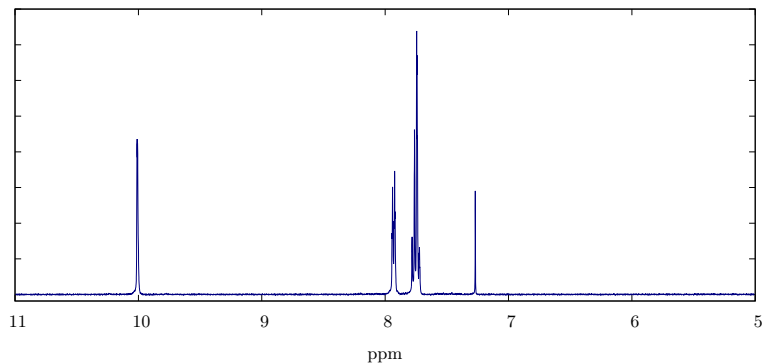


Figure 4.1: ^1H -NMR of 2-bromo-6-formylpyridine.

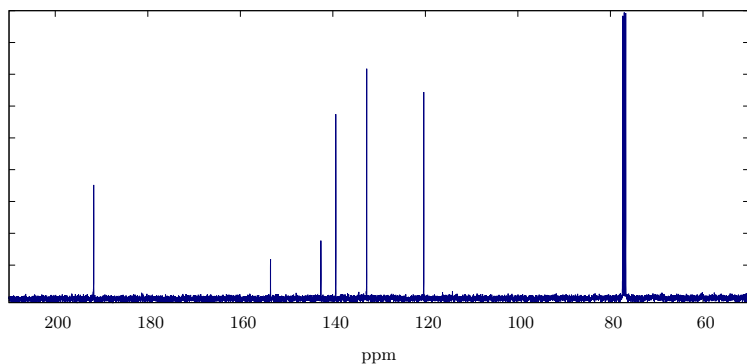


Figure 4.2: ^{13}C -NMR of 2-bromo-6-formylpyridine.

6-Phenyl-2-pyridinecarbaldehyde

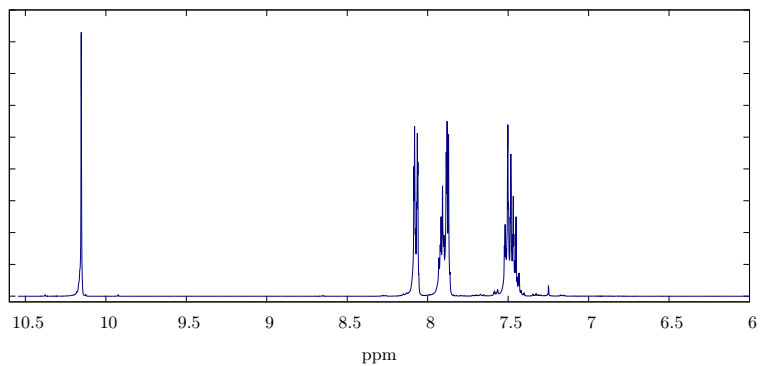


Figure 4.3: ^1H -NMR of 6-phenyl-2-pyridinecarbaldehyde.

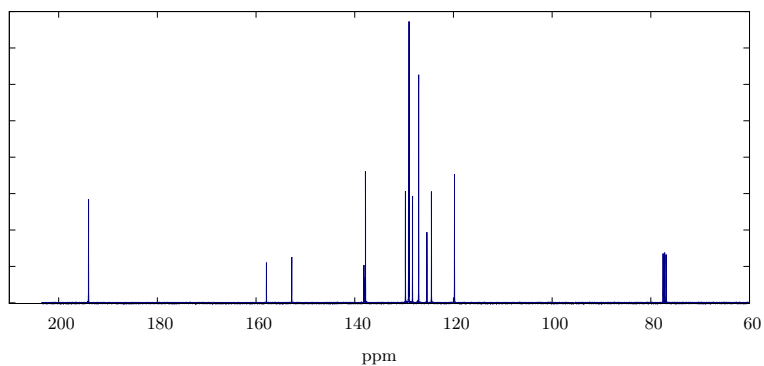


Figure 4.4: ^{13}C -NMR of 6-phenyl-2-pyridinecarbaldehyde.

6-Phenyl-2-pyridinemethanol

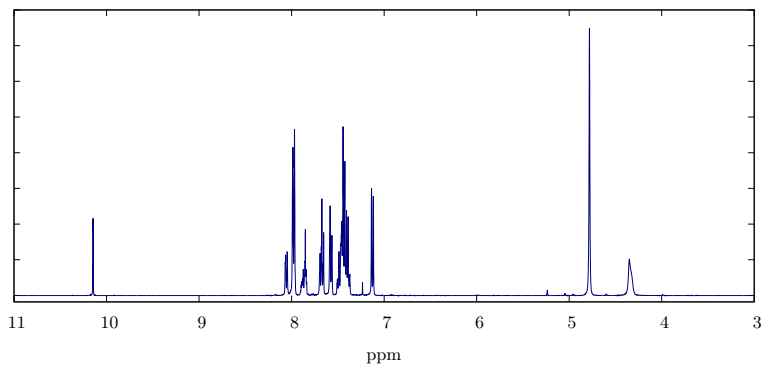


Figure 4.5: ^1H -NMR of 6-phenyl-2-pyridinemethanol.

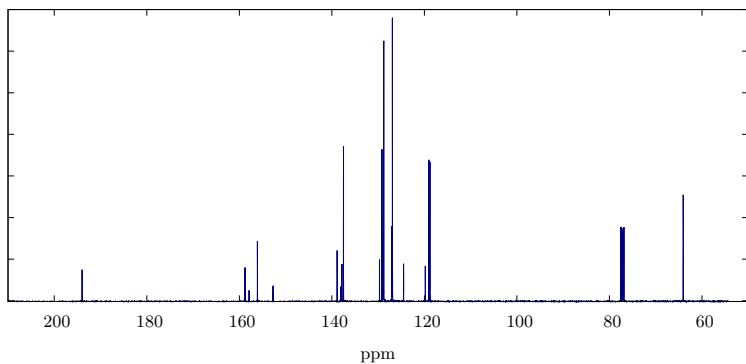


Figure 4.6: ^{13}C -NMR of 6-phenyl-2-pyridinemethanol.

2-(Chloromethyl)-6-phenylpyridine hydrochloride

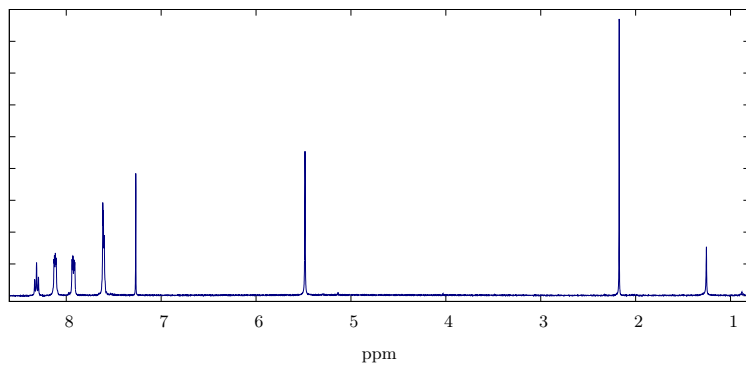


Figure 4.7: ^1H -NMR of 2-(chloromethyl)-6-phenylpyridine hydrochloride.

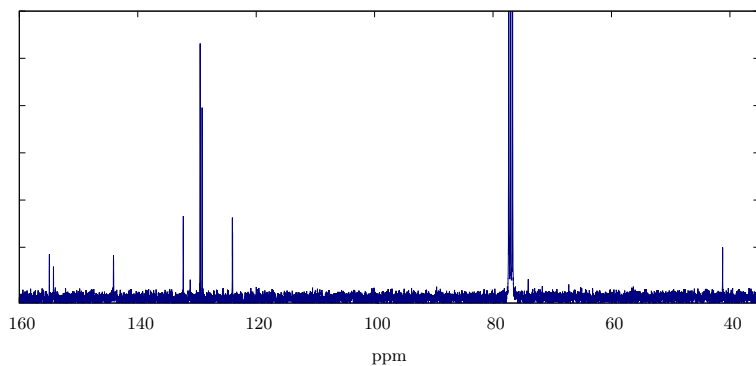


Figure 4.8: ^{13}C -NMR of 2-(chloromethyl)-6-phenylpyridine hydrochloride.

2-(Diethylaminomethyl)-6-phenylpyridine

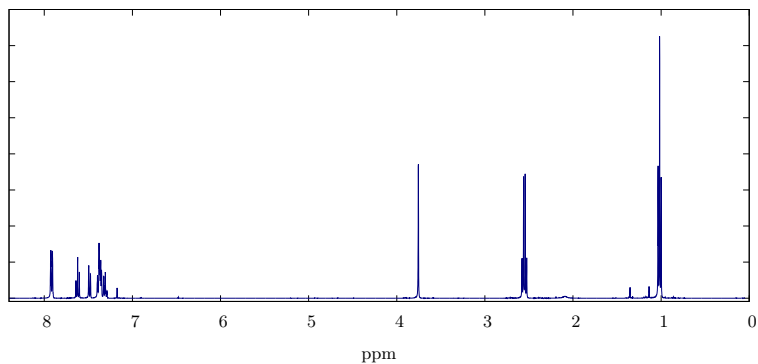


Figure 4.9: ^1H -NMR of 2-(diethylaminomethyl)-6-phenylpyridine.

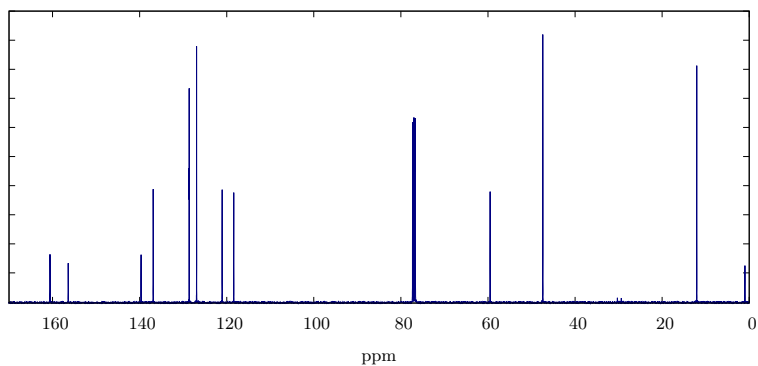


Figure 4.10: ^{13}C -NMR of 2-(diethylaminomethyl)-6-phenylpyridine.

***N'*-Benzylidene-*N,N*-diethyl-ethylendiamine (BDED)**

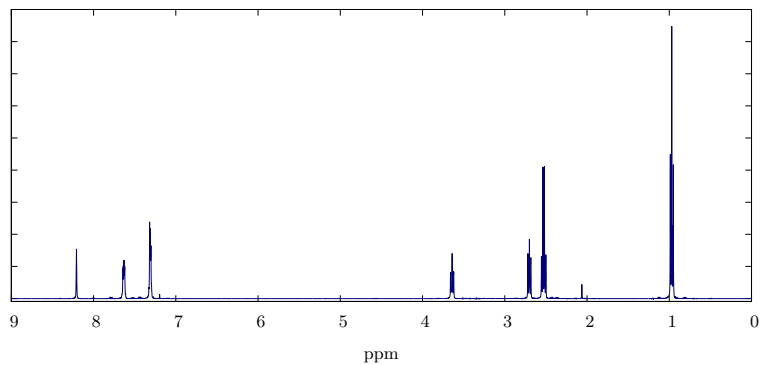


Figure 4.11: ^1H -NMR of *N'*-benzylidene-*N,N*-diethyl-ethylendiamine.

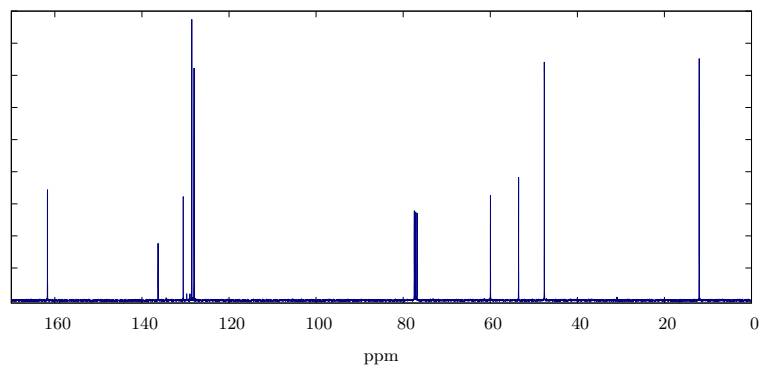


Figure 4.12: ^{13}C -NMR of *N'*-benzylidene-*N,N*-diethyl-ethylendiamine.

***N'*-Benzyl-*N,N*-diethyl-ethylendiamine (H_2BDED)**

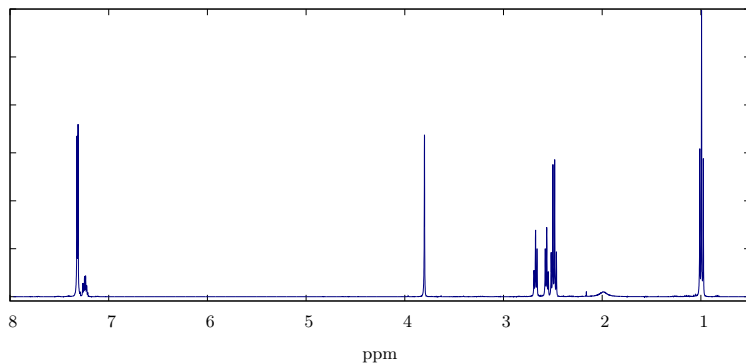


Figure 4.13: 1H -NMR of *N'*-benzyl-*N,N*-diethyl-ethylendiamine.

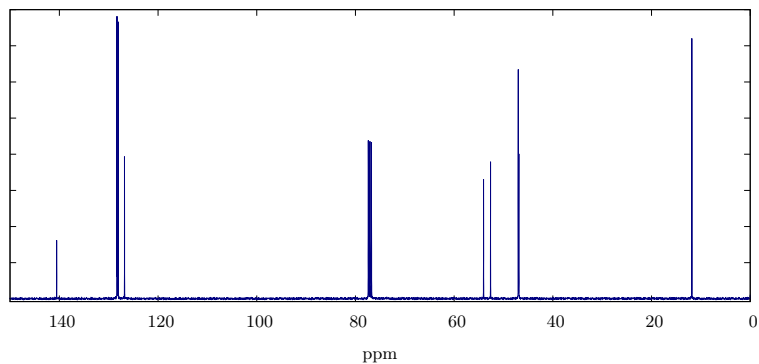


Figure 4.14: ^{13}C -NMR of *N'*-benzyl-*N,N*-diethyl-ethylendiamine.

Salicylaldehyde from synthetic hydroxylation

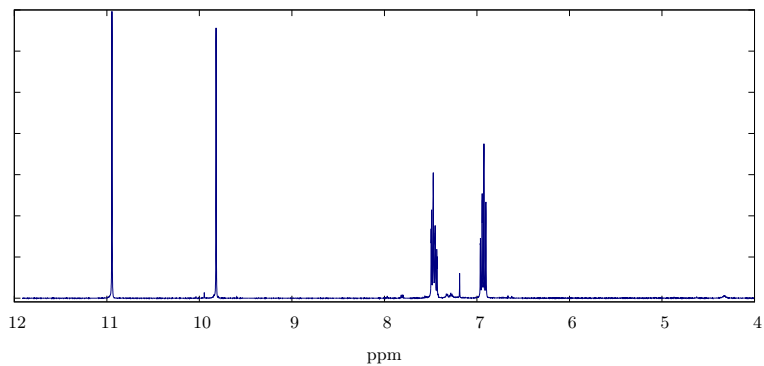


Figure 4.15: ^1H -NMR of salicylaldehyde.

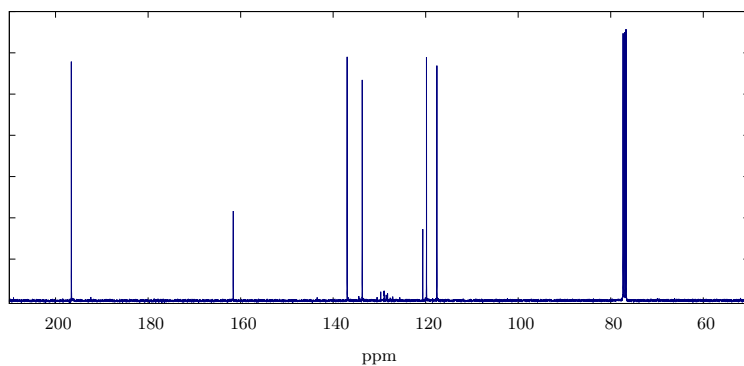


Figure 4.16: ^{13}C -NMR of salicylaldehyde.

2-(diethylamino)ethyl(4-methoxy-phenyl)methylideneamine

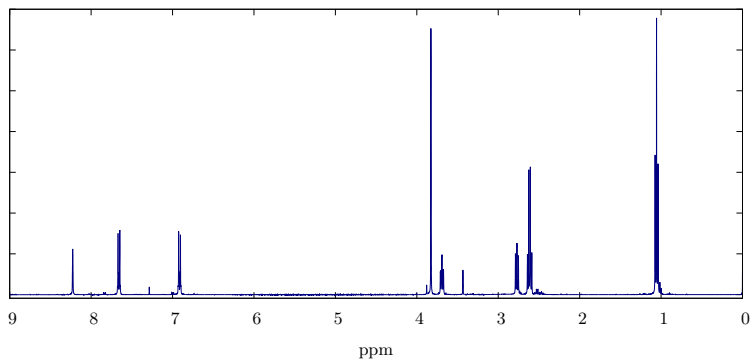


Figure 4.17: ^1H -NMR of 2-(diethylamino)ethyl(4-methoxy-phenyl)methylideneamine.

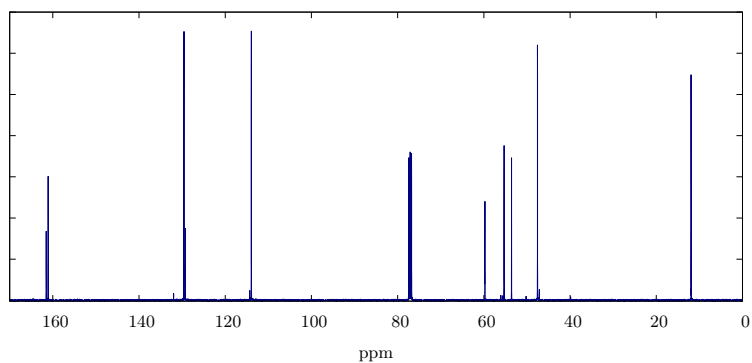


Figure 4.18: ^{13}C -NMR of 2-(diethylamino)ethyl(4-methoxy-phenyl)methylideneamine.

2-(diethylamino)ethyl(4-nitrophenyl)methylideneamine

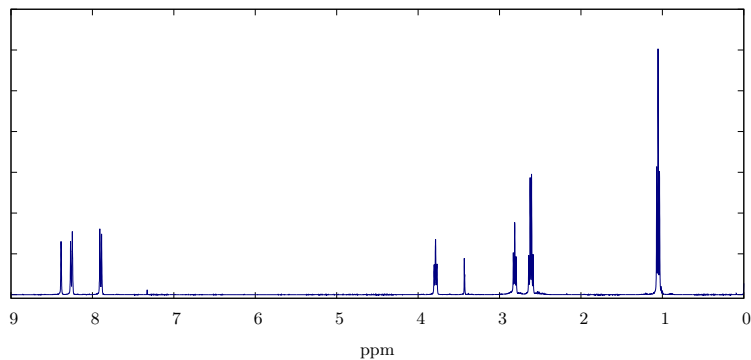


Figure 4.19: ^1H -NMR of 2-(diethylamino)ethyl(4-nitrophenyl)methylideneamine.

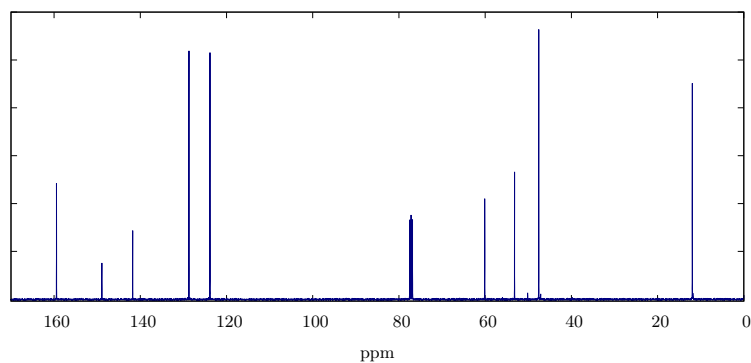


Figure 4.20: ^{13}C -NMR of 2-(diethylamino)ethyl(4-nitrophenyl)methylideneamine.

2-(diethylamino)ethyl(4-methyl)methylideneamine

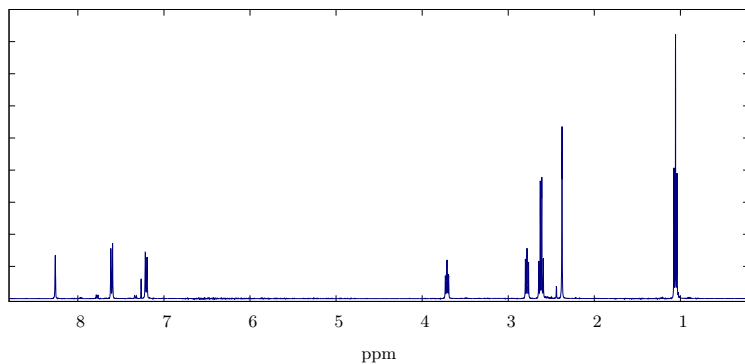


Figure 4.21: ^1H -NMR of 2-(diethylamino)ethyl(4-methyl)methylideneamine.

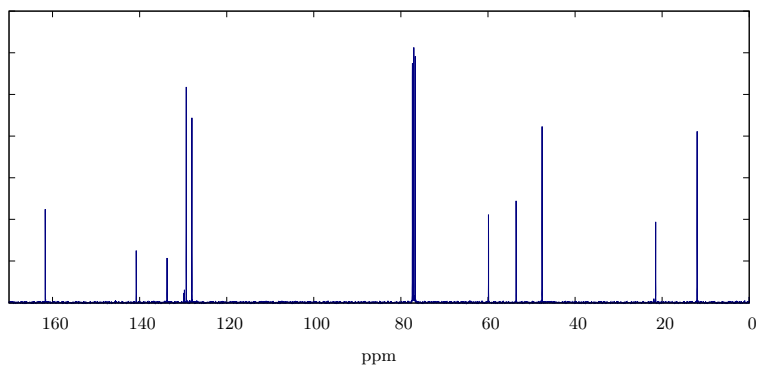


Figure 4.22: ^{13}C -NMR of 2-(diethylamino)ethyl(4-methyl)methylideneamine.

2-(diethylamino)ethyl(4-chloro)methylideneamine

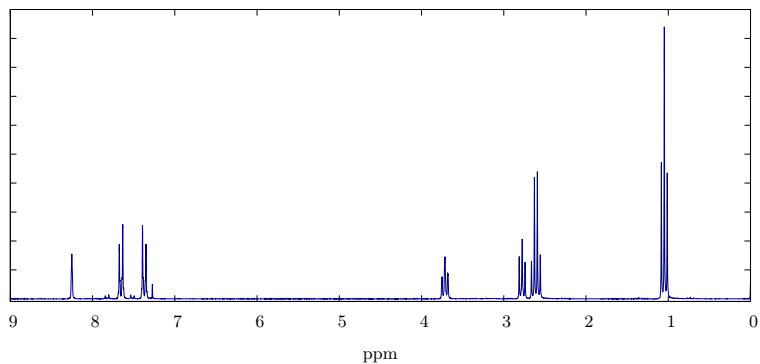


Figure 4.23: ^1H -NMR of 2-(diethylamino)ethyl(4-chloro)methylideneamine.

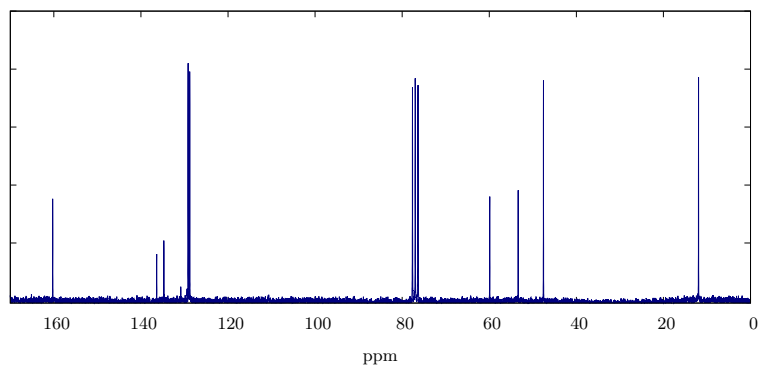


Figure 4.24: ^{13}C -NMR of 2-(diethylamino)ethyl(4-chloro)methylideneamine.

2-(diethylamino)ethyl(3-nitrophenyl)methylideneamine

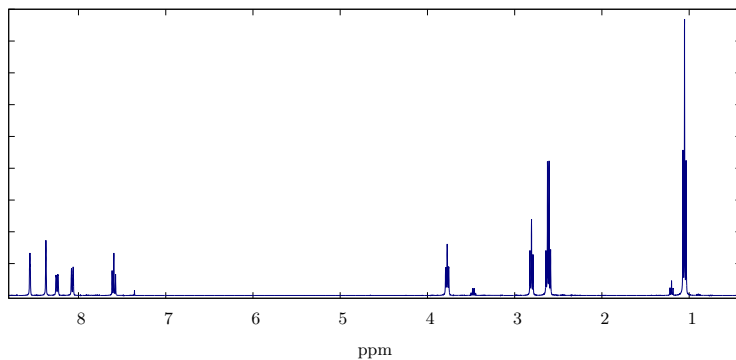


Figure 4.25: ^1H -NMR of 2-(diethylamino)ethyl(3-nitrophenyl)methylideneamine.

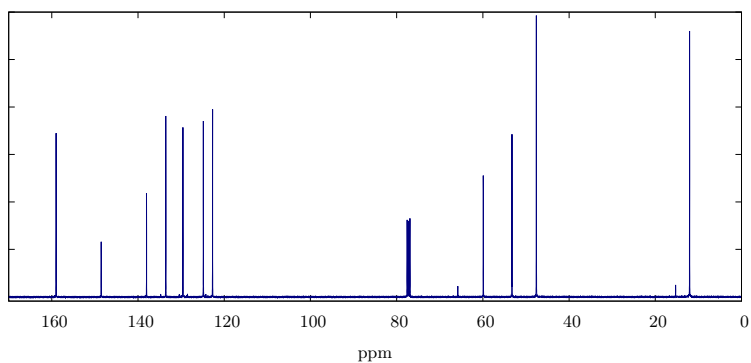


Figure 4.26: ^{13}C -NMR of 2-(diethylamino)ethyl(3-nitrophenyl)methylideneamine.

2-(diethylamino)ethyl(3-methyl)methylideneamine

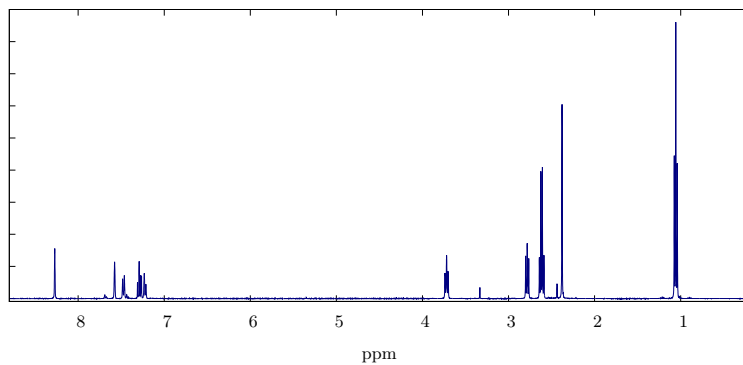


Figure 4.27: ^1H -NMR of 2-(diethylamino)ethyl(3-methyl)methylideneamine.

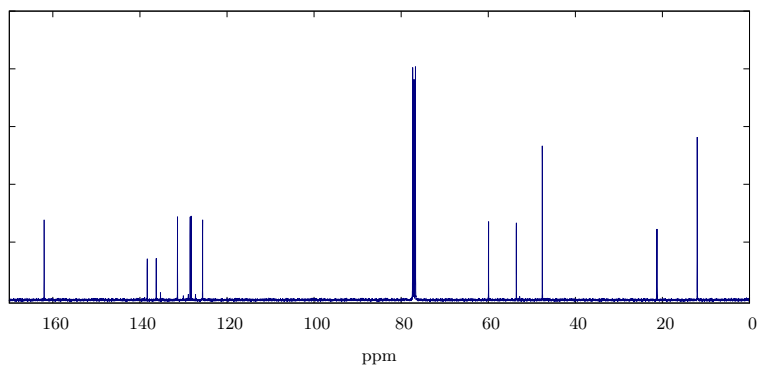


Figure 4.28: ^{13}C -NMR of 2-(diethylamino)ethyl(3-methyl)methylideneamine.

***N'*-Benzylidene-*N,N*-dimethyl-ethylendiamine**

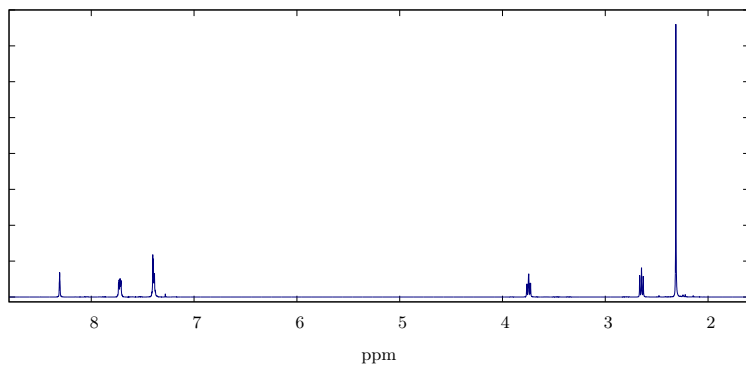


Figure 4.29: ^1H -NMR of *N'*-benzylidene-*N,N*-dimethyl-ethylendiamine.

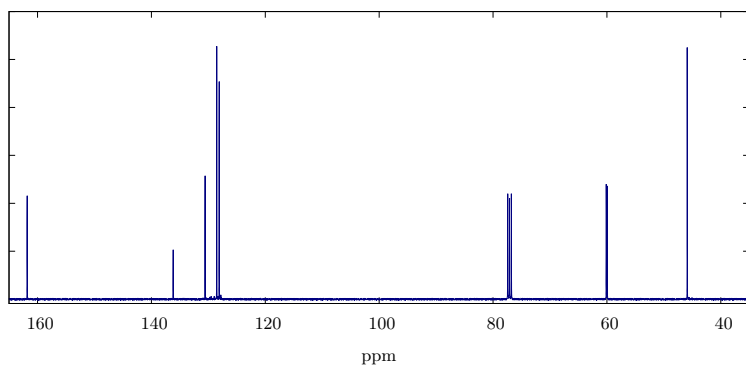


Figure 4.30: ^{13}C -NMR of *N'*-benzylidene-*N,N*-dimethyl-ethylendiamine.

2-(diethylamino)ethyl(4-hydroxy-phenyl)methylideneamine

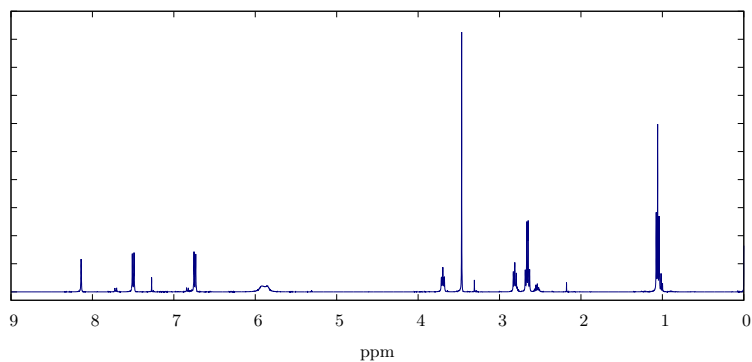


Figure 4.31: ^1H -NMR of 2-(diethylamino)ethyl(4-hydroxy-phenyl)methylideneamine.

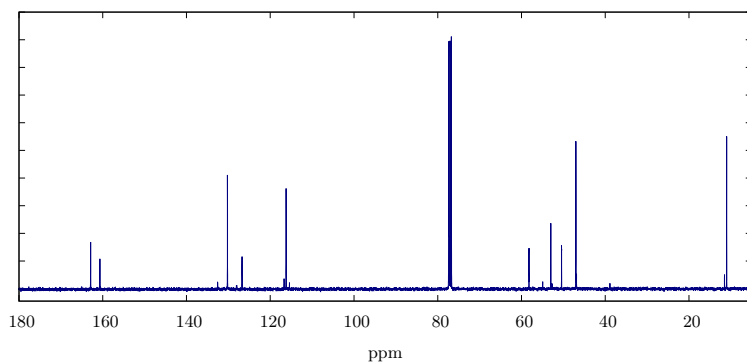


Figure 4.32: ^{13}C -NMR of 2-(diethylamino)ethyl(4-hydroxy-phenyl)methylideneamine.

4.1.2 Crystallographic Data

Table 4.1: Crystal data and structure refinement for $[\text{Cu}_2(\text{PPN})_2(\text{OH})_2](\text{CF}_3\text{SO}_3)_2$.

CCDC number	1032911
Empirical formula	$\text{C}_{34}\text{H}_{42}\text{Cu}_2\text{F}_6\text{N}_4\text{O}_8\text{S}_2$
Formula weight	939.92
Temperature	170(2) K
Wavelength	0.71073 Å
Crystal system	Monoclinic
Space group	$P2_1/n$
Unit cell dimensions	$a = 10.2427(6)$ Å $\alpha = 90^\circ$ $b = 17.3109(9)$ Å $\beta = 105.159(7)^\circ$ $c = 11.1938(7)$ Å $\gamma = 90^\circ$
Volume	$1915.71(19)$ Å ³
Z	2
Density (calculated)	1.629 Mg/m ³
Absorption coefficient	1.304 mm ⁻¹
F(000)	964
Crystal Size	$0.3 \times 0.2 \times 0.2$ mm ³
Theta range for data collection	2.22 to 25.96°
Index ranges	$-12 \leq h \leq 11$, $-20 \leq k \leq 21$, $-13 \leq l \leq 13$
Reflections collected	10720
Independent reflections	3703 [R(int) = 0.0364]
Completeness to theta = 25.96°	98.7%
Refinement method	Full-matrix least-squares on F ²
Data / restraints / parameters	3703 / 0 / 255
Goodness-of-fit on F ²	1.020
Final R indices [I > 2sigma(I)]	R1 = 0.0310, wR2 = 0.0750
R indices (all data)	R1 = 0.0394, wR2 = 0.0783
Extinction coefficient	0.0056(9)
Largest diff. peak and hole	0.424 and -0.483 e.Å ⁻³

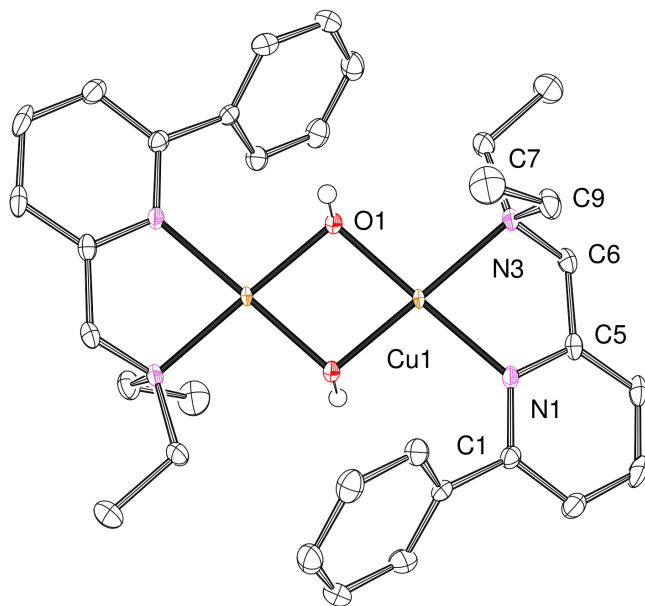
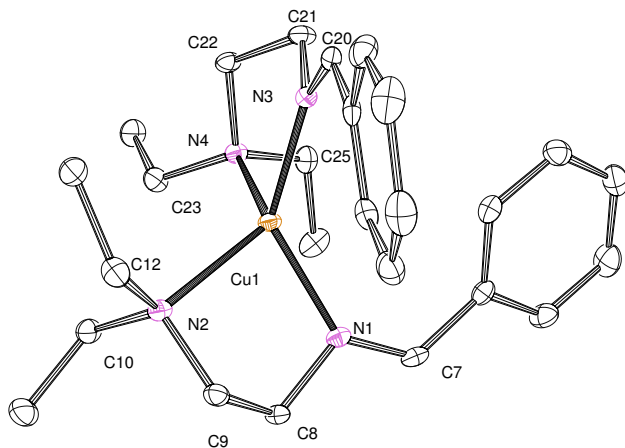


Table 4.2: Selected bond lengths [\AA] and angles [$^\circ$] for $[\text{Cu}_2(\text{PPN})_2(\text{OH})_2](\text{CF}_3\text{SO}_3)_2$.

Cu(1)-O(1)	1.9118(14)	Cu(1)-N(1)	2.0280(17)
Cu(1)-O(1A)	1.9173(14)	Cu(1)-N(3)	2.0434(17)
Cu(1)-Cu(1A)	2.9049(5)		
O(1)-Cu(1)-O(1A)	81.31(7)	N(1)-Cu(1)-N(3)	81.56(7)
O(1)-Cu(1)-N(1)	177.95(7)	O(1)-Cu(1)-Cu(1A)	40.73(4)
O(1A)-Cu(1)-N(1)	99.64(7)	O(1A)-Cu(1)-Cu(1A)	40.59(4)
O(1)-Cu(1)-N(3)	97.66(7)	N(1)-Cu(1)-Cu(1A)	140.19(5)
O(1A)-Cu(1)-N(3)	174.82(6)	N(3)-Cu(1)-Cu(1A)	138.17(5)
Cu(1)-O(1)-Cu(1A)	98.69(7)		

[Cu(BDED)₂]CF₃SO₃Table 4.3: Crystal data and structure refinement for [Cu(BDED)₂]CF₃SO₃.

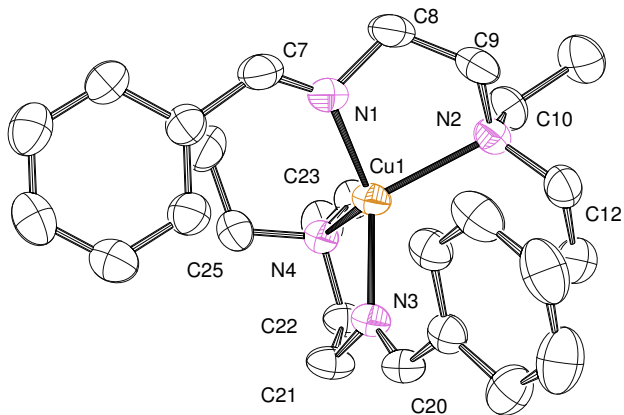
CCDC number	1047583
Empirical formula	C ₂₇ H ₄₀ CuF ₃ N ₄ O ₃ S
Formula weight	621.23
Temperature	100(2) K
Wavelength	0.71073 Å
Crystal system	Monoclinic
Space group	<i>P</i> 2 ₁ / <i>n</i>
Unit cell dimensions	a = 10.7621(5) Å α = 90° b = 12.5348(6) Å β = 91.521(2)° c = 21.6124(10) Å γ = 90°
Volume	2914.5(2) Å ³
Z	4
Density (calculated)	1.416 Mg/m ³
Absorption coefficient	0.875 mm ⁻¹
F(000)	1304
Crystal Size	0.643 x 0.328 x 0.325 mm ³
Theta range for data collection	2.489 to 25.105°
Index ranges	-12 ≤ h ≤ 12, -13 ≤ k ≤ 14, -25 ≤ l ≤ 25
Reflections collected	53815
Independent reflections	5172 [R(int) = 0.0467]
Completeness to theta = 25.96°	99.6%
Absorption correction	Semi-empirical from equivalents
Refinement method	Full-matrix least-squares on F ²
Data / restraints / parameters	5172 / 0 / 356
Goodness-of-fit on F ²	1.104
Final R indices [I > 2σ(I)]	R1 = 0.0310, wR2 = 0.0667
R indices (all data)	R1 = 0.0367, wR2 = 0.0688
Largest diff. peak and hole	0.278 and -0.357 e.Å ⁻³

Table 4.4: Selected bond lengths [Å] and angles [°] for [Cu(BDED)₂]CF₃SO₃.

N(1)-Cu(1)	2.0161(16)	Cu(1)-N(4)	2.1801(16)
Cu(1)-N(3)	2.0298(16)	Cu(1)-N(2)	2.2338(16)
N(1)-Cu(1)-N(3)	131.78(6)	C(10)-N(2)-Cu(1)	112.50(11)
N(1)-Cu(1)-N(4)	117.12(6)	C(20)-N(3)-Cu(1)	136.85(14)
N(3)-Cu(1)-N(4)	86.38(6)	C(21)-N(3)-Cu(1)	107.96(11)
N(1)-Cu(1)-N(2)	85.51(6)	C(25)-N(4)-Cu(1)	110.21(12)
N(3)-Cu(1)-N(2)	121.83(6)	C(22)-N(4)-Cu(1)	100.54(11)
N(4)-Cu(1)-N(2)	117.77(6)	C(23)-N(4)-Cu(1)	114.71(11)
C(9)-N(2)-Cu(1)	98.84(11)	C(7)-N(1)-Cu(1)	135.58(14)
C(12)-N(2)-Cu(1)	113.28(11)	C(8)-N(1)-Cu(1)	108.19(12)

[Cu(BDED)₂][SbF₆]Table 4.5: Crystal data and structure refinement for [Cu(BDED)₂][SbF₆].

CCDC number	1047584
Empirical formula	C ₂₆ H ₄₀ CuF ₆ N ₄ Sb
Formula weight	707.91
Temperature	190(2) K
Wavelength	0.71073 Å
Crystal system	Monoclinic
Space group	<i>P</i> 2 ₁ / <i>n</i>
Unit cell dimensions	a = 12.888(3) Å α = 90° b = 12.906(3) Å β = 97.81(3)° c = 18.244(4) Å γ = 90°
Volume	3006.4(11) Å ³
Z	4
Density (calculated)	1.564 Mg/m ³
Absorption coefficient	1.665 mm ⁻¹
F(000)	1432
Crystal Size	0.50 x 0.25 x 0.20 mm ³
Theta range for data collection	1.823 to 27.479°
Index ranges	-16 ≤ h ≤ 16, -16 ≤ k ≤ 15, -23 ≤ l ≤ 23
Reflections collected	25252
Independent reflections	6884 [R(int) = 0.0516]
Completeness to theta = 25.96°	99.9%
Refinement method	Full-matrix least-squares on F ²
Data / restraints / parameters	6884 / 0 / 347
Goodness-of-fit on F ²	1.022
Absorption correction	Empirical
Max. and min. transmission	0.51737 and 0.41605
Final R indices [I > 2σ(I)]	R1 = 0.0426, wR2 = 0.1091
R indices (all data)	R1 = 0.0676, wR2 = 0.1210
Largest diff. peak and hole	0.745 and -0.853 e.Å ⁻³

Table 4.6: Selected bond lengths [Å] and angles [°] for $[\text{Cu}(\text{BDED})_2]\text{SbF}_6$.

N(1)-Cu(1)	2.015(3)	Cu(1)-N(4)	2.190(3)
Cu(1)-N(3)	2.026(3)	Cu(1)-N(2)	2.239(3)
C(7)-N(1)-Cu(1)	136.4(3)	C(20)-N(3)-Cu(1)	134.5(2)
C(8)-N(1)-Cu(1)	106.7(2)	C(21)-N(3)-Cu(1)	108.9(2)
N(1)-Cu(1)-N(3)	133.15(11)	C(23)-N(4)-Cu(1)	115.9(2)
N(1)-Cu(1)-N(4)	119.37(11)	C(22)-N(4)-Cu(1)	100.26(18)
N(3)-Cu(1)-N(4)	86.18(10)	C(25)-N(4)-Cu(1)	109.8(2)
N(1)-Cu(1)-N(2)	86.12(11)	C(9)-N(2)-Cu(1)	99.3(2)
N(3)-Cu(1)-N(2)	117.16(11)	C(10)-N(2)-Cu(1)	112.0(2)
N(4)-Cu(1)-N(2)	118.50(10)	C(12)-N(2)-Cu(1)	113.5(2)

[Cu(H₂BDED)Cl₂] · acetoneTable 4.7: Crystal data and structure refinement for [Cu(H₂BDED)Cl₂]·acetone.

CCDC number	1047586	
Empirical formula	C ₁₆ H ₂₈ Cl ₂ CuN ₂ O	
Formula weight	398.84	
Temperature	293(2) K	
Wavelength	0.71073 Å	
Crystal system	Orthorhombic	
Space group	<i>Pbca</i>	
Unit cell dimensions	a = 10.875(2) Å	α = 90°
	b = 21.157(4) Å	β = 90°
	c = 16.997(3) Å	γ = 90°
Volume	3910.7(12) Å ³	
Z	8	
Density (calculated)	1.355 Mg/m ³	
Absorption coefficient	1.393 mm ⁻¹	
F(000)	1672	
Crystal Size	0.40 x 0.08 x 0.06 mm ³	
Theta range for data collection	2.942 to 28.131°	
Index ranges	-14<=h<=13, -22<=k<=26, -16<=l<=22	
Reflections collected	16191	
Independent reflections	4594 [R(int) = 0.2422]	
Completeness to theta = 25.96°	97.4%	
Absorption correction	None	
Refinement method	Full-matrix least-squares on F ²	
Data / restraints / parameters	4594 / 0 / 203	
Goodness-of-fit on F ²	0.961	
Final R indices [I>2sigma(I)]	R1 = 0.0934, wR2 = 0.2312	
R indices (all data)	R1 = 0.1498, wR2 = 0.2770	
Largest diff. peak and hole	2.327 and -1.552 e.Å ⁻³	

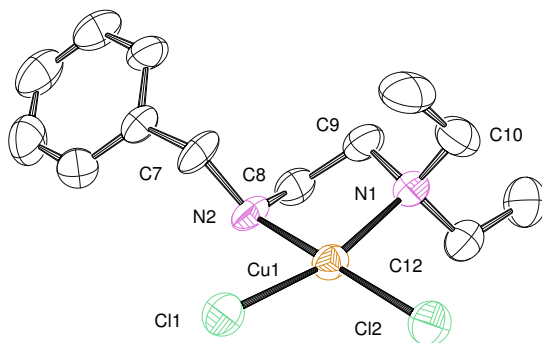


Table 4.8: Selected bond lengths [Å] and angles [°] for [Cu(H₂BDED)Cl₂]
acetone.

N(2)-Cu(1)	2.025(6)	Cl(1)-Cu(1)	2.3071(18)
Cl(2)-Cu(1)	2.245(2)	Cu(1)-N(1)	2.114(5)
C(8)-N(2)-Cu(1)	106.1(4)	N(1)-Cu(1)-Cl(1)	164.70(18)
C(7)-N(2)-Cu(1)	114.7(4)	Cl(2)-Cu(1)-Cl(1)	91.69(8)
N(2)-Cu(1)-N(1)	84.7(2)	C(9)-N(1)-Cu(1)	106.3(4)
N(2)-Cu(1)-Cl(2)	177.68(17)	C(12)-N(1)-Cu(1)	107.7(4)
N(1)-Cu(1)-Cl(2)	94.13(17)	C(10)-N(1)-Cu(1)	109.4(4)
N(2)-Cu(1)-Cl(1)	89.92(17)		

[Cu₂(Et₂en)OH₂](CF₃SO₃)₂ · 4 H₂OTable 4.9: Crystal data and structure refinement for [Cu₂(Et₂en)OH₂](CF₃SO₃)₂ · 4 H₂O.

CCDC number	1047585
Empirical formula	C ₇ H ₂₁ CuF ₃ N ₂ O ₆ S
Formula weight	381.86
Temperature	150(2) K
Wavelength	0.71073 Å
Crystal system	Monoclinic
Space group	<i>P</i> 2 ₁ / <i>n</i>
Unit cell dimensions	a = 7.3784(15) Å α = 90° b = 13.327(3) Å β = 95.56(3)° c = 15.307(3) Å γ = 90°
Volume	1498.1(5) Å ³
Z	4
Density (calculated)	1.693 Mg/m ³
Absorption coefficient	1.654 mm ⁻¹
F(000)	788
Crystal Size	0.38 x 0.35 x 0.25 mm ³
Theta range for data collection	2.674 to 27.573°
Index ranges	-9 ≤ h ≤ 9, -17 ≤ k ≤ 16, -19 ≤ l ≤ 19
Reflections collected	34892
Independent reflections	3458 [R(int) = 0.0887]
Completeness to theta = 25.96°	99.8%
Absorption correction	Empirical
Max. and min. transmission	0.7456 and 0.6103
Refinement method	Full-matrix least-squares on F ²
Data / restraints / parameters	3458 / 0 / 203
Goodness-of-fit on F ²	1.008
Final R indices [I > 2σ(I)]	R1 = 0.0295, wR2 = 0.0672
R indices (all data)	R1 = 0.0477, wR2 = 0.0723
Largest diff. peak and hole	0.314 and -0.378 e.Å ⁻³

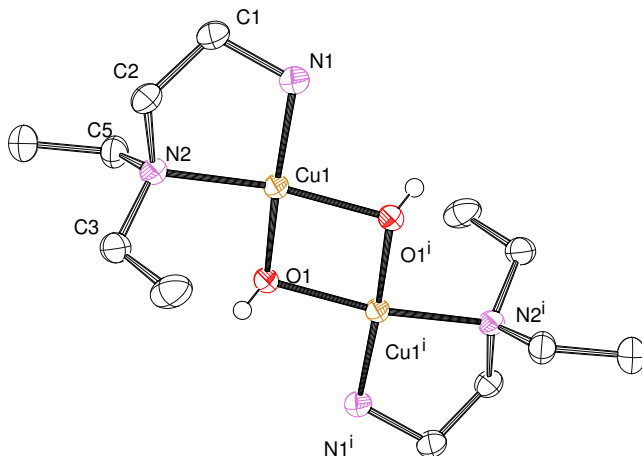


Table 4.10: Selected bond lengths [\AA] and angles [$^\circ$] for $[\text{Cu}_2(\text{Et}_2\text{en})\text{OH}_2](\text{CF}_3\text{SO}_3)_2 \cdot 4\text{H}_2\text{O}$.

Cu(1)-O(1)	1.9318(15)	Cu(1)-N(2)	2.0614(17)
Cu(1)-O(1)#1	1.9644(15)	Cu(1)-Cu(1)#1	2.9486(6)
Cu(1)-N(1)	1.9815(17)	O(1)-Cu(1)#1	1.9644(15)
O(1)-Cu(1)-O(1)#1	81.64(7)	N(1)-Cu(1)-Cu(1)#1	135.74(5)
O(1)-Cu(1)-N(1)	174.62(7)	N(2)-Cu(1)-Cu(1)#1	137.53(5)
O(1)#1-Cu(1)-N(1)	95.51(6)	Cu(1)-O(1)-Cu(1)#1	98.36(7)
O(1)-Cu(1)-N(2)	98.05(7)	C(1)-N(1)-Cu(1)	108.23(12)
O(1)#1-Cu(1)-N(2)	165.81(7)	C(3)-N(2)-Cu(1)	111.59(13)
N(1)-Cu(1)-N(2)	85.84(7)	C(2)-N(2)-Cu(1)	105.82(12)
O(1)-Cu(1)-Cu(1)#1	41.23(4)	C(5)-N(2)-Cu(1)	107.79(12)
O(1)#1-Cu(1)-Cu(1)#1	40.40(4)		

Symmetry transformations used to generate equivalent atoms:

#1 $-x + 1, -y + 1, -z + 1$

[Cu(m-Me-BDED)₂](CF₃SO₃)Table 4.11: Crystal data and structure refinement for [Cu(m-Me-BDED)₂](CF₃SO₃).

CCDC number	1047582
Empirical formula	C ₂₉ H ₄₄ CuF ₃ N ₄ O ₃ S
Formula weight	649.28
Temperature	100(2) K
Wavelength	0.71073 Å
Crystal system	Orthorhombic
Space group	<i>P</i> 2 ₁ 2 ₁ 2 ₁
Unit cell dimensions	a = 9.4788(4) Å α = 90° b = 13.7438(5) Å β = 90° c = 24.5303(9) Å γ = 90°
Volume	3195.7(2) Å ³
Z	4
Density (calculated)	1.350 Mg/m ³
Absorption coefficient	0.802 mm ⁻¹
F(000)	1368
Crystal Size	0.224 x 0.203 x 0.058 mm ³
Theta range for data collection	2.226 to 25.080°
Index ranges	-11 ≤ h ≤ 11, -16 ≤ k ≤ 16, -28 ≤ l ≤ 29
Reflections collected	50580
Independent reflections	5683 [R(int) = 0.0691]
Completeness to theta = 25.96°	99.9%
Absorption correction	Semi-empirical from equivalents
Max. and min. transmission	0.7452 and 0.6726
Refinement method	Full-matrix least-squares on F ²
Data / restraints / parameters	5683 / 521 / 460
Goodness-of-fit on F ²	1.053
Final R indices [I > 2σ(I)]	R1 = 0.0457, wR2 = 0.1045
R indices (all data)	R1 = 0.0543, wR2 = 0.1088
Absolute structure parameter	0.018(6)
Largest diff. peak and hole	0.662 and -0.386 e.Å ⁻³

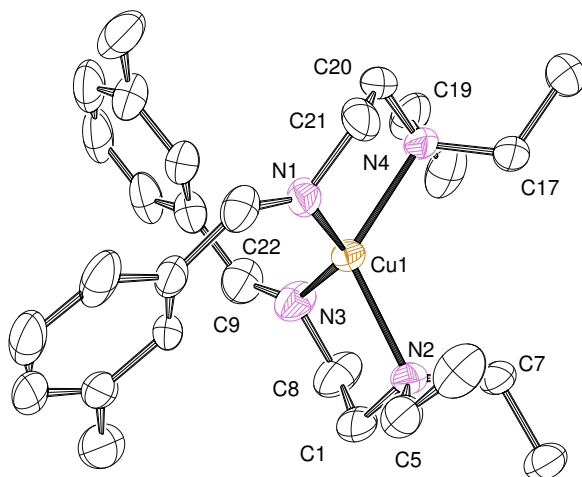


Table 4.12: Selected bond lengths [Å] and angles [°] for [Cu(m-Me-BDED)₂]
CF₃SO₃.

Cu(1)-N(1)	2.018(4)	Cu(1)-N(4)	2.177(4)
Cu(1)-N(3)	2.019(4)	Cu(1)-N(2)	2.191(4)
N(1)-Cu(1)-N(3)	134.28(19)	C(1)-N(2)-Cu(1)	99.8(3)
N(1)-Cu(1)-N(4)	86.33(19)	C(7)-N(2)-Cu(1)	113.7(3)
N(3)-Cu(1)-N(4)	115.7(2)	C(5)-N(2)-Cu(1)	110.9(3)
N(1)-Cu(1)-N(2)	116.98(18)	C(9)-N(3)-Cu(1)	137.6(4)
N(3)-Cu(1)-N(2)	86.63(18)	C(8)-N(3)-Cu(1)	106.8(4)
N(4)-Cu(1)-N(2)	121.06(17)	C(19)-N(4)-Cu(1)	112.1(4)
C(22)-N(1)-Cu(1)	136.9(4)	C(20)-N(4)-Cu(1)	99.4(3)
C(21)-N(1)-Cu(1)	106.9(4)	C(17)-N(4)-Cu(1)	112.0(3)

4.1.3 Computational Details

Total Electronic Energies and Gibbs Free Energies

Table 4.13: Total electronic energies and Gibbs free energies (203 K) of the molecules present in Figure 2.5. Employed DFT method: RI-BLYP-D3/def2-TZVP(SDD)+COSMO(acetone) // BLYP-D2/def2-TZVP(SDD)/auto.

Molecule	E _{Tot} [au]	G ₂₀₃ [au]	Imaginary Frequency
1	-1850.208647	-1849.710507	
TS12	-1850.207357	-1849.708615	<i>i</i> 204
2	-1850.227588	-1849.726182	
TS23	-1850.206165	-1849.705056	<i>i</i> 246
3	-1850.206316	-1849.704837	
TS34	-1850.189241	-1849.690623	<i>i</i> 126
4	-1850.307647	-1849.806281	
TS35	-1850.198696	-1849.703222	<i>i</i> 409
5	-1850.251153	-1849.751598	
TS56	-1850.235161	-1849.740532	<i>i</i> 1103
6	-1850.300625	-1849.800845	

Table 4.14: Total electronic energies and Gibbs free energies (203 K) of the molecules present in Table 2.1. Employed DFT method: RI- BLYP-D3/def2-TZVP(SDD)+COSMO(acetone)//BLYP-D2/def2-TZVP(SDD)/auto.

Molecule	E _{Tot} [au]	G ₂₀₃ [au]	Imaginary Frequency
2-OCH₃	-2079.321966	-2078.761990	
TS35-OCH₃	-2079.300798	-2078.746415	<i>i</i> 868
2-OH	-2000.743607	-2000.235683	
TS35-OH	-2000.720284	-2000.217911	<i>i</i> 865
2-CH₃	-1928.846125	-1928.294675	
TS35-CH₃	-1928.820301	-1928.274375	<i>i</i> 634
2-CH=CH₂	-2005.024034	-2004.462463	
TS35-CH=CH₂	-2004.996852	-2004.440720	<i>i</i> 801
2-F	-2048.794870	-2048.311312	
TS35-F	-2048.765107	-2048.286683	<i>i</i> 707
2-CHO	-2076.950540	-2076.435716	
TS35-CHO	-2076.915208	-2076.405920	<i>i</i> 501
2-CF₃	-2524.579132	-2524.075664	
TS35-CF₃	-2524.540808	-2524.042989	<i>i</i> 312
2-NO₂	-2259.417992	-2258.918237	
TS35-NO₂	-2259.380388	-2258.886410	<i>i</i> 445

Table 4.15: Total electronic energies and Gibbs free energies (203 K) of the molecules present in Figure 2.10. Employed DFT method: RI- BLYP-D3 / def2-TZVP(SDD)+COSMO(acetone) // BLYP-D2 / def2-TZVP(SDD) / auto.

Molecule	E _{Tot} [au]	G ₂₀₃ [au]	Imaginary Frequency
1'	-1621.514572	-1621.051592	
2'	-1621.533721	-1621.065493	
3'	-1621.517569	-1621.049690	
TS34'	-1621.494128	-1621.029223	<i>i</i> 97
TS35'	-1621.506116	-1621.043892	<i>i</i> 67

Cartesian Coordinates of Optimized Structures

DFT method: BLYP-D2/def2-TZVP(SDD)/auto

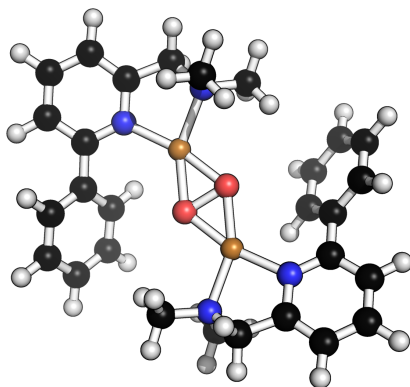
Scheme 3

Figure 4.33: 1.

Table 4.16: 1.

Cu	1.531930000	0.825910000	-0.085080000
Cu	-1.551070000	-0.849617000	-0.064378000
O	0.330153000	-0.694002000	-0.143514000
O	-0.349342000	0.674118000	0.068131000
N	2.009227000	2.814634000	-0.108985000
N	-1.927684000	-2.810257000	-0.518813000
N	3.461772000	0.529645000	-0.371027000
C	6.155491000	0.455663000	-1.056579000
C	4.159496000	-0.632394000	-0.207237000
C	4.084411000	1.650817000	-0.832343000
C	5.433731000	1.651862000	-1.170654000
C	5.516345000	-0.685669000	-0.574009000
H	5.904834000	2.565990000	-1.525847000
H	6.061380000	-1.615183000	-0.432234000
H	7.211087000	0.423735000	-1.320560000
C	3.194932000	2.863951000	-1.029264000
H	3.758500000	3.797294000	-0.879596000
H	2.810692000	2.863470000	-2.059400000
N	-3.512672000	-0.608296000	-0.034106000
C	-6.224349000	-0.618324000	-0.667904000

continue next page

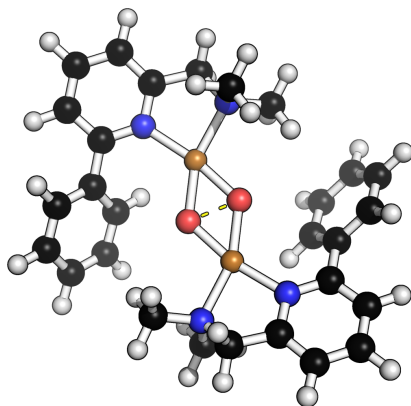
Table 4.16: 1.

C	-4.192911000	0.575008000	-0.080368000
C	-4.168536000	-1.787334000	-0.246219000
C	-5.520117000	-1.827423000	-0.568171000
C	-5.560736000	0.579982000	-0.413714000
H	-6.009807000	-2.783822000	-0.738052000
H	-6.091136000	1.528263000	-0.433822000
H	-7.282621000	-0.617569000	-0.922955000
C	-3.334616000	-3.037878000	-0.050964000
H	-3.778685000	-3.900225000	-0.569477000
H	-3.291571000	-3.270407000	1.022736000
C	3.482619000	-1.797744000	0.400145000
C	2.307012000	-4.035778000	1.632117000
C	3.689442000	-3.089904000	-0.124371000
C	2.683391000	-1.642213000	1.550650000
C	2.104381000	-2.755506000	2.165934000
C	3.095403000	-4.200425000	0.483107000
H	4.306213000	-3.219329000	-1.012414000
H	2.560164000	-0.654211000	1.993402000
H	1.521081000	-2.627879000	3.076455000
H	3.260575000	-5.194247000	0.070687000
H	1.872360000	-4.905907000	2.121887000
C	-0.972301000	-3.761043000	0.126058000
H	0.044099000	-3.516681000	-0.198662000
H	-1.217791000	-4.795128000	-0.162992000
H	-1.039661000	-3.654941000	1.213940000
C	-1.846638000	-2.934329000	-2.010855000
H	-0.829764000	-2.684156000	-2.331035000
H	-2.561685000	-2.243859000	-2.472460000
H	-2.086633000	-3.966841000	-2.308968000
C	2.401176000	3.236743000	1.274212000
H	2.724045000	4.289384000	1.262005000
H	3.223039000	2.604970000	1.628446000
H	1.535176000	3.124944000	1.935137000
C	0.901651000	3.682723000	-0.614506000
H	0.616457000	3.351565000	-1.618927000
H	1.235524000	4.731709000	-0.649817000
H	0.043467000	3.588839000	0.058560000
C	-3.495240000	1.825735000	0.286535000
C	-2.329727000	4.247843000	1.114471000
C	-3.747185000	3.017535000	-0.423557000
C	-2.649353000	1.861289000	1.413857000
C	-2.075113000	3.067328000	1.827264000
C	-3.158808000	4.218804000	-0.017124000
H	-4.399092000	2.998876000	-1.295493000
H	-2.485033000	0.954360000	1.992316000
H	-1.460437000	3.091895000	2.725957000
H	-3.361319000	5.134087000	-0.570408000

continue next page

Table 4.16: **1**.

H	-1.902508000	5.191593000	1.450377000
---	--------------	-------------	-------------

Figure 4.34: **TS12**.Table 4.17: **TS12**.

Cu	1.437764000	0.842147000	-0.087189000
Cu	-1.453655000	-0.859949000	-0.076637000
O	0.401615000	-0.738432000	-0.147947000
O	-0.420435000	0.725900000	0.093307000
N	1.883807000	2.831531000	-0.133730000
N	-1.794957000	-2.817564000	-0.544017000
N	3.376423000	0.580279000	-0.370073000
C	6.063786000	0.534537000	-1.084891000
C	4.089760000	-0.572387000	-0.207521000
C	3.980614000	1.705024000	-0.846344000
C	5.326468000	1.720937000	-1.198312000
C	5.442985000	-0.611401000	-0.589288000
H	5.782301000	2.638646000	-1.564058000
H	6.000297000	-1.533686000	-0.448148000
H	7.116812000	0.513428000	-1.359983000
C	3.073197000	2.902929000	-1.047379000
H	3.619141000	3.846137000	-0.894587000

continue next page

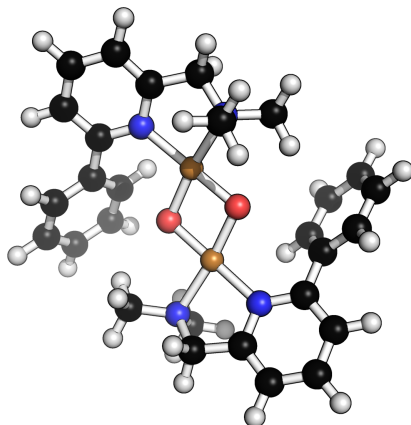
Table 4.17: **TS12.**

H	2.695279000	2.895870000	-2.079791000
N	-3.423650000	-0.665725000	-0.042392000
C	-6.132356000	-0.726167000	-0.688428000
C	-4.126983000	0.503723000	-0.086216000
C	-4.055553000	-1.856008000	-0.263956000
C	-5.404985000	-1.921509000	-0.590832000
C	-5.492973000	0.483646000	-0.426532000
H	-5.875084000	-2.886639000	-0.766533000
H	-6.041611000	1.421502000	-0.444789000
H	-7.189372000	-0.744744000	-0.947946000
C	-3.194126000	-3.087948000	-0.076948000
H	-3.615959000	-3.957038000	-0.602435000
H	-3.144315000	-3.327753000	0.994810000
C	3.439603000	-1.743852000	0.418088000
C	2.346954000	-3.994106000	1.703793000
C	3.665201000	-3.037337000	-0.095823000
C	2.660158000	-1.593281000	1.583073000
C	2.123465000	-2.712666000	2.225324000
C	3.112331000	-4.153996000	0.538354000
H	4.266632000	-3.163304000	-0.994824000
H	2.519904000	-0.602806000	2.014093000
H	1.556075000	-2.587293000	3.146114000
H	3.292529000	-5.148697000	0.134402000
H	1.945470000	-4.868379000	2.214016000
C	-0.806371000	-3.737990000	0.093429000
H	0.200826000	-3.445116000	-0.220438000
H	-1.006711000	-4.776552000	-0.212980000
H	-0.883938000	-3.650110000	1.182001000
C	-1.708908000	-2.926545000	-2.036982000
H	-0.700399000	-2.639572000	-2.352746000
H	-2.446111000	-2.256530000	-2.493773000
H	-1.913658000	-3.964071000	-2.343257000
C	2.253929000	3.277705000	1.247912000
H	2.548628000	4.338299000	1.226962000
H	3.089506000	2.671356000	1.614223000
H	1.385866000	3.148925000	1.902942000
C	0.754546000	3.660641000	-0.655366000
H	0.491352000	3.315023000	-1.660815000
H	1.054560000	4.719597000	-0.691864000
H	-0.106606000	3.540586000	0.009161000
C	-3.460242000	1.767208000	0.295904000
C	-2.384636000	4.214411000	1.175152000
C	-3.741294000	2.960453000	-0.399984000
C	-2.626118000	1.813508000	1.433087000
C	-2.097338000	3.032763000	1.871606000
C	-3.198453000	4.174251000	0.032187000
H	-4.382892000	2.934393000	-1.279291000

continue next page

Table 4.17: **TS12**.

H	−2.442757000	0.905427000	2.002967000
H	−1.492793000	3.063173000	2.776858000
H	−3.425030000	5.090729000	−0.509714000
H	−1.993892000	5.166785000	1.530358000

Figure 4.35: **2**.Table 4.18: **2**.

Cu	1.083645000	0.865931000	−0.116036000
Cu	−1.107246000	−0.936653000	−0.078973000
O	0.709812000	−0.926994000	−0.171315000
O	−0.724973000	0.847472000	0.140311000
N	1.271158000	2.875302000	−0.178680000
N	−1.208983000	−2.905330000	−0.515290000
N	3.034084000	0.883060000	−0.448634000
C	5.629470000	1.142263000	−1.412488000
C	3.908925000	−0.152308000	−0.286350000
C	3.439191000	2.046293000	−1.033072000
C	4.734135000	2.216104000	−1.510759000
C	5.214789000	−0.037989000	−0.797745000
H	5.029811000	3.162836000	−1.957802000

continue next page

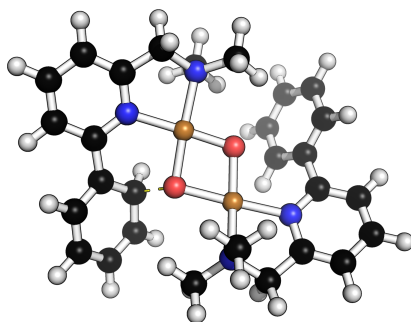
Table 4.18: **2.**

H	5.902000000	-0.868612000	-0.659306000
H	6.646759000	1.238275000	-1.787782000
C	2.365110000	3.098833000	-1.184606000
H	2.775519000	4.114192000	-1.078248000
H	1.912927000	3.018907000	-2.183370000
N	-3.096686000	-0.969401000	-0.116366000
C	-5.699089000	-1.292752000	-1.067784000
C	-3.924931000	0.115343000	-0.184377000
C	-3.570717000	-2.210898000	-0.442074000
C	-4.860396000	-2.407262000	-0.919658000
C	-5.232214000	-0.037923000	-0.686703000
H	-5.199894000	-3.410086000	-1.168929000
H	-5.878318000	0.835013000	-0.729553000
H	-6.711248000	-1.411190000	-1.450448000
C	-2.606657000	-3.340937000	-0.180519000
H	-2.868100000	-4.245464000	-0.747460000
H	-2.628705000	-3.588429000	0.890257000
C	3.501782000	-1.344169000	0.485682000
C	2.908370000	-3.597953000	2.056071000
C	3.867494000	-2.632928000	0.045673000
C	2.836734000	-1.199505000	1.721893000
C	2.550391000	-2.319374000	2.505285000
C	3.560048000	-3.753393000	0.821389000
H	4.384229000	-2.752120000	-0.905430000
H	2.581982000	-0.204150000	2.081631000
H	2.069819000	-2.194470000	3.474117000
H	3.844833000	-4.745434000	0.475202000
H	2.700185000	-4.470652000	2.673177000
C	-0.191074000	-3.711754000	0.224923000
H	0.803336000	-3.314841000	0.000842000
H	-0.261298000	-4.763360000	-0.092241000
H	-0.382724000	-3.631180000	1.299632000
C	-0.960668000	-2.996769000	-1.992725000
H	0.032196000	-2.584776000	-2.196335000
H	-1.724897000	-2.419622000	-2.525650000
H	-1.009927000	-4.051443000	-2.302418000
C	1.687368000	3.343339000	1.184082000
H	1.845786000	4.432003000	1.160955000
H	2.614853000	2.839738000	1.475232000
H	0.888650000	3.098879000	1.891488000
C	0.016623000	3.572520000	-0.594925000
H	-0.283654000	3.209480000	-1.582443000
H	0.201260000	4.657188000	-0.627930000
H	-0.770124000	3.346678000	0.129813000
C	-3.488117000	1.416830000	0.360987000
C	-2.919342000	3.893036000	1.568669000
C	-2.832952000	1.470513000	1.612755000

continue next page

Table 4.18: **2**.

C	−3.842172000	2.619477000	−0.283249000
C	−3.549829000	3.848672000	0.311780000
C	−2.561668000	2.704471000	2.215054000
H	−2.592644000	0.546045000	2.131278000
H	−4.344748000	2.587846000	−1.248509000
H	−3.829883000	4.772963000	−0.190483000
H	−2.096172000	2.733558000	3.198798000
H	−2.726724000	4.853230000	2.044747000

Figure 4.36: **TS23**.Table 4.19: **TS23**.

Cu	−1.204535000	−0.775422000	−0.318329000
Cu	1.144356000	0.908664000	−0.035036000
O	−0.843855000	1.035469000	0.173540000
O	0.587480000	−0.850228000	−0.214337000
N	−1.461793000	−2.746249000	−0.653921000
N	1.554111000	2.824705000	−0.674407000
N	−3.164813000	−0.674848000	−0.317011000
C	−5.922894000	−0.762764000	−0.633355000
C	−3.906452000	0.428040000	0.008692000
C	−3.759387000	−1.794267000	−0.807728000
C	−5.142713000	−1.881179000	−0.955728000
C	−5.303939000	0.396004000	−0.164568000
H	−5.595120000	−2.798702000	−1.325951000

continue next page

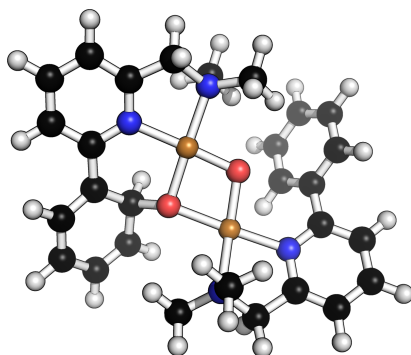
Table 4.19: **TS23**.

H	-5.892773000	1.268290000	0.105297000
H	-7.005332000	-0.798959000	-0.741914000
C	-2.818282000	-2.882682000	-1.283040000
H	-3.227192000	-3.884719000	-1.085649000
H	-2.692231000	-2.780900000	-2.370521000
N	3.156726000	0.677094000	-0.062045000
C	5.806201000	0.569133000	-0.920500000
C	3.829261000	-0.508899000	-0.008927000
C	3.800084000	1.808451000	-0.466784000
C	5.119860000	1.791459000	-0.905926000
C	5.162451000	-0.576339000	-0.457338000
H	5.596830000	2.713969000	-1.229692000
H	5.685786000	-1.527094000	-0.397102000
H	6.837079000	0.519952000	-1.266701000
C	2.994138000	3.080202000	-0.345852000
H	3.396553000	3.876853000	-0.989392000
H	3.036234000	3.429589000	0.695977000
C	-3.218821000	1.609171000	0.552731000
C	-2.035558000	3.876051000	1.797605000
C	-3.714085000	2.895821000	0.309341000
C	-2.002215000	1.446870000	1.360420000
C	-1.495952000	2.633397000	2.036633000
C	-3.134258000	4.018310000	0.911786000
H	-4.567372000	3.028616000	-0.353044000
H	-1.958398000	0.532580000	1.957955000
H	-0.668973000	2.505072000	2.732709000
H	-3.546799000	5.006172000	0.715548000
H	-1.636488000	4.754299000	2.302385000
C	0.704323000	3.942099000	-0.174541000
H	-0.339264000	3.719124000	-0.408624000
H	1.006571000	4.884247000	-0.659381000
H	0.825131000	4.028145000	0.909288000
C	1.380269000	2.704954000	-2.161856000
H	0.332465000	2.467249000	-2.371340000
H	2.026230000	1.906519000	-2.543751000
H	1.651044000	3.659129000	-2.640981000
C	-1.438162000	-3.362150000	0.714707000
H	-1.607623000	-4.445958000	0.625754000
H	-2.228303000	-2.914951000	1.328475000
H	-0.455486000	-3.169913000	1.157790000
C	-0.397193000	-3.366431000	-1.503422000
H	-0.404291000	-2.890701000	-2.489372000
H	-0.595488000	-4.444634000	-1.603226000
H	0.567511000	-3.196923000	-1.015868000
C	3.183750000	-1.688940000	0.601974000
C	2.109800000	-3.950437000	1.877533000
C	2.484759000	-1.556493000	1.819251000

continue next page

Table 4.19: **TS23**.

C	3.342218000	−2.967704000	0.031982000
C	2.794643000	−4.090034000	0.659502000
C	1.960940000	−2.682388000	2.457996000
H	2.388020000	−0.572565000	2.274009000
H	3.884903000	−3.076803000	−0.905847000
H	2.921380000	−5.075234000	0.213734000
H	1.457991000	−2.576804000	3.418025000
H	1.717265000	−4.831323000	2.383564000

Figure 4.37: **3**.Table 4.20: **3**.

Cu	−1.233939000	−0.746044000	−0.380149000
Cu	1.165481000	0.897037000	−0.068586000
O	−0.879256000	1.091883000	0.108290000
O	0.557459000	−0.842427000	−0.283782000
N	−1.532552000	−2.711193000	−0.715762000
N	1.647979000	2.798949000	−0.725481000
N	−3.188006000	−0.614488000	−0.312964000
C	−5.953952000	−0.649045000	−0.543870000
C	−3.897063000	0.499569000	0.051024000
C	−3.815796000	−1.715399000	−0.801088000
C	−5.204489000	−1.776548000	−0.907398000
C	−5.301577000	0.492132000	−0.078810000

continue next page

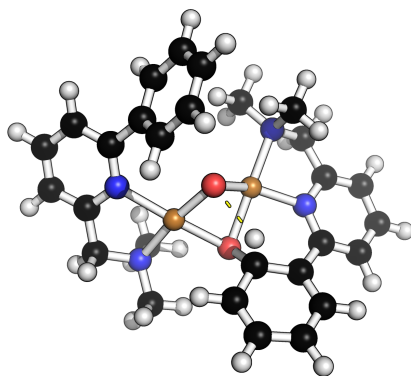
Table 4.20: **3.**

H	-5.685057000	-2.680784000	-1.274754000
H	-5.870357000	1.367750000	0.220810000
H	-7.039728000	-0.664979000	-0.618344000
C	-2.905868000	-2.814216000	-1.314656000
H	-3.328727000	-3.811207000	-1.120629000
H	-2.803647000	-2.699619000	-2.403385000
N	3.173173000	0.610678000	-0.042219000
C	5.833376000	0.411704000	-0.848171000
C	3.808715000	-0.593644000	0.041490000
C	3.856640000	1.716249000	-0.451756000
C	5.183457000	1.653597000	-0.865513000
C	5.147554000	-0.706938000	-0.380020000
H	5.693150000	2.556435000	-1.194863000
H	5.641620000	-1.671392000	-0.295180000
H	6.868521000	0.326622000	-1.174085000
C	3.087302000	3.013706000	-0.368362000
H	3.529959000	3.787067000	-1.014026000
H	3.117259000	3.377799000	0.668884000
C	-3.169618000	1.654134000	0.591298000
C	-1.872250000	3.875084000	1.830635000
C	-3.682003000	2.948176000	0.456676000
C	-1.856795000	1.448675000	1.272619000
C	-1.302374000	2.635932000	1.956053000
C	-3.053939000	4.044712000	1.057710000
H	-4.586903000	3.113001000	-0.124929000
H	-1.847583000	0.559586000	1.920189000
H	-0.402812000	2.485943000	2.550948000
H	-3.485084000	5.037534000	0.943303000
H	-1.432523000	4.736631000	2.330616000
C	0.828843000	3.959287000	-0.272647000
H	-0.217517000	3.767744000	-0.522344000
H	1.173885000	4.877164000	-0.775470000
H	0.931705000	4.071323000	0.810566000
C	1.505745000	2.653973000	-2.214261000
H	0.455128000	2.451900000	-2.446545000
H	2.129381000	1.823604000	-2.563692000
H	1.823887000	3.586635000	-2.706759000
C	-1.494019000	-3.333056000	0.649447000
H	-1.685320000	-4.413181000	0.559242000
H	-2.264117000	-2.873734000	1.279473000
H	-0.500618000	-3.160441000	1.075747000
C	-0.498215000	-3.347544000	-1.589906000
H	-0.518323000	-2.869302000	-2.574507000
H	-0.716288000	-4.422117000	-1.688019000
H	0.478563000	-3.193328000	-1.121724000
C	3.116707000	-1.743890000	0.657387000
C	1.952815000	-3.952038000	1.946388000

continue next page

Table 4.20: **3**.

C	2.397288000	-1.570795000	1.857109000
C	3.249041000	-3.035565000	0.111100000
C	2.656952000	-4.131475000	0.745166000
C	1.828447000	-2.670331000	2.502822000
H	2.322135000	-0.577316000	2.295196000
H	3.806770000	-3.175297000	-0.813726000
H	2.764228000	-5.127222000	0.318142000
H	1.309484000	-2.535018000	3.450566000
H	1.524895000	-4.812566000	2.458731000

Figure 4.38: **TS34 (broken-symmetry singlet geometry)**.Table 4.21: **TS34 (broken-symmetry singlet geometry)**.

Cu	1.038861000	0.668713000	-0.321370000
Cu	-1.023857000	-1.094523000	0.056561000
O	1.035039000	-1.422700000	-0.362759000
O	-0.299792000	0.385556000	0.937751000
N	1.163848000	2.675845000	-0.873654000
N	-1.532760000	-2.795278000	-1.030320000
N	2.984857000	0.678653000	-0.650326000
C	5.680868000	0.884356000	-1.222413000
C	3.827991000	-0.285659000	-0.172401000
C	3.444987000	1.757937000	-1.316233000

continue next page

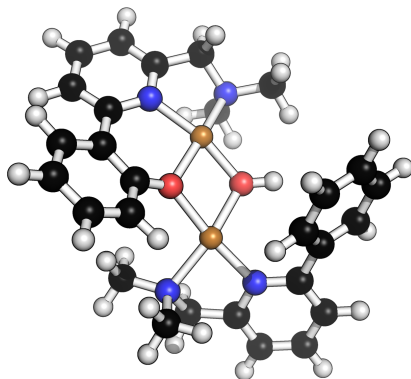
Table 4.21: **TS34 (broken-symmetry singlet geometry).**

C	4.802014000	1.900400000	-1.618454000
C	5.200752000	-0.204061000	-0.491151000
H	5.156137000	2.773680000	-2.162623000
H	5.887222000	-0.985778000	-0.181004000
H	6.738855000	0.947052000	-1.470045000
C	2.378902000	2.752836000	-1.752162000
H	2.782562000	3.777200000	-1.763735000
H	2.067641000	2.504653000	-2.777409000
N	-3.070182000	-0.699342000	-0.081751000
C	-5.641471000	-0.316174000	-1.118380000
C	-3.697302000	0.501833000	0.093281000
C	-3.726477000	-1.710131000	-0.720991000
C	-5.003464000	-1.556340000	-1.250817000
C	-4.986649000	0.707266000	-0.440257000
H	-5.483274000	-2.391244000	-1.756985000
H	-5.470350000	1.666534000	-0.275938000
H	-6.639864000	-0.160645000	-1.523442000
C	-2.989586000	-3.028246000	-0.790411000
H	-3.413299000	-3.679003000	-1.570007000
H	-3.085942000	-3.546508000	0.174885000
C	3.271786000	-1.332709000	0.707986000
C	2.288640000	-3.422882000	2.449358000
C	4.122203000	-2.053202000	1.552266000
C	1.792433000	-1.589377000	0.821035000
C	1.397405000	-2.743604000	1.654826000
C	3.656509000	-3.069390000	2.400404000
H	5.186343000	-1.832380000	1.566457000
H	1.370271000	-0.737757000	1.531771000
H	0.333142000	-2.967712000	1.675412000
H	4.370904000	-3.596214000	3.031311000
H	1.955147000	-4.228026000	3.101456000
C	-0.746485000	-4.019876000	-0.708088000
H	0.315743000	-3.791325000	-0.840358000
H	-1.036666000	-4.845419000	-1.377106000
H	-0.943401000	-4.313128000	0.329468000
C	-1.288809000	-2.420158000	-2.460453000
H	-0.223639000	-2.194821000	-2.579889000
H	-1.889732000	-1.538827000	-2.712914000
H	-1.569552000	-3.255460000	-3.121199000
C	1.368891000	3.442576000	0.396150000
H	1.489885000	4.513629000	0.169137000
H	2.266245000	3.069712000	0.902724000
H	0.494066000	3.287441000	1.036523000
C	-0.045161000	3.187986000	-1.581863000
H	-0.204175000	2.602555000	-2.495034000
H	0.087965000	4.249803000	-1.845716000
H	-0.905556000	3.083191000	-0.912398000

continue next page

Table 4.21: **TS34 (broken-symmetry singlet geometry)**.

C	-3.063722000	1.572404000	0.891631000
C	-2.019568000	3.643140000	2.485094000
C	-2.472005000	1.284621000	2.137731000
C	-3.135276000	2.911171000	0.457306000
C	-2.604380000	3.939397000	1.243171000
C	-1.961815000	2.317333000	2.932044000
H	-2.447150000	0.258378000	2.493564000
H	-3.604848000	3.144252000	-0.497594000
H	-2.666041000	4.970713000	0.899391000
H	-1.529896000	2.086252000	3.903959000
H	-1.633431000	4.447037000	3.109954000

Figure 4.39: **4.**Table 4.22: **4.**

Cu	1.380337000	-1.065776000	-0.106263000
Cu	-1.183029000	0.734669000	-0.201756000
O	0.809757000	0.799636000	0.240511000
O	-0.527508000	-1.153852000	-0.286281000
N	1.973077000	-2.872857000	-0.869616000
N	-1.599143000	2.681209000	-0.885147000
N	3.285722000	-0.559822000	-0.102524000
C	5.834653000	-0.018574000	-1.065310000

continue next page

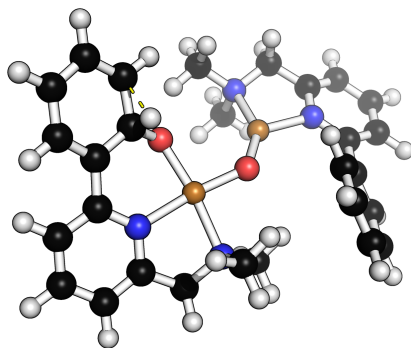
Table 4.22: 4.

C	3.769640000	0.718455000	0.002041000
C	4.060759000	-1.562738000	-0.609207000
C	5.341951000	-1.332850000	-1.091455000
C	5.056085000	0.995376000	-0.519194000
H	5.935861000	-2.156050000	-1.481988000
H	5.425019000	2.016302000	-0.507567000
H	6.819457000	0.207795000	-1.470029000
C	3.437672000	-2.940223000	-0.529877000
H	3.950994000	-3.656387000	-1.187753000
H	3.516222000	-3.303990000	0.504460000
N	-3.137465000	0.456918000	-0.579167000
C	-5.747528000	0.257523000	-1.509890000
C	-3.941254000	-0.531590000	-0.097807000
C	-3.610498000	1.353311000	-1.483480000
C	-4.916026000	1.291422000	-1.963093000
C	-5.258494000	-0.654829000	-0.574365000
H	-5.270007000	2.030844000	-2.678454000
H	-5.892190000	-1.442516000	-0.174660000
H	-6.772284000	0.179664000	-1.868732000
C	-2.596743000	2.370599000	-1.966825000
H	-3.091434000	3.293517000	-2.306785000
H	-2.038570000	1.951751000	-2.816780000
C	2.993108000	1.757173000	0.709289000
C	1.647045000	3.660323000	2.345252000
C	3.688501000	2.796333000	1.371066000
C	1.569455000	1.711423000	0.875919000
C	0.931544000	2.638036000	1.729122000
C	3.036939000	3.746382000	2.157413000
H	4.773553000	2.831523000	1.312535000
H	-0.139258000	2.524784000	1.883970000
H	-1.086776000	-1.900960000	-0.001528000
H	3.613250000	4.521817000	2.656819000
H	1.135438000	4.373000000	2.990025000
C	-0.418306000	3.387430000	-1.461818000
H	0.299292000	3.585965000	-0.659095000
H	-0.730815000	4.341298000	-1.916226000
H	0.044042000	2.750303000	-2.223660000
C	-2.242950000	3.542268000	0.155559000
H	-1.505405000	3.785352000	0.924937000
H	-3.087899000	3.008111000	0.602726000
H	-2.601024000	4.475674000	-0.307332000
C	1.786258000	-2.793838000	-2.355083000
H	2.146051000	-3.723562000	-2.822785000
H	2.356502000	-1.943365000	-2.745947000
H	0.721494000	-2.654246000	-2.565694000
C	1.243760000	-4.057150000	-0.325091000
H	1.342651000	-4.072546000	0.765883000

continue next page

Table 4.22: 4.

H	1.662536000	-4.984080000	-0.747825000
H	0.188427000	-3.975522000	-0.604161000
C	-3.399616000	-1.433747000	0.941701000
C	-2.362307000	-3.150139000	2.914900000
C	-3.606844000	-2.825145000	0.854255000
C	-2.678486000	-0.912457000	2.035852000
C	-2.166639000	-1.764705000	3.017819000
C	-3.081404000	-3.678328000	1.832303000
H	-4.166543000	-3.235051000	0.014640000
H	-2.551169000	0.165867000	2.130093000
H	-1.634844000	-1.350378000	3.872598000
H	-3.245375000	-4.751905000	1.756603000
H	-1.974100000	-3.813748000	3.685764000

Figure 4.40: **TS35**.Table 4.23: **TS35**.

Cu	1.361953000	0.466596000	-0.123517000
Cu	-1.551017000	-0.891657000	-0.037736000
O	1.746254000	-1.417888000	-0.057259000
O	-0.366134000	0.334225000	0.411839000
N	1.132943000	2.518425000	-0.483846000
N	-1.900346000	-2.743089000	-0.958222000
N	3.322590000	0.896096000	-0.489101000

continue next page

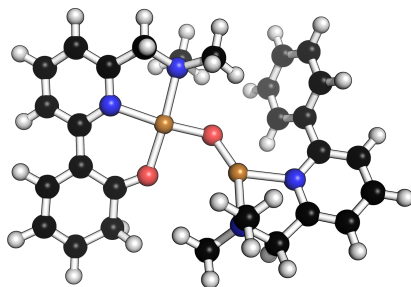
Table 4.23: **TS35.**

C	5.867437000	1.699126000	-1.297565000
C	4.394433000	0.085417000	-0.230593000
C	3.503806000	2.090189000	-1.097378000
C	4.767725000	2.533426000	-1.502717000
C	5.681189000	0.470809000	-0.660828000
H	4.874445000	3.503645000	-1.984039000
H	6.531983000	-0.187724000	-0.519947000
H	6.860689000	1.998794000	-1.626381000
C	2.251819000	2.893943000	-1.392012000
H	2.461023000	3.973866000	-1.331551000
H	1.937468000	2.675177000	-2.423308000
N	-3.573235000	-0.842710000	0.061962000
C	-6.319617000	-0.947870000	-0.395881000
C	-4.323823000	0.281578000	0.237864000
C	-4.166277000	-2.007607000	-0.314633000
C	-5.533977000	-2.097716000	-0.555735000
C	-5.712187000	0.240946000	0.004398000
H	-5.970425000	-3.044559000	-0.866562000
H	-6.298174000	1.141667000	0.167401000
H	-7.392761000	-0.984224000	-0.574786000
C	-3.228338000	-3.190826000	-0.429390000
H	-3.658522000	-3.981244000	-1.063878000
H	-3.058863000	-3.610905000	0.572769000
C	4.179477000	-1.185230000	0.492258000
C	3.878876000	-3.748108000	1.822479000
C	5.253276000	-1.856417000	1.089962000
C	2.812852000	-1.785683000	0.656451000
C	2.755734000	-3.128198000	1.295116000
C	5.122421000	-3.109638000	1.712725000
H	6.243905000	-1.409863000	1.071438000
H	2.693806000	-1.493898000	1.811423000
H	1.753990000	-3.541209000	1.395225000
H	6.008991000	-3.578544000	2.136751000
H	3.789803000	-4.713514000	2.317169000
C	-0.845673000	-3.754294000	-0.663946000
H	0.115826000	-3.362505000	-1.012328000
H	-1.071704000	-4.708849000	-1.168171000
H	-0.804170000	-3.915963000	0.419875000
C	-1.986120000	-2.522639000	-2.435203000
H	-1.019313000	-2.153158000	-2.793899000
H	-2.763514000	-1.779858000	-2.646177000
H	-2.232667000	-3.468181000	-2.945749000
C	1.274117000	3.169083000	0.854336000
H	1.183998000	4.261871000	0.748432000
H	2.252196000	2.920072000	1.281894000
H	0.473756000	2.787126000	1.495097000
C	-0.189681000	2.873158000	-1.073624000

continue next page

Table 4.23: **TS35**.

H	-0.288886000	2.385445000	-2.049361000
H	-0.260914000	3.966166000	-1.190340000
H	-0.968832000	2.511252000	-0.397994000
C	-3.670579000	1.527378000	0.701959000
C	-2.547883000	3.922199000	1.664026000
C	-2.729612000	1.502580000	1.749764000
C	-4.040324000	2.766502000	0.139832000
C	-3.474226000	3.955316000	0.611239000
C	-2.179868000	2.694771000	2.231230000
H	-2.452464000	0.555104000	2.204656000
H	-4.765228000	2.794549000	-0.672356000
H	-3.765255000	4.905725000	0.167243000
H	-1.481789000	2.664827000	3.066445000
H	-2.130053000	4.850775000	2.050330000

Figure 4.41: **5**.Table 4.24: **5**.

Cu	1.334182000	-0.574335000	0.079075000
Cu	-1.496707000	0.902582000	-0.026582000
O	1.748823000	1.252805000	-0.523820000
O	-0.424641000	-0.450800000	-0.380068000
N	1.051470000	-2.579624000	0.554526000
N	-1.779424000	2.843969000	0.704477000
N	3.287700000	-0.972811000	0.463048000
C	5.828194000	-2.119476000	0.431844000
C	4.354756000	-0.215545000	0.075100000

continue next page

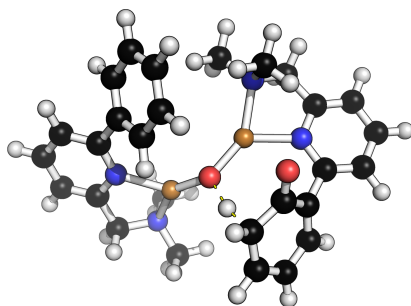
Table 4.24: 5.

C	3.477677000	-2.254171000	0.883618000
C	4.731894000	-2.856806000	0.893359000
C	5.637998000	-0.802885000	0.021184000
H	4.840291000	-3.884733000	1.232184000
H	6.481322000	-0.238870000	-0.364938000
H	6.817919000	-2.569743000	0.383358000
C	2.235323000	-2.960324000	1.380130000
H	2.371781000	-4.052216000	1.377495000
H	2.034345000	-2.644303000	2.414036000
N	-3.523764000	0.911153000	-0.109756000
C	-6.258943000	1.172747000	0.354251000
C	-4.317947000	-0.195589000	-0.157161000
C	-4.069590000	2.133244000	0.135782000
C	-5.429657000	2.302848000	0.374502000
C	-5.700962000	-0.075046000	0.084608000
H	-5.826848000	3.294872000	0.578737000
H	-6.321883000	-0.965124000	0.025918000
H	-7.327540000	1.269731000	0.537730000
C	-3.086034000	3.282952000	0.115995000
H	-3.483183000	4.158563000	0.652303000
H	-2.895016000	3.575603000	-0.926770000
C	4.165534000	1.215089000	-0.284411000
C	4.092782000	4.027762000	-1.091288000
C	5.245683000	2.091192000	-0.214755000
C	2.881169000	1.800674000	-0.646693000
C	2.858530000	3.203772000	-1.232536000
C	5.224762000	3.476370000	-0.588742000
H	6.189119000	1.717738000	0.179200000
H	2.652559000	3.071920000	-2.315161000
H	1.969485000	3.732210000	-0.855352000
H	6.135284000	4.060211000	-0.472725000
H	4.057347000	5.065834000	-1.419234000
C	-0.693762000	3.790519000	0.326466000
H	0.247479000	3.424735000	0.751884000
H	-0.905664000	4.800923000	0.714250000
H	-0.615130000	3.824411000	-0.766332000
C	-1.888945000	2.771894000	2.195571000
H	-0.940871000	2.403630000	2.602676000
H	-2.694388000	2.080537000	2.466270000
H	-2.105975000	3.770298000	2.609007000
C	1.064550000	-3.280137000	-0.767661000
H	0.947790000	-4.364058000	-0.610261000
H	2.014745000	-3.083264000	-1.277807000
H	0.229912000	-2.892209000	-1.357164000
C	-0.227391000	-2.865719000	1.263850000
H	-0.226282000	-2.344154000	2.227036000
H	-0.318178000	-3.951427000	1.424594000

continue next page

Table 4.24: **5**.

H	-1.048989000	-2.502179000	0.641435000
C	-3.727866000	-1.507196000	-0.506660000
C	-2.763441000	-4.033987000	-1.281367000
C	-2.827294000	-1.625687000	-1.583387000
C	-4.134365000	-2.668377000	0.182227000
C	-3.644668000	-3.922573000	-0.195220000
C	-2.359690000	-2.884616000	-1.973427000
H	-2.522334000	-0.739218000	-2.133402000
H	-4.828816000	-2.584808000	1.016945000
H	-3.962194000	-4.812109000	0.346078000
H	-1.698157000	-2.967612000	-2.834339000
H	-2.409812000	-5.014787000	-1.595961000

Figure 4.42: **TS56**.Table 4.25: **TS56**.

Cu	1.280117000	0.565950000	-0.205737000
Cu	-1.528606000	-1.079725000	-0.085847000
O	2.802981000	0.105477000	2.217061000
O	0.019192000	-0.462838000	0.605322000
N	1.777363000	2.417961000	-0.937072000
N	-2.432117000	-2.652876000	-1.092015000
N	3.225653000	0.181329000	-0.674396000
C	5.858415000	-0.148073000	-1.472430000
C	3.936968000	-0.882882000	-0.200841000
C	3.798841000	1.091837000	-1.488065000

continue next page

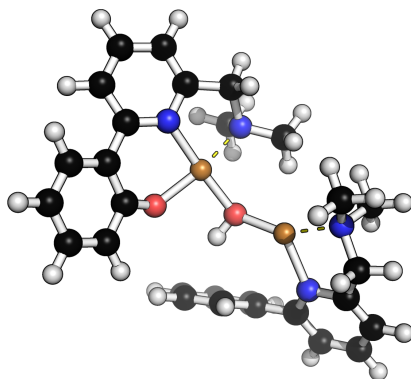
Table 4.25: **TS56.**

C	5.126460000	0.962972000	-1.905451000
C	5.263177000	-1.077601000	-0.611289000
H	5.568245000	1.710155000	-2.561577000
H	5.828291000	-1.916772000	-0.213131000
H	6.893848000	-0.277222000	-1.782676000
C	2.871935000	2.198854000	-1.945862000
H	3.421659000	3.136321000	-2.120003000
H	2.396139000	1.904554000	-2.892454000
N	-3.399320000	-0.292067000	-0.076991000
C	-6.035943000	0.501431000	-0.519663000
C	-3.754209000	1.006498000	0.154558000
C	-4.335915000	-1.192819000	-0.488116000
C	-5.657909000	-0.831244000	-0.727416000
C	-5.084650000	1.414173000	-0.071263000
H	-6.372083000	-1.578249000	-1.067285000
H	-5.360149000	2.443174000	0.142838000
H	-7.063244000	0.817541000	-0.692140000
C	-3.853477000	-2.621224000	-0.620263000
H	-4.499984000	-3.199240000	-1.297867000
H	-3.882973000	-3.100614000	0.369195000
C	3.232368000	-1.746579000	0.763445000
C	1.398981000	-3.252141000	2.345023000
C	3.150510000	-3.115961000	0.651640000
C	2.537285000	-1.057230000	1.883188000
C	1.381666000	-1.809531000	2.456577000
C	2.269489000	-3.884749000	1.480776000
H	3.730418000	-3.628439000	-0.117321000
H	0.977273000	-1.387392000	3.383681000
H	0.594655000	-1.272715000	1.569967000
H	2.271948000	-4.969434000	1.393489000
H	0.714984000	-3.839153000	2.957282000
C	-1.818651000	-3.986501000	-0.813306000
H	-0.778700000	-3.974952000	-1.156987000
H	-2.369069000	-4.779158000	-1.345632000
H	-1.851625000	-4.179941000	0.264669000
C	-2.374237000	-2.367157000	-2.561717000
H	-1.326312000	-2.352798000	-2.880846000
H	-2.834683000	-1.393115000	-2.761214000
H	-2.915476000	-3.150024000	-3.116572000
C	2.306018000	3.178923000	0.244930000
H	2.682479000	4.159273000	-0.087275000
H	3.109901000	2.604903000	0.717951000
H	1.488379000	3.317934000	0.958880000
C	0.641150000	3.163396000	-1.556947000
H	0.251003000	2.586131000	-2.402946000
H	0.985709000	4.147952000	-1.913489000
H	-0.140166000	3.303324000	-0.804257000

continue next page

Table 4.25: **TS56**.

C	-2.763186000	1.970299000	0.687644000
C	-1.033747000	3.878448000	1.832735000
C	-1.850359000	1.597153000	1.694246000
C	-2.796972000	3.316913000	0.263250000
C	-1.940330000	4.263203000	0.833032000
C	-0.986264000	2.543102000	2.256458000
H	-1.847342000	0.579181000	2.072717000
H	-3.496810000	3.620455000	-0.513548000
H	-1.985754000	5.299984000	0.504174000
H	-0.302537000	2.243856000	3.049016000
H	-0.384748000	4.621367000	2.294153000

Figure 4.43: **6**.Table 4.26: **6**.

Cu	-1.509153000	-0.328985000	0.416428000
Cu	1.775211000	-0.729393000	-0.444458000
O	-1.863859000	1.507869000	0.079414000
O	0.362288000	0.037810000	0.524094000
N	-1.366067000	-2.120948000	1.472298000
N	2.680297000	-2.293759000	-1.464386000
N	-3.404710000	-0.845968000	0.149499000
C	-6.062701000	-1.516079000	0.628198000

continue next page

Table 4.26: 6.

C	-4.388155000	0.019115000	-0.258107000
C	-3.723811000	-2.031647000	0.742653000
C	-5.037196000	-2.403734000	0.993561000
C	-5.739070000	-0.318297000	0.004853000
H	-5.253954000	-3.362819000	1.458683000
H	-6.519872000	0.391511000	-0.250189000
H	-7.102492000	-1.759104000	0.839334000
C	-2.542988000	-2.934862000	1.017381000
H	-2.788026000	-3.708353000	1.759755000
H	-2.253058000	-3.434631000	0.081733000
N	3.657027000	0.125663000	-0.520238000
C	6.404040000	0.530428000	-0.313155000
C	4.128614000	1.124964000	0.274269000
C	4.520591000	-0.640701000	-1.236450000
C	5.900134000	-0.469826000	-1.157486000
C	5.514793000	1.334014000	0.399877000
H	6.563305000	-1.106549000	-1.739396000
H	5.872019000	2.144450000	1.030295000
H	7.477802000	0.686824000	-0.225837000
C	3.864022000	-1.661910000	-2.144238000
H	4.581189000	-2.434190000	-2.460864000
H	3.488739000	-1.151106000	-3.042469000
C	-4.041168000	1.259131000	-0.963063000
C	-3.388068000	3.606988000	-2.439306000
C	-4.962747000	1.843701000	-1.853702000
C	-2.748344000	1.894913000	-0.812957000
C	-2.439325000	3.045666000	-1.599273000
C	-4.654591000	3.000327000	-2.575422000
H	-5.923455000	1.364311000	-2.026578000
H	-1.456384000	3.493924000	-1.470528000
H	-5.386680000	3.413786000	-3.265887000
H	-3.152360000	4.506705000	-3.005116000
C	1.824876000	-2.982846000	-2.477412000
H	0.974346000	-3.448036000	-1.965437000
H	2.397786000	-3.764946000	-3.001801000
H	1.461297000	-2.247876000	-3.204344000
C	3.167785000	-3.296794000	-0.462536000
H	2.307210000	-3.743528000	0.046109000
H	3.808614000	-2.795533000	0.271485000
H	3.741898000	-4.088618000	-0.969713000
C	-1.511823000	-1.734528000	2.913939000
H	-1.487080000	-2.636242000	3.545702000
H	-2.466833000	-1.215779000	3.053198000
H	-0.685469000	-1.067566000	3.180482000
C	-0.093652000	-2.854809000	1.267065000
H	0.032893000	-3.060561000	0.196952000
H	-0.103205000	-3.804009000	1.826359000

continue next page

Table 4.26: **6**.

H	0.730392000	−2.227906000	1.623760000
C	3.151214000	2.004694000	0.953455000
C	1.318556000	3.729059000	2.215005000
C	2.061255000	2.538641000	0.232365000
C	3.324224000	2.362368000	2.302843000
C	2.406452000	3.212904000	2.931509000
C	1.151606000	3.397138000	0.861460000
H	1.956143000	2.304488000	−0.826096000
H	4.167471000	1.961087000	2.863188000
H	2.544071000	3.475865000	3.978798000
H	0.323691000	3.819398000	0.295471000
H	0.614855000	4.401745000	2.701989000
H	0.439054000	1.017745000	0.553575000

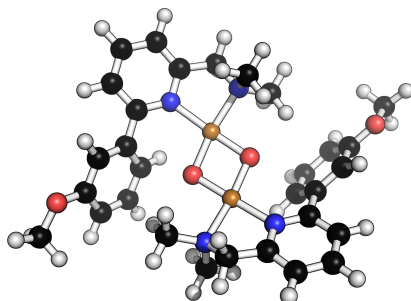
Figure 4.44: **2–OCH₃**.

Table 1

Table 4.27: **2–OCH₃**.

Cu	−0.398270000	−1.342385000	−0.016083000
Cu	0.390241000	1.385866000	−0.012548000
O	−1.108458000	0.348851000	−0.025323000
O	1.080281000	−0.298148000	0.327833000
N	0.592953000	−3.108223000	−0.104205000
N	−0.652279000	3.037157000	−0.568084000
N	−1.995118000	−2.453836000	−0.468974000
C	−3.936323000	−4.155228000	−1.515887000

continue next page

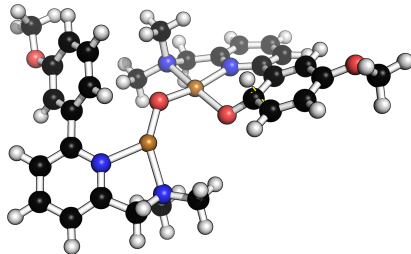
Table 4.27: **2-OCH₃**.

C	-3.309939000	-2.095954000	-0.388713000
C	-1.642130000	-3.642532000	-1.032881000
C	-2.585967000	-4.525524000	-1.548509000
C	-4.294203000	-2.939056000	-0.936484000
H	-2.266987000	-5.473801000	-1.975918000
H	-5.336458000	-2.641700000	-0.856851000
H	-4.699706000	-4.818381000	-1.918872000
C	-0.155260000	-3.895724000	-1.139310000
H	0.078856000	-4.967076000	-1.046109000
H	0.196539000	-3.557920000	-2.124651000
N	2.010201000	2.559605000	-0.134680000
C	3.945262000	4.311764000	-1.125668000
C	3.312481000	2.154535000	-0.202461000
C	1.677883000	3.835084000	-0.495787000
C	2.614485000	4.732413000	-0.995331000
C	4.291697000	3.026710000	-0.717101000
H	2.307059000	5.737558000	-1.275096000
H	5.323912000	2.689289000	-0.752764000
H	4.701824000	4.987414000	-1.520647000
C	0.233828000	4.206453000	-0.260570000
H	-0.064827000	5.080147000	-0.857676000
H	0.097102000	4.453593000	0.801850000
C	-3.696781000	-0.862793000	0.331520000
C	-4.591672000	1.362263000	1.805582000
C	-4.699245000	-0.037566000	-0.190688000
C	-3.131627000	-0.571298000	1.595530000
C	-3.593811000	0.528224000	2.321616000
C	-5.144548000	1.085609000	0.533893000
H	-5.146775000	-0.241416000	-1.161566000
H	-2.377812000	-1.230082000	2.018437000
C	-1.971005000	3.153759000	0.123495000
H	-2.548690000	2.244683000	-0.068880000
H	-2.506598000	4.035718000	-0.260351000
H	-1.802852000	3.255077000	1.200497000
C	-0.864658000	2.900925000	-2.046348000
H	-1.443132000	1.989261000	-2.222841000
H	0.106989000	2.832940000	-2.548686000
H	-1.412836000	3.780046000	-2.418198000
C	0.486476000	-3.761723000	1.240835000
H	0.974126000	-4.748182000	1.208432000
H	-0.569355000	-3.880775000	1.505917000
H	0.985804000	-3.123444000	1.976623000
C	2.029430000	-2.968555000	-0.488505000
H	2.092537000	-2.472087000	-1.461530000
H	2.488877000	-3.967879000	-0.541061000
H	2.536670000	-2.355783000	0.261023000
C	3.703951000	0.839645000	0.350498000

continue next page

Table 4.27: **2**–OCH₃.

C	4.655867000	–1.515691000	1.577656000
C	3.149946000	0.398282000	1.579137000
C	4.706935000	0.088383000	–0.267606000
C	5.185841000	–1.094869000	0.333479000
C	3.647014000	–0.764617000	2.183191000
H	2.417450000	1.011369000	2.093309000
H	5.142753000	0.399062000	–1.214975000
H	5.041203000	–2.404875000	2.068841000
H	–4.950013000	2.204724000	2.390421000
H	3.254077000	–1.076478000	3.149371000
H	–3.186278000	0.732961000	3.310088000
O	6.152072000	–1.749985000	–0.351988000
O	–6.102759000	1.834065000	–0.071388000
C	6.775776000	–2.913199000	0.257814000
H	7.243366000	–2.636969000	1.213380000
H	7.534589000	–3.241640000	–0.457113000
H	6.032026000	–3.707591000	0.417578000
C	–6.689831000	2.937479000	0.667102000
H	–7.157123000	2.572621000	1.592994000
H	–7.446321000	3.361636000	0.001428000
H	–5.925771000	3.692673000	0.905412000

Figure 4.45: **TS35**–OCH₃.Table 4.28: **TS35**–OCH₃.

Cu	1.013956000	0.730627000	–0.311428000
Cu	–1.300247000	–1.480009000	–0.170750000
O	2.023026000	–0.921581000	–0.309739000

continue next page

Table 4.28: **TS35–OCH₃**.

O	–0.525002000	0.021546000	0.334098000
N	0.087254000	2.592983000	–0.608918000
N	–1.170194000	–3.278558000	–1.247752000
N	2.677311000	1.790213000	–0.823225000
C	4.726363000	3.324547000	–1.917510000
C	3.969848000	1.371997000	–0.687835000
C	2.398782000	2.955157000	–1.453524000
C	3.402549000	3.762412000	–1.995028000
C	5.010775000	2.121887000	–1.268186000
H	3.143046000	4.699093000	–2.484539000
H	6.035273000	1.765545000	–1.226843000
H	5.530452000	3.910584000	–2.358558000
C	0.929301000	3.299278000	–1.613193000
H	0.778681000	4.389429000	–1.555149000
H	0.605111000	2.973254000	–2.612499000
N	–3.236450000	–2.054816000	0.046097000
C	–5.858800000	–2.941256000	–0.256918000
C	–4.264654000	–1.221606000	0.368742000
C	–3.490993000	–3.310926000	–0.405698000
C	–4.787904000	–3.788422000	–0.573478000
C	–5.594834000	–1.656946000	0.216925000
H	–4.953336000	–4.796549000	–0.947757000
H	–6.402522000	–0.986165000	0.498134000
H	–6.885438000	–3.283807000	–0.373835000
C	–2.257974000	–4.143956000	–0.689316000
H	–2.487437000	–4.977727000	–1.371359000
H	–1.888437000	–4.567590000	0.255957000
C	4.246023000	0.132541000	0.081964000
C	4.927977000	–2.314735000	1.490458000
C	5.511346000	–0.107294000	0.580038000
C	3.183448000	–0.891839000	0.322228000
C	3.623470000	–2.111500000	1.033247000
C	5.883445000	–1.312402000	1.256953000
H	6.301029000	0.632749000	0.472476000
H	3.041021000	–0.818952000	1.571707000
H	2.841422000	–2.851745000	1.193494000
H	5.172024000	–3.221060000	2.036264000
C	0.155453000	–3.947275000	–1.118317000
H	0.928648000	–3.259280000	–1.476612000
H	0.178753000	–4.880857000	–1.705466000
H	0.334010000	–4.176456000	–0.061213000
C	–1.444482000	–2.980375000	–2.687039000
H	–0.662246000	–2.313003000	–3.064782000
H	–2.419089000	–2.487394000	–2.775356000
H	–1.448854000	–3.913281000	–3.274823000
C	0.142189000	3.271700000	0.721024000
H	–0.299878000	4.278272000	0.643848000

continue next page

Table 4.28: **TS35**–**OCH₃**.

H	1.184832000	3.352865000	1.049325000
H	−0.430210000	2.664843000	1.429296000
C	−1.329646000	2.490273000	−1.057499000
H	−1.361336000	1.984215000	−2.028333000
H	−1.764955000	3.498604000	−1.144760000
H	−1.876719000	1.899265000	−0.318111000
C	−3.960722000	0.126789000	0.906030000
C	−3.511281000	2.674617000	2.024968000
C	−2.967059000	0.301987000	1.894021000
C	−4.716944000	1.226272000	0.478692000
C	−4.493696000	2.505109000	1.027574000
C	−2.761491000	1.568579000	2.445418000
H	−2.394033000	−0.549129000	2.248840000
H	−5.485280000	1.117039000	−0.284503000
H	−2.019250000	1.695985000	3.231979000
H	−3.345725000	3.647714000	2.478992000
O	7.158457000	−1.355124000	1.647810000
O	−5.272651000	3.503409000	0.526608000
C	7.657006000	−2.552081000	2.328343000
H	8.709901000	−2.343958000	2.531394000
H	7.552659000	−3.423682000	1.668555000
H	7.103331000	−2.702821000	3.265011000
C	−5.176517000	4.815989000	1.131794000
H	−5.417580000	4.763840000	2.203765000
H	−5.911117000	5.433602000	0.607650000
H	−4.166281000	5.232744000	0.998061000

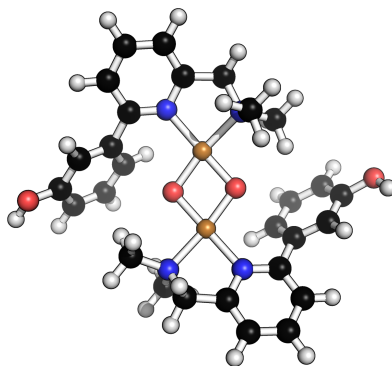
Figure 4.46: **2**–**OH**.

Table 4.29: **2-OH**.

Cu	-0.788204000	-1.143510000	-0.047237000
Cu	0.791419000	1.218970000	-0.018153000
O	-0.951186000	0.685442000	-0.065607000
O	0.935093000	-0.597526000	0.285905000
N	-0.366848000	-3.123502000	-0.156883000
N	0.322820000	3.123379000	-0.530632000
N	-2.654387000	-1.733931000	-0.438674000
C	-5.053806000	-2.792267000	-1.377301000
C	-3.803417000	-1.009888000	-0.299526000
C	-2.689573000	-2.972819000	-1.004071000
C	-3.872591000	-3.539518000	-1.468720000
C	-5.014942000	-1.527404000	-0.792622000
H	-3.864562000	-4.538110000	-1.900398000
H	-5.921486000	-0.941769000	-0.664658000
H	-5.995059000	-3.203441000	-1.737731000
C	-1.347426000	-3.649772000	-1.164430000
H	-1.434039000	-4.743285000	-1.076833000
H	-0.945677000	-3.421604000	-2.162051000
N	2.694724000	1.827377000	-0.100950000
C	5.089730000	2.889483000	-1.062972000
C	3.801795000	1.031317000	-0.173244000
C	2.785095000	3.148083000	-0.439881000
C	3.961469000	3.709591000	-0.923007000
C	5.008731000	1.554113000	-0.676158000
H	3.991507000	4.765150000	-1.183901000
H	5.880653000	0.906878000	-0.718057000
H	6.023366000	3.296081000	-1.447561000
C	1.529776000	3.950415000	-0.198390000
H	1.523161000	4.884328000	-0.778312000
H	1.470007000	4.208179000	0.868623000
C	-3.774217000	0.280195000	0.422730000
C	-3.852436000	2.682357000	1.882427000
C	-4.499772000	1.377927000	-0.074832000
C	-3.095348000	0.388134000	1.654112000
C	-3.150823000	1.584990000	2.378462000
C	-4.525596000	2.581840000	0.645442000
H	-5.023644000	1.303117000	-1.027991000
H	-2.567517000	-0.472119000	2.057729000
H	-2.655246000	1.655504000	3.344984000
H	-3.914611000	3.616505000	2.437661000
C	-0.895535000	3.630706000	0.169302000
H	-1.728085000	2.953294000	-0.041845000
H	-1.127920000	4.645099000	-0.189305000
H	-0.707286000	3.648655000	1.247467000
C	0.086322000	3.095300000	-2.011399000
H	-0.745462000	2.412580000	-2.208655000

continue next page

Table 4.29: **2–OH**.

H	0.991145000	2.740473000	–2.517901000
H	–0.159009000	4.110049000	–2.359992000
C	–0.615189000	–3.722710000	1.194785000
H	–0.445070000	–4.809309000	1.149870000
H	–1.648017000	–3.523071000	1.499099000
H	0.078544000	–3.266003000	1.907800000
C	1.034656000	–3.407592000	–0.588633000
H	1.206282000	–2.953823000	–1.569490000
H	1.183798000	–4.497124000	–0.644457000
H	1.722029000	–2.967049000	0.138260000
C	3.755306000	–0.343947000	0.370007000
C	3.917158000	–2.876689000	1.587125000
C	3.106067000	–0.586779000	1.605259000
C	4.459489000	–1.375983000	–0.263128000
C	4.534978000	–2.643955000	0.337277000
C	3.210559000	–1.848450000	2.209461000
H	2.607388000	0.226291000	2.122446000
H	4.959995000	–1.217254000	–1.216016000
H	2.753279000	–2.019873000	3.182258000
H	4.011475000	–3.853584000	2.062537000
O	5.219126000	–3.605739000	–0.342191000
H	5.307999000	–4.416321000	0.195345000
O	–5.172621000	3.701971000	0.208467000
H	–5.681406000	3.516702000	–0.603696000

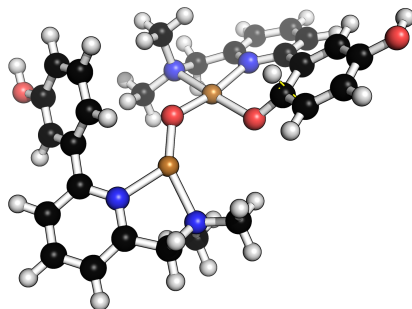
Figure 4.47: **TS35–OH**.

Table 4.30: **TS35–OH**.

Cu	1.197426000	0.613774000	−0.207282000
Cu	−1.454300000	−1.190267000	−0.105032000
O	1.895991000	−1.192894000	−0.207953000
O	−0.464920000	0.186867000	0.378369000
N	0.636110000	2.613089000	−0.514187000
N	−1.597961000	−3.012384000	−1.133113000
N	3.046933000	1.356827000	−0.638883000
C	5.383658000	2.503598000	−1.628468000
C	4.236655000	0.710401000	−0.458729000
C	3.009820000	2.557652000	−1.260602000
C	4.165063000	3.173963000	−1.751256000
C	5.418796000	1.264507000	−0.985501000
H	4.099170000	4.145431000	−2.237262000
H	6.359421000	0.727346000	−0.913519000
H	6.297546000	2.937097000	−2.030217000
C	1.634556000	3.164147000	−1.472059000
H	1.681304000	4.262886000	−1.401657000
H	1.300268000	2.912163000	−2.489273000
N	−3.462632000	−1.428349000	0.072409000
C	−6.186060000	−1.868311000	−0.303015000
C	−4.344068000	−0.424962000	0.339278000
C	−3.911698000	−2.636509000	−0.358395000
C	−5.265139000	−2.893186000	−0.559897000
C	−5.723174000	−0.633039000	0.149023000
H	−5.587430000	−3.869350000	−0.916262000
H	−6.413816000	0.172748000	0.384067000
H	−7.251676000	−2.035805000	−0.449265000
C	−2.827659000	−3.670086000	−0.584813000
H	−3.175275000	−4.473653000	−1.252615000
H	−2.556853000	−4.120758000	0.381155000
C	4.251246000	−0.566086000	0.298293000
C	4.419115000	−3.119159000	1.666113000
C	5.432198000	−1.036612000	0.852963000
C	3.015551000	−1.386494000	0.464135000
C	3.195252000	−2.681944000	1.162134000
C	5.542894000	−2.297580000	1.509324000
H	6.334632000	−0.429031000	0.795433000
H	2.844441000	−1.312609000	1.708481000
H	2.286582000	−3.271028000	1.270654000
H	4.504190000	−4.066559000	2.193769000
C	−0.406044000	−3.889052000	−0.952679000
H	0.477752000	−3.352051000	−1.313383000
H	−0.528771000	−4.831900000	−1.511773000
H	−0.288453000	−4.111749000	0.114431000
C	−1.785710000	−2.712719000	−2.586360000
H	−0.895965000	−2.192696000	−2.957610000

continue next page

Table 4.30: **TS35–OH**.

H	−2.664379000	−2.070487000	−2.712967000
H	−1.929625000	−3.648054000	−3.152089000
C	0.754688000	3.260804000	0.826965000
H	0.514245000	4.333030000	0.745439000
H	1.777562000	3.141733000	1.202273000
H	0.046429000	2.767307000	1.499270000
C	−0.756023000	2.768817000	−1.022949000
H	−0.831057000	2.299651000	−2.009889000
H	−1.007695000	3.838752000	−1.096877000
H	−1.428371000	2.263736000	−0.324036000
C	−3.832380000	0.866258000	0.859187000
C	−2.991430000	3.322398000	1.939617000
C	−2.867453000	0.893936000	1.886958000
C	−4.367434000	2.068404000	0.369150000
C	−3.941662000	3.296039000	0.901671000
C	−2.464994000	2.120966000	2.424597000
H	−2.467095000	−0.034312000	2.283026000
H	−5.109642000	2.070271000	−0.426767000
H	−1.748006000	2.140034000	3.243703000
H	−2.684639000	4.277175000	2.368462000
O	6.701302000	−2.734032000	2.032087000
O	−4.484369000	4.427473000	0.354760000
H	7.437256000	−2.106396000	1.888341000
H	−4.215264000	5.214884000	0.864291000

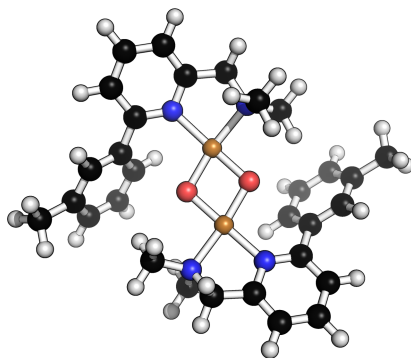
Figure 4.48: **2–CH₃**.

Table 4.31: **2-CH₃**.

Cu	-0.764887000	-1.160485000	-0.109247000
Cu	0.767029000	1.230358000	-0.085766000
O	-0.956968000	0.661740000	-0.195675000
O	0.947338000	-0.581185000	0.180507000
N	-0.320929000	-3.132613000	-0.164057000
N	0.270309000	3.127553000	-0.576476000
N	-2.617353000	-1.779806000	-0.438714000
C	-5.016068000	-2.846532000	-1.355390000
C	-3.766969000	-1.060413000	-0.281712000
C	-2.649568000	-3.022370000	-0.997449000
C	-3.833833000	-3.593678000	-1.450560000
C	-4.979201000	-1.582308000	-0.769876000
H	-3.827610000	-4.594607000	-1.876776000
H	-5.886639000	-0.999298000	-0.636210000
H	-5.957873000	-3.260194000	-1.711525000
C	-1.303592000	-3.692783000	-1.153886000
H	-1.379062000	-4.784306000	-1.037167000
H	-0.908688000	-3.486171000	-2.158793000
N	2.651673000	1.873412000	-0.092799000
C	5.053180000	2.970566000	-0.992214000
C	3.773796000	1.094287000	-0.124958000
C	2.729248000	3.195848000	-0.432390000
C	3.908513000	3.774311000	-0.885029000
C	4.984288000	1.636706000	-0.600218000
H	3.929732000	4.829698000	-1.147382000
H	5.867591000	1.003819000	-0.613962000
H	5.989887000	3.391011000	-1.353804000
C	1.455870000	3.976771000	-0.219511000
H	1.443985000	4.909501000	-0.800914000
H	1.368999000	4.234275000	0.845621000
C	-3.737899000	0.217332000	0.458839000
C	-3.843094000	2.585242000	1.948644000
C	-4.476910000	1.322687000	-0.008607000
C	-3.053209000	0.310750000	1.687545000
C	-3.116199000	1.492015000	2.430522000
C	-4.530943000	2.519419000	0.717671000
H	-5.006476000	1.251432000	-0.958381000
H	-2.507621000	-0.549539000	2.070282000
C	-0.968203000	3.595251000	0.116446000
H	-1.783997000	2.904035000	-0.115548000
H	-1.216606000	4.610223000	-0.229800000
H	-0.793579000	3.600382000	1.196958000
C	0.052499000	3.110111000	-2.060811000
H	-0.760220000	2.410209000	-2.276266000
H	0.972420000	2.783110000	-2.558783000
H	-0.212536000	4.122797000	-2.400374000

continue next page

Table 4.31: **2-CH₃**.

C	-0.553854000	-3.698208000	1.205124000
H	-0.370523000	-4.783253000	1.186625000
H	-1.586890000	-3.502411000	1.510607000
H	0.140670000	-3.215612000	1.900108000
C	1.082417000	-3.409624000	-0.595578000
H	1.241919000	-2.980662000	-1.589570000
H	1.243846000	-4.498444000	-0.621578000
H	1.769098000	-2.943125000	0.116125000
C	3.737075000	-0.275153000	0.426919000
C	3.899878000	-2.801230000	1.633453000
C	3.073398000	-0.522517000	1.649817000
C	4.466371000	-1.312726000	-0.185243000
C	4.551305000	-2.584361000	0.396307000
C	3.171520000	-1.784228000	2.251734000
H	2.547173000	0.284889000	2.150908000
H	4.973749000	-1.127705000	-1.131407000
H	3.985952000	-3.775922000	2.113981000
H	-3.898061000	3.500650000	2.538025000
H	2.696887000	-1.959848000	3.215823000
H	-2.613517000	1.553952000	3.394329000
C	5.337130000	-3.695089000	-0.259314000
H	4.706413000	-4.581947000	-0.423277000
H	6.168644000	-4.012759000	0.387684000
H	5.752234000	-3.379166000	-1.224174000
C	-5.333309000	3.700620000	0.219411000
H	-6.243399000	3.829174000	0.825086000
H	-5.639008000	3.566186000	-0.825834000
H	-4.759668000	4.634840000	0.302291000

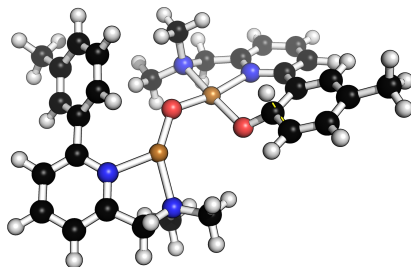
Figure 4.49: **TS35-CH₃**.

Table 4.32: **TS35**–**CH₃**.

Cu	1.193145000	0.637244000	–0.208698000
Cu	–1.440680000	–1.204185000	–0.099674000
O	1.901201000	–1.156961000	–0.240629000
O	–0.464218000	0.185903000	0.370235000
N	0.606011000	2.632805000	–0.475100000
N	–1.544635000	–3.035571000	–1.116585000
N	3.033226000	1.411289000	–0.620497000
C	5.363927000	2.635437000	–1.530488000
C	4.233208000	0.782176000	–0.438337000
C	2.983252000	2.630321000	–1.204629000
C	4.133921000	3.283869000	–1.656619000
C	5.413765000	1.379129000	–0.923716000
H	4.056187000	4.268452000	–2.113579000
H	6.364867000	0.862283000	–0.846550000
H	6.276126000	3.100206000	–1.899777000
C	1.600440000	3.217455000	–1.417139000
H	1.627376000	4.315374000	–1.327787000
H	1.277168000	2.975952000	–2.440516000
N	–3.440731000	–1.487793000	0.090370000
C	–6.154230000	–2.006482000	–0.263239000
C	–4.348269000	–0.506035000	0.355904000
C	–3.860140000	–2.712216000	–0.326458000
C	–5.206616000	–3.007925000	–0.517258000
C	–5.722722000	–0.755907000	0.175454000
H	–5.503623000	–3.995824000	–0.862956000
H	–6.434008000	0.031968000	0.409212000
H	–7.215708000	–2.205029000	–0.400579000
C	–2.751268000	–3.719335000	–0.550461000
H	–3.083432000	–4.539403000	–1.206049000
H	–2.459871000	–4.151295000	0.418078000
C	4.263868000	–0.519899000	0.267172000
C	4.472529000	–3.113635000	1.522770000
C	5.451671000	–1.002481000	0.810748000
C	3.033626000	–1.355124000	0.427556000
C	3.238426000	–2.689982000	1.042308000
C	5.596010000	–2.279086000	1.414621000
H	6.344393000	–0.381788000	0.769913000
H	2.882178000	–1.220944000	1.628181000
H	2.333624000	–3.285262000	1.148701000
H	4.561188000	–4.092792000	1.991005000
C	–0.328255000	–3.878237000	–0.940184000
H	0.537542000	–3.320058000	–1.312171000
H	–0.430463000	–4.828667000	–1.490701000
H	–0.195791000	–4.088701000	0.127765000
C	–1.753202000	–2.751918000	–2.569941000
H	–0.880383000	–2.212341000	–2.953248000

continue next page

Table 4.32: **TS35**—**CH₃**.

H	−2.649051000	−2.133196000	−2.692786000
H	−1.878502000	−3.695027000	−3.127195000
C	0.709110000	3.255956000	0.879387000
H	0.451595000	4.325394000	0.817494000
H	1.732396000	3.145467000	1.256249000
H	0.005563000	2.739006000	1.538658000
C	−0.785958000	2.779521000	−0.987342000
H	−0.850181000	2.327212000	−1.982908000
H	−1.048739000	3.847889000	−1.042535000
H	−1.455636000	2.256247000	−0.299679000
C	−3.873561000	0.803694000	0.858369000
C	−3.085125000	3.296347000	1.872707000
C	−2.895476000	0.876256000	1.866800000
C	−4.447752000	1.993756000	0.367159000
C	−4.059291000	3.249391000	0.855839000
C	−2.513500000	2.122796000	2.374026000
H	−2.458901000	−0.034332000	2.267896000
H	−5.201082000	1.940870000	−0.418627000
H	−1.780408000	2.173153000	3.177865000
H	−2.787919000	4.262865000	2.280279000
C	6.927754000	−2.697194000	1.969768000
H	7.753248000	−2.312316000	1.356133000
H	7.004442000	−3.788390000	2.048019000
H	7.055758000	−2.280197000	2.983220000
C	−4.685577000	4.520749000	0.326114000
H	−3.917943000	5.260164000	0.054930000
H	−5.322560000	4.986049000	1.093607000
H	−5.307270000	4.323291000	−0.556266000

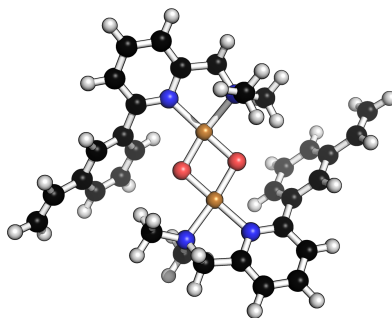
Figure 4.50: **2**—**CH=CH₂**.

Table 4.33: **2-CH=CH₂**.

Cu	-0.423637000	-1.339372000	-0.053551000
Cu	0.396390000	1.380015000	-0.044797000
O	-1.111626000	0.361290000	-0.102865000
O	1.066907000	-0.312949000	0.264320000
N	0.542110000	-3.119092000	-0.130314000
N	-0.607645000	3.058609000	-0.578678000
N	-2.038604000	-2.434096000	-0.437293000
C	-4.042446000	-4.102678000	-1.407451000
C	-3.342189000	-2.046274000	-0.322931000
C	-1.724460000	-3.638537000	-0.989895000
C	-2.702236000	-4.506440000	-1.466782000
C	-4.359164000	-2.870638000	-0.836040000
H	-2.417703000	-5.469136000	-1.886265000
H	-5.392104000	-2.547885000	-0.734271000
H	-4.830233000	-4.753496000	-1.782647000
C	-0.245451000	-3.922992000	-1.124918000
H	-0.027768000	-4.995009000	-1.005242000
H	0.088517000	-3.621005000	-2.127846000
N	2.034096000	2.522504000	-0.107249000
C	4.027584000	4.235505000	-1.043738000
C	3.327895000	2.086992000	-0.150606000
C	1.737078000	3.808605000	-0.461894000
C	2.704702000	4.687427000	-0.934361000
C	4.336658000	2.939099000	-0.640236000
H	2.427643000	5.702633000	-1.209542000
H	5.361211000	2.577198000	-0.658814000
H	4.807023000	4.896823000	-1.417964000
C	0.297431000	4.207821000	-0.246508000
H	0.024635000	5.092209000	-0.839828000
H	0.149148000	4.447994000	0.815898000
C	-3.672457000	-0.799334000	0.399743000
C	-4.428071000	1.474242000	1.857140000
C	-4.625593000	0.091857000	-0.120839000
C	-3.096530000	-0.540477000	1.660584000
C	-3.490923000	0.588738000	2.387155000
C	-5.005060000	1.251749000	0.581254000
H	-5.068533000	-0.103562000	-1.097251000
H	-2.378858000	-1.240854000	2.082621000
H	-3.075004000	0.766779000	3.377375000
H	-4.731876000	2.342250000	2.439098000
C	-1.929677000	3.184143000	0.104987000
H	-2.517650000	2.285627000	-0.102789000
H	-2.454083000	4.075814000	-0.271356000
H	-1.768192000	3.270259000	1.184232000
C	-0.809403000	2.947665000	-2.060874000
H	-1.398789000	2.046888000	-2.256062000

continue next page

Table 4.33: **2-CH=CH₂**.

H	0.165494000	2.874077000	-2.556173000
H	-1.342438000	3.839964000	-2.422786000
C	0.470242000	-3.738181000	1.233381000
H	0.949715000	-4.728713000	1.210702000
H	-0.578143000	-3.841923000	1.532334000
H	0.997159000	-3.085838000	1.936967000
C	1.968439000	-2.999972000	-0.558534000
H	2.006580000	-2.535907000	-1.548711000
H	2.424051000	-4.001779000	-0.590266000
H	2.498276000	-2.367173000	0.157618000
C	3.675057000	0.760600000	0.401799000
C	4.524619000	-1.630855000	1.609506000
C	3.110504000	0.340129000	1.627568000
C	4.646235000	-0.040580000	-0.218240000
C	5.079255000	-1.251714000	0.357551000
C	3.557216000	-0.847297000	2.229407000
H	2.394387000	0.976977000	2.137993000
H	5.075230000	0.270827000	-1.170151000
H	3.154873000	-1.142042000	3.197138000
H	4.868788000	-2.541826000	2.094477000
C	-5.974361000	2.171184000	-0.031837000
H	-6.357981000	1.855239000	-1.004771000
C	6.080540000	-2.057640000	-0.348917000
H	6.418794000	-1.644698000	-1.301865000
C	6.608681000	-3.223629000	0.069763000
H	7.356981000	-3.741362000	-0.527127000
H	6.328957000	-3.687781000	1.015166000
C	-6.418223000	3.329742000	0.487323000
H	-6.088032000	3.702211000	1.457016000
H	-7.147203000	3.935805000	-0.047080000

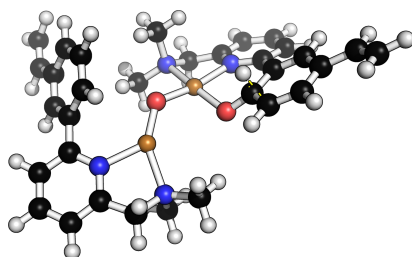
Figure 4.51: **TS35-CH=CH₂**.

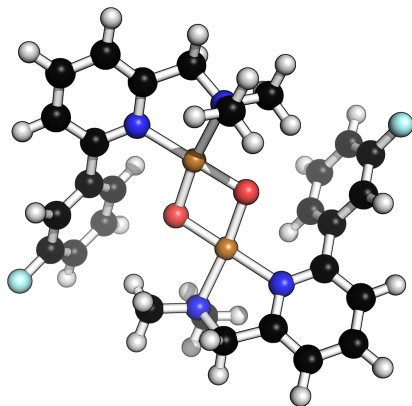
Table 4.34: **TS35**–**CH=CH₂**.

Cu	1.012952000	0.729948000	–0.271697000
Cu	–1.334546000	–1.454654000	–0.122733000
O	1.965120000	–0.950943000	–0.345426000
O	–0.540269000	0.043046000	0.363773000
N	0.137220000	2.624901000	–0.497779000
N	–1.245862000	–3.265408000	–1.184043000
N	2.703765000	1.755647000	–0.756655000
C	4.795998000	3.294642000	–1.761363000
C	3.985876000	1.298878000	–0.636434000
C	2.457621000	2.958123000	–1.326911000
C	3.483655000	3.767610000	–1.822172000
C	5.047546000	2.054306000	–1.172697000
H	3.249147000	4.734231000	–2.263709000
H	6.063013000	1.672274000	–1.146489000
H	5.616418000	3.882714000	–2.168283000
C	0.998451000	3.345879000	–1.475214000
H	0.874890000	4.436377000	–1.377335000
H	0.668156000	3.064224000	–2.485948000
N	–3.286684000	–1.973291000	0.081000000
C	–5.933782000	–2.757440000	–0.276396000
C	–4.288608000	–1.102885000	0.387549000
C	–3.578877000	–3.217962000	–0.378986000
C	–4.889869000	–3.644852000	–0.572936000
C	–5.630965000	–1.484548000	0.206191000
H	–5.086770000	–4.645237000	–0.952664000
H	–6.418119000	–0.783937000	0.472932000
H	–6.970051000	–3.060570000	–0.415148000
C	–2.370985000	–4.093423000	–0.641891000
H	–2.617515000	–4.919946000	–1.326637000
H	–2.031243000	–4.527497000	0.309777000
C	4.229856000	0.013491000	0.061569000
C	4.866884000	–2.526334000	1.287501000
C	5.493512000	–0.291672000	0.551373000
C	3.144218000	–0.990134000	0.255028000
C	3.565780000	–2.278502000	0.863303000
C	5.857324000	–1.534850000	1.151264000
H	6.282025000	0.454647000	0.480938000
H	3.036975000	–0.959851000	1.489706000
H	2.764679000	–3.004448000	0.988310000
H	5.102623000	–3.491844000	1.729110000
C	0.055185000	–3.975809000	–1.029936000
H	0.854323000	–3.315399000	–1.383518000
H	0.056976000	–4.914351000	–1.609490000
H	0.210880000	–4.202561000	0.031475000
C	–1.485152000	–2.963731000	–2.629097000
H	–0.677076000	–2.320277000	–2.993662000

continue next page

Table 4.34: **TS35**–**CH=CH₂**.

H	–2.443356000	–2.443094000	–2.736180000
H	–1.506233000	–3.897911000	–3.214403000
C	0.207892000	3.253437000	0.856202000
H	–0.216244000	4.269610000	0.816574000
H	1.252798000	3.302869000	1.183730000
H	–0.374333000	2.632124000	1.543187000
C	–1.281152000	2.573344000	–0.950174000
H	–1.321441000	2.123487000	–1.948088000
H	–1.701391000	3.591409000	–0.976751000
H	–1.837495000	1.951672000	–0.244431000
C	–3.938052000	0.228217000	0.936171000
C	–3.372164000	2.746096000	2.044122000
C	–2.983023000	0.350568000	1.962275000
C	–4.597308000	1.378388000	0.468724000
C	–4.316830000	2.655133000	0.994998000
C	–2.718632000	1.609307000	2.517722000
H	–2.477212000	–0.532927000	2.342195000
H	–5.329869000	1.289722000	–0.333458000
H	–2.007350000	1.693476000	3.337980000
H	–3.159337000	3.714238000	2.493426000
C	7.235658000	–1.705755000	1.605016000
H	7.920149000	–0.897120000	1.342796000
C	–5.006366000	3.824591000	0.429376000
H	–5.729496000	3.596621000	–0.357297000
C	7.705605000	–2.750175000	2.315297000
H	8.753712000	–2.798258000	2.604668000
H	7.070002000	–3.574816000	2.637246000
C	–4.832950000	5.108800000	0.787446000
H	–5.403637000	5.902657000	0.309529000
H	–4.138345000	5.407975000	1.572421000

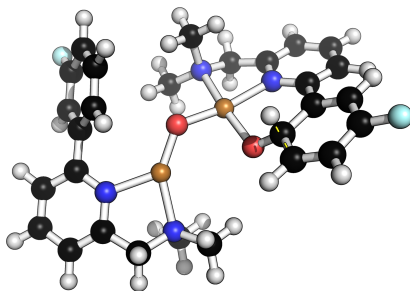
Figure 4.52: **2-F**.Table 4.35: **2-F**.

Cu	-0.81850000	-1.129793000	-0.091695000
Cu	0.807440000	1.196512000	-0.075036000
O	-0.938817000	0.698779000	-0.164093000
O	0.912574000	-0.619587000	0.212149000
N	-0.464417000	-3.119323000	-0.164206000
N	0.382963000	3.106779000	-0.583471000
N	-2.687868000	-1.664973000	-0.464513000
C	-5.110281000	-2.594743000	-1.461970000
C	-3.806070000	-0.897470000	-0.318368000
C	-2.763466000	-2.891732000	-1.051848000
C	-3.963063000	-3.394886000	-1.545854000
C	-5.029212000	-1.345917000	-0.845179000
H	-3.994190000	-4.385298000	-1.995061000
H	-5.911780000	-0.723727000	-0.719321000
H	-6.061199000	-2.954603000	-1.850816000
C	-1.446163000	-3.620842000	-1.187235000
H	-1.573203000	-4.709202000	-1.088478000
H	-1.017714000	-3.418898000	-2.179267000
N	2.716982000	1.765926000	-0.116089000
C	5.149739000	2.759566000	-1.055716000
C	3.807721000	0.945246000	-0.156880000
C	2.842933000	3.081178000	-0.468955000
C	4.039329000	3.607990000	-0.941174000
C	5.032621000	1.432089000	-0.650669000
H	4.098686000	4.659341000	-1.213691000

continue next page

Table 4.35: **2–F**.

H	5.889705000	0.763874000	−0.669771000
H	6.097578000	3.139008000	−1.433278000
C	1.604392000	3.913598000	−0.249155000
H	1.620325000	4.839848000	−0.840499000
H	1.540783000	4.185506000	0.814076000
C	−3.724201000	0.357463000	0.460209000
C	−3.701670000	2.692565000	2.035943000
C	−4.339871000	1.527905000	−0.020604000
C	−3.103094000	0.360600000	1.726792000
C	−3.105680000	1.517881000	2.510358000
C	−4.297296000	2.673579000	0.770194000
H	−4.824900000	1.560588000	−0.993756000
H	−2.654360000	−0.554418000	2.107397000
H	−2.656968000	1.504327000	3.501756000
H	−3.727424000	3.605171000	2.628126000
C	−0.829034000	3.631643000	0.115497000
H	−1.671218000	2.968676000	−0.102738000
H	−1.043641000	4.650159000	−0.241931000
H	−0.643420000	3.643532000	1.194275000
C	0.148562000	3.080765000	−2.065972000
H	−0.692155000	2.409736000	−2.265057000
H	1.050178000	2.715010000	−2.570358000
H	−0.083157000	4.098790000	−2.413253000
C	−0.758132000	−3.694680000	1.189986000
H	−0.616504000	−4.785567000	1.159997000
H	−1.790927000	−3.463403000	1.470371000
H	−0.065498000	−3.250340000	1.911929000
C	0.935931000	−3.453035000	−0.564186000
H	1.139380000	−3.022532000	−1.549250000
H	1.053900000	−4.546890000	−0.595380000
H	1.621568000	−3.020810000	0.169566000
C	3.723502000	−0.417529000	0.410854000
C	3.793618000	−2.947157000	1.659450000
C	3.097429000	−0.619702000	1.662432000
C	4.373889000	−1.490467000	−0.224683000
C	4.379899000	−2.733220000	0.404183000
C	3.151694000	−1.874633000	2.284111000
H	2.629902000	0.219505000	2.168910000
H	4.861524000	−1.374319000	−1.190076000
H	2.708219000	−2.009508000	3.268812000
H	3.863046000	−3.929009000	2.123417000
F	−4.850070000	3.815189000	0.289703000
F	4.975223000	−3.774982000	−0.221627000

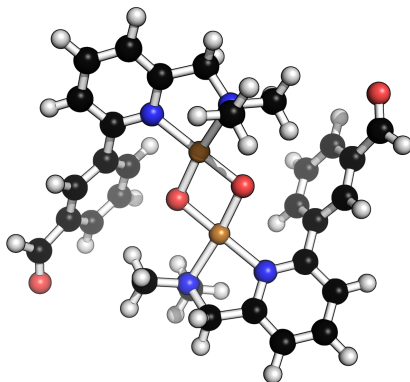
Figure 4.53: **TS35–F**.Table 4.36: **TS35–F**.

Cu	1.197661000	0.605185000	−0.214615000
Cu	−1.474696000	−1.177673000	−0.109405000
O	1.879003000	−1.204856000	−0.181755000
O	−0.471270000	0.192957000	0.364600000
N	0.650337000	2.602011000	−0.531714000
N	−1.639497000	−2.997186000	−1.135571000
N	3.054544000	1.331803000	−0.642436000
C	5.410692000	2.490269000	−1.578709000
C	4.243551000	0.687226000	−0.443431000
C	3.028703000	2.536596000	−1.256299000
C	4.192829000	3.156661000	−1.723329000
C	5.436344000	1.249134000	−0.939145000
H	4.133738000	4.130724000	−2.205091000
H	6.378803000	0.718899000	−0.845272000
H	6.331986000	2.928919000	−1.957205000
C	1.658705000	3.146998000	−1.483722000
H	1.707463000	4.245527000	−1.415808000
H	1.332800000	2.892798000	−2.503156000
N	−3.484183000	−1.395517000	0.077363000
C	−6.213361000	−1.800895000	−0.300086000
C	−4.354945000	−0.384065000	0.349314000
C	−3.947742000	−2.596877000	−0.357979000
C	−5.304673000	−2.835797000	−0.559495000
C	−5.735793000	−0.572590000	0.156859000
H	−5.638968000	−3.806891000	−0.918611000
H	−6.417177000	0.240419000	0.394653000
H	−7.280783000	−1.955007000	−0.447748000
C	−2.876747000	−3.642551000	−0.588445000
H	−3.233797000	−4.439479000	−1.258947000
H	−2.611278000	−4.099878000	0.375874000

continue next page

Table 4.36: **TS35–F**.

C	4.250367000	−0.594780000	0.298408000
C	4.395753000	−3.167424000	1.658333000
C	5.433752000	−1.081948000	0.843103000
C	3.003963000	−1.405212000	0.487968000
C	3.174338000	−2.718227000	1.162377000
C	5.501838000	−2.339482000	1.477737000
H	6.358376000	−0.512195000	0.794394000
H	2.853645000	−1.252445000	1.699094000
H	2.254787000	−3.285199000	1.292021000
H	4.490171000	−4.116927000	2.181063000
C	−0.457586000	−3.888036000	−0.956397000
H	0.432194000	−3.361406000	−1.317845000
H	−0.591777000	−4.828429000	−1.516636000
H	−0.342382000	−4.113639000	0.110353000
C	−1.824022000	−2.693989000	−2.589138000
H	−0.928907000	−2.183075000	−2.960081000
H	−2.696104000	−2.042787000	−2.715417000
H	−1.977490000	−3.627327000	−3.155325000
C	0.762034000	3.253290000	0.809558000
H	0.520420000	4.324560000	0.723793000
H	1.783087000	3.135827000	1.190226000
H	0.050455000	2.761019000	1.479052000
C	−0.736966000	2.765510000	−1.051744000
H	−0.805444000	2.301743000	−2.041744000
H	−0.983814000	3.836641000	−1.120658000
H	−1.415824000	2.259170000	−0.360443000
C	−3.824142000	0.895818000	0.876527000
C	−2.905543000	3.335663000	1.955026000
C	−2.874115000	0.904028000	1.915913000
C	−4.314135000	2.114986000	0.370481000
C	−3.831987000	3.306095000	0.910085000
C	−2.432163000	2.116839000	2.455645000
H	−2.506082000	−0.035992000	2.316844000
H	−5.042437000	2.146326000	−0.437112000
H	−1.726744000	2.112097000	3.284637000
H	−2.585438000	4.292057000	2.363335000
F	6.686846000	−2.723163000	1.956176000
F	−4.275005000	4.480955000	0.392223000

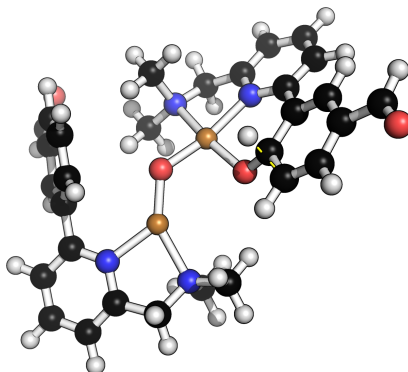
Figure 4.54: **2-CHO**.Table 4.37: **2-CHO**.

Cu	-0.530464000	-1.300638000	-0.184902000
Cu	0.469338000	1.364321000	-0.173579000
O	-1.095605000	0.444792000	-0.306154000
O	1.020796000	-0.373473000	0.073850000
N	0.310317000	-3.141184000	-0.254384000
N	-0.377135000	3.116992000	-0.723194000
N	-2.218798000	-2.306889000	-0.423336000
C	-4.391375000	-3.844183000	-1.222471000
C	-3.481971000	-1.841390000	-0.202280000
C	-2.022073000	-3.534108000	-0.980051000
C	-3.088571000	-4.336307000	-1.375939000
C	-4.586125000	-2.594743000	-0.630771000
H	-2.900899000	-5.318682000	-1.804156000
H	-5.586122000	-2.208061000	-0.449679000
H	-5.245039000	-4.442366000	-1.536190000
C	-0.575760000	-3.916950000	-1.190567000
H	-0.417058000	-4.996711000	-1.052439000
H	-0.275035000	-3.659724000	-2.216114000
N	2.175832000	2.389089000	-0.103468000
C	4.356646000	3.950231000	-0.871494000
C	3.434087000	1.861136000	-0.047961000
C	2.002367000	3.697023000	-0.462906000
C	3.067487000	4.501210000	-0.852340000
C	4.536897000	2.632391000	-0.455576000
H	2.889594000	5.536571000	-1.134404000
H	5.529571000	2.192482000	-0.400030000

continue next page

Table 4.37: **2-CHO**.

H	5.208767000	4.551619000	-1.183192000
C	0.586704000	4.201441000	-0.337902000
H	0.412006000	5.097744000	-0.949217000
H	0.391866000	4.459721000	0.712662000
C	-3.647889000	-0.578184000	0.548507000
C	-3.929403000	1.808513000	2.006345000
C	-4.479225000	0.445833000	0.063388000
C	-2.994099000	-0.409703000	1.786196000
C	-3.159356000	0.766759000	2.525343000
C	-4.582879000	1.652861000	0.766763000
H	-4.997339000	0.329028000	-0.889175000
H	-2.379923000	-1.218378000	2.179668000
H	-2.684830000	0.866389000	3.500038000
H	-4.045336000	2.750450000	2.540299000
C	-1.720627000	3.330211000	-0.106131000
H	-2.351265000	2.474586000	-0.358865000
H	-2.165395000	4.258565000	-0.493462000
H	-1.613974000	3.393332000	0.980967000
C	-0.507329000	3.024380000	-2.216562000
H	-1.144695000	2.166327000	-2.450152000
H	0.485269000	2.888678000	-2.660966000
H	-0.960970000	3.951816000	-2.596738000
C	0.274298000	-3.717581000	1.130427000
H	0.698432000	-4.732526000	1.112288000
H	-0.761001000	-3.753670000	1.484875000
H	0.875692000	-3.076966000	1.783576000
C	1.718272000	-3.116354000	-0.753334000
H	1.731111000	-2.708510000	-1.768861000
H	2.129939000	-4.136835000	-0.745362000
H	2.305717000	-2.474980000	-0.093153000
C	3.633454000	0.513464000	0.527254000
C	4.101754000	-1.986972000	1.733685000
C	3.032676000	0.183975000	1.762044000
C	4.489686000	-0.416349000	-0.088980000
C	4.690860000	-1.675804000	0.487987000
C	3.292363000	-1.050677000	2.374067000
H	2.398266000	0.914988000	2.257868000
H	4.964294000	-0.179356000	-1.041897000
H	2.863957000	-1.268645000	3.350931000
H	4.298819000	-2.965101000	2.169993000
C	-5.298292000	2.805950000	0.143810000
H	-6.009237000	2.543570000	-0.675451000
O	-5.092734000	3.964604000	0.463565000
C	5.450678000	-2.717972000	-0.266540000
H	6.074057000	-2.337544000	-1.110611000
O	5.367843000	-3.908329000	-0.018826000

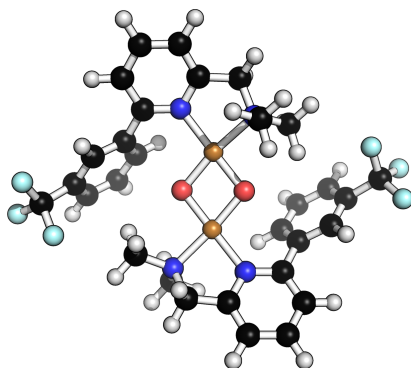
Figure 4.55: **TS35–CHO**.Table 4.38: **TS35–CHO**.

Cu	0.988776000	0.785024000	−0.297239000
Cu	−1.425947000	−1.343323000	−0.138130000
O	1.828844000	−0.942141000	−0.441239000
O	−0.610823000	0.162213000	0.298801000
N	0.241109000	2.727552000	−0.451653000
N	−1.356071000	−3.155291000	−1.204519000
N	2.760884000	1.720495000	−0.669995000
C	4.990265000	3.227631000	−1.402192000
C	4.011475000	1.188122000	−0.508839000
C	2.612945000	2.978249000	−1.144918000
C	3.708564000	3.769655000	−1.508069000
C	5.142685000	1.933220000	−0.902149000
H	3.548740000	4.779208000	−1.881614000
H	6.137333000	1.504256000	−0.837926000
H	5.863500000	3.803862000	−1.702021000
C	1.188795000	3.458358000	−1.340295000
H	1.116235000	4.545164000	−1.178196000
H	0.897442000	3.257780000	−2.381928000
N	−3.370934000	−1.868320000	0.101034000
C	−6.032829000	−2.608067000	−0.237159000
C	−4.359218000	−0.996867000	0.446194000
C	−3.684121000	−3.097835000	−0.384669000
C	−5.004821000	−3.501391000	−0.567897000
C	−5.707554000	−1.350078000	0.273634000
H	−5.221435000	−4.490173000	−0.966864000
H	−6.481595000	−0.644310000	0.565209000

continue next page

Table 4.38: **TS35–CHO**.

H	−7.074478000	−2.894307000	−0.371244000
C	−2.490904000	−3.982274000	−0.679858000
H	−2.752055000	−4.784867000	−1.386757000
H	−2.154628000	−4.449022000	0.257464000
C	4.150901000	−0.161741000	0.075414000
C	4.555759000	−2.844359000	1.120222000
C	5.380330000	−0.599435000	0.581480000
C	2.988418000	−1.102908000	0.192988000
C	3.295129000	−2.477978000	0.684316000
C	5.597434000	−1.900398000	1.072362000
H	6.233037000	0.078023000	0.595581000
H	2.857943000	−0.998339000	1.382657000
H	2.430970000	−3.135203000	0.755743000
H	4.760981000	−3.843755000	1.503015000
C	−0.062427000	−3.881057000	−1.059311000
H	0.742158000	−3.224035000	−1.406570000
H	−0.070429000	−4.812695000	−1.649370000
H	0.090167000	−4.123202000	−0.000541000
C	−1.588131000	−2.827429000	−2.646208000
H	−0.774196000	−2.183873000	−2.997150000
H	−2.542561000	−2.298798000	−2.748151000
H	−1.613788000	−3.751689000	−3.246410000
C	0.274687000	3.269330000	0.942838000
H	−0.112529000	4.299918000	0.949085000
H	1.305341000	3.255735000	1.315927000
H	−0.359901000	2.628287000	1.561313000
C	−1.153354000	2.783978000	−0.974230000
H	−1.160603000	2.439771000	−2.014404000
H	−1.535807000	3.814342000	−0.908816000
H	−1.760366000	2.115079000	−0.359490000
C	−3.957861000	0.311533000	1.015674000
C	−3.117134000	2.783960000	2.063463000
C	−3.050639000	0.364559000	2.090742000
C	−4.465558000	1.509335000	0.485672000
C	−4.010021000	2.742896000	0.975072000
C	−2.659659000	1.595954000	2.632485000
H	−2.667775000	−0.562059000	2.512715000
H	−5.166374000	1.486995000	−0.349942000
H	−1.992362000	1.617758000	3.492437000
H	−2.796171000	3.755397000	2.435619000
C	6.975052000	−2.287414000	1.558125000
H	7.749962000	−1.490765000	1.473260000
C	−4.379889000	3.994548000	0.256121000
H	−5.272468000	3.918105000	−0.409667000
O	7.219489000	−3.390201000	1.998870000
O	−3.732650000	5.026934000	0.335144000

Figure 4.56: **2-CF₃**.Table 4.39: **2-CF₃**.

Cu	-0.146666000	-1.388113000	-0.051461000
Cu	0.120722000	1.432547000	-0.069696000
O	-1.151397000	0.138788000	-0.173433000
O	1.106446000	-0.091749000	0.234142000
N	1.126203000	-2.953269000	-0.061085000
N	-1.163313000	2.876620000	-0.657938000
N	-1.508544000	-2.773125000	-0.416156000
C	-3.157845000	-4.755245000	-1.450305000
C	-2.860836000	-2.642881000	-0.294616000
C	-0.968115000	-3.883282000	-0.991862000
C	-1.765397000	-4.902051000	-1.504629000
C	-3.703918000	-3.625148000	-0.840184000
H	-1.305272000	-5.783712000	-1.945807000
H	-4.779790000	-3.507437000	-0.736425000
H	-3.808043000	-5.528199000	-1.856191000
C	0.540367000	-3.885131000	-1.086699000
H	0.953978000	-4.896366000	-0.957882000
H	0.846805000	-3.517862000	-2.076331000
N	1.497506000	2.867025000	-0.069321000
C	3.173985000	4.912191000	-0.958386000
C	2.850136000	2.686561000	-0.043351000
C	0.979139000	4.070457000	-0.462550000
C	1.786626000	5.109376000	-0.910143000
C	3.702535000	3.702340000	-0.512593000
H	1.337165000	6.051422000	-1.216306000
H	4.776554000	3.536420000	-0.481592000

continue next page

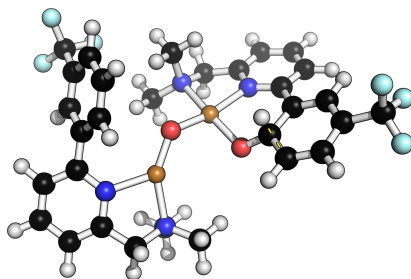
Table 4.39: **2-CF₃**.

H	3.831331000	5.702107000	-1.317344000
C	-0.516963000	4.188003000	-0.316283000
H	-0.931604000	4.988585000	-0.944693000
H	-0.758466000	4.414707000	0.731908000
C	-3.408327000	-1.505020000	0.475187000
C	-4.535549000	0.557161000	2.014133000
C	-4.494009000	-0.766557000	-0.026645000
C	-2.893104000	-1.202896000	1.751835000
C	-3.465021000	-0.187823000	2.521286000
C	-5.038812000	0.271086000	0.734655000
H	-4.900881000	-0.988443000	-1.010738000
H	-2.068868000	-1.791490000	2.150900000
H	-3.089328000	0.014407000	3.522425000
H	-4.992992000	1.344779000	2.609304000
C	-2.512730000	2.746893000	-0.029137000
H	-2.907894000	1.754174000	-0.256920000
H	-3.184100000	3.515297000	-0.438536000
H	-2.417456000	2.867900000	1.054654000
C	-1.276267000	2.708944000	-2.146246000
H	-1.665445000	1.706455000	-2.346833000
H	-0.287266000	2.828586000	-2.603103000
H	-1.963488000	3.470994000	-2.542744000
C	1.107240000	-3.573656000	1.304860000
H	1.762180000	-4.457696000	1.310613000
H	0.084294000	-3.869087000	1.558878000
H	1.475308000	-2.835709000	2.024881000
C	2.524928000	-2.573093000	-0.425278000
H	2.529896000	-2.123150000	-1.422095000
H	3.163847000	-3.467737000	-0.412531000
H	2.889553000	-1.845767000	0.303383000
C	3.417761000	1.464301000	0.566858000
C	4.668393000	-0.693100000	1.862531000
C	2.985450000	1.049964000	1.844720000
C	4.472909000	0.781989000	-0.063482000
C	5.077882000	-0.302507000	0.575021000
C	3.623545000	-0.012475000	2.493670000
H	2.185383000	1.593169000	2.341915000
H	4.812461000	1.087056000	-1.050724000
H	3.318033000	-0.296055000	3.498985000
H	5.177029000	-1.515295000	2.361728000
C	6.125209000	-1.121645000	-0.156834000
C	-6.128137000	1.146895000	0.142771000
F	6.768841000	-0.407736000	-1.116417000
F	7.051752000	-1.644086000	0.683062000
F	5.508960000	-2.188461000	-0.794062000
F	-6.977575000	1.623888000	1.084926000
F	-5.551071000	2.246642000	-0.475067000

continue next page

Table 4.39: **2**–**CF₃**.

F	–6.856498000	0.500907000	–0.805022000
---	--------------	-------------	--------------

Figure 4.57: **TS35**–**CF₃**.Table 4.40: **TS35**–**CF₃**.

Cu	–0.739156000	–0.576842000	–0.590048000
Cu	1.378859000	1.815663000	–0.206138000
O	–1.914488000	0.944429000	–0.534270000
O	0.678590000	0.245257000	0.190449000
N	0.411551000	–2.257842000	–1.030725000
N	1.287013000	3.604342000	–1.298332000
N	–2.270687000	–1.792681000	–1.154115000
C	–4.132596000	–3.614060000	–2.149817000
C	–3.604971000	–1.566102000	–0.949041000
C	–1.860779000	–2.905096000	–1.803974000
C	–2.765643000	–3.848502000	–2.305180000
C	–4.554816000	–2.469584000	–1.470843000
H	–2.397398000	–4.734318000	–2.819060000
H	–5.618013000	–2.276847000	–1.370679000
H	–4.865151000	–4.312672000	–2.549535000
C	–0.368127000	–3.036432000	–2.035580000
H	–0.063229000	–4.094470000	–2.030981000
H	–0.138833000	–2.629884000	–3.031778000
N	3.268774000	2.444124000	0.176325000
C	5.914072000	3.272382000	–0.061413000
C	4.268576000	1.622981000	0.600038000
C	3.559259000	3.669145000	–0.333938000

continue next page

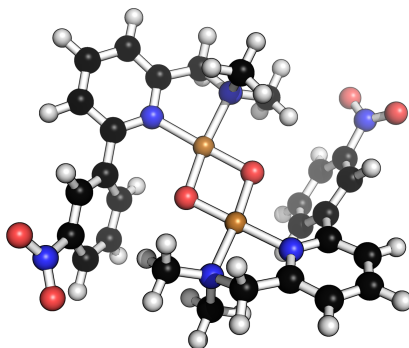
Table 4.40: **TS35**–**CF₃**.

C	4.871581000	4.117232000	–0.466841000
C	5.610561000	2.020358000	0.476539000
H	5.071446000	5.101330000	–0.885621000
H	6.395010000	1.355024000	0.829026000
H	6.950128000	3.592217000	–0.157511000
C	2.347307000	4.492397000	–0.717529000
H	2.613815000	5.296530000	–1.420346000
H	1.931325000	4.954818000	0.189316000
C	–4.023798000	–0.368255000	–0.194159000
C	–4.996010000	2.007855000	1.161619000
C	–5.319714000	–0.275818000	0.324787000
C	–3.082046000	0.770114000	0.090498000
C	–3.685018000	1.976018000	0.721689000
C	–5.806075000	0.878326000	0.960081000
H	–6.006662000	–1.110874000	0.223594000
H	–2.919160000	0.492901000	1.237953000
H	–2.990487000	2.794849000	0.898144000
H	–5.396367000	2.892400000	1.652490000
C	–0.047598000	4.267602000	–1.237004000
H	–0.798800000	3.574709000	–1.631536000
H	–0.047883000	5.195812000	–1.832247000
H	–0.278927000	4.504475000	–0.192026000
C	1.622385000	3.279628000	–2.720221000
H	0.862722000	2.596353000	–3.115140000
H	2.605598000	2.797009000	–2.759439000
H	1.640932000	4.200078000	–3.326381000
C	0.535902000	–3.004505000	0.259794000
H	1.157596000	–3.900122000	0.112119000
H	–0.461852000	–3.292164000	0.611571000
H	1.012731000	–2.337259000	0.983951000
C	1.769631000	–1.915958000	–1.543023000
H	1.667008000	–1.370643000	–2.487738000
H	2.354396000	–2.835290000	–1.692738000
H	2.251713000	–1.278885000	–0.796464000
C	3.893795000	0.329253000	1.219882000
C	3.227018000	–2.103203000	2.459769000
C	2.921070000	0.289712000	2.235985000
C	4.523673000	–0.860685000	0.817532000
C	4.171559000	–2.072169000	1.422495000
C	2.606054000	–0.917862000	2.865089000
H	2.435782000	1.211269000	2.548594000
H	5.269777000	–0.846453000	0.025971000
H	1.882337000	–0.933298000	3.677593000
H	2.990050000	–3.048286000	2.944071000
C	–7.235052000	0.866584000	1.512284000
C	4.735153000	–3.378052000	0.902176000
F	–8.052829000	0.100218000	0.743482000

continue next page

Table 4.40: **TS35**–**CF₃**.

F	–7.219059000	0.342231000	2.770529000
F	–7.750218000	2.116563000	1.573947000
F	3.818138000	–3.966807000	0.032770000
F	4.959966000	–4.278630000	1.891100000
F	5.885948000	–3.216579000	0.199567000

Figure 4.58: **2**–**NO₂**.Table 4.41: **2**–**NO₂**.

Cu	–0.314918000	–1.376683000	–0.110397000
Cu	0.234585000	1.410355000	–0.123461000
O	–1.161784000	0.248105000	–0.228069000
O	1.062018000	–0.209405000	0.164297000
N	0.795526000	–3.067258000	–0.172511000
N	–0.878980000	2.987060000	–0.731123000
N	–1.813343000	–2.627989000	–0.425907000
C	–3.695642000	–4.434915000	–1.376610000
C	–3.138448000	–2.370979000	–0.236485000
C	–1.410590000	–3.782421000	–1.025309000
C	–2.328467000	–4.716113000	–1.498728000
C	–4.100183000	–3.259842000	–0.738573000
H	–1.978678000	–5.636593000	–1.961472000
H	–5.153307000	–3.037044000	–0.583736000
H	–4.436694000	–5.138502000	–1.751851000

continue next page

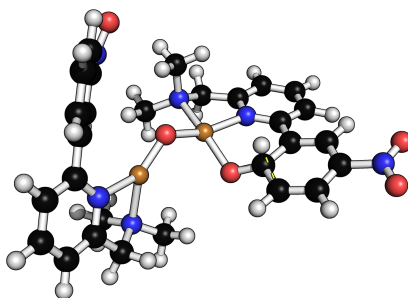
Table 4.41: **2-NO₂**.

C	0.085148000	-3.928746000	-1.182205000
H	0.405314000	-4.975858000	-1.076209000
H	0.386919000	-3.582015000	-2.180670000
N	1.750509000	2.702154000	-0.086998000
C	3.648326000	4.573657000	-0.912352000
C	3.076860000	2.386517000	-0.031696000
C	1.367152000	3.956065000	-0.476457000
C	2.288083000	4.911291000	-0.892203000
C	4.040424000	3.311410000	-0.468620000
H	1.944948000	5.897543000	-1.196928000
H	5.090897000	3.035233000	-0.416521000
H	4.391049000	5.295228000	-1.248021000
C	-0.111774000	4.224022000	-0.363055000
H	-0.428848000	5.066110000	-0.993984000
H	-0.354773000	4.467708000	0.681029000
C	-3.514964000	-1.181483000	0.560134000
C	-4.197642000	1.073160000	2.100239000
C	-4.439667000	-0.253729000	0.057094000
C	-2.960994000	-0.993025000	1.842980000
C	-3.324453000	0.111002000	2.618839000
C	-4.729627000	0.874303000	0.822307000
H	-4.889298000	-0.369381000	-0.926036000
H	-2.267853000	-1.732872000	2.239978000
H	-2.927528000	0.225762000	3.625471000
H	-4.472855000	1.961060000	2.663785000
C	-2.250453000	2.998226000	-0.139780000
H	-2.736255000	2.054280000	-0.396448000
H	-2.823945000	3.843427000	-0.547442000
H	-2.176295000	3.088895000	0.947894000
C	-0.965919000	2.838560000	-2.223823000
H	-1.450870000	1.883091000	-2.444619000
H	0.042641000	2.857278000	-2.652207000
H	-1.558677000	3.669827000	-2.633594000
C	0.767021000	-3.695604000	1.190239000
H	1.333971000	-4.638042000	1.165732000
H	-0.269522000	-3.893101000	1.481364000
H	1.232233000	-3.002750000	1.898887000
C	2.209996000	-2.819361000	-0.582353000
H	2.222512000	-2.376367000	-1.582885000
H	2.768870000	-3.766961000	-0.575954000
H	2.653550000	-2.123888000	0.132888000
C	3.497442000	1.105636000	0.579914000
C	4.415095000	-1.233660000	1.855069000
C	3.022424000	0.750187000	1.861226000
C	4.448125000	0.293236000	-0.059039000
C	4.856292000	-0.877433000	0.573947000
C	3.504919000	-0.395572000	2.504608000

continue next page

Table 4.41: **2**–NO₂.

H	2.307333000	1.397204000	2.363988000
H	4.841911000	0.538199000	−1.042399000
H	4.786028000	−2.146342000	2.314719000
N	−5.572351000	1.948706000	0.210090000
O	−5.411206000	3.097855000	0.653193000
O	−6.327939000	1.629575000	−0.712983000
H	3.173002000	−0.632398000	3.513540000
N	5.740571000	−1.821137000	−0.178698000
O	6.439773000	−1.353519000	−1.082465000
O	5.670319000	−3.017898000	0.143998000

Figure 4.59: **TS35**–NO₂.Table 4.42: **TS35**–NO₂.

Cu	1.008540000	0.890736000	−0.569012000
Cu	−1.789059000	−0.603482000	−0.756111000
O	1.620978000	−0.945621000	−0.772651000
O	−0.651600000	0.478201000	0.061046000
N	0.523769000	2.863575000	−0.855448000
N	−2.062907000	−1.465738000	−2.655220000
N	2.915035000	1.563512000	−0.691579000
C	5.399573000	2.791479000	−0.969781000
C	4.044294000	0.867136000	−0.360617000
C	3.000855000	2.839914000	−1.128059000
C	4.231060000	3.493983000	−1.267696000
C	5.308082000	1.473127000	−0.517262000

continue next page

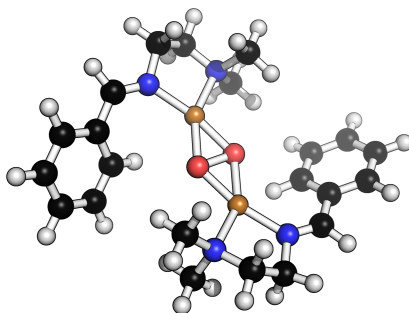
Table 4.42: **TS35–NO₂**.

H	4.262580000	4.524775000	−1.615172000
H	6.218812000	0.920929000	−0.308741000
H	6.374482000	3.261110000	−1.085939000
C	1.696733000	3.494223000	−1.537811000
H	1.718838000	4.576528000	−1.339802000
H	1.572749000	3.358358000	−2.622319000
N	−3.481379000	−1.643486000	−0.343226000
C	−5.699628000	−3.313148000	−0.046127000
C	−4.316482000	−1.475002000	0.723030000
C	−3.741232000	−2.620287000	−1.254271000
C	−4.844134000	−3.463804000	−1.144061000
C	−5.430406000	−2.316240000	0.891522000
H	−5.023682000	−4.224069000	−1.901512000
H	−6.090655000	−2.153351000	1.739421000
H	−6.571952000	−3.954304000	0.066826000
C	−2.712464000	−2.776962000	−2.356371000
H	−3.167450000	−3.208219000	−3.262238000
H	−1.925240000	−3.464661000	−2.013979000
C	3.914199000	−0.518222000	0.137930000
C	3.826351000	−3.294888000	1.009257000
C	4.988653000	−1.134997000	0.786946000
C	2.639594000	−1.307100000	−0.001087000
C	2.704354000	−2.739903000	0.412480000
C	4.944854000	−2.476117000	1.181614000
H	5.910286000	−0.597760000	0.991120000
H	2.339933000	−1.237965000	1.155933000
H	1.772279000	−3.289848000	0.299723000
H	3.849796000	−4.332257000	1.335861000
C	−0.781049000	−1.664643000	−3.389228000
H	−0.345919000	−0.682769000	−3.606199000
H	−0.956297000	−2.199757000	−4.337081000
H	−0.088910000	−2.231385000	−2.757470000
C	−2.985377000	−0.606842000	−3.460055000
H	−2.518265000	0.372503000	−3.610248000
H	−3.929890000	−0.480074000	−2.919962000
H	−3.181355000	−1.074789000	−4.438605000
C	0.335841000	3.421726000	0.523207000
H	−0.042481000	4.451974000	0.461850000
H	1.295501000	3.400948000	1.052623000
H	−0.385734000	2.787964000	1.041270000
C	−0.723016000	3.045865000	−1.660165000
H	−0.562435000	2.625130000	−2.659721000
H	−0.962525000	4.117285000	−1.735958000
H	−1.530203000	2.522207000	−1.146284000
C	−4.030473000	−0.390989000	1.692634000
C	−3.440278000	1.640721000	3.568484000
C	−4.161177000	−0.625039000	3.077856000

continue next page

Table 4.42: **TS35–NO₂**.

C	–3.641777000	0.882133000	1.249768000
C	–3.338211000	1.864954000	2.191711000
C	–3.872395000	0.383322000	4.004545000
H	–4.467581000	–1.608681000	3.429442000
H	–3.588110000	1.123451000	0.193461000
H	–3.974048000	0.186701000	5.069745000
H	–3.194092000	2.435816000	4.267050000
N	6.182311000	–3.065842000	1.838794000
O	7.156189000	–2.316480000	1.957557000
O	6.107600000	–4.244995000	2.186534000
N	–2.859059000	3.186147000	1.703283000
O	–2.298312000	3.933483000	2.516692000
O	–3.009333000	3.449195000	0.495683000

Figure 4.60: **1'**.

Scheme 6

Table 4.43: **1'**.

Cu	–0.973980000	–1.448670000	–0.043499000
Cu	0.968920000	1.494086000	–0.066031000
O	–0.638569000	0.480416000	0.089585000
O	0.602651000	–0.410336000	–0.082733000
N	–0.286642000	–3.360855000	–0.335129000
N	0.426334000	3.476297000	–0.076600000
N	–2.803510000	–2.164907000	–0.137115000
C	–3.955299000	–1.569220000	–0.231256000

continue next page

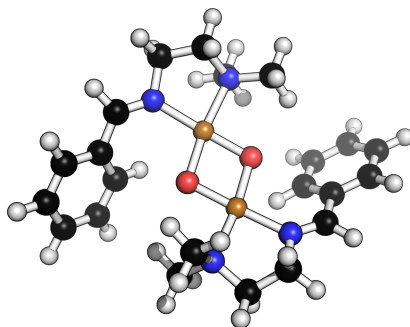
Table 4.43: 1'.

C	-2.757239000	-3.642636000	-0.329518000
C	-1.446642000	-4.024760000	-1.023979000
H	-1.307794000	-5.116688000	-1.026694000
H	-1.454538000	-3.666723000	-2.060784000
N	2.816118000	2.064462000	-0.413179000
C	3.948825000	1.430815000	-0.419671000
C	2.771729000	3.475071000	-0.889809000
C	1.736330000	4.220561000	-0.042073000
H	1.592886000	5.250565000	-0.400813000
H	2.070117000	4.251209000	1.001939000
C	-4.250834000	-0.182219000	0.077817000
C	-4.987408000	2.463010000	0.664650000
C	-5.408063000	0.386915000	-0.506367000
C	-3.484347000	0.582692000	0.987841000
C	-3.858943000	1.893124000	1.280653000
C	-5.760136000	1.709269000	-0.231152000
H	-6.020754000	-0.212758000	-1.179162000
H	-2.640516000	0.131441000	1.502571000
H	-3.300161000	2.463889000	2.020538000
H	-6.645201000	2.144145000	-0.691093000
H	-5.281960000	3.482772000	0.907718000
C	-0.427518000	3.844867000	1.094292000
H	-1.355771000	3.265922000	1.045489000
H	-0.660287000	4.920946000	1.063841000
H	0.109754000	3.613122000	2.020733000
C	-0.320692000	3.755350000	-1.345924000
H	-1.231269000	3.147352000	-1.357724000
H	0.302020000	3.495815000	-2.208632000
H	-0.583398000	4.823687000	-1.392178000
C	0.007511000	-4.000226000	0.986535000
H	0.279317000	-5.056642000	0.834760000
H	-0.870218000	-3.938539000	1.638008000
H	0.844615000	-3.468976000	1.451528000
C	0.937611000	-3.399979000	-1.192943000
H	0.720633000	-2.915425000	-2.150924000
H	1.237177000	-4.445372000	-1.366296000
H	1.743031000	-2.862871000	-0.680548000
C	4.197415000	0.085210000	0.069635000
C	4.808542000	-2.513478000	0.942210000
C	5.335799000	-0.590694000	-0.431073000
C	3.390368000	-0.545138000	1.044787000
C	3.699573000	-1.833764000	1.477283000
C	5.626404000	-1.890501000	-0.011780000
H	5.980138000	-0.093564000	-1.155825000
H	2.560863000	-0.008342000	1.496462000
H	3.103852000	-2.300192000	2.260593000
H	6.497842000	-2.408017000	-0.407728000

continue next page

Table 4.43: **1'**.

H	5.052997000	-3.514683000	1.293781000
H	4.819408000	1.952716000	-0.840436000
H	-4.809418000	-2.171301000	-0.571790000
H	3.755691000	3.955284000	-0.805536000
H	2.474861000	3.475279000	-1.948560000
H	-2.818228000	-4.111614000	0.662467000
H	-3.615629000	-3.990754000	-0.920937000

Figure 4.61: **2'**.Table 4.44: **2'**.

Cu	0.473148000	1.332872000	-0.210632000
Cu	-0.488573000	-1.327740000	-0.208430000
O	1.078313000	-0.400000000	-0.049925000
O	-1.089212000	0.402839000	-0.197377000
N	-0.453710000	3.113856000	-0.481990000
N	0.439336000	-3.125834000	-0.351643000
N	2.163553000	2.352215000	-0.371223000
C	3.394155000	1.929031000	-0.379594000
C	1.914338000	3.761884000	-0.798862000
C	0.502441000	3.870464000	-1.363845000
H	0.181065000	4.920044000	-1.439417000
H	0.448895000	3.410895000	-2.358114000
N	-2.167808000	-2.298963000	-0.512010000
C	-3.409373000	-1.926296000	-0.430358000

continue next page

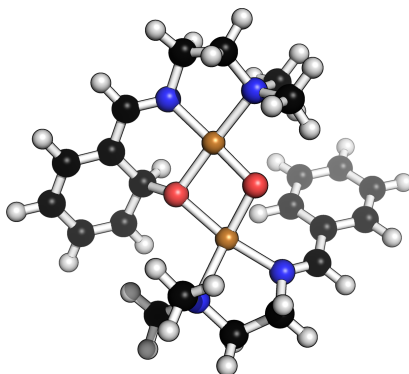
Table 4.44: 2'.

C	-1.836873000	-3.596245000	-1.166172000
C	-0.647058000	-4.171722000	-0.402506000
H	-0.258562000	-5.085847000	-0.873222000
H	-0.940867000	-4.396224000	0.629306000
C	3.914786000	0.719787000	0.224627000
C	5.100918000	-1.517340000	1.432022000
C	5.119876000	0.185253000	-0.290651000
C	3.327799000	0.138595000	1.374939000
C	3.928355000	-0.968214000	1.975910000
C	5.694663000	-0.942949000	0.295077000
H	5.594606000	0.657058000	-1.150653000
H	2.446287000	0.592271000	1.816968000
H	3.502446000	-1.388662000	2.885311000
H	6.616499000	-1.357018000	-0.108542000
H	5.572865000	-2.372602000	1.913421000
C	1.355826000	-3.344929000	0.809761000
H	2.091556000	-2.535865000	0.825188000
H	1.859694000	-4.317017000	0.697182000
H	0.769220000	-3.337771000	1.734906000
C	1.235551000	-3.100557000	-1.623072000
H	1.938522000	-2.264280000	-1.567132000
H	0.563803000	-2.962050000	-2.476918000
H	1.775325000	-4.053374000	-1.728697000
C	-0.620588000	3.757715000	0.861715000
H	-1.022726000	4.773749000	0.731010000
H	0.342755000	3.804911000	1.378094000
H	-1.322120000	3.152930000	1.444732000
C	-1.788332000	2.992193000	-1.146161000
H	-1.663136000	2.503822000	-2.116938000
H	-2.210046000	3.999975000	-1.279966000
H	-2.443928000	2.386977000	-0.513429000
C	-3.937604000	-0.761832000	0.253153000
C	-5.100822000	1.451341000	1.526086000
C	-3.293456000	-0.160298000	1.360942000
C	-5.189766000	-0.264540000	-0.180274000
C	-5.755734000	0.851203000	0.438085000
C	-3.879887000	0.935843000	1.993162000
H	-2.371653000	-0.584752000	1.745960000
H	-5.705224000	-0.751430000	-1.007809000
H	-6.713724000	1.236969000	0.095290000
H	-3.406586000	1.372799000	2.870996000
H	-5.559772000	2.299629000	2.031717000
H	4.138414000	2.573611000	-0.868818000
H	2.029231000	4.403527000	0.085320000
H	2.654364000	4.080905000	-1.546072000
H	-4.153037000	-2.564951000	-0.926911000
H	-2.693696000	-4.282243000	-1.141235000

continue next page

Table 4.44: **2'**.

H	-1.570845000	-3.406780000	-2.216146000
---	--------------	--------------	--------------

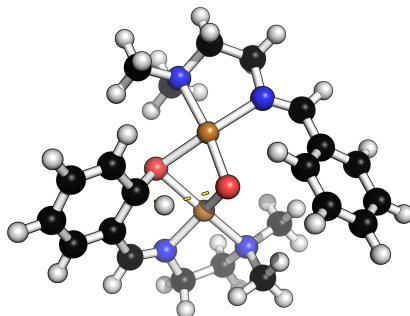
Figure 4.62: **3'**.Table 4.45: **3'**.

Cu	-0.638539000	-1.402701000	-0.460704000
Cu	0.365351000	1.348844000	-0.363726000
O	-1.349466000	0.332112000	0.087215000
O	0.791326000	-0.385593000	-0.854894000
N	0.126406000	-3.116911000	-1.194438000
N	-0.234466000	3.321141000	-0.729978000
N	-2.175916000	-2.452946000	0.096875000
C	-3.341289000	-1.909393000	0.344615000
C	-2.067509000	-3.881296000	-0.282516000
C	-1.078440000	-3.991362000	-1.449065000
H	-0.750975000	-5.030199000	-1.605003000
H	-1.546192000	-3.623728000	-2.369814000
N	2.209719000	2.012072000	-0.591858000
C	3.354668000	1.532537000	-0.218406000
C	2.144724000	3.215651000	-1.450914000
C	1.046690000	4.108192000	-0.872769000
H	0.867979000	4.990889000	-1.504709000
H	1.339765000	4.441977000	0.129751000

continue next page

Table 4.45: $\mathbf{3}'$.

C	-3.480180000	-0.565084000	0.823059000
C	-3.789466000	2.074428000	1.829988000
C	-4.737168000	0.051876000	0.820087000
C	-2.264521000	0.168185000	1.312121000
C	-2.536922000	1.514976000	1.855085000
C	-4.900655000	1.350309000	1.312581000
H	-5.598733000	-0.490412000	0.431399000
H	-1.681055000	-0.449926000	2.013020000
H	-1.692059000	2.054052000	2.278437000
H	-5.888200000	1.807666000	1.313166000
H	-3.949925000	3.072013000	2.236674000
C	-1.137083000	4.035565000	0.221217000
H	-2.096295000	3.515879000	0.256818000
H	-1.290969000	5.070460000	-0.123986000
H	-0.678632000	4.050754000	1.216104000
C	-0.928000000	3.200554000	-2.056941000
H	-1.828778000	2.593007000	-1.924350000
H	-0.265043000	2.714184000	-2.780891000
H	-1.198943000	4.202596000	-2.424943000
C	1.013080000	-3.677052000	-0.123805000
H	1.424381000	-4.640464000	-0.461556000
H	0.436112000	-3.823477000	0.795005000
H	1.820743000	-2.961409000	0.059180000
C	0.914103000	-2.922896000	-2.451294000
H	0.259864000	-2.505016000	-3.223087000
H	1.311459000	-3.895040000	-2.781491000
H	1.728477000	-2.223821000	-2.239911000
C	3.610478000	0.419128000	0.676761000
C	4.285895000	-1.722873000	2.365498000
C	2.657922000	-0.099725000	1.584505000
C	4.913735000	-0.132879000	0.654022000
C	5.243410000	-1.209604000	1.480027000
C	2.997977000	-1.157456000	2.423361000
H	1.670222000	0.347639000	1.653490000
H	5.660240000	0.284261000	-0.021648000
H	6.245419000	-1.632704000	1.449800000
H	2.275110000	-1.533832000	3.145543000
H	4.547336000	-2.544108000	3.031071000
H	-4.253133000	-2.500340000	0.189669000
H	-1.700431000	-4.432954000	0.594853000
H	-3.043758000	-4.299760000	-0.566036000
H	4.250803000	2.029330000	-0.616875000
H	3.107574000	3.745056000	-1.472018000
H	1.896327000	2.902928000	-2.475263000

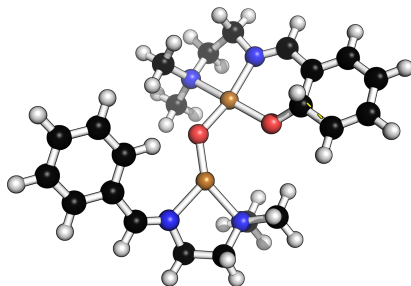
Figure 4.63: **TS34'** (open-shell broken-symmetry singlet).Table 4.46: **TS34'** (open-shell broken-symmetry singlet).

Cu	-0.388622000	-1.158823000	-0.556126000
Cu	0.043677000	1.471780000	-0.008034000
O	-1.753388000	0.457445000	-0.440639000
O	0.423850000	-0.181470000	0.792722000
N	0.874106000	-2.716164000	-1.103682000
N	-0.648081000	3.210898000	-0.933983000
N	-1.841383000	-2.425964000	-0.914367000
C	-2.979446000	-2.321678000	-0.294413000
C	-1.396787000	-3.714746000	-1.495278000
C	0.027468000	-3.523458000	-2.051108000
H	0.501487000	-4.497650000	-2.245630000
H	-0.018581000	-2.962921000	-2.992879000
N	1.906677000	2.302487000	-0.260260000
C	3.090051000	1.793093000	-0.100454000
C	1.802140000	3.519936000	-1.116689000
C	0.470662000	4.205591000	-0.826039000
H	0.299570000	5.045878000	-1.515949000
H	0.469757000	4.587756000	0.202347000
C	-3.352820000	-1.174878000	0.511946000
C	-4.183678000	0.946986000	2.261220000
C	-4.543758000	-1.256064000	1.237449000
C	-2.450460000	0.017221000	0.710888000
C	-3.005922000	1.090436000	1.561785000
C	-4.960687000	-0.223377000	2.094407000
H	-5.173912000	-2.138310000	1.124084000
H	-1.593338000	-0.363141000	1.421916000
H	-2.395599000	1.984276000	1.665526000
H	-5.902356000	-0.325212000	2.631728000

continue next page

Table 4.46: **TS34'** (open-shell broken-symmetry singlet).

H	-4.532637000	1.737915000	2.922950000
C	-1.890284000	3.768739000	-0.327275000
H	-2.681535000	3.015784000	-0.402364000
H	-2.198673000	4.678589000	-0.865749000
H	-1.701157000	4.019961000	0.723323000
C	-0.932142000	2.859021000	-2.362213000
H	-1.717632000	2.096514000	-2.376549000
H	-0.028235000	2.461544000	-2.835529000
H	-1.265829000	3.754835000	-2.908993000
C	1.222186000	-3.482917000	0.131463000
H	1.844462000	-4.352822000	-0.131387000
H	0.305767000	-3.824077000	0.624642000
H	1.768453000	-2.816596000	0.807261000
C	2.123152000	-2.244898000	-1.769564000
H	1.860786000	-1.660899000	-2.659591000
H	2.740933000	-3.106545000	-2.069738000
H	2.681615000	-1.623253000	-1.060837000
C	3.460371000	0.668621000	0.740618000
C	4.277386000	-1.521233000	2.293416000
C	2.770844000	0.347092000	1.932027000
C	4.593437000	-0.090730000	0.363276000
C	4.984202000	-1.195297000	1.122958000
C	3.184919000	-0.741625000	2.702759000
H	1.957406000	0.980520000	2.268820000
H	5.156269000	0.187498000	-0.527949000
H	5.851403000	-1.781963000	0.825689000
H	2.671063000	-0.971107000	3.634307000
H	4.602761000	-2.362142000	2.904168000
H	-3.683561000	-3.164674000	-0.298626000
H	-1.420286000	-4.488927000	-0.714787000
H	-2.075428000	-4.027813000	-2.301654000
H	3.918858000	2.250031000	-0.662344000
H	2.630548000	4.210215000	-0.910749000
H	1.863063000	3.219382000	-2.172521000

Figure 4.64: **TS35'**.Table 4.47: **TS35'**.

Cu	1.287781000	−0.993541000	0.301931000
Cu	−1.207960000	1.076671000	0.379842000
O	1.982468000	0.727537000	−0.285990000
O	−0.461754000	−0.511533000	0.165497000
N	0.708586000	−2.733218000	1.350908000
N	−0.864963000	3.077325000	0.897751000
N	3.080488000	−1.874469000	0.238745000
C	4.191927000	−1.377362000	−0.206294000
C	3.048591000	−3.270532000	0.727374000
C	1.983147000	−3.358732000	1.826155000
H	1.810675000	−4.405419000	2.118765000
H	2.316099000	−2.796545000	2.706843000
N	−3.154243000	1.561289000	0.372875000
C	−4.221285000	0.973808000	−0.079413000
C	−3.324702000	2.866275000	1.065021000
C	−2.170002000	3.780999000	0.655546000
H	−2.200021000	4.733576000	1.207179000
H	−2.236714000	3.991123000	−0.418909000
C	4.317266000	−0.048466000	−0.769995000
C	4.721884000	2.552921000	−1.924865000
C	5.574961000	0.366447000	−1.219962000
C	3.130851000	0.854683000	−0.970987000
C	3.447279000	2.205497000	−1.509526000
C	5.785760000	1.643314000	−1.767085000
H	6.420347000	−0.314689000	−1.119024000
H	2.977817000	0.550413000	−2.103498000
H	2.595817000	2.871770000	−1.633650000
H	6.788063000	1.926777000	−2.084603000
H	4.902713000	3.535448000	−2.357760000
C	0.222375000	3.705193000	0.093065000

continue next page

Table 4.47: **TS35'**.

H	1.146274000	3.143492000	0.266762000
H	0.356581000	4.759676000	0.387012000
H	-0.046075000	3.653449000	-0.968737000
C	-0.495401000	3.127548000	2.346462000
H	0.439538000	2.575089000	2.490216000
H	-1.284115000	2.663893000	2.948387000
H	-0.359510000	4.173664000	2.666182000
C	-0.023004000	-3.593344000	0.374244000
H	-0.353088000	-4.519895000	0.869379000
H	0.628819000	-3.839727000	-0.471209000
H	-0.886007000	-3.023282000	0.015998000
C	-0.190975000	-2.409914000	2.496138000
H	0.351494000	-1.786963000	3.216099000
H	-0.518832000	-3.341006000	2.985186000
H	-1.048899000	-1.860695000	2.098150000
C	-4.359609000	-0.289593000	-0.786102000
C	-4.875903000	-2.677918000	-2.185024000
C	-3.291960000	-1.140584000	-1.159438000
C	-5.685199000	-0.660742000	-1.128120000
C	-5.941985000	-1.845748000	-1.818341000
C	-3.556682000	-2.319546000	-1.854246000
H	-2.263223000	-0.889949000	-0.914979000
H	-6.511371000	-0.007547000	-0.846970000
H	-6.964310000	-2.117807000	-2.073079000
H	-2.732695000	-2.966388000	-2.152565000
H	-5.068876000	-3.600718000	-2.729898000
H	5.109210000	-1.980916000	-0.174949000
H	2.774826000	-3.912236000	-0.123533000
H	4.032353000	-3.592409000	1.097441000
H	-5.175171000	1.497381000	0.081252000
H	-4.287769000	3.331713000	0.811521000
H	-3.307542000	2.688206000	2.149907000

4.2 Supporting Information for Chapter 3

4.2.1 Kinetic Rate Constants

Formation of the Bis(μ -oxido) Complex from the Reaction of [CuDPDen]CF₃SO₃ with O₂

T (°C)	T (K)	k _{obs} (s ⁻¹)	σ k _{obs} (10 ⁻⁶ s ⁻¹)
-80.9	192.3	0.65	4.8
-79.3	193.9	0.69	7.2
-77.7	195.5	0.76	5.5
-76.4	196.8	0.87	12.4
-74.4	198.8	1.08	4.5
-72.9	200.3	1.07	5.3
-71.3	201.9	1.20	7.9
-69.9	203.3	1.33	15.4
-68.4	204.8	1.39	29.4
-66.6	206.6	1.57	31.3
-65.1	208.1	1.72	41.5
-63.6	209.6	1.89	58.9

Decay of the Bis(μ -oxido) Complex with the Ligand DPDen

T (°C)	T (K)	k _{obs} (10 ⁻² s ⁻¹)	σ k _{obs} (10 ⁻⁶ s ⁻¹)
-89.0	184.2	0.37	0.8
-86.0	187.2	0.58	0.9
-80.0	193.2	0.67	0.4
-77.0	196.2	0.70	0.6
-74.9	198.3	0.74	0.2
-73.0	200.2	0.88	0.3
-71.0	202.2	0.85	6.8
-67.9	205.2	1.02	0.7
-64.0	209.2	1.01	1.4
-58.9	214.3	1.40	0.8
-54.0	219.2	2.75	0.9
-45.0	228.2	7.57	0.4
-35.0	238.2	24.23	0.6

4.2.2 NMR Data

N'-(2,2-dimethylpropylidene)-*N,N*-diethyl-ethylendiamine (DPDen)

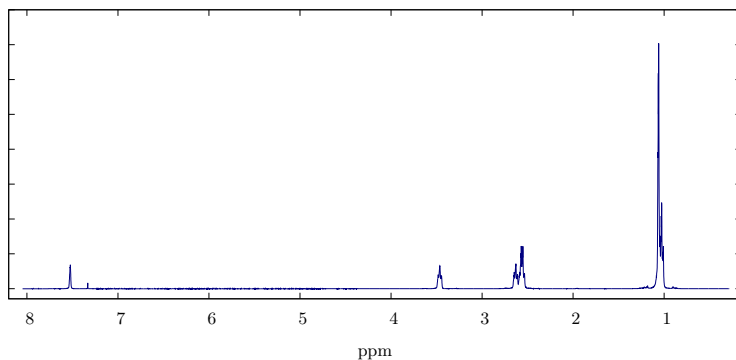


Figure 4.65: ^1H -NMR of *N'*-(2,2-dimethylpropylidene)-*N,N*-diethyl-ethylendiamine.

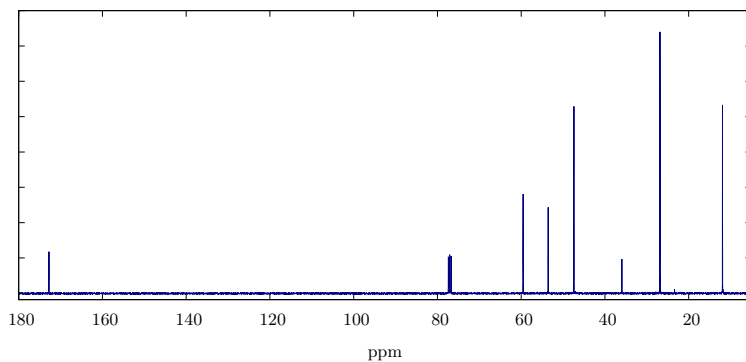


Figure 4.66: ^{13}C -NMR of *N'*-(2,2-dimethylpropylidene)-*N,N*-diethyl-ethylendiamine.

***N'*-Cyclohexylmethylene-*N,N*-diethyl-ethane-1,2-diamine**

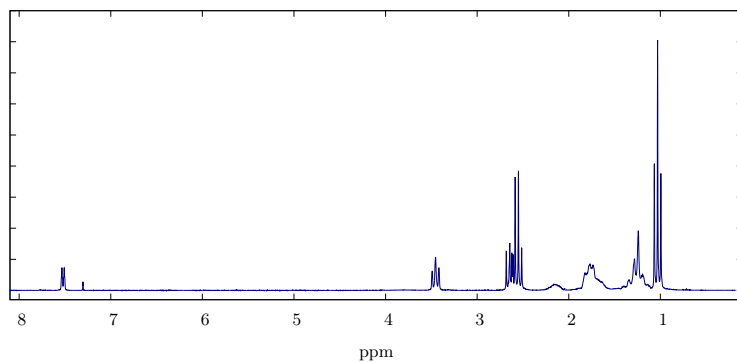


Figure 4.67: ^1H -NMR of *N'*-cyclohexylmethylene-*N,N*-diethyl-ethane-1,2-diamine.

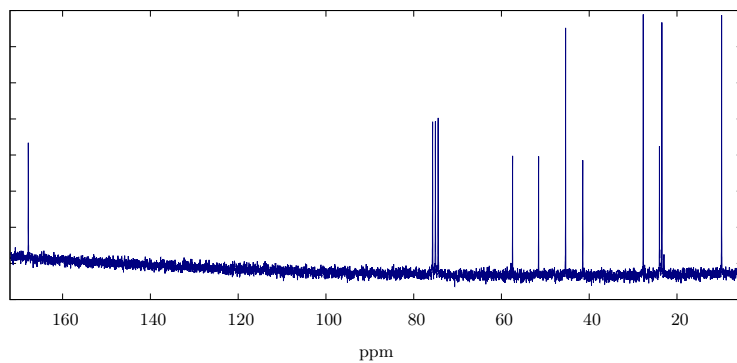


Figure 4.68: ^{13}C -NMR of *N'*-cyclohexylmethylene-*N,N*-diethyl-ethane-1,2-diamine.

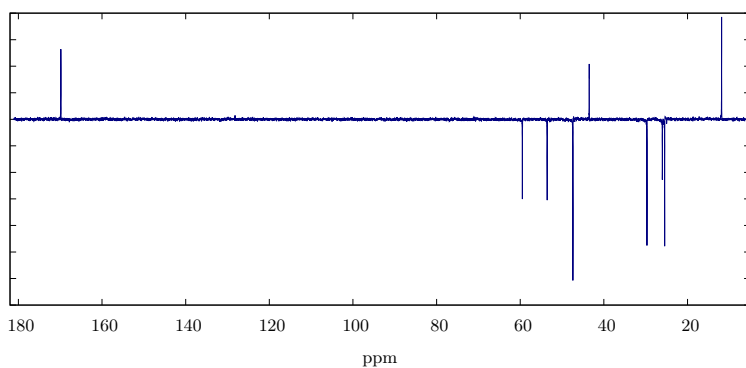


Figure 4.69: DEPT135 ^{13}C -NMR of *N'*-cyclohexylmethylene-*N,N*-diethylethane-1,2-diamine.

Adamantanylmethylidene-diethylaminomethylamine

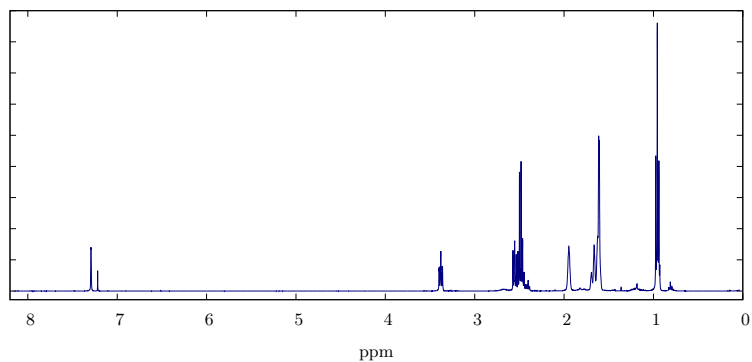


Figure 4.70: ^1H -NMR of adamantanylmethylidene-diethylaminomethylamine.

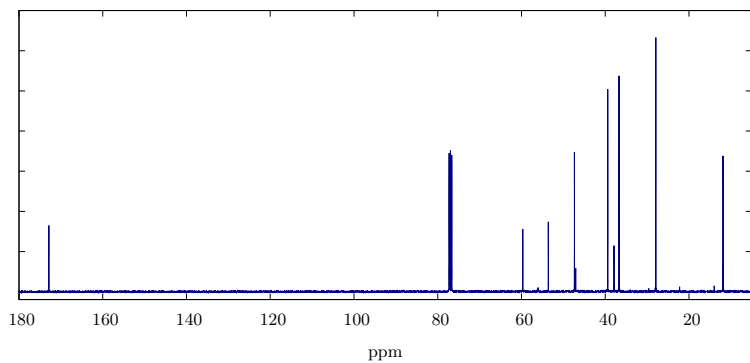


Figure 4.71: ^{13}C -NMR of adamantanylmethylidene-diethylaminomethylamine.

2-Hydroxy-adamantancarbaldehyde

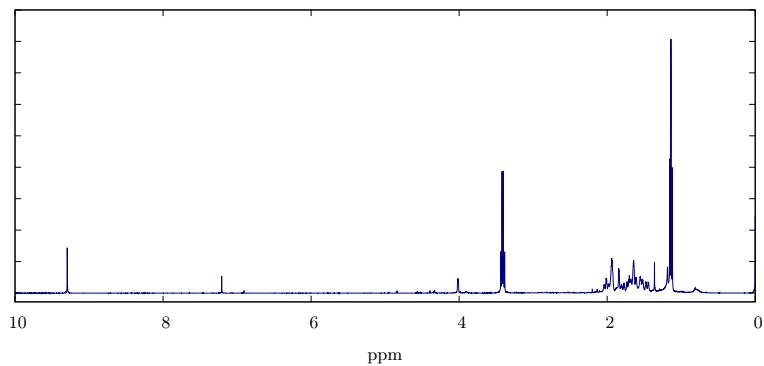


Figure 4.72: ^1H -NMR of 2-hydroxy-adamantancarbaldehyde.

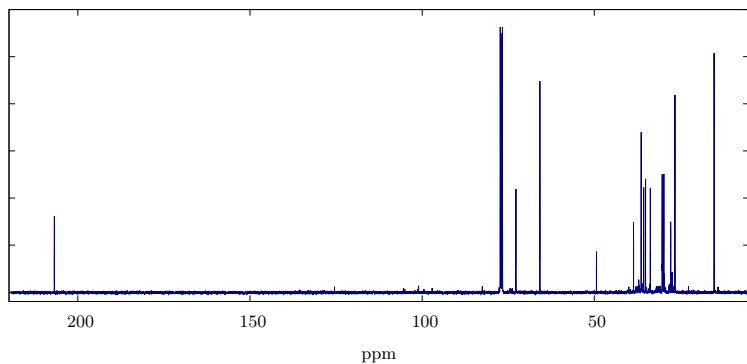


Figure 4.73: ^{13}C -NMR of 2-hydroxy-adamantancarbaldehyde.

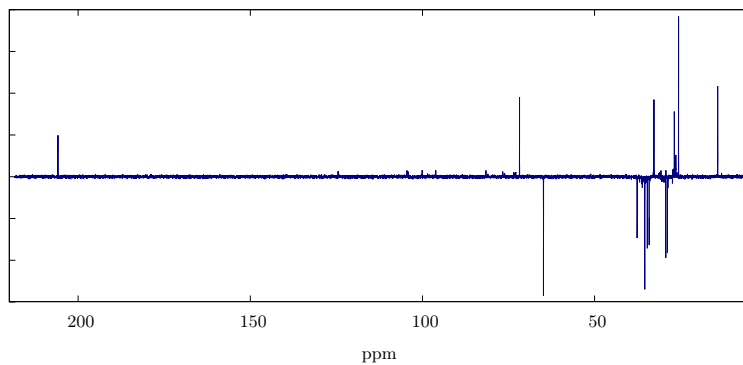


Figure 4.74: DEPT135 ^{13}C -NMR of 2-hydroxy-adamantancarbaldehyde.

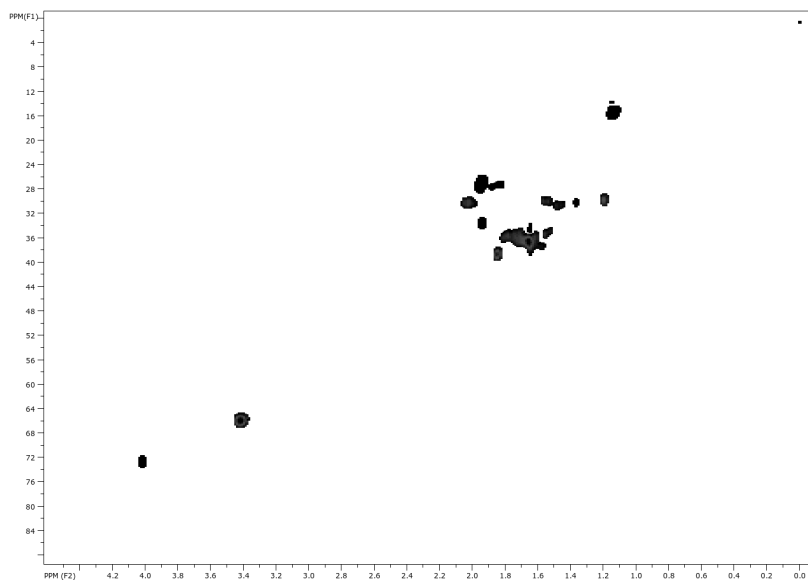


Figure 4.75: HSQC (y: ^{13}C) of 2-hydroxy-adamantancarbaldehyde.

Pentafluorophenylhydrazin-1-ylidenemethyladamantan-2-ol

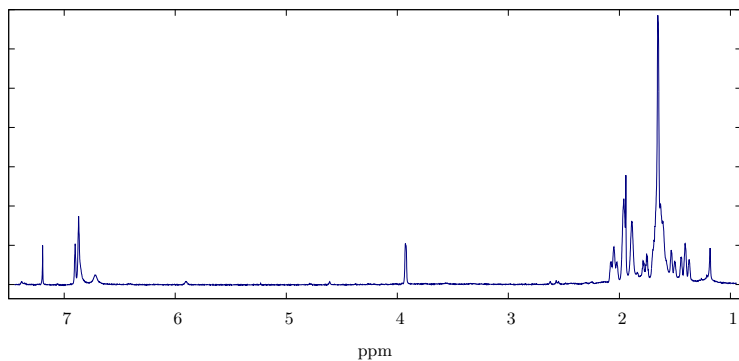


Figure 4.76: ^1H -NMR of pentafluorophenylhydrazin-1-ylidenemethyladamantan-2-ol.

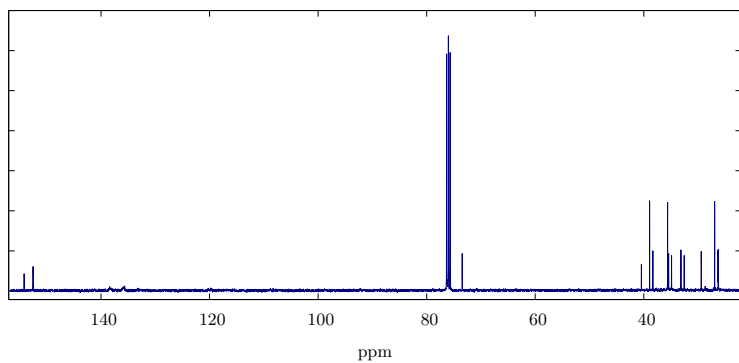


Figure 4.77: ^{13}C -NMR of pentafluorophenylhydrazin-1-ylidenemethyladamantan-2-ol.

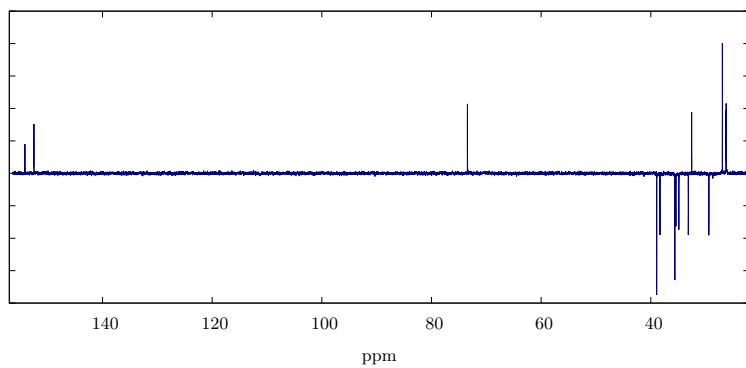


Figure 4.78: DEPT135 ^{13}C -NMR of pentafluorophenylhydrazin-1-ylidene-methyladamantan-2-ol.

Diamantane-1-carboxylic acid

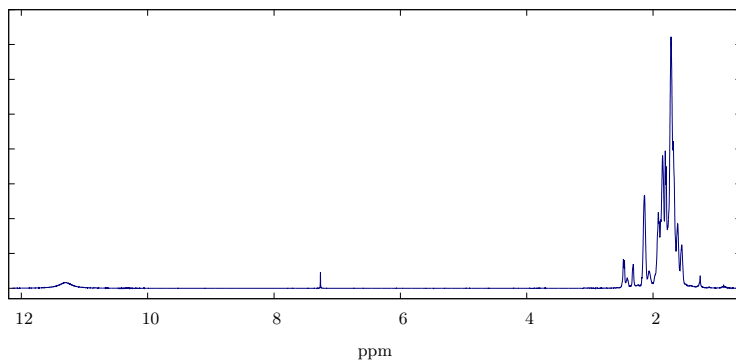


Figure 4.79: ^1H -NMR of diamantane-1-carboxylic acid.

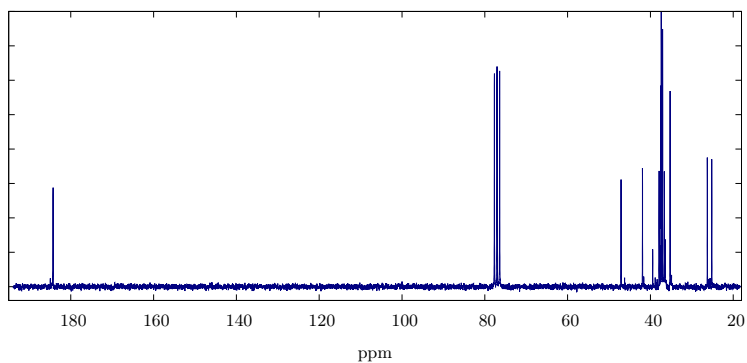


Figure 4.80: ^{13}C -NMR of diamantane-1-carboxylic acid.

Diamantane-1-carboxylic acid methylester

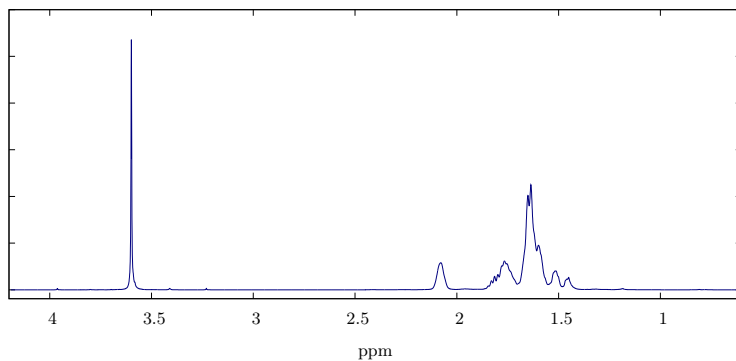


Figure 4.81: ^1H -NMR of diamantane-1-carboxylic acid methylester.

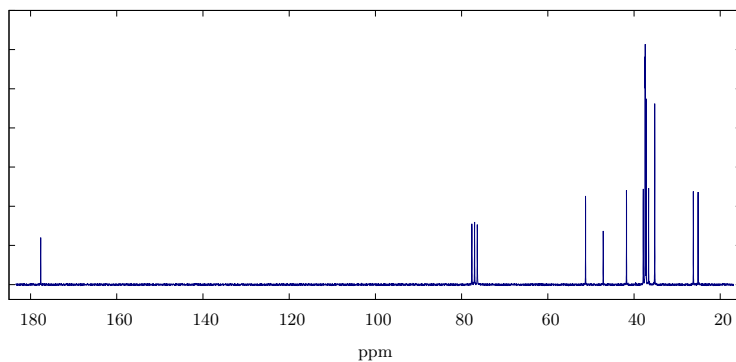


Figure 4.82: ^{13}C -NMR of diamantane-1-carboxylic acid methylester.

1-Hydroxymethyldiamantane

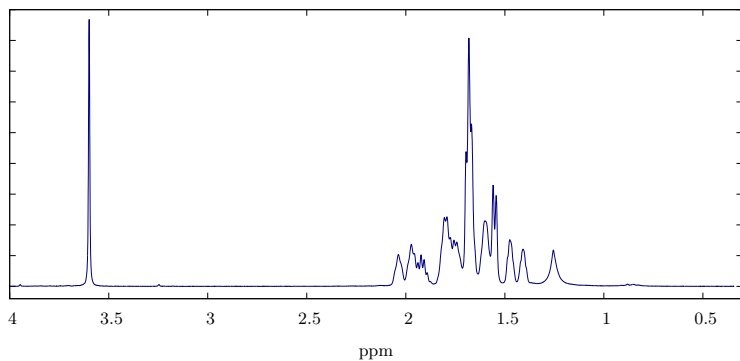


Figure 4.83: ^1H -NMR of 1-hydroxymethyldiamantane.

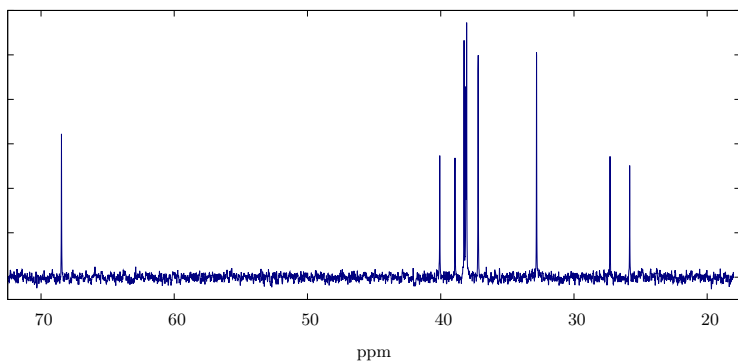


Figure 4.84: ^{13}C -NMR of 1-hydroxymethyldiamantane.

Diamantane-1-carbaldehyde

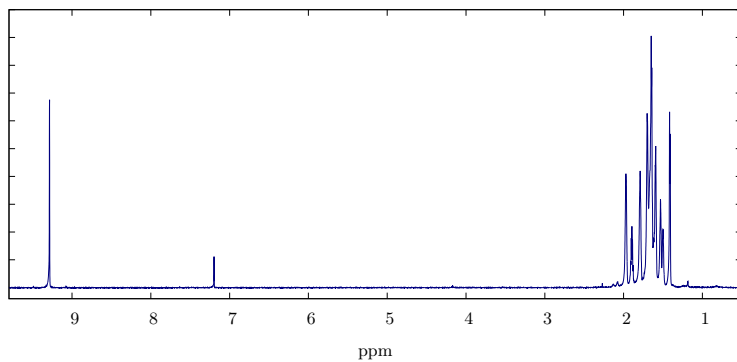


Figure 4.85: ^1H -NMR of diamantane-1-carbaldehyde.

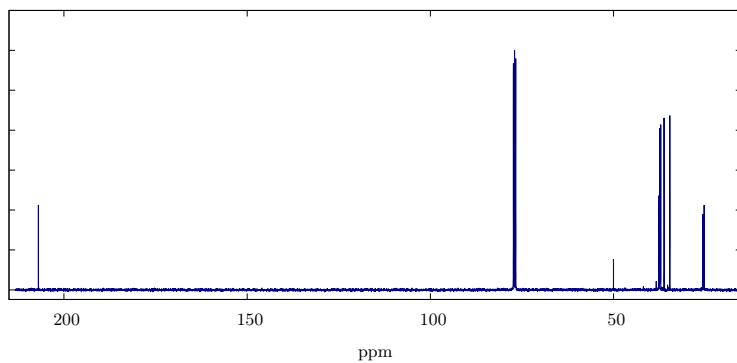


Figure 4.86: ^{13}C -NMR of diamantane-1-carbaldehyde.

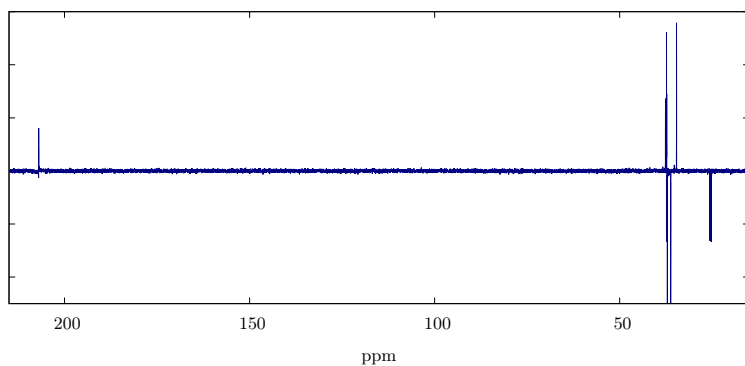


Figure 4.87: DEPT135 ^{13}C -NMR of diamantane-1-carbaldehyde.

Diamantylmethylidene-diethylaminomenthylamine

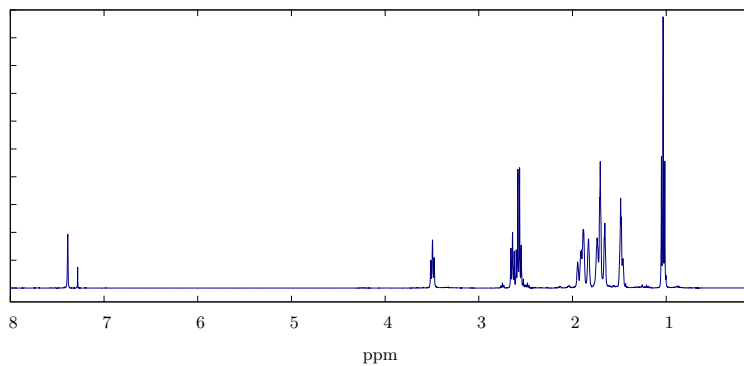


Figure 4.88: ^1H -NMR of diamantylmethylidene-diethylaminomenthylamine.

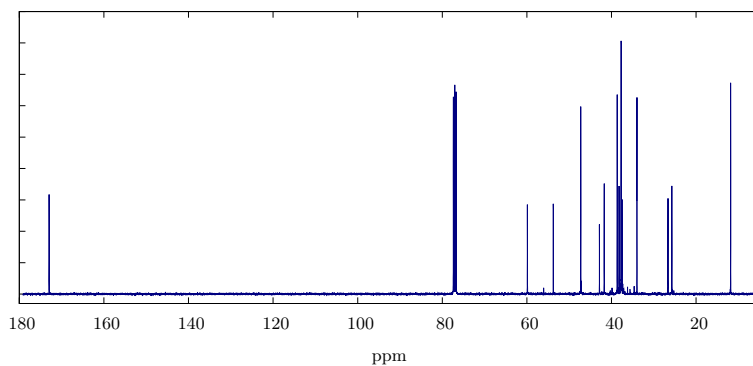


Figure 4.89: ^{13}C -NMR of diamantylmethylidene-diethylaminomenthylamine.

2-Hydroxy-diamantancarbaldehyde

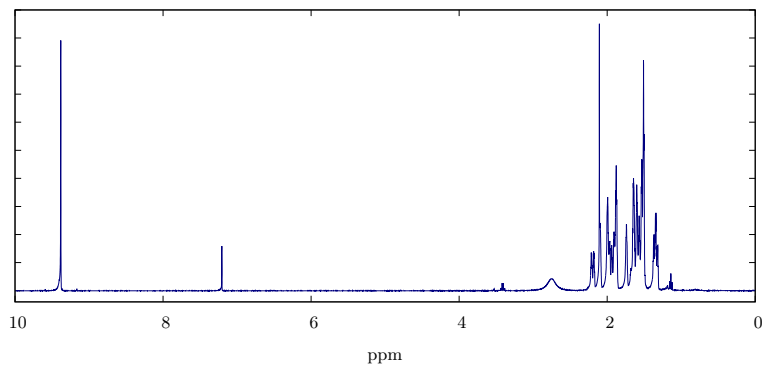


Figure 4.90: ^1H -NMR of 2-hydroxy-diamantancarbaldehyde.

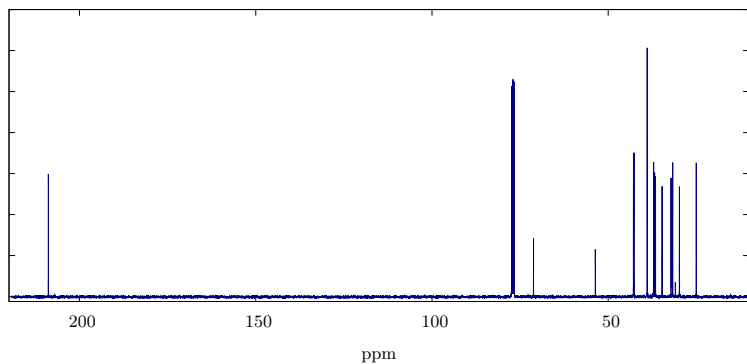


Figure 4.91: ^{13}C -NMR of 2-hydroxy-diamantancarbaldehyde.

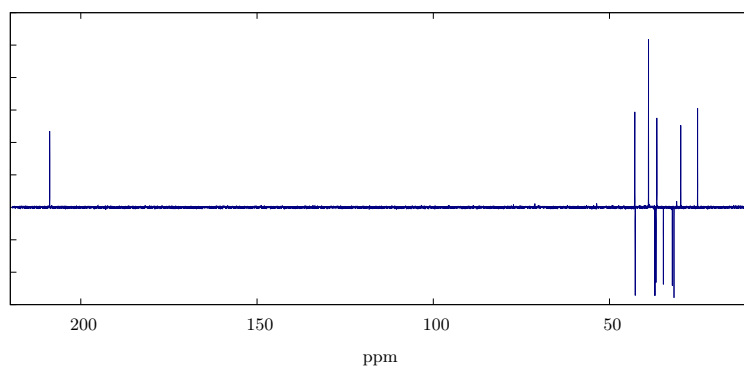


Figure 4.92: DEPT135 ^{13}C -NMR of 2-hydroxy-diamantancarbaldehyde.

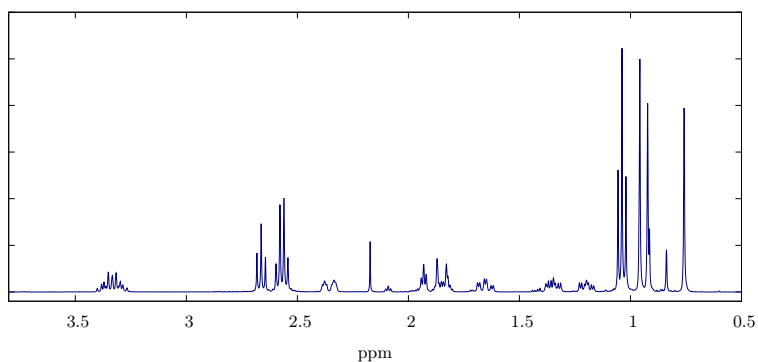
***N,N*-Diethyl-*N'*-(1,7,7-trimethyl-bicyclo[2.2.1]hept-2-ylidene)-ethane-1,2-diamine**

Figure 4.93: ^1H -NMR of *N,N*-diethyl-*N'*-(1,7,7-trimethyl-bicyclo[2.2.1]hept-2-ylidene)-ethane-1,2-diamine.

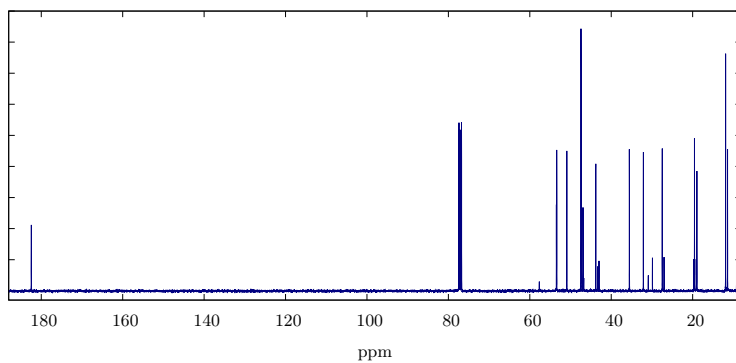


Figure 4.94: ^{13}C -NMR of *N,N*-diethyl-*N'*-(1,7,7-trimethyl-bicyclo[2.2.1]hept-2-ylidene)-ethane-1,2-diamine.

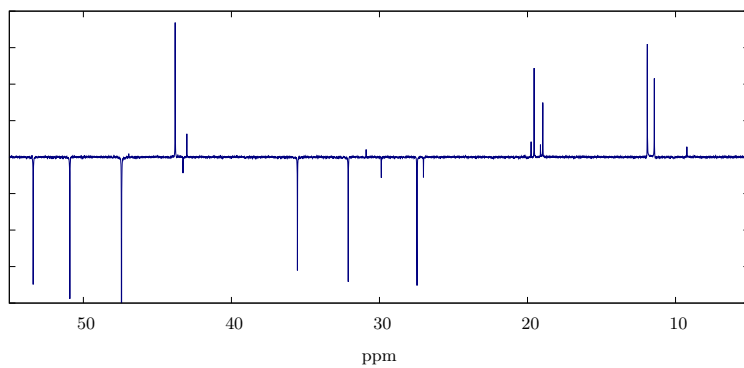


Figure 4.95: DEPT135 ^{13}C -NMR of *N,N*-diethyl-*N'*-(1,7,7-trimethyl-bicyclo[2.2.1]hept-2-ylidene)-ethane-1,2-diamine.

4.2.3 Mass Spectra

3-Hydroxy-2,2-dimethyl-propionaldehyde

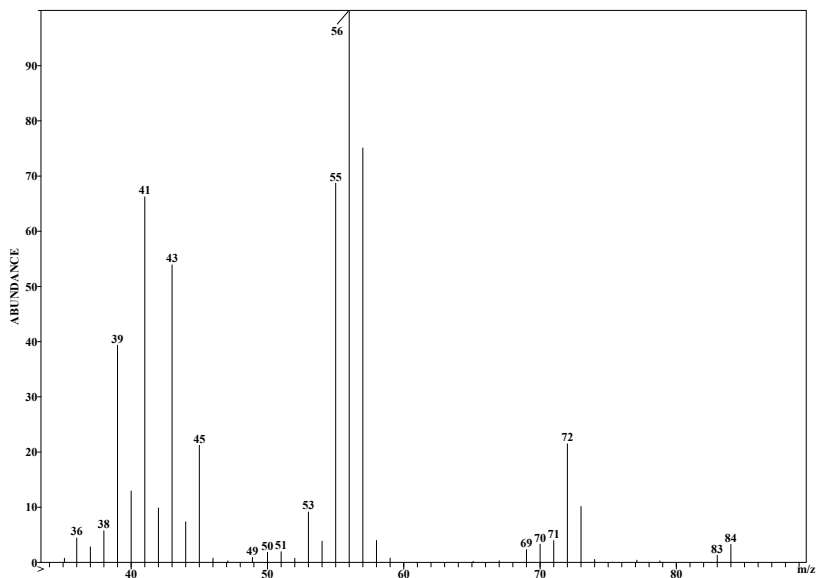


Figure 4.96: Mass spectrum of 3-hydroxy-2,2-dimethyl-propionaldehyde.

2-Hydroxy-adamantancarbaldehyde

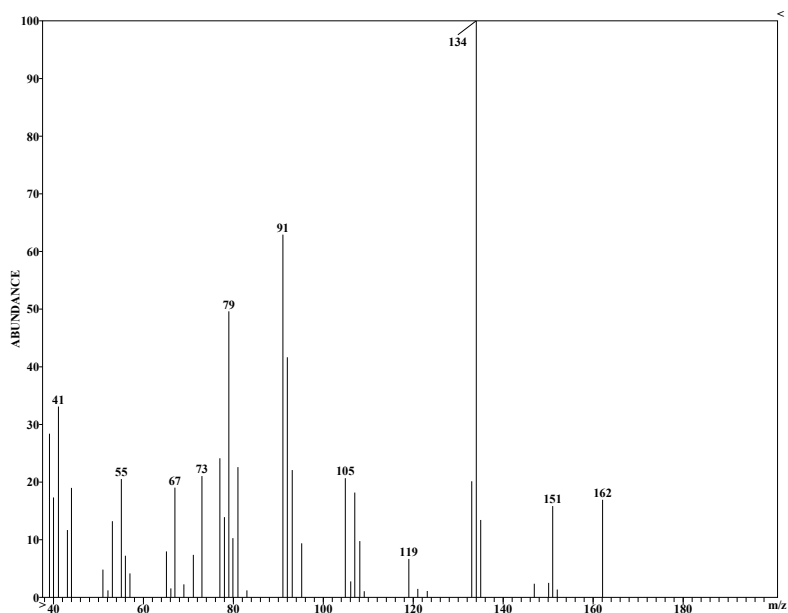
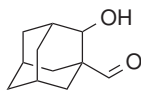


Figure 4.97: Mass spectrum of 2-hydroxy-adamantancarbaldehyde.

4.2.4 IR Spectra

2-Hydroxy-adamantancarbaldehyde

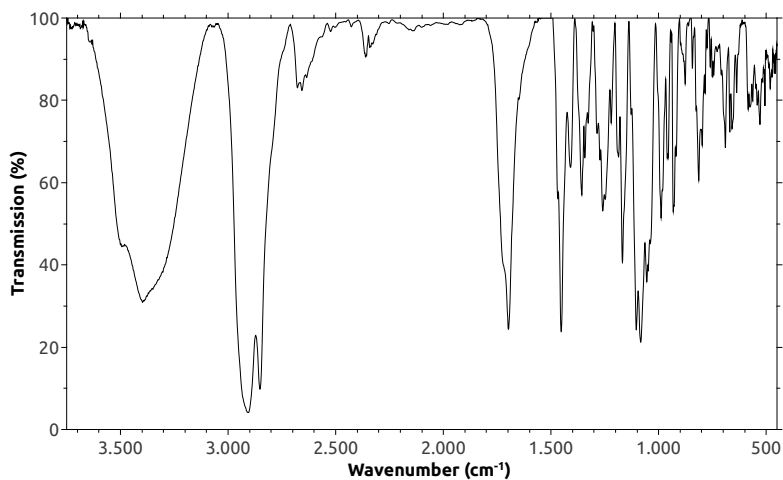
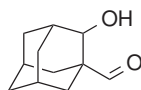


Figure 4.98: IR spectrum of 2-hydroxy-adamantancarbaldehyde.

4.2.5 Crystallographic Data

Adamantane-1-carboxylic acid methylester

Table 4.48: Crystal data and structure refinement for adamantane-1-carboxylic acid methylester.

CCDC number	1059670
Empirical formula	C ₁₂ H ₁₈ O ₂
Formula weight	194.26
Temperature	193(2) K
Wavelength	0.71073 Å
Crystal system	Monoclinic
Space group	<i>P</i> 2 ₁ / <i>c</i>
Unit cell dimensions	a = 10.569(2) Å α = 90° b = 7.3850(15) Å β = 108.72(3)° c = 14.032(3) Å γ = 90°
Volume	1037.3(4) Å ³
Z	4
Density (calculated)	1.244 Mg/m ³
Absorption coefficient	0.083 mm ⁻¹
F(000)	424
Crystal Size	0.65 x 0.30 x 0.25 mm ³
Theta range for data collection	2.035 to 25.026°
Index ranges	-12 ≤ h ≤ 12, -8 ≤ k ≤ 8, -16 ≤ l ≤ 16
Reflections collected	7331
Independent reflections	1843 [R(int) = 0.0458]
Completeness to theta = 25.96°	99.9%
Absorption correction	Empirical
Max. and min. transmission	0.9796 and 0.9483
Refinement method	Full-matrix least-squares on F ²
Data / restraints / parameters	1843 / 0 / 199
Goodness-of-fit on F ²	1.054
Final R indices [I > 2σ(I)]	R1 = 0.0405, wR2 = 0.1003
R indices (all data)	R1 = 0.0530, wR2 = 0.1080
Largest diff. peak and hole	0.147 and -0.249 e.Å ⁻³

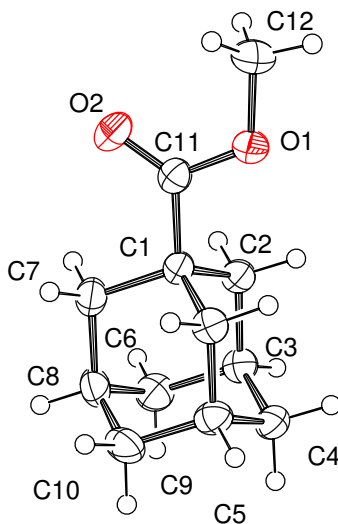


Table 4.49: Bond lengths [\AA] and angles [$^\circ$] for adamantane-1-carboxylic acid methylester.

C(1)-C(11)	1.5178(19)	C(3)-C(9)	1.528(2)
C(1)-C(7)	1.535(2)	C(3)-C(4)	1.534(2)
C(1)-C(6)	1.5442(19)	C(4)-C(5)	1.530(2)
C(1)-C(2)	1.5475(19)	C(5)-C(10)	1.529(2)
O(1)-C(11)	1.3436(18)	C(5)-C(6)	1.533(2)
O(1)-C(12)	1.4438(19)	C(7)-C(8)	1.534(2)
C(2)-C(3)	1.534(2)	C(8)-C(10)	1.528(3)
O(2)-C(11)	1.2020(17)	C(8)-C(9)	1.533(2)
C(11)-C(1)-C(7)	109.65(11)	C(10)-C(5)-C(6)	109.55(13)
C(11)-C(1)-C(6)	110.98(11)	C(4)-C(5)-C(6)	109.65(13)
C(7)-C(1)-C(6)	108.94(13)	C(5)-C(6)-C(1)	109.66(12)
C(11)-C(1)-C(2)	109.33(12)	C(8)-C(7)-C(1)	109.85(12)
C(7)-C(1)-C(2)	109.08(12)	C(10)-C(8)-C(9)	109.68(13)
C(6)-C(1)-C(2)	108.83(11)	C(10)-C(8)-C(7)	109.83(14)
C(11)-O(1)-C(12)	115.63(12)	C(9)-C(8)-C(7)	109.42(14)
C(3)-C(2)-C(1)	109.58(12)	C(3)-C(9)-C(8)	109.23(12)

continue next page

Table 4.49: Bond lengths [Å] and angles [°] for adamantane-1-carboxylic acid methylester.

C(9)-C(3)-C(2)	110.10(12)	C(8)-C(10)-C(5)	109.31(13)
C(9)-C(3)-C(4)	109.62(13)	O(2)-C(11)-O(1)	122.43(13)
C(2)-C(3)-C(4)	109.03(12)	O(2)-C(11)-C(1)	125.26(13)
C(5)-C(4)-C(3)	109.50(12)	O(1)-C(11)-C(1)	112.30(11)
C(10)-C(5)-C(4)	109.58(13)		

1-Hydroxymethyladamantane

Table 4.50: Crystal data and structure refinement for 1-hydroxymethyladamantane.

CCDC number	1059672
Empirical formula	C ₃₃ H ₅₄ O ₃
Formula weight	498.76
Temperature	190(2) K
Wavelength	0.71073 Å
Crystal system	Monoclinic
Space group	<i>P</i> 2 ₁ / <i>n</i> 11
Unit cell dimensions	a = 11.353(2) Å α = 90° b = 13.113(3) Å β = 90.00(3)° c = 19.503(4) Å γ = 90°
Volume	2903.4(10) Å ³
Z	4
Density (calculated)	1.141 Mg/m ³
Absorption coefficient	0.070 mm ⁻¹
F(000)	1104
Crystal Size	0.50 x 0.45 x 0.40 mm ³
Theta range for data collection	1.044 to 25.017°
Index ranges	-13<= <i>h</i> <=13, -15<= <i>k</i> <=14, -23<= <i>l</i> <=23
Reflections collected	32276
Independent reflections	5102 [R(int) = 0.0601]
Completeness to theta = 25.96°	99.9%
Absorption correction	Empirical
Max. and min. transmission	1.03880 and 0.89112
Refinement method	Full-matrix least-squares on F ²
Data / restraints / parameters	5102 / 0 / 542
Goodness-of-fit on F ²	1.005
Final R indices [I>2sigma(I)]	R1 = 0.0412, wR2 = 0.0994
R indices (all data)	R1 = 0.0700, wR2 = 0.1101
Largest diff. peak and hole	0.183 and -0.144 e.Å ⁻³

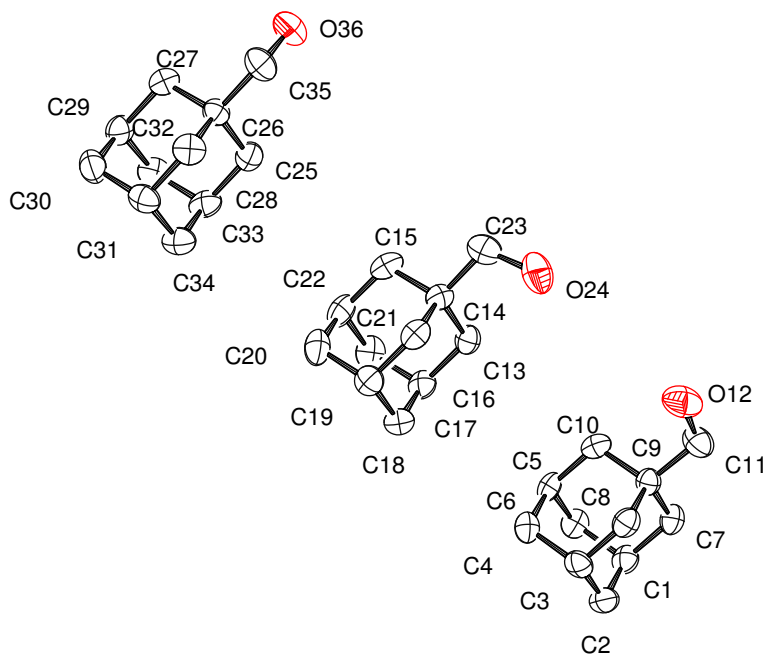


Table 4.51: Bond lengths [Å] and angles [°] for 1-hydroxymethyladamantane.

C(1)-C(7)	1.520(3)	C(17)-C(18)	1.520(3)
C(1)-C(2)	1.522(3)	C(17)-C(21)	1.531(3)
C(1)-C(6)	1.527(3)	C(18)-C(19)	1.532(3)
C(2)-C(3)	1.530(3)	C(19)-C(20)	1.525(3)
C(3)-C(8)	1.526(3)	C(20)-C(22)	1.527(3)
C(3)-C(4)	1.531(3)	C(21)-C(22)	1.526(3)
C(4)-C(5)	1.526(3)	C(23)-O(24)	1.419(3)
C(5)-C(10)	1.521(3)	C(25)-C(33)	1.526(3)
C(5)-C(6)	1.533(3)	C(25)-C(26)	1.534(3)
C(7)-C(9)	1.540(3)	C(26)-C(35)	1.522(3)
C(8)-C(9)	1.530(3)	C(26)-C(27)	1.527(3)
C(9)-C(11)	1.516(3)	C(26)-C(28)	1.527(3)
C(9)-C(10)	1.542(3)	C(27)-C(29)	1.539(3)

continue next page

Table 4.51: Bond lengths [\AA] and angles [$^\circ$] for 1-hydroxymethyladamantane.

C(11)-O(12)	1.430(3)	C(28)-C(31)	1.532(4)
C(13)-C(17)	1.531(3)	C(29)-C(30)	1.520(3)
C(13)-C(14)	1.539(3)	C(29)-C(32)	1.532(3)
C(14)-C(23)	1.520(2)	C(30)-C(31)	1.523(3)
C(14)-C(16)	1.529(3)	C(31)-C(34)	1.527(3)
C(14)-C(15)	1.539(3)	C(32)-C(33)	1.525(3)
C(15)-C(22)	1.523(3)	C(33)-C(34)	1.522(3)
C(16)-C(19)	1.529(4)	C(35)-O(36)	1.412(3)
C(7)-C(1)-C(2)	109.7(2)	C(13)-C(17)-C(21)	109.9(2)
C(7)-C(1)-C(6)	109.5(2)	C(17)-C(18)-C(19)	109.64(16)
C(2)-C(1)-C(6)	109.4(2)	C(20)-C(19)-C(16)	109.3(2)
C(1)-C(2)-C(3)	109.52(19)	C(20)-C(19)-C(18)	109.34(19)
C(8)-C(3)-C(2)	110.1(2)	C(16)-C(19)-C(18)	109.18(19)
C(8)-C(3)-C(4)	109.30(19)	C(19)-C(20)-C(22)	109.72(19)
C(2)-C(3)-C(4)	108.97(19)	C(22)-C(21)-C(17)	109.61(19)
C(5)-C(4)-C(3)	109.25(18)	C(15)-C(22)-C(21)	109.5(2)
C(10)-C(5)-C(4)	110.3(2)	C(15)-C(22)-C(20)	109.6(2)
C(10)-C(5)-C(6)	109.3(2)	C(21)-C(22)-C(20)	108.93(18)
C(4)-C(5)-C(6)	109.22(19)	O(24)-C(23)-C(14)	114.18(17)
C(1)-C(6)-C(5)	109.24(18)	C(33)-C(25)-C(26)	110.36(18)
C(1)-C(7)-C(9)	110.67(18)	C(35)-C(26)-C(27)	111.09(19)
C(3)-C(8)-C(9)	110.42(18)	C(35)-C(26)-C(28)	108.5(2)
C(11)-C(9)-C(8)	112.2(2)	C(27)-C(26)-C(28)	109.13(19)
C(11)-C(9)-C(7)	107.59(19)	C(35)-C(26)-C(25)	111.1(2)
C(8)-C(9)-C(7)	108.85(18)	C(27)-C(26)-C(25)	108.74(18)
C(11)-C(9)-C(10)	111.59(19)	C(28)-C(26)-C(25)	108.20(18)
C(8)-C(9)-C(10)	108.61(18)	C(26)-C(27)-C(29)	109.84(19)
C(7)-C(9)-C(10)	107.89(18)	C(26)-C(28)-C(31)	111.07(18)
C(5)-C(10)-C(9)	110.25(18)	C(30)-C(29)-C(32)	109.43(19)
O(12)-C(11)-C(9)	114.0(2)	C(30)-C(29)-C(27)	110.2(2)
C(17)-C(13)-C(14)	110.21(17)	C(32)-C(29)-C(27)	108.7(2)
C(23)-C(14)-C(16)	111.8(2)	C(29)-C(30)-C(31)	109.9(2)
C(23)-C(14)-C(15)	108.68(16)	C(30)-C(31)-C(34)	109.3(2)
C(16)-C(14)-C(15)	108.67(18)	C(30)-C(31)-C(28)	108.8(2)
C(23)-C(14)-C(13)	111.1(2)	C(34)-C(31)-C(28)	109.1(2)
C(16)-C(14)-C(13)	108.58(15)	C(33)-C(32)-C(29)	109.48(19)
C(15)-C(14)-C(13)	107.94(18)	C(34)-C(33)-C(32)	109.4(2)
C(22)-C(15)-C(14)	110.85(16)	C(34)-C(33)-C(25)	109.7(2)
C(19)-C(16)-C(14)	110.83(18)	C(32)-C(33)-C(25)	109.34(19)
C(18)-C(17)-C(13)	109.76(19)	C(33)-C(34)-C(31)	109.7(2)
C(18)-C(17)-C(21)	108.86(18)	O(36)-C(35)-C(26)	114.9(2)

3-hydroxy-2,2-dimethyl-propionic acid

Table 4.52: Crystal data and structure refinement for 3-hydroxy-2,2-dimethyl-propionic acid.

CCDC number	1059671
Empirical formula	C ₁₅ H ₃₀ O ₉
Formula weight	354.39
Temperature	190(2) K
Wavelength	0.71073 Å
Crystal system	Monoclinic
Space group	<i>P</i> 2 ₁ / <i>n</i>
Unit cell dimensions	a = 6.0890(12) Å α = 90° b = 30.670(6) Å β = 93.24(3)° c = 9.868(2) Å γ = 90°
Volume	1839.9(6) Å ³
Z	4
Density (calculated)	1.279 Mg/m ³
Absorption coefficient	0.105 mm ⁻¹
F(000)	768
Crystal Size	1.05 x 0.35 x 0.25 mm ³
Theta range for data collection	2.17 to 27.51°
Index ranges	-7<= <i>h</i> <=7, -39<= <i>k</i> <=39, -12<= <i>l</i> <=11
Reflections collected	11758
Independent reflections	4068 [R(int) = 0.0588]
Completeness to theta = 25.96°	96.4%
Absorption correction	Empirical
Max. and min. transmission	0.9742 and 0.8976
Refinement method	Full-matrix least-squares on F ²
Data / restraints / parameters	4068 / 0 / 337
Goodness-of-fit on F ²	0.934
Final R indices [I>2sigma(I)]	R1 = 0.0452, wR2 = 0.1107
R indices (all data)	R1 = 0.0742, wR2 = 0.1239
Largest diff. peak and hole	0.214 and -0.251 e.Å ⁻³

4 Supporting Information

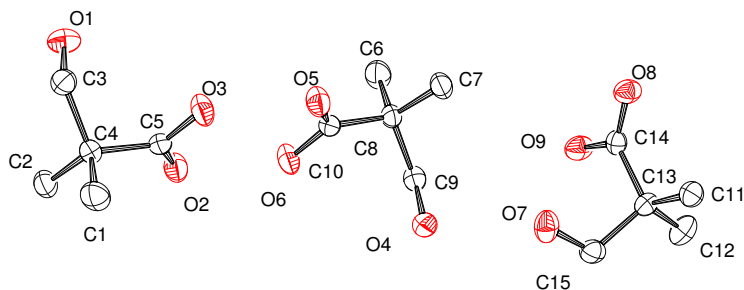


Table 4.53: Bond lengths [Å] and angles [°] for 3-hydroxy-2,2-dimethylpropionic acid.

O(1)-C(3)	1.4229(17)	C(7)-C(8)	1.5290(18)
C(1)-C(4)	1.5408(19)	C(8)-C(10)	1.5166(18)
O(2)-C(5)	1.2243(16)	C(8)-C(9)	1.5296(19)
C(2)-C(4)	1.5267(18)	O(7)-C(15)	1.4262(18)
O(3)-C(5)	1.3152(15)	O(8)-C(14)	1.2233(16)
C(3)-C(4)	1.5249(19)	O(9)-C(14)	1.3181(15)
C(4)-C(5)	1.5180(18)	C(11)-C(13)	1.5266(18)
O(4)-C(9)	1.4239(17)	C(12)-C(13)	1.534(2)
O(5)-C(10)	1.2226(16)	C(13)-C(14)	1.5138(18)
O(6)-C(10)	1.3128(15)	C(13)-C(15)	1.5336(19)
C(6)-C(8)	1.535(2)		
O(1)-C(3)-C(4)	109.91(11)	C(9)-C(8)-C(6)	108.08(11)
C(5)-C(4)-C(3)	109.08(11)	O(4)-C(9)-C(8)	112.24(11)
C(5)-C(4)-C(2)	109.88(11)	O(5)-C(10)-O(6)	122.91(12)
C(3)-C(4)-C(2)	110.91(11)	O(5)-C(10)-C(8)	122.92(11)
C(5)-C(4)-C(1)	108.02(11)	O(6)-C(10)-C(8)	114.15(12)
C(3)-C(4)-C(1)	108.21(11)	C(14)-C(13)-C(11)	109.75(11)
C(2)-C(4)-C(1)	110.66(12)	C(14)-C(13)-C(15)	108.32(10)
O(2)-C(5)-O(3)	122.58(12)	C(11)-C(13)-C(15)	111.24(12)
O(2)-C(5)-C(4)	123.39(11)	C(14)-C(13)-C(12)	108.90(12)
O(3)-C(5)-C(4)	114.01(12)	C(11)-C(13)-C(12)	110.39(12)
C(10)-C(8)-C(7)	109.88(11)	C(15)-C(13)-C(12)	108.18(12)
C(10)-C(8)-O(9)	109.84(11)	O(8)-C(14)-O(9)	122.73(12)
C(7)-C(8)-C(9)	110.52(11)	O(8)-C(14)-C(13)	123.36(11)
C(10)-C(8)-C(6)	107.82(11)	O(9)-C(14)-C(13)	113.90(11)
C(7)-C(8)-C(6)	110.65(12)	O(7)-C(15)-C(13)	112.24(11)

Pentafluorophenylhydrazin-1-ylidenemethyladamantan-2-ol

Table 4.54: Crystal data and structure refinement for pentafluorophenylhydrazin-1-ylidenemethyladamantan-2-ol.

CCDC number	1059674
Empirical formula	C ₁₇ H ₁₇ F ₅ N ₂ O
Formula weight	360.32
Temperature	150(2) K
Wavelength	0.71073 Å
Crystal system	Monoclinic
Space group	<i>P</i> 2 ₁ / <i>c</i>
Unit cell dimensions	a = 13.503(3) Å α = 90° b = 10.452(2) Å β = 108.39(3)° c = 11.595(2) Å γ = 90°
Volume	1552.8(6) Å ³
Z	4
Density (calculated)	1.541 Mg/m ³
Absorption coefficient	0.138 mm ⁻¹
F(000)	744
Crystal Size	0.40 x 0.09 x 0.07 mm ³
Theta range for data collection	2.515 to 27.452°
Index ranges	-13<= <i>h</i> <=17, -13<= <i>k</i> <=11, -14<= <i>l</i> <=13
Reflections collected	10282
Independent reflections	3543 [R(int) = 0.0538]
Completeness to theta = 25.96°	100.0%
Absorption correction	Empirical
Max. and min. transmission	0.95665 and 0.90996
Refinement method	Full-matrix least-squares on F ²
Data / restraints / parameters	3543 / 3 / 242
Goodness-of-fit on F ²	1.055
Final R indices [I>2sigma(I)]	R1 = 0.0603, wR2 = 0.1437
R indices (all data)	R1 = 0.1129, wR2 = 0.1638
Largest diff. peak and hole	0.607 and -0.312 e.Å ⁻³

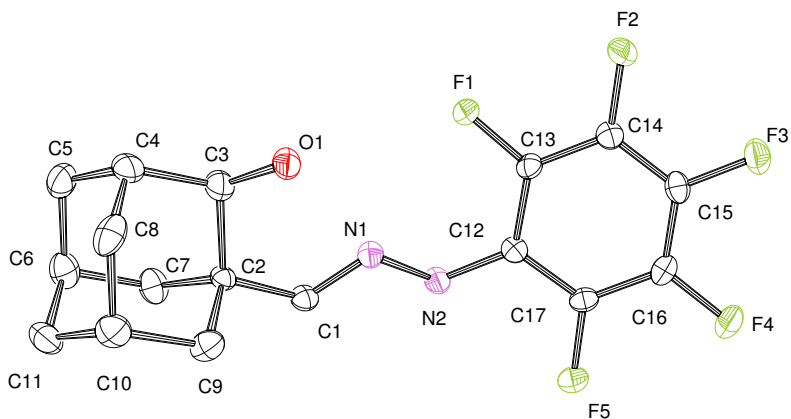


Table 4.55: Bond lengths [Å] and angles [°] for pentapentafluorophenylhydrazin-1-ylidenemethyladamantan-2-ol.

F(1)-C(13)	1.345(3)	C(4)-C(8)	1.529(5)
N(1)-C(1)	1.275(3)	C(5)-C(6)	1.502(5)
N(1)-N(2)	1.392(3)	F(5)-C(17)	1.348(3)
C(1)-C(2)	1.500(3)	C(6)-C(11)	1.516(4)
F(2)-C(14)	1.348(3)	C(6)-C(7)	1.547(4)
N(2)-C(12)	1.384(3)	C(9)-C(10)	1.546(4)
C(2)-C(9)	1.535(4)	C(8)-C(10)	1.519(4)
C(2)-C(7)	1.535(4)	C(10)-C(11)	1.517(4)
C(2)-C(3)	1.539(4)	C(12)-C(17)	1.392(4)
C(3)-O(2)	1.218(12)	C(12)-C(13)	1.397(4)
C(3)-O(1)	1.392(4)	C(13)-C(14)	1.381(4)
C(3)-C(4)	1.546(4)	C(14)-C(15)	1.368(4)
F(3)-C(15)	1.347(3)	C(15)-C(16)	1.374(4)
F(4)-C(16)	1.345(3)	C(16)-C(17)	1.378(4)
C(4)-C(5)	1.506(5)		
C(1)-N(1)-N(2)	116.4(2)	C(10)-C(8)-C(4)	110.5(2)
N(1)-C(1)-C(2)	122.4(2)	C(11)-C(10)-C(8)	109.9(3)
C(12)-N(2)-N(1)	117.5(2)	C(11)-C(10)-C(9)	109.1(2)
C(1)-C(2)-C(9)	108.4(2)	C(8)-C(10)-C(9)	108.3(2)
C(1)-C(2)-C(7)	108.5(2)	C(6)-C(11)-C(10)	110.3(2)
C(9)-C(2)-C(7)	108.8(2)	N(2)-C(12)-C(17)	121.1(2)
C(1)-C(2)-C(3)	113.3(2)	N(2)-C(12)-C(13)	123.1(2)
C(9)-C(2)-C(3)	110.2(2)	C(17)-C(12)-C(13)	115.8(2)

continue next page

Table 4.55: Bond lengths [Å] and angles [°] for pentafluorophenylhydrazin-1-ylidenemethyladamantan-2-ol.

C(7)-C(2)-C(3)	107.6(2)	F(1)-C(13)-C(14)	117.9(2)
O(2)-C(3)-C(2)	130.4(7)	F(1)-C(13)-C(12)	120.2(2)
O(1)-C(3)-C(2)	114.3(2)	C(14)-C(13)-C(12)	121.8(2)
O(2)-C(3)-C(4)	116.9(7)	F(2)-C(14)-C(15)	119.7(2)
O(1)-C(3)-C(4)	109.2(2)	F(2)-C(14)-C(13)	119.7(2)
C(2)-C(3)-C(4)	109.3(2)	C(15)-C(14)-C(13)	120.5(2)
C(5)-C(4)-C(8)	110.0(2)	F(3)-C(15)-C(14)	120.2(2)
C(5)-C(4)-C(3)	108.5(2)	F(3)-C(15)-C(16)	120.4(2)
C(8)-C(4)-C(3)	109.3(3)	C(14)-C(15)-C(16)	119.4(2)
C(6)-C(5)-C(4)	110.6(3)	F(4)-C(16)-C(15)	120.1(2)
C(5)-C(6)-C(11)	111.2(3)	F(4)-C(16)-C(17)	120.0(2)
C(5)-C(6)-C(7)	108.4(2)	C(15)-C(16)-C(17)	119.8(2)
C(11)-C(6)-C(7)	108.0(3)	F(5)-C(17)-C(16)	118.8(2)
C(2)-C(7)-C(6)	110.4(2)	F(5)-C(17)-C(12)	118.6(2)
C(2)-C(9)-C(10)	109.8(2)	C(16)-C(17)-C(12)	122.7(2)

2-diethylamino-ethyl-ammonium adamantancarboxylate

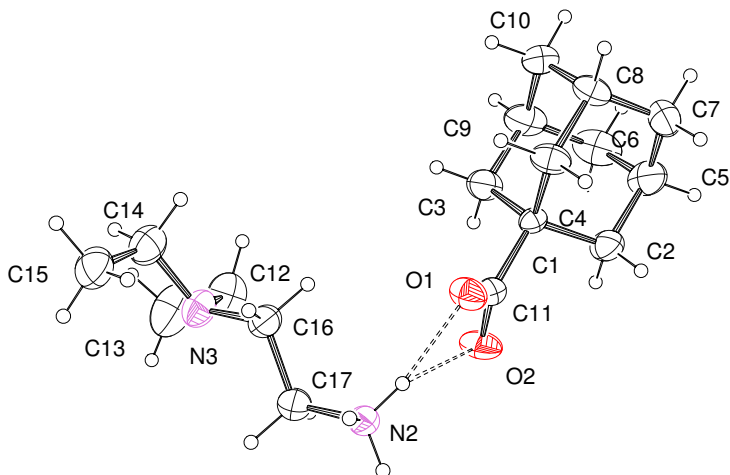
Table 4.56: Crystal data and structure refinement for 2-diethylamino-ethyl-ammonium adamantancarboxylate.

CCDC number	1059673	
Empirical formula	C ₁₇ H ₃₂ N ₂ O ₂	
Formula weight	296.44	
Temperature	190(2) K	
Wavelength	0.71073 Å	
Crystal system	Monoclinic	
Space group	<i>P</i> 2 ₁	
Unit cell dimensions	a = 10.743(2) Å	α = 90°
	b = 6.6370(13) Å	β = 94.14(3)°
	c = 12.390(3) Å	γ = 90°
Volume	881.1(3) Å ³	
Z	2	
Density (calculated)	1.117 Mg/m ³	
Absorption coefficient	0.073 mm ⁻¹	
F(000)	328	
Crystal Size	0.10 x 0.10 x 0.05 mm ³	
Theta range for data collection	1.648 to 25.027°	
Index ranges	-12 ≤ h ≤ 12, -7 ≤ k ≤ 7, -14 ≤ l ≤ 14	
Reflections collected	8503	
Independent reflections	2914 [R(int) = 0.0541]	
Completeness to theta = 25.96°	99.8%	

continue next page

Table 4.56: Crystal data and structure refinement for 2-diethylamino-ethyl-ammonium adamantancarboxylate.

Absorption correction	Empirical
Max. and min. transmission	1.07548 and 0.84628
Refinement method	Full-matrix least-squares on F^2
Data / restraints / parameters	2914 / 1 / 193
Goodness-of-fit on F^2	1.034
Final R indices [$I > 2\sigma(I)$]	$R1 = 0.0508$, $wR2 = 0.1222$
R indices (all data)	$R1 = 0.0723$, $wR2 = 0.1436$
Largest diff. peak and hole	0.142 and -0.176 $e.\text{\AA}^{-3}$

Table 4.57: Bond lengths [\AA] and angles [$^\circ$] for 2-diethylamino-ethyl-ammonium adamantancarboxylate.

O(1)-C(11)	1.250(4)	C(3)-C(9)	1.538(6)
C(1)-C(3)	1.513(5)	C(4)-C(8)	1.534(5)
C(1)-C(4)	1.522(5)	C(5)-C(6)	1.491(8)

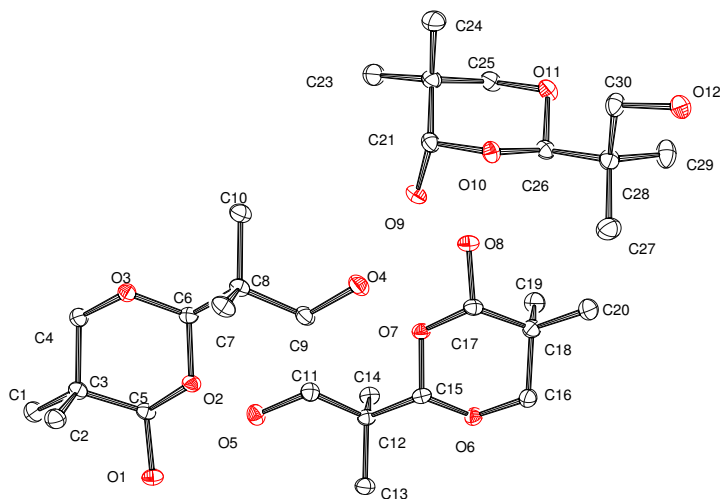
continue next page

Table 4.57: Bond lengths [Å] and angles [°] for 2-diethylamino-ethyl-ammonium adamantancarboxylate.

C(1)-C(2)	1.523(5)	C(5)-C(7)	1.500(8)
C(1)-C(11)	1.529(5)	C(6)-C(9)	1.521(9)
O(2)-C(11)	1.243(4)	C(7)-C(8)	1.487(7)
N(2)-C(17)	1.471(5)	C(8)-C(10)	1.500(6)
C(2)-C(5)	1.538(6)	C(9)-C(10)	1.519(8)
N(3)-C(16)	1.450(5)	C(12)-C(13)	1.484(8)
N(3)-C(12)	1.466(6)	C(14)-C(15)	1.485(7)
N(3)-C(14)	1.467(7)	C(16)-C(17)	1.500(6)
C(3)-C(1)-C(4)	108.4(3)	C(8)-C(7)-C(5)	110.9(4)
C(3)-C(1)-C(2)	108.9(4)	C(7)-C(8)-C(10)	110.6(4)
C(4)-C(1)-C(2)	108.8(3)	C(7)-C(8)-C(4)	109.2(4)
C(3)-C(1)-C(11)	109.0(3)	C(10)-C(8)-C(4)	109.0(3)
C(4)-C(1)-C(11)	113.0(3)	C(10)-C(9)-C(6)	109.9(4)
C(2)-C(1)-C(11)	108.7(3)	C(10)-C(9)-C(3)	107.6(4)
C(1)-C(2)-C(5)	110.3(3)	C(6)-C(9)-C(3)	108.9(4)
C(16)-N(3)-C(12)	110.2(4)	C(8)-C(10)-C(9)	109.7(4)
C(16)-N(3)-C(14)	111.4(4)	O(2)-C(11)-O(1)	122.4(3)
C(12)-N(3)-C(14)	111.7(4)	O(2)-C(11)-C(1)	118.3(3)
C(1)-C(3)-C(9)	110.4(3)	O(1)-C(11)-C(1)	119.3(3)
C(1)-C(4)-C(8)	110.0(3)	N(3)-C(12)-C(13)	114.0(5)
C(6)-C(5)-C(7)	109.5(4)	N(3)-C(14)-C(15)	112.8(4)
C(6)-C(5)-C(2)	107.7(5)	N(3)-C(16)-C(17)	110.8(3)
C(7)-C(5)-C(2)	109.7(4)	N(2)-C(17)-C(16)	111.6(3)
C(5)-C(6)-C(9)	110.9(4)		

2-*tert*-butyl-5,5-dimethyl-[1,3]dioxan-4-olTable 4.58: Crystal data and structure refinement for 2-*tert*-butyl-5,5-dimethyl-[1,3]dioxan-4-ol.

CCDC number	1059669
Empirical formula	C ₃₀ H ₆₀ O ₁₂
Formula weight	612.78
Temperature	100(2) K
Wavelength	1.54178 Å
Crystal system	Triclinic
Space group	<i>P</i> $\bar{1}$
Unit cell dimensions	a = 5.9538(3) Å α = 94.834(2)° b = 14.5123(7) Å β = 92.571(2)° c = 19.3329(10) Å γ = 92.894(2)°
Volume	1660.34(14) Å ³
Z	2
Density (calculated)	1.226 Mg/m ³
Absorption coefficient	0.769 mm ⁻¹
F(000)	672
Crystal Size	1.017 x 0.366 x 0.284 mm ³
Theta range for data collection	3.664 to 66.583°
Index ranges	-7 ≤ h ≤ 7, -17 ≤ k ≤ 17, -22 ≤ l ≤ 22
Reflections collected	66765
Independent reflections	5798 [R(int) = 0.0413]
Completeness to theta = 25.96°	99.2%
Absorption correction	Semi-empirical from equivalents
Max. and min. transmission	0.7528 and 0.5637
Refinement method	Full-matrix least-squares on F ²
Data / restraints / parameters	5798 / 0 / 415
Goodness-of-fit on F ²	1.084
Final R indices [I > 2sigma(I)]	R1 = 0.0367, wR2 = 0.0898
R indices (all data)	R1 = 0.0395, wR2 = 0.0913
Largest diff. peak and hole	0.252 and -0.266 e.Å ⁻³

Table 4.59: Bond lengths [Å] and angles [°] for 2-*tert*-butyl-5,5-dimethyl-[1,3]dioxan-4-ol.

O(1)-C(5)	1.3927(15)	C(12)-C(14)	1.5318(17)
C(1)-C(3)	1.5282(17)	C(12)-C(13)	1.5348(17)
O(2)-C(6)	1.4181(15)	C(12)-C(11)	1.5351(17)
O(2)-C(5)	1.4382(14)	O(12)-C(30)	1.4385(15)
C(2)-C(3)	1.5312(18)	O(11)-C(26)	1.4092(15)
C(3)-C(5)	1.5288(17)	O(11)-C(25)	1.4304(15)
C(3)-C(4)	1.5296(17)	O(10)-C(21)	1.4221(15)
O(3)-C(6)	1.4097(15)	O(10)-C(26)	1.4255(15)
O(3)-C(4)	1.4322(15)	C(16)-C(18)	1.5325(18)
O(4)-C(9)	1.4323(15)	C(17)-C(18)	1.5296(18)
O(5)-C(11)	1.4266(15)	C(18)-C(20)	1.5284(18)
O(6)-C(15)	1.4084(15)	C(18)-C(19)	1.5297(18)
O(6)-C(16)	1.4304(15)	C(21)-C(22)	1.5341(18)
C(6)-C(8)	1.5292(17)	C(22)-C(23)	1.5271(18)
O(7)-C(15)	1.4261(15)	C(22)-C(25)	1.5273(18)
O(7)-C(17)	1.4328(15)	C(22)-C(24)	1.5340(18)
C(7)-C(8)	1.5317(17)	C(26)-C(28)	1.5291(17)

continue next page

Table 4.59: Bond lengths [\AA] and angles [$^\circ$] for 2-*tert*-butyl-5,5-dimethyl-[1,3]dioxan-4-ol.

O(8)-C(17)	1.3975(15)	C(27)-C(28)	1.5306(19)
C(8)-C(9)	1.5309(18)	C(28)-C(29)	1.5300(18)
C(8)-C(10)	1.5347(17)	C(28)-C(30)	1.5372(18)
O(9)-C(21)	1.4112(15)	C(12)-C(15)	1.5281(17)
C(6)-O(2)-C(5)	112.20(9)	O(6)-C(15)-O(7)	110.73(10)
C(1)-C(3)-C(5)	109.47(10)	O(6)-C(15)-C(12)	109.13(10)
C(1)-C(3)-C(4)	108.88(10)	O(7)-C(15)-C(12)	109.50(10)
C(5)-C(3)-C(4)	106.66(10)	O(6)-C(16)-C(18)	111.13(10)
C(1)-C(3)-C(2)	110.69(11)	O(8)-C(17)-O(7)	106.79(9)
C(5)-C(3)-C(2)	110.31(10)	O(8)-C(17)-C(18)	110.66(10)
C(4)-C(3)-C(2)	110.72(10)	O(7)-C(17)-C(18)	110.52(10)
C(6)-O(3)-C(4)	111.00(9)	C(20)-C(18)-C(17)	109.72(10)
O(3)-C(4)-C(3)	111.39(10)	C(20)-C(18)-C(19)	110.51(11)
O(1)-C(5)-O(2)	106.20(9)	C(17)-C(18)-C(19)	110.51(10)
O(1)-C(5)-C(3)	111.31(10)	C(20)-C(18)-C(16)	109.49(11)
O(2)-C(5)-C(3)	110.01(10)	C(17)-C(18)-C(16)	105.82(10)
C(15)-O(6)-C(16)	111.12(9)	C(19)-C(18)-C(16)	110.69(11)
O(3)-C(6)-O(2)	111.23(10)	O(9)-C(21)-O(10)	111.31(10)
O(3)-C(6)-C(8)	108.40(10)	O(9)-C(21)-C(22)	110.49(10)
O(2)-C(6)-C(8)	108.95(10)	O(10)-C(21)-C(22)	110.51(10)
C(15)-O(7)-C(17)	111.71(9)	C(23)-C(22)-C(25)	109.18(11)
C(6)-C(8)-C(9)	107.33(10)	C(23)-C(22)-C(24)	110.36(11)
C(6)-C(8)-C(7)	110.08(10)	C(25)-C(22)-C(24)	110.71(11)
C(9)-C(8)-C(7)	110.44(11)	C(23)-C(22)-C(21)	111.25(11)
C(6)-C(8)-C(10)	108.74(10)	C(25)-C(22)-C(21)	107.01(10)
C(9)-C(8)-C(10)	109.82(10)	C(24)-C(22)-C(21)	108.28(11)
C(7)-C(8)-C(10)	110.37(10)	O(11)-C(25)-C(22)	110.82(10)
O(4)-C(9)-C(8)	111.24(10)	O(11)-C(26)-O(10)	110.92(10)
C(15)-C(12)-C(14)	110.67(10)	O(11)-C(26)-C(28)	109.47(10)
C(15)-C(12)-C(13)	108.64(10)	O(10)-C(26)-C(28)	108.29(10)
C(14)-C(12)-C(13)	109.72(10)	C(26)-C(28)-C(29)	108.73(11)
C(15)-C(12)-C(11)	107.32(10)	C(26)-C(28)-C(27)	109.06(11)
C(14)-C(12)-C(11)	110.61(10)	C(29)-C(28)-C(27)	110.18(11)
C(13)-C(12)-C(11)	109.83(10)	C(26)-C(28)-C(30)	108.67(10)
O(5)-C(11)-C(12)	112.87(10)	C(29)-C(28)-C(30)	110.38(11)
C(26)-O(11)-C(25)	110.25(9)	C(27)-C(28)-C(30)	109.78(11)
C(21)-O(10)-C(26)	113.62(9)	O(12)-C(30)-C(28)	111.93(10)

5 Summary/Zusammenfassung

5.1 Summary

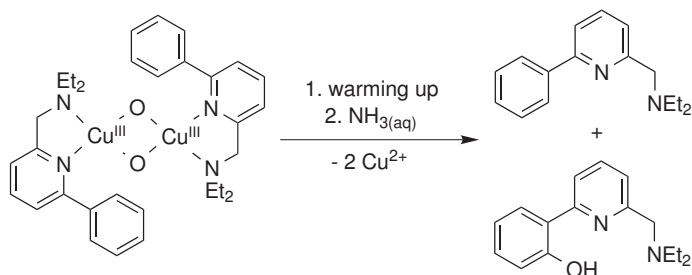
Selective oxidations under mild conditions are of great interest. In nature a variety of enzymes catalyze these reactions and most of them contain metal ions at their active site. For copper containing metalloenzymes several examples are known to hydroxylate organic substrates using dioxygen. This reactivity is of interest not only to understand biological mechanisms, but also for applications in laboratory and industrial processes. Effort by the scientific community to model the active sites or the catalytic activity of these enzymes have been successful; however, fundamental steps in the oxidation process are still discussed. The understanding of these steps would offer more options for targeted optimizations and better understanding of natural processes. Although there were attempts to utilize copper activated oxygen in synthesis, the number of applications is limited so far. Therefore it is desirable to develop more general synthetic applications using copper complexes for several reasons: As mentioned above the mild conditions and the selectivity are of interest, but furthermore copper is a less expensive alternative to rare, noble metals. In addition using dioxygen as oxidizing agent is a "greener" alternative compared to other oxidants.

In this work both, mechanistic and synthetic challenges had been addressed. The results are discussed separately for the hydroxylation of aromatic and of aliphatic compounds.

5.1.1 Selective Aromatic Hydroxylations

For dinuclear "copper dioxygen adduct" complexes different binding of dioxygen is possible, peroxido complexes contain copper(II) and bis(μ -oxido) complexes contain copper(III) ions. It was found for some model systems that there is a rapid equilibrium between both of them. This gave rise to the question whether the bis(μ -oxido) complex could be the hydroxylating species. To address this, Holland et al. applied the ligand PPN in their investigations [65]. The reactivity of this system is shown in Figure 5.1.

In this work the reactivity of $[\text{CuPPN}]^+$ towards dioxygen was reinvestigated using "stopped-flow" techniques at low temperatures. As described by Holland et al. a bis(μ -oxido) complex could be detected and no other

Figure 5.1: Selective *o*-hydroxylation of the ligand PPN.

intermediates were observed. For the formation of the bis(μ -oxido) complex a kinetic pseudo-first order was found; however a full kinetic analysis was not possible because the copper(I) complex solution was not stable over time. The mechanism was further studied by DFT methods. It was found in full agreement with the experimental results that in this system the bis(μ -oxido) complex is preferred to the μ - η^2 : η^2 -peroxido complex. The optimized structures showed that one oxygen atom is in close proximity to one of the phenyl groups, causing an *ortho*-hydroxylation at this position which exhibits strong electrophilic character of this reaction. The formed dienone intermediate was found to be thermodynamically unstable and reacts in two possible pathways to a (μ -OH)(μ -O)-dicopper complex. Although this can be considered important to probably many aromatic hydroxylations, the ligand PPN is synthetically demanding and thus the selective hydroxylation of minor synthetic interest.

The ligand BDED (Figure 5.2) was introduced not only to be a synthetic easily accessible alternative to PPN, but to offer possible synthetic applications for the selective aromatic hydroxylation with the according copper(I) complex.

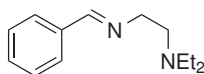


Figure 5.2: The ligand BDED.

BDED can be prepared by a one-step Schiff-base reaction and the reactivity of the corresponding copper(I) complex towards dioxygen is very similar to the reactivity of the copper(I) complexes with the ligand PPN. This is also supported by DFT studies. As formation and cleavage of the imine bond are

both simple reactions, this ligand can be used for selective hydroxylation of aromatic aldehydes in synthesis. This is a more general approach with more possible applications than similar procedures described previously by Feringa et al. [126], yet this huge advantage has to be paid with 50% maximum yield. The method was tested with different substituted aldehydes demonstrating the large range of possible substrates (Figure 5.3).

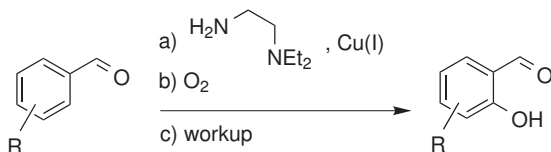


Figure 5.3: General formulation of the selective *o*-hydroxylation of aromatic aldehydes using a simple Cu(I) complex and O₂.

5.1.2 Selective Aliphatic Hydroxylations

Compared to selective hydroxylations of aromatic substrates less examples are known regarding the hydroxylation of aliphatic substrates. This is owed to the fact that less is known about the aliphatic C-H bond activation such as in pMMO compared to the aromatic C-H activation in tyrosinase and to the non-preactivated nature of such hydrocarbons. In this work the design of the aromatic ligand BDED was directly transferred to an aliphatic ligand, DPDen (Figure 5.4).

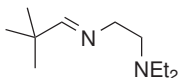


Figure 5.4: The ligand DPDen.

The copper(I) complex of the ligand DPDen exhibits similar intramolecular ligand hydroxylation reactions with dioxygen as the complex with the BDED ligand. In low temperature "stopped flow" experiments with an excess of dioxygen a pseudo-first order kinetics for the formation of a bis(μ -oxido) complex was observed. It was possible to determine the activation enthalpy for this formation which is similar to known examples from literature. In addition the activation entropy was determined which could suggest an interchange mechanism. The decay of the "oxygen adduct" complex was

also analyzed and evidence for different rate determining steps in different temperature ranges was observed.

The described simple copper(I) complexes with imine ligands are also a useful way for synthetic selective hydroxylations. Different aldehydes such as adamantane-1-carbaldehyde and cyclohexanecarbaldehyde were used for ligand synthesis and analyzed regarding the hydroxylation reaction. Although working with the very unstable adamantane-1-carbaldehyde is synthetically challenging, it offers a unique way to β -hydroxylated adamantane compounds. As Schiff-base with a hydrazine the stabilized product could be isolated and structurally characterized (Figure 5.5).

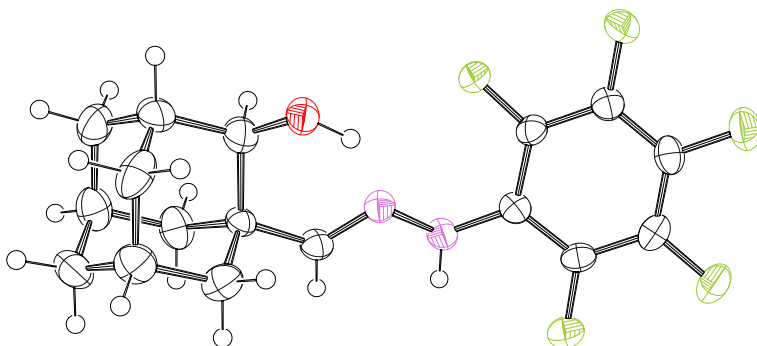


Figure 5.5: ORTEP plot of the molecular structure of pentafluorophenylhydrazin-1-ylidenemethyladamantan-2-ol; ellipsoids are drawn at 50 % probability.

Using cyclohexanecarbaldehyde and adamantane-1-carbaldehyde gave further insight into the selectivity of the reaction. It was found that in all cases only the β -position was hydroxylated. This is noteworthy because in the case of cyclohexanecarbaldehyde the α -position was also accessible and for adamantane-1-carbaldehyde the γ -position should be strongly favored (Figure 5.6).

Similar selectivity was reported previously by Schönecker et al. [89]-[92]. The fact that only β -hydroxylation occurs for adamantancarbaldehyde is a strong evidence for a concerted mechanism of the hydroxylation, as a radical intermediate would not exhibit such reactivity.

Cyclohexanecarbaldehyde as substrate also demonstrates possible applica-



Figure 5.6: Different accessible C–H bonds for cyclohexanecarbaldehyde (a) and adamantane-1-carbaldehyde (b).

tions for the aliphatic hydroxylation for a wide range of substrates and diamantane-1-carbaldehyde is another example for the capabilities regarding ligand hydroxylations (overview in Figure 5.7).

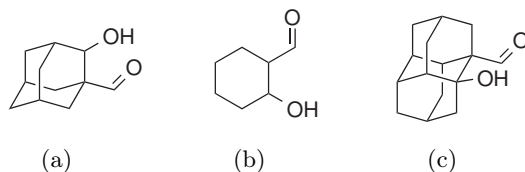


Figure 5.7: Products of the selective hydroxylation of adamantane-1-carbaldehyde (a), cyclohexanecarbaldehyde (b) and diamantane-1-carbaldehyde (c).

With these reactions new and unique compounds can be accessed in good yields. Furthermore only a few synthetic steps are required.

5.2 Zusammenfassung

Selektive Oxidationsreaktionen unter milden Bedingungen sind von großem Interesse. In der Natur katalysiert eine Vielzahl an Enzymen derartige Reaktionen worunter die meisten Metallionen im aktiven Zentrum beinhalten. Für Proteine, die Kupfer enthalten, sind einige Beispiele bekannt, welche organische Substrate mittels molekularem Sauerstoff hydroxylieren. Diese Reaktivität ist nicht nur interessant um biologische Mechanismen zu verstehen, sondern auch für den Einsatz in Labor und Industrie von Interesse. Bisherige wissenschaftliche Bemühungen die aktiven Zentren oder die katalytische Aktivität dieser Enzyme zu modellieren waren erfolgreich, jedoch sind fundamentale Schritte in diesem Oxidationsprozess noch immer nicht vollständig verstanden. Das genaue Verständnis dieser Schritte würde allerdings neue

Möglichkeiten zur gezielten Optimierung von Reaktionen eröffnen und das Verständnis für natürliche Prozesse voranbringen. Auch wenn es Versuche gab die Aktivierung von molekularem Sauerstoff mittels Kupferkomplexen für die Synthese einzusetzen, ist die Zahl der Anwendungen noch begrenzt. Daher ist es von Interesse allgemeinere synthetische Verfahren mit Kupferkomplexen zu entwickeln, auch aus folgenden Gründen: Wie schon beschrieben sind die milden Bedingungen und die Selektivität erstrebenswert. Weiterhin ist Kupfer verglichen zu seltenen Edelmetallen eine kostensparende Alternative. Außerdem ist molekularer Sauerstoff eine weitaus „grünere“ Alternative zu anderen Oxidationsmitteln.

In dieser Arbeit wurden sowohl mechanistische als auch synthetische Fragen adressiert. Die Ergebnisse werden hier separat für die Hydroxylierung von aromatischen und aliphatischen Verbindungen diskutiert.

5.2.1 Selektive aromatische Hydroxylierungen

Für dinukleare „Kupfer-Disauerstoff-Addukt“ Komplexe sind verschiedene Anbindungen von molekularem Sauerstoff möglich, dabei enthalten Peroxido-Komplexe Kupfer(II)- und Bis(μ -oxido)-Komplexe Kupfer(III)-Ionen. Mit manchen Modellsystem wurde ein schnelles Gleichgewicht zwischen diesen beiden nachgewiesen. Dabei kam die Frage auf ob der Bis(μ -oxido)-Komplex die für die Hydroxylierung verantwortliche Spezies sein kann. Um dies zu beantworten benutzten Holland et al. [65] den Liganden PPN. Die mit diesem System durchgeführte Reaktion ist in Abbildung 5.8 gezeigt.

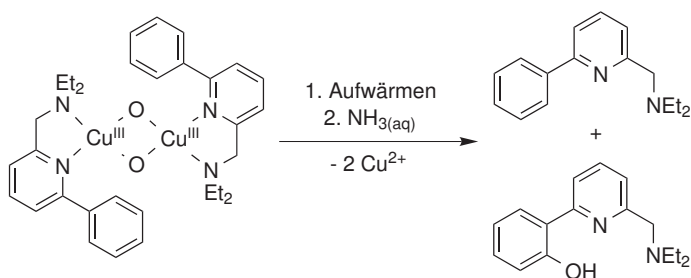


Abbildung 5.8: Selektive *o*-Hydroxylierung des Liganden PPN.

In dieser Arbeit wurde die Reaktivität von $[\text{CuPPN}]^+$ gegenüber molekularem Sauerstoff mittels der „Stopped-flow“-Technik bei tiefen Temperaturen weiterführend untersucht. Wie schon von Holland et al. beschrieben, konnte ein Bis(μ -oxido)-Komplex nachgewiesen werden, wobei keine weiteren Inter-

mediate beobachtet wurden. Für die Bildung dieses Bis(μ -oxido)-Komplexes konnte eine Kinetik pseudo-erster Ordnung ermittelt werden. Eine vollständige kinetische Analyse war aber nicht möglich, da der Kupfer(I)-Komplex in Lösung nicht über den benötigten Zeitraum stabil war. Ergänzend hierzu wurde der Mechanismus der Reaktion mit DFT Methoden untersucht. In vollständiger Übereinstimmung mit den experimentellen Ergebnissen wurde weiterhin gezeigt, dass mit diesem System der Bis(μ -oxido)-Komplex gegenüber dem μ - η^2 : η^2 -Peroxo-Komplex bevorzugt ist. Die optimierte Struktur zeigte, dass eines der Sauerstoffatome bereits in der unmittelbaren Nähe einer der Phenylgruppen war. Als direkte Folge hiervon wurde der aromatische Ring in *ortho*-Position hydroxyliert, was den starken elektrophilen Charakter dieser Reaktion zeigt. Es wurde herausgefunden, dass das dabei gebildete Dienon-Intermediat thermodynamisch nicht stabil war und in zwei verschiedenen Reaktionsmechanismen zum (μ -OH)(μ -O)-Dikupferkomplex weiter reagierte. Dies ist vermutlich auch für das Verständnis vieler weiterer aromatischer Hydroxylierungen wichtig. Von Nachteil ist jedoch die aufwendige Synthese des Liganden PPN, welcher somit für eine synthetische Anwendung nur von geringem Interesse ist.

Der Ligand BDED (Abbildung 5.9) wurde nicht nur als synthetisch viel besser zugängliche Alternative zu PPN eingeführt, er bietet als Kupfer(I)-Komplex auch mögliche synthetische Anwendungen für selektive aromatische Hydroxylierungsreaktionen.

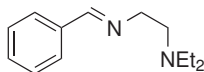


Abbildung 5.9: Der Ligand BDED.

BDED kann in einer einstufigen Schiffbasensynthese dargestellt werden. Die Reaktivität des zugehörigen Kupfer(I)-Komplexes gegenüber molekularem Sauerstoff ist außerdem vergleichbar mit der des Kupfer(I)-Komplexes mit dem Liganden PPN. Die auch in diesem Fall durchgeführten DFT-Berechnungen unterstützen diese Ähnlichkeit in Bezug auf die Reaktivität. Da sowohl die Bildung als auch das Brechen der Iminbindung einfache Reaktionen sind, kann der Ligand zur selektiven Hydroxylierung von aromatischen Aldehyden in der Synthese eingesetzt werden. Dies ist ein allgemeinerer Ansatz, welcher ein größeres Anwendungsfeld erlaubt als die bisher von Feringa et al. [126] beschriebenen Verfahren. Dieser große Vorteil wird allerdings mit einer maximalen Ausbeute von 50 % bezahlt. Die Methode wurde mit verschiedenen substituierten Aldehyden getestet und es konnte gezeigt werden,

dass eine Vielzahl von verschiedenen Substraten verwendbar sind (Abbildung 5.10).

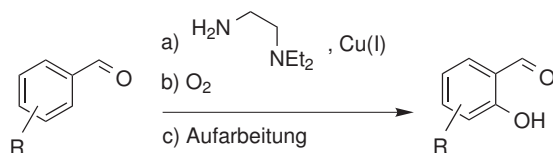


Abbildung 5.10: Allgemeine Beschreibung der selektiven *o*-Hydroxylierung von aromatischen Aldehyden mittels eines einfachen Kupfer(I)-Komplexes und O_2 .

5.2.2 Selektive aliphatische Hydroxylierungen

Verglichen mit der selektiven Hydroxylierung von Aromatischen Substraten sind weniger Beispiele bekannt, bei denen aliphatische Substrate hydroxyliert werden. Dies ist auch der Tatsache geschuldet, dass weniger über die aliphatische C–H Bindungsaktivierung in pMMO verglichen zur aromatischen C–H Bindungsaktivierung in Tyrosinase bekannt ist. Außerdem sind die C–H Bindungen in derartigen aliphatischen Kohlenwasserstoffen nicht voraktiviert. In dieser Arbeit wurde das Design des aromatischen Liganden BDDE direkt auf den aliphatischen Liganden DPDen übertragen (Abbildung 5.11).

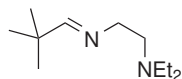


Abbildung 5.11: Der Ligand DPDen.

Der Kupfer(I)-Komplex mit dem Liganden DPDen zeigt ähnliche intramolekulare Ligandhydroxylierung wie der Komplex des Liganden BDDE. Mit einem Überschuss an molekularem Sauerstoff konnte in „Stopped-flow“-Experimenten bei tiefen Temperaturen eine Reaktion pseudo-erster Ordnung für die Bildung eines Bis(μ -oxido)-Komplexes beobachtet werden. Es war möglich die Aktivierungsenthalpie für diesen Prozess zu bestimmen, wobei diese in guter Übereinstimmung mit bekannten Beispielen aus der Literatur ist. Außerdem wurde die Aktivierungsentropie bestimmt, die einen möglichen Austausch-Mechanismus nahelegt. Auch der Abbau des „Sauerstoff-Addukt“-Komplexes wurde analysiert und es wurden Hinweise für verschiedene ge-

schwindigkeitsbestimmende Schritte in verschiedenen Temperaturbereichen gefunden.

Die beschriebenen einfachen Kupfer(I)-Komplexe mit Iminliganden sind außerdem ein nützliches Verfahren für synthetische, selektive Hydroxylierungen. Verschiedene Aldehyde wie Adamantan-1-carbaldehyd oder Cyclohexancarbaldehyd wurden zur Ligandsynthese eingesetzt und daraufhin bezüglich der Hydroxylierungsreaktion untersucht. Auch wenn das Arbeiten mit dem sehr instabilen Adamantan-1-carbaldehyd synthetisch anspruchsvoll war, ermöglicht es einen einzigartigen Zugang zu β -hydroxylierten Adamantanverbindungen. Das Produkt konnte als Schiffbase mit einem Hydrazinderivat stabilisiert, isoliert und mittels Strukturanalyse charakterisiert werden (Abbildung 5.12).

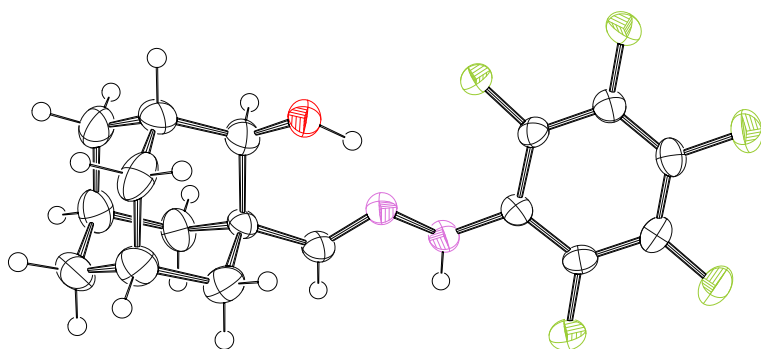


Abbildung 5.12: ORTEP Darstellung der Molekülstruktur von Pentafluorophenylhydrazin-1-ylidenmethyadamantan-2-ol; Temperatur ellipsoide sind mit 50 % Aufenthaltswahrscheinlichkeit gezeigt.

Der Einsatz von Cyclohexancarbaldehyd und Adamantan-1-carbaldehyd gab weiteren Einblick in die Selektivität der beschriebenen Reaktion. In allen Fällen wurde nur die β -Position hydroxyliert. Dies ist bemerkenswert, da im Falle von Cyclohexancarbaldehyd auch die α -Position theoretisch zugänglich war und bei Adamantan-1-carbaldehyd die γ -Position starkt bevorzugt sein sollte (Abbildung 5.13).

Eine vergleichbare Selektivität wurde bereits von Schönecker et al. beschrieben [89]-[92]. Die Tatsache, dass nur eine β -Hydroxylierung zu beobachten ist, ist ein starker Beweis für einen konzertierten Mechanismus der Hydroxylierung,



Abbildung 5.13: Die verschiedenen zugänglichen C–H Bindungen für Cyclohexancarbaldehyd (a) und Adamantan-1-carbaldehyd (b).

da ein radikalisches Intermediat eine derartige Reaktivität nicht aufweisen würde.

Cyclohexancarbaldehyd als Substrat zeigt außerdem mögliche Anwendungen für die aliphatische Hydroxylierung bei einem größeren Spektrum von Substraten. Diamantan-1-carbaldehyd ist ein weiteres Beispiel für die Möglichkeiten der Ligandhydroxylierungen (Überblick in Abbildung 5.14).

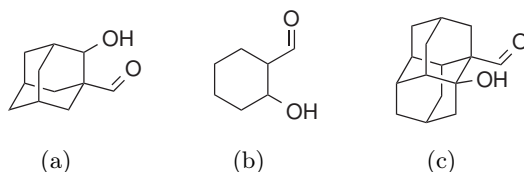


Abbildung 5.14: Produkte der selektiven Hydroxylierung von Adamantan-1-carbaldehyd (a), Cyclohexancarbaldehyd (b) und Diamantan-1-carbaldehyd (c).

Durch diese Reaktionen sind somit neue und einzigartige Verbindungen in guten Ausbeuten zugänglich. Zusätzlich sind dafür nur wenige Syntheseschritte notwendig.

6 Bibliography

- [1] A. F. Hollemann, E. Wiberg, and N. Wiberg. *Lehrbuch der Anorganischen Chemie*. 102. Walter de Gruyter, **2007**, pp. 1433–1452.
- [2] E. Anders and M. Ebihara. *Geochim. Cosmochim. Acta* 46, **1982**, pp. 2363–2380.
- [3] W. F. McDonough. “The Composition of the Earth”. *Earthquake Thermodynamics and Phase Transformation in the Earth’s Interior*. Ed. by R. Teisseyre and E. Majewski. **2000**. Chap. 1, pp. 3–23.
- [4] W. Kaim and B. Schwederski. *Bioanorganische Chemie*. 4. Auflage. Teubner, **2005**.
- [5] D. J. Spira-Solomon, M. D. Allendorf, and E. I. Solomon. *J. Am. Chem. Soc.* 108, **1986**, pp. 5318–5328.
- [6] H. Aoyama, T. Tomizaki, H. Yamaguchi, R. Nakashima, R. Yaono, and S. Yoshikawa. *Science* 272, **1995**, pp. 1136–1144.
- [7] B. G. Malmström. *Chem. Rev.* 90, **1990**, pp. 1247–1260.
- [8] E. I. Solomon, U. M. Sundaram, and T. E. Machonkin. *Chem. Rev.* 96, **1996**, pp. 2563–2606.
- [9] R. H. Holm, P. Kennepohl, and E. I. Solomon. *Chem. Rev.* 96, **1996**, pp. 2239–2314.
- [10] B. G. Malmström. *Eur. J. Biochem.* 223, **1994**, pp. 711–718.
- [11] K. Paraskevopoulos, M. Sundararajan, R. Surendran, M. A. Hough, R. R. Eady, I. H. S. Hillier, and S. Hasnain. *Dalton Trans.* 25, **2006**, p. 3067.
- [12] D. Subhadra, A. Anupama, J. Chirag, S. Ramaswamy, and P. Sai Sudha. *to be published*, **2015**.
- [13] I. A. Koval, P. Gamez, C. Belle, K. Selmeczi, and J. Reedijk. *Chem. Soc. Rev.* 35, **2006**, pp. 814–840.
- [14] Y. Matoba, T. Kumagai, A. Yamamoto, H. Yoshitsu, and M. Sugiyama. *J. Biol. Chem.* 281, **2006**, pp. 8981–8990.
- [15] P. Gamez, I. a. Koval, and J. Reedijk. *Dalton Trans.* **2004**, pp. 4079–4088.

- [16] J. M. Guss, P. R. Harrowell, M. Murata, V. A. Norris, and H. C. Freeman. *J. Mol. Biol.* 192, **1986**, pp. 361–387.
- [17] R. J. Deeth. *Inorg. Chem.* 46, **2007**, pp. 4492–4503.
- [18] D. E. Nikles, M. J. Powers, and F. L. Urbach. *Inorg. Chem.* 22, **1983**, pp. 3210–3217.
- [19] S. Knapp, T. P. Keenan, X. H. Zhang, R. Fikar, J. A. Potenza, and H. J. Schugar. *J. Am. Chem. Soc.* 112, **1990**, pp. 3452–3464.
- [20] A. G. Sykes. *Adv. Inorg. Chem.* 36, **1991**, pp. 377–408.
- [21] T. Tsukihara, H. Aoyama, E. Yamashita, T. Tomizaki, H. Yamaguchi, K. Shinzawa-Itoh, R. Nakashima, R. Yaono, and S. Yoshikawa. *Science* 269, **1995**, pp. 1069–1074.
- [22] C. S. Stoj and D. J. Kosman. “Copper Proteins: Oxidases”. *Encyclopedia of Inorganic Chemistry*. John Wiley & Sons, Ltd, **2006**, pp. 1814–1846.
- [23] P. J. Hart, A. M. Nersissian, and S. DeBeer George. “Copper Proteins with Type 1 Sites”. *Encyclopedia of Inorganic Chemistry*. John Wiley & Sons, Ltd, **2006**, pp. 1814–1846.
- [24] E. Bouwman, W. L. Driessen, and J. Reedijk. *Coord. Chem. Rev.* 104, **1990**, pp. 143–172.
- [25] P. K. Bharadwaj, J. A. Potenza, and H. J. Schugar. *J. Am. Chem. Soc.* 108, **1986**, pp. 1351–1352.
- [26] J. A. Tainer, E. D. Getzoff, K. M. Beem, J. S. Richardson, and D. C. Richardson. *J. Mol. Biol.* 160, **1982**, pp. 181–217.
- [27] J. A. Tainer, E. D. Getzoff, J. S. Richardson, and D. C. Richardson. *Nature* 306, **1983**, pp. 284–287.
- [28] S. Schindler. *Eur. J. Inorg. Chem.* **2000**, pp. 2311–2326.
- [29] K. Yoshizawa, N. Kihara, T. Kamachi, and Y. Shiota. *Inorg. Chem.* 45, **2006**, pp. 3034–3041.
- [30] J. P. Klinman. *Chem. Rev.* 96, **1996**, pp. 2541–2561.
- [31] M. A. McGuirl and D. M. Dooley. “Copper Proteins with Type 2 Sites”. *Encyclopedia of Inorganic Chemistry*. John Wiley & Sons, Ltd, **2006**, pp. 1814–1846.
- [32] K. Fujisawa, M. Tanaka, Y. Moro-oka, and N. Kitajima. *J. Am. Chem. Soc.* 116, **1994**, pp. 12079–12080.

- [33] C. Würtele, E. Goutchenova, K. Harms, M. C. Holthausen, J. Sundermeyer, and S. Schindler. *Angew. Chem., Int. Ed.* 45, **2006**, pp. 3867–3869.
- [34] V. Mahadevan, R. K. Gebbink, and T. D. Stack. *Curr. Opin. Chem. Biol.* 4, **2000**, pp. 228–34.
- [35] Y. Wang, J. L. DuBois, B. Hedman, K. O. Hodgson, and T. D. P. Stack. *Science* 279, **1998**, pp. 537–540.
- [36] L. M. Mirica, X. Ottenwaelde, and T. D. P. Stack. *Chem. Rev.* 104, **2004**, pp. 1013–1045.
- [37] P. K. Ross and E. I. Solomon. *J. Am. Chem. Soc.* 112, **1990**, pp. 5871–5872.
- [38] K. A. Magnus, H. Ton-That, and J. E. Carpenter. *Chem. Rev.* 94, **1994**, pp. 727–735.
- [39] H. Decker and F. Tuczek. *Trends Biochem. Sci.* 25, **2000**, pp. 392–397.
- [40] M. Maria, N. Bostan, and R. Aslam. *Int. J. Biotechnol.* 4, **2011**, pp. 575–581.
- [41] S. Itoh, H. Kumei, M. Taki, S. Nagamoto, T. Kitagawa, and S. Fukuzumi. *J. Am. Chem. Soc.* 123, **2001**, pp. 6708–6709.
- [42] E. I. Solomon, P. Chen, M. Metz, S. K. Lee, and A. E. Palmer. *Angew. Chem., Int. Ed.* 40, **2001**, pp. 4570–4590.
- [43] M. Rolff, J. Schottenheim, H. Decker, and F. Tuczek. *Chem. Soc. Rev.* 40, **2011**, pp. 4077–4098.
- [44] E. A. Lewis and W. B. Tolman. *Chem. Rev.* 104, **2004**, pp. 1047–1076.
- [45] O. Sander, A. Henß, C. Näther, C. Würtele, M. C. Holthausen, S. Schindler, and F. Tuczek. *Chem. Eur. J.* 14, **2008**, pp. 9714–9729.
- [46] L. M. Mirica, M. Vance, D. J. Rudd, B. Hedman, K. O. Hodgson, E. I. Solomon, and T. D. P. Stack. *Science* 308, **2005**, pp. 1890–1892.
- [47] M. Rolff, J. Schottenheim, G. Peters, and F. Tuczek. *Angew. Chem., Int. Ed.* 49, **2010**, pp. 6438–6442.
- [48] J. Schottenheim, N. Fateeva, W. Thimm, J. Krahmer, and F. Tuczek. *Z. Anorg. Allg. Chem.* 639, **2013**, pp. 1491–1497.
- [49] A. Hoffmann, C. Citek, S. Binder, A. Goos, M. Rübhausen, O. Troeppe, I. Ivanović-Burmazović, E. C. Wasinger, T. D. P. Stack, and S. Herres-Pawlis. *Angew. Chem., Int. Ed.* 52, **2013**, pp. 5398–5401.
- [50] R. L. Lieberman and A. C. Rosenzweig. *Nature* 434, **2005**, pp. 177–182.

- [51] R. A. Himes and K. D. Karlin. *Curr. Opin. Chem. Biol.* 13, **2009**, pp. 119–131.
- [52] K. Yoshizawa and Y. Shiota. *J. Am. Chem. Soc.* 128, **2006**, pp. 9873–9881.
- [53] S. I. Chan, V. C. C. Wang, J. C. H. Lai, S. S. F. Yu, P. P. Y. Chen, K. H. C. Chen, C. L. Chen, and M. K. Chan. *Angew. Chem., Int. Ed.* 46, **2007**, pp. 1992–1994.
- [54] R. L. Osborne, J. P. Klinman, J. Kaizer, S. J. Pap, G. Speier, D. Rokhsana, E. M. Shepard, D. E. Brown, D. M. Dooley, A. Paulus, S. de Vries, T. Sakurai, K. Kataoka, J. P. Roth, K. Yoshizawa, S. Itoh, Z. Halime, K. D. Karlin, J.-N. Rebilly, O. Renaud, and M. C. Kozlowski. *Copper-Oxygen Chemistry*. Ed. by S. I. Kenneth D. Karlin. John Wiley & Sons, Inc., **2011**.
- [55] S. J. Blanksby and G. B. Ellison. *Acc. Chem. Res.* 36, **2003**, pp. 255–263.
- [56] E. Pidcock, H. V. Obias, C. X. Zhang, K. D. Karlin, and E. I. Solomon. *J. Am. Chem. Soc.* 120, **1998**, pp. 7841–7847.
- [57] R. W. Cruse, S. Kaderli, K. D. Karlin, and A. D. Zuberbühler. *J. Am. Chem. Soc.* 110, **1988**, pp. 6882–6883.
- [58] K. D. Karlin, M. S. Nasir, B. I. Cohen, R. W. Cruse, S. Kaderli, and A. D. Zuberbühler. *J. Am. Chem. Soc.* 116, **1994**, pp. 1324–1336.
- [59] P. Rys, P. Skrabal, and H. Zollinger. *Angew. Chem., Int. Ed.* 11, **1972**, p. 874.
- [60] M. Becker, S. Schindler, K. D. Karlin, T. A. Kaden, S. Kaderli, T. Palanché, and A. D. Zuberbühler. *Inorg. Chem.* 38, **1999**, pp. 1989–1995.
- [61] P. Chen and E. I. Solomon. *J. Inorg. Biochem* 88, **2002**, pp. 368–374.
- [62] M. S. Nasir, B. I. Cohen, and K. D. Karlin. *J. Am. Chem. Soc.* 114, **1992**, pp. 2482–2494.
- [63] A. M. Reynolds, E. A. Lewis, N. W. Aboeella, and W. B. Tolman. *Chem. Commun.* **2005**, pp. 2014–2016.
- [64] D. Maiti, H. R. Lucas, A. A. Narducci Sarjeant, and K. D. Karlin. *J. Am. Chem. Soc.* 129, **2007**, pp. 6998–6999.
- [65] P. L. Holland, K. R. Rodgers, and W. B. Tolman. *Angew. Chem., Int. Ed.* 38, **1999**, pp. 1139–1142.
- [66] M. Régier, C. Jorand, and B. Waegell. *J. Chem. Soc., Chem. Comm.* 24, **1990**, pp. 1752–1755.

- [67] E. Monzani, L. Quinti, A. Perotti, L. Casella, M. Gullotti, L. Randaccio, S. Geremia, G. Nardin, P. Faleschini, and G. Tabbì. *Inorg. Chem.* 37, **1998**, pp. 553–562.
- [68] I. Garcia-Bosch, A. Company, J. R. Frisch, M. Torrent-Sucarrat, M. Cardellach, I. Gamba, M. Güell, L. Casella, L. Que, X. Ribas, J. M. Luis, and M. Costas. *Angew. Chem., Int. Ed.* 49, **2010**, pp. 2406–2409.
- [69] I. Garcia-Bosch, X. Ribas, and M. Costas. *Chem. Eur. J.* 18, **2012**, pp. 2113–22.
- [70] A. Company, S. Palavicini, I. Garcia-Bosch, R. Mas-Ballesté, L. Que, E. V. Rybak-Akimova, L. Casella, X. Ribas, and M. Costas. *Chem. Eur. J.* 14, **2008**, pp. 3535–3538.
- [71] S. Herres-Pawlis, P. Verma, R. Haase, P. Kang, C. T. Lyons, E. C. Wasinger, U. Flörke, G. Henkel, and T. D. P. Stack. *J. Am. Chem. Soc.* 131, **2009**, pp. 1154–1169.
- [72] P. Kang, E. Bobyr, J. Dustman, K. O. Hodgson, B. Hedman, E. I. Solomon, and T. D. P. Stack. *Inorg. Chem.* 49, **2010**, pp. 11030–11038.
- [73] D. Maiti, H. C. Fry, J. S. Woertink, M. A. Vance, E. I. Solomon, and K. D. Karlin. *J. Am. Chem. Soc.* 129, **2007**, pp. 264–265.
- [74] M. Güell, J. M. Luis, P. E. M. Siegbahn, and M. Solà. *J. Biol. Inorg. Chem.* 14, **2009**, pp. 273–285.
- [75] W. E. Allen and T. N. Sorrell. *Inorg. Chem.* 36, **1997**, pp. 1732–1734.
- [76] S. Itoh, M. Taki, H. Nakao, P. L. Holland, W. B. Tolman, L. Que, and S. Fukuzumi. *Angew. Chem., Int. Ed.* 39, **2000**, pp. 398–400.
- [77] P. Spuhler and M. C. Holthausen. *Angew. Chem., Int. Ed.* 42, **2003**, pp. 5961–5965.
- [78] G. Tian, J. A. Berry, and J. P. Klinman. *Biochemistry* 33, **1994**, pp. 226–234.
- [79] P. F. Fitzpatrick, D. R. Flory, and J. J. Villafranca. *Biochemistry* 24, **1985**, pp. 2108–2114.
- [80] C. Würtele, O. Sander, V. Lutz, T. Waitz, F. Tuczek, and S. Schindler. *J. Am. Chem. Soc.* 131, **2009**, pp. 7544–7545.
- [81] H. R. Lucas, L. Li, A. A. N. Sarjeant, M. A. Vance, E. I. Solomon, and K. D. Karlin. *J. Am. Chem. Soc.* 131, **2009**, pp. 3230–3245.
- [82] A. Berkessel and R. K. Thauer. *Angew. Chem., Int. Ed.* 34, **1995**, pp. 2247–2250.
- [83] P. R. Schreiner and A. A. Fokin. *Chem. Rec.* 3, **2004**, pp. 247–257.

- [84] C. Limberg. *Angew. Chem., Int. Ed.* 42, **2003**, pp. 5932–5954.
- [85] J. S. Thompson. *J. Am. Chem. Soc.* 106, **1984**, pp. 8308–8309.
- [86] J. A. Halfen, V. G. Young, and W. B. Tolman. *Inorg. Chem.* 37, **1998**, pp. 2102–2103.
- [87] I. Blain, M. Giorgi, I. D. Riggi, and M. Réglér. *Eur. J. Inorg. Chem.* 2000, **2000**, pp. 393–398.
- [88] H. Arai, Y. Saito, S. Nagatomo, T. Kitagawa, Y. Funahashi, K. Jitsukawa, and H. Masuda. *Chem. Lett.* 32, **2003**, pp. 156–157.
- [89] B. Schönecker, T. Zheldakova, Y. Liu, M. Kötteritzsch, W. Günther, and H. Görls. *Angew. Chem., Int. Ed.* 42, **2003**, pp. 3240–3244.
- [90] B. Schönecker, T. Zheldakova, C. Lange, W. Günther, H. Görls, and M. Bohl. *Chem. Eur. J.* 10, **2004**, pp. 6029–6042.
- [91] B. Schönecker, C. Lange, T. Zheldakova, W. Günther, H. Görls, and G. Vaughan. *Tetrahedron* 61, **2005**, pp. 103–114.
- [92] B. Schönecker and C. Lange. *J. Organomet. Chem.* 691, **2006**, pp. 2107–2124.
- [93] H. Decker, R. Dillinger, and F. Tuczek. *Angew. Chem., Int. Ed.* 39, **2000**, pp. 1591–1595.
- [94] Á. Sánchez-Ferrer, J. N. Rodríguez-López, F. García-Cánovas, and F. García-Carmona. *Biochim. Biophys. Acta* 1247, **1995**, pp. 1–11.
- [95] H. Decker, T. Schweikardt, and F. Tuczek. *Angew. Chem., Int. Ed.* 45, **2006**, pp. 4546–4550.
- [96] L. Que and W. B. Tolman. *Nature* 455, **2008**, pp. 333–340.
- [97] L. Q. Hatcher and K. D. Karlin. *J. Biol. Inorg. Chem.* 9, **2004**, pp. 669–683.
- [98] K. D. Karlin, S. Kaderli, and A. D. Zuberbühler. *Acc. Chem. Res.* 30, **1997**, pp. 139–147.
- [99] K. D. Karlin, J. C. Hayes, Y. Gultneh, R. W. Cruse, J. W. McKown, J. P. Hutchinson, and J. Zubieta. *J. Am. Chem. Soc.* 106, **1984**, pp. 2121–2128.
- [100] T. Osako, K. Ohkubo, M. Taki, Y. Tachi, S. Fukuzumi, and S. Itoh. *J. Am. Chem. Soc.* 125, **2003**, pp. 11027–11033.
- [101] S. Itoh and S. Fukuzumi. *Acc. Chem. Res.* 40, **2007**, pp. 592–600.
- [102] S. Palavicini, A. Granata, E. Monzani, and L. Casella. *J. Am. Chem. Soc.* 127, **2005**, pp. 18031–18036.

- [103] K. D. Karlin, C. X. Zhang, A. L. Rheingold, B. Galliker, S. Kaderli, and A. D. Zuberbühler. *Inorg. Chim. Acta* 389, **2012**, pp. 138–150.
- [104] M. S. Nasir, B. I. Cohen, and K. D. Karlin. *J. Am. Chem. Soc.* 114, **1992**, pp. 2482–2494.
- [105] L. Casella, M. Gullotti, R. Radaelli, and P. Di Gennaro. *J. Chem. Soc., Chem. Commun.* **1991**, pp. 1611–1612.
- [106] L. Santagostini, M. Gullotti, E. Monzani, L. Casella, R. Dillinger, and F. Tuczek. *Chem. Eur. J.* 6, **2000**, pp. 519–522.
- [107] B. T. O. T. Holt, M. A. Vance, L. M. Mirica, D. E. Heppner, T. D. P. Stack, and E. I. Solomon. *J. Am. Chem. Soc.* 131, **2009**, pp. 6421–6438.
- [108] J. A. Halfen, S. Mahapatra, E. C. Wilkinson, S. Kaderli, V. G. Young, L. Que, A. D. Zuberbühler, and W. B. Tolman. *Science* 271, **1996**, pp. 1397–1400.
- [109] L. Que and W. B. Tolman. *Angew. Chem., Int. Ed.* 41, **2002**, pp. 1114–1137.
- [110] K. V. N. Esguerra, Y. Fall, and J. P. Lumb. *Angew. Chem., Int. Ed.* 53, **2014**, pp. 5877–5881.
- [111] K. V. N. Esguerra, Y. Fall, L. Petitjean, and J. P. Lumb. *J. Am. Chem. Soc.* 136, **2014**, pp. 7662–7668.
- [112] A. Orita, H. Taniguchi, and J. Otera. *Chem. Asian J.* 1, **2006**, pp. 430–437.
- [113] C.-I. Chuang, K. Lim, Q. Chen, J. Zubieta, and J. W. Canary. *Inorg. Chem.* 34, **1995**, pp. 2562–2568.
- [114] M. M. Makowska-Grzyska, E. Szajna, C. Shipley, A. M. Arif, M. H. Mitchell, J. A. Halfen, and L. M. Berreau. *Inorg. Chem.* 42, **2003**, pp. 7472–7488.
- [115] Y. F. Liu, J. G. Yu, P. E. M. Siegbahn, and M. R. A. Blomberg. *Chem. Eur. J.* 19, **2013**, pp. 1942–1954.
- [116] A. Poater and M. Solà. *Beilstein J. Org. Chem.* 9, **2013**, pp. 585–593.
- [117] A. Poater, X. Ribas, A. Llobet, L. Cavallo, and M. Solà. *J. Am. Chem. Soc.* 130, **2008**, pp. 17710–17717.
- [118] S. Herres, A. J. Heuwing, U. Flörke, J. Schneider, and G. Henkel. *Inorg. Chim. Acta* 358, **2005**, pp. 1089–1095.
- [119] A. R. Surrey. *J. Am. Chem. Soc.* 71, **1949**, pp. 2941–2942.

- [120] X. Li, Y.-H. Liu, W.-J. Gu, B. Li, F.-J. Chen, and B.-F. Shi. *Org. Lett.* 16, **2014**, pp. 3904–3907.
- [121] F. Mo, L. J. Trzepakowski, and G. Dong. *Angew. Chem., Int. Ed.* 51, **2012**, pp. 13075–13079.
- [122] E. Amadéi, E. H. Alilou, F. Eydoux, M. Pierrot, M. Réglier, and B. Waegell. *J. Chem. Soc., Chem. Commun.* **1992**, pp. 1782–1784.
- [123] I. Blain, P. Bruno, M. Giorgi, E. Lojou, D. Lexa, and M. Re. *Eur. J. Inorg. Chem.* **1998**, pp. 1297–1304.
- [124] P. Naumov and S. W. Ng. *J. Coord. Chem.* 59, **2006**, pp. 1307–1309.
- [125] S. Kozuch and J. M. L. Martin. *Chem. Phys. Chem.* 12, **2011**, pp. 1413–1418.
- [126] C. Zondervan, E. K. van den Beuken, H. Kooijman, A. L. Spek, and B. L. Feringa. *Tetrahedron Lett.* 38, **1997**, pp. 3111–3114.
- [127] G. J. Kubas. *Inorg. Synth.* 19, **1979**, p. 1990.
- [128] P. Lühning and A. Schumpe. *J. Chem. Eng. Data* 34, **1989**, pp. 250–252.
- [129] G. M. Sheldrick. *Acta Crystallogr., Sect. A* 64, **2007**, pp. 112–122.
- [130] G. M. Sheldrick. *Acta Crystallogr., Sect. A* 71, **2015**, pp. 3–8.
- [131] A. L. Spek. *Acta Crystallogr., Sect. D* 65, **2009**, pp. 148–155.
- [132] M. J. Frisch, G. W. Trucks, H. B. Schlegel, G. E. Scuseria, M. A. Robb, J. R. Cheeseman, G. Scalmani, V. Barone, B. Mennucci, G. A. Petersson, H. Nakatsuji, M. Caricato, X. Li, H. P. Hratchian, A. F. Izmaylov, J. Bloino, G. Zheng, J. L. Sonnenberg, M. Hada, M. Ehara, K. Toyota, R. Fukuda, J. Hasegawa, M. Ishida, T. Nakajima, Y. Honda, O. Kitao, H. Nakai, T. Vreven, J. A. M. Jr., J. E. Peralta, F. Ogliaro, M. Bearpark, J. J. Heyd, E. Brothers, K. N. Kudin, V. N. Staroverov, T. Keith, R. Kobayashi, J. Normand, K. Raghavachari, A. Rendell, J. C. Burant, S. S. Iyengar, J. Tomasi, M. Cossi, N. Rega, J. M. Millam, M. Klene, J. E. Knox, J. B. Cross, V. Bakken, C. Adamo, J. Jaramillo, R. Gomperts, R. E. Stratmann, O. Yazyev, A. J. Austin, R. Cammi, C. Pomelli, J. W. Ochterski, R. L. Martin, K. Morokuma, V. G. Zakrzewski, G. A. Voth, P. Salvador, J. J. Dannenberg, S. Dapprich, A. D. Daniels, O. Farkas, J. B. Foresman, J. V. Ortiz, J. Cioslowski, and D. J. Fox. *Gaussian 09*. Wallingford, CT, **2009**.
- [133] C. Lee, W. Yang, and R. G. Parr. *Phys. Rev. B* 37, **1988**, pp. 785–789.
- [134] B. Miehlich, A. Savin, H. Stoll, and H. Preuss. *Chem. Phys. Lett.* 157, **1989**, pp. 200–206.

- [135] S. Grimme. *J. Comput. Chem.* 27, **2006**, pp. 1787–1799.
- [136] A. Schäfer, C. Huber, and R. Ahlrichs. *J. Chem. Phys.* 97, **1992**, pp. 2571–2577.
- [137] F. Weigend and R. Ahlrichs. *Phys. Chem. Chem. Phys.* 7, **2005**, pp. 3297–3305.
- [138] M. Dolg, U. Wedig, H. Stoll, and H. Preuss. *J. Chem. Phys.* 86, **1987**, pp. 866–872.
- [139] B. I. Dunlap. *J. Chem. Phys.* 78, **1983**, pp. 3140–3142.
- [140] B. I. Dunlap. *J. Mol. Struct.: THEOCHEM* 529, **2000**, pp. 37–40.
- [141] S. Grimme, J. Antony, S. Ehrlich, and H. Krieg. *J. Chem. Phys.* 132, **2010**, pp. 154104–154119.
- [142] A. Klamt and G. Schüürmann. *J. Chem. Soc., Perkin Trans. 2*, **1993**, pp. 799–805.
- [143] F. Neese, U. Becker, D. Bykov, D. Ganyushin, A. Hansen, R. Izsak, D. G. Liakos, C. Kollmar, S. Kossmann, D. A. Pantazis, T. Petrenko, C. Reimann, C. Riplinger, M. Roemelt, B. Sandhöfer, I. Schapiro, K. Sivalingam, and B. Weizsla. *ORCA - An ab initio, DFT and semiempirical SCF-MO package*. **2012**.
- [144] R. A. Kendall and H. A. Früchtl. *Theor. Chem. Acc.* 97, **1997**, pp. 158–163.
- [145] K. Eichkorn, O. Treutler, H. Öhm, M. Häser, and R. Ahlrichs. *Chem. Phys. Lett.* 240, **1995**, pp. 283–290.
- [146] K. Eichkorn, F. Weigend, O. Treutler, and R. Ahlrichs. *Theor. Chem. Acc.* 97, **1997**, pp. 119–124.
- [147] F. Weigend. *Phys. Chem. Chem. Phys.* 8, **2006**, pp. 1057–1065.
- [148] K. Yamaguchi, Y. Takahara, and T. Fueno. “Ab-Initio Molecular Orbital Studies of Structure and Reactivity of Transition Metal-OXO Compounds”. *Applied Quantum Chemistry*. Ed. by K. Morokuma, V. Smith, and H. F. Schaefer. V.H. Smith, **1986**, pp. 155–184.
- [149] T. Soda, Y. Kitagawa, T. Onishi, Y. Takano, Y. Shigeta, H. Nagao, Y. Yoshioka, and K. Yamaguchi. *Chem. Phys. Lett.* 319, **2000**, pp. 223–230.
- [150] C. Y. Legault. *CYLview*. Sherbrooke, QC, **2009**.
- [151] S. M. H. Ali, Y.-K. Yan, P. P. F. Lee, K. Z. X. Khong, M. A. Sk, K. H. Lim, B. Klejevska, and R. Vilar. *Dalton Trans.* 43, **2014**, pp. 1449–1459.

- [152] M. Aresta, D. H. Lee, B. Mondal, K. D. Karlin, J. Peters, M. Mehn, J. W. Tye, M. Hall, C. N. Cornall, M. Sigman, A. Borovik, P. J. Zinn, M. K. Zart, R. Periana, L. Berreau, P. W. N. M. van Leeuwen, and Z. Freixa. *Activation of Small Molecules: Organometallic and Bioinorganic Perspectives*. Ed. by W. B. Tolman. WILEY-VCH, **2006**.
- [153] D. H. R. Barton, A. E. Martell, and D. T. Sawyer, eds. *The Activation of Dioxygen and Homogeneous Catalytic Oxidation*. Springer US, **1993**.
- [154] E. Roduner, W. Kaim, B. Sarkar, V. B. Urlacher, J. Pleiss, R. Gläser, W. D. Einicke, G. a. Sprenger, U. Beifuß, E. Klemm, C. Liebner, H. Hieronymus, S. F. Hsu, B. Plietker, and S. Laschat. *ChemCatChem* 5, **2013**, pp. 82–112.
- [155] S. E. Allen, R. R. Walvoord, R. Padilla-salinas, and M. C. Kozlowski. *Chem. Rev.* 113, **2013**, pp. 6234–6458.
- [156] J. Reedijk and E. Bouwman, eds. *Bioinorganic catalysis*. New York: Elsevier, **2013**.
- [157] T. Inoue, Y. Shiota, and K. Yoshizawa. *J. Am. Chem. Soc.* 130, **2008**, pp. 16890–7.
- [158] D. Maiti, D.-H. Lee, K. Gaoutchenova, C. Würtele, M. C. Holthausen, A. A. N. Sarjeant, J. Sundermeyer, S. Schindler, and K. D. Karlin. *Angew. Chem., Int. Ed.* 47, **2007**, pp. 82–85.
- [159] M. H. Baik, M. Newcomb, R. A. Friesner, and S. J. Lippard. *Chem. Rev.* 103, **2003**, pp. 2385–2419.
- [160] B. Wilkinson, M. Zhu, N. D. Priestley, H. T. Nguyen, H. Morimoto, P. G. Williams, S. I. Chan, H. G. Floss, V. Uni, L. Berkeley, C. Road, and R. A. R. V. Microbiol. *J. Am. Chem. Soc.* 118, **1996**, pp. 921–922.
- [161] J. Becker, P. Gupta, F. Angersbach, F. Tucek, C. Näther, M. C. Holthausen, and S. Schindler. *Chem. Eur. J. (accepted for publication)*, **2015**.
- [162] J. Astner, M. Weitzer, S. P. Foxon, S. Schindler, F. W. Heinemann, J. Mukherjee, R. Gupta, V. Mahadevan, and R. Mukherjee. *Inorg. Chim. Acta* 361, **2008**, pp. 279–292.
- [163] D. E. Applequist and L. Kaplan. *J. Am. Chem. Soc.* 87, **1965**, pp. 2194–2200.
- [164] H. Koch and W. Haaf. *Angew. Chem.* 72, **1960**, p. 628.
- [165] F. Bélanger-Gariépy, F. Brisse, P. D. Harvey, D. F. R. Gilson, and I. S. Butler. *Ca. J. Chem.* 68, **1990**, pp. 1163–1169.

- [166] G. Tojo and M. Fernández. *Oxidation of Alcohols to Aldehydes and Ketones*. Basic Reactions in Organic Synthesis. New York: Springer, **2006**.
- [167] S. Kaihara, S. Matsumura, and J. P. Fisher. *Macromolecules* 40, **2007**, pp. 7625–7632.
- [168] C. B. Hübschle, G. M. Sheldrick, and B. Dittrich. *J. Appl. Crystallogr.* 44, **2011**, pp. 1281–1284.
- [169] L. J. Farrugia. *J. Appl. Crystallogr.* 30, **1997**, p. 565.

7 List of Figures

1.1	Abundance of selected elements in Earth's crust and humans.	9
1.2	Type I binding site for copper in azurin II	11
1.3	Type II binding site for copper in Hydra Cu-Zn superoxide dismutase.	12
1.4	Active site of tyrosinase.	13
1.5	Overview over several functions performed by proteins con- taining copper.	14
1.6	Model system for type I copper proteins.	15
1.7	Binding of dioxygen as 1:1 copper adduct complexes.	16
1.8	Ligands used for the first crystallization of η^2 (a) and η^1 (b) Cu/O ₂ adducts.	17
1.9	Ligand of the catalytically active model system of galactose oxidase.	17
1.10	Binding of dioxygen as 2:1 copper adduct complexes	17
1.11	<i>o</i> -hydroxylation of tyrosine by tyrosinase.	19
1.12	Ligands used for dinuclear complexes capable of tyrosinase-like, intramolecular hydroxylation reactions.	19
1.13	Intramolecular aromatic hydroxylation of the [Cu ₂ DAPA] ²⁺ complex with dioxygen.	20
1.14	Ligands used for mononuclear complexes with tyrosinase-like activity towards external substrates as oxygen binding dimer.	20
1.15	Proposed mechanistic cycle of the tyrosinase-like activity of mononuclear complexes [48].	21
1.16	Model complex for the trinuclear copper site in pMMO.	22
1.17	Intramolecular hydroxylation of mononuclear η^2 -peroxido cop- per(III) complex.	23
1.18	Intramolecular hydroxylation with a bis(μ -oxido) copper(III) complex.	24
1.19	Intramolecular benzylic hydroxylation.	25
1.20	Intramolecular aliphatic ligand hydroxylation.	26
1.21	Stereo-selective β -hydroxylation of a steroid amine ligand with copper dioxygen complexes.	26
1.22	Stereo-selective γ -hydroxylation of a steroid imine ligand with copper dioxygen complexes.	27

1.23	BDED (colored) is quite similar to PPN	28
2.1	The ligands PPN (a: R=Et, X=H) and BDED (b: R=Et, X=Y=H).	31
2.2	Synthesis of PPN.	32
2.3	Time resolved UV-vis spectra of the reaction of [Cu(PPN)] CF ₃ SO ₃ with dioxygen	33
2.4	Oxidation of [Cu(PPN)CH ₃ CN]SbF ₆ with dioxygen (scheme redrawn from reference [65])	34
2.5	Computed reaction pathways for the intramolecular aromatic hydroxylation reaction of the PPN ligand	35
2.6	Molecular Structure of the cation of [Cu ₂ (PPN) ₂ (OH) ₂] (CF ₃ SO ₃) ₂	38
2.7	ORTEP plot of the molecular structure of [Cu(BDED) ₂] ⁺	39
2.8	Time resolved UV-vis spectra of the reaction of [Cu(BDED)] CF ₃ SO ₃ with dioxygen	40
2.9	Oxidation of [Cu(I)BDED] with dioxygen.	41
2.10	Selected reaction steps computed for the intramolecular aromatic hydroxylation reaction for the BDED ligand	42
2.11	The ligand H ₂ BDED.	43
2.12	Molecular structure of the cation of [Cu ₂ (Et ₂ en)(OH) ₂] (CF ₃ SO ₃) ₂	44
2.13	ORTEP plot of the molecular structure of [Cu(BDED) ₂] ⁺	54
2.14	ORTEP plot of the molecular structure of [Cu(m-Me-BDED) ₂] ⁺	54
2.15	Molecular Structure of [Cu(H ₂ BDED)Cl ₂]	56
2.16	UV/vis of [CuBDED] ⁺ complex without and with O ₂	57
2.17	IR of [CuBDED] ⁺ complex without and with O ₂	58
3.1	Selective <i>o</i> -hydroxylation using a simple Cu(I) complex and O ₂	65
3.2	Oxidation of the [Cu ^I DPDen] ⁺ complex with dioxygen.	66
3.3	ORTEP plot of the molecular structure of 3-hydroxy-2,2-dimethyl-propionic acid	67
3.4	Time resolved UV-vis spectra of the reaction of [Cu(DPDen)] CF ₃ SO ₃ with dioxygen	68
3.5	Plot ln(k _{obs} /T) versus 1/T according to the Eyring-Polanyi equation for k _{obs} in the temperature range -80.9 to -63.6 °C for the formation of the bis(μ-oxido) complex with linear fit	69
3.6	Plot ln(k/T) versus 1/T according to the Eyring-Polanyi equation for k in the temperature range -89.0 to -35.0 °C for the decay of the bis(μ-oxido) complex with linear fits	70
3.7	α and β positions for the hydroxylation of cyclohexanecarbaldehyde	71

3.8	Oxidation of the copper(I) complex of <i>N'</i> -cyclohexylmethylene- <i>N,N</i> -diethyl-ethane-1,2-diamine with dioxygen.	71
3.9	Synthetic route for adamantane-1-carbaldehyde.	72
3.10	ORTEP plot of the molecular structure of adamantane-1-carboxylic acid methylester	73
3.11	ORTEP plot of the molecular structure of 1-hydroxymethyl-adamantane	74
3.12	ORTEP plot of the molecular structure of pentafluorophenyl-hydrazin-1-ylidenemethyladamantan-2-ol	74
3.13	Synthetic route for diadamantane-1-carbaldehyde.	75
3.14	UV/vis of [DPDen] ⁺ complex without and with O ₂	82
3.15	No hydroxylation of ketones such as camphor was observed.	83
3.16	ORTEP plot of the molecular structure of 2-diethylamino-ethyl-ammonium adamantancarboxylate	84
3.17	ORTEP plot of the molecular structure of 2- <i>tert</i> -butyl-5,5-dimethyl-[1,3]dioxan-4-ol	86
4.1	¹ H-NMR 2-Bromo-6-formylpyridine	89
4.2	¹³ C-NMR 2-Bromo-6-formylpyridine	89
4.3	¹ H-NMR 6-Phenyl-2-pyridinecarbaldehyde	90
4.4	¹³ C-NMR 6-Phenyl-2-pyridinecarbaldehyde	90
4.5	¹ H-NMR 6-Phenyl-2-pyridinemethanol	91
4.6	¹³ C-NMR 6-Phenyl-2-pyridinemethanol	91
4.7	¹ H-NMR 2-(Chloromethyl)-6-phenylpyridine hydrochloride	92
4.8	¹³ C-NMR 2-(Chloromethyl)-6-phenylpyridine hydrochloride	92
4.9	¹ H-NMR 2-(Diethylaminomethyl)-6-phenylpyridine	93
4.10	¹³ C-NMR 2-(Diethylaminomethyl)-6-phenylpyridine	93
4.11	¹ H-NMR <i>N'</i> -Benzylidene- <i>N,N</i> -diethyl-ethylendiamine	94
4.12	¹³ C-NMR <i>N'</i> -Benzylidene- <i>N,N</i> -diethyl-ethylendiamine	94
4.13	¹ H-NMR <i>N'</i> -Benzyl- <i>N,N</i> -diethyl-ethylendiamine	95
4.14	¹³ C-NMR <i>N'</i> -Benzyl- <i>N,N</i> -diethyl-ethylendiamine	95
4.15	¹ H-NMR Salicylaldehyde	96
4.16	¹³ C-NMR Salicylaldehyde	96
4.17	¹ H-NMR 2-(diethylamino)ethyl(4-methoxy-phenyl)methylideneamine	97
4.18	¹³ C-NMR 2-(diethylamino)ethyl(4-methoxy-phenyl)methylideneamine	97
4.19	¹ H-NMR 2-(diethylamino)ethyl(4-nitrophenyl)methylideneamine	98
4.20	¹³ C-NMR 2-(diethylamino)ethyl(4-nitrophenyl)methylideneamine	98
4.21	¹ H-NMR 2-(diethylamino)ethyl(4-methyl)methylideneamine	99
4.22	¹³ C-NMR 2-(diethylamino)ethyl(4-methyl)methylideneamine	99

7 List of Figures

4.23	¹ H-NMR 2-(diethylamino)ethyl(4-chloro)methylideneamine .	100
4.24	¹³ C-NMR 2-(diethylamino)ethyl(4-chloro)methylideneamine .	100
4.25	¹ H-NMR 2-(diethylamino)ethyl(3-nitrophenyl)methylideneamine	101
4.26	¹³ C-NMR 2-(diethylamino)ethyl(3-nitrophenyl)methylidene- amine	101
4.27	¹ H-NMR 2-(diethylamino)ethyl(3-methyl)methylideneamine .	102
4.28	¹³ C-NMR 2-(diethylamino)ethyl(3-methyl)methylideneamine	102
4.29	¹ H-NMR <i>N'</i> -Benzylidene- <i>N,N</i> -dimethyl-ethylendiamine . . .	103
4.30	¹³ C-NMR <i>N'</i> -Benzylidene- <i>N,N</i> -dimethyl-ethylendiamine . . .	103
4.31	¹ H-NMR 2-(diethylamino)ethyl(4-hydroxyphenyl)methylide- neamine	104
4.32	¹³ C-NMR 2-(diethylamino)ethyl(4-hydroxyphenyl)methylide- neamine	104
4.65	¹ H-NMR <i>N'</i> -(2,2-Dimethylpropylidene)- <i>N,N</i> -diethyl-ethylen- diamine	185
4.66	¹³ C-NMR <i>N'</i> -(2,2-Dimethylpropylidene)- <i>N,N</i> -diethyl-ethylen- diamine	185
4.67	¹ H-NMR <i>N'</i> -Cyclohexylmethylene- <i>N,N</i> -diethyl-ethane-1,2- diamine	186
4.68	¹³ C-NMR <i>N'</i> -Cyclohexylmethylene- <i>N,N</i> -diethyl-ethane-1,2- diamine	186
4.69	DEPT135 ¹³ C-NMR <i>N'</i> -Cyclohexylmethylene- <i>N,N</i> -diethyl- ethane-1,2-diamine	187
4.70	¹ H-NMR Adamantanylmethylidene-diethylaminomethylamine	188
4.71	¹³ C-NMR Adamantanylmethylidene-diethylaminomethylamine	188
4.72	¹ H-NMR 2-Hydroxy-adamantancarbaldehyde	189
4.73	¹³ C-NMR 2-Hydroxy-adamantancarbaldehyde	189
4.74	DEPT135 ¹³ C-NMR 2-Hydroxy-adamantancarbaldehyde . . .	190
4.75	HSQC 2-Hydroxy-adamantancarbaldehyde	190
4.76	¹ H-NMR Pentafluorophenylhydrazin-1-ylidenemethyladaman- tan-2-ol	191
4.77	¹³ C-NMR Penta-fluorophenylhydrazin-1-ylidenemethylada- mantan-2-ol	191
4.78	DEPT135 ¹³ C-NMR Penta-fluorophenylhydrazin-1-ylidene- methyladamantan-2-ol	192
4.79	¹ H-NMR Diamantane-1-carboxylic acid	193
4.80	¹³ C-NMR Diamantane-1-carboxylic acid	193
4.81	¹ H-NMR Diamantane-1-carboxylic acid methylester	194
4.82	¹³ C-NMR Diamantane-1-carboxylic acid methylester	194
4.83	¹ H-NMR 1-Hydroxymethyldiamantane	195
4.84	¹³ C-NMR 1-Hydroxymethyldiamantane	195
4.85	¹ H-NMR Diamantane-1-carbaldehyde	196

4.86	^{13}C -NMR Diamantane-1-carbaldehyde	196
4.87	DEPT135 ^{13}C -NMR Diamantane-1-carbaldehyde	197
4.88	^1H -NMR diamantylmethylidene-diethylaminomethylamine	198
4.89	^{13}C -NMR diamantylmethylidene-diethylaminomethylamine	198
4.90	^1H -NMR 2-hydroxy-diamantancarbaldehyde	199
4.91	^{13}C -NMR 2-hydroxy-diamantancarbaldehyde	199
4.92	DEPT135 ^{13}C -NMR 2-hydroxy-diamantancarbaldehyde	200
4.93	^1H -NMR <i>N,N</i> -Diethyl- <i>N'</i> -(1,7,7-trimethyl-bicyclo[2.2.1]hept-2-ylidene)-ethane-1,2-diamine	201
4.94	^{13}C -NMR <i>N,N</i> -Diethyl- <i>N'</i> -(1,7,7-trimethyl-bicyclo[2.2.1]hept-2-ylidene)-ethane-1,2-diamine	201
4.95	DEPT135 ^{13}C -NMR <i>N,N</i> -Diethyl- <i>N'</i> -(1,7,7-trimethyl-bicyclo[2.2.1]hept-2-ylidene)-ethane-1,2-diamine	202
4.96	Mass spectrum of 3-hydroxy-2,2-dimethyl-propionaldehyde	203
4.97	Mass spectrum of 2-hydroxy-adamantancarbaldehyde	204
4.98	IR spectrum of 2-hydroxy-adamantancarbaldehyde	205
5.1	Selective <i>o</i> -hydroxylation of the ligand PPN.	222
5.2	The ligand BDED.	222
5.3	General formulation of the selective <i>o</i> -hydroxylation of aromatic aldehydes using a simple Cu(I) complex and O_2	223
5.4	The ligand DPDen.	223
5.5	ORTEP plot of the molecular structure of pentafluorophenylhydrazin-1-ylidenemethyladamantan-2-ol	224
5.6	Different accessible C–H bonds for cyclohexancarbaldehyde and adamantane-1-carbaldehyde	225
5.7	Products of the selective hydroxylation of adamantane-1-carbaldehyde, cyclohexancarbaldehyde and diamantane-1-carbaldehyde	225
5.8	Selektive <i>o</i> -Hydroxylierung des Liganden PPN.	226
5.9	Der Ligand BDED.	227
5.10	Allgemeine Beschreibung der selektiven <i>o</i> -Hydroxylierung von aromatischen Aldehyden mittels eines einfachen Kupfer(I)-Komplexes und O_2	228
5.11	Der Ligand DPDen.	228
5.12	ORTEP Darstellung der Molekülstruktur von Pentafluorophenylhydrazin-1-ylidenmethyladamantan-2-ol	229
5.13	Die verschiedenen zugänglichen C–H Bindungen für Cyclohexancarbaldehyd und Adamantan-1-carbaldehyd	230
5.14	Produkte der selektiven Hydroxylierung von Adamantan-1-carbaldehyd, Cyclohexancarbaldehyd und Diamantan-1-carbaldehyd	230

8 List of Tables

1.1	Approximate UV-vis absorption of some Cu/O ₂ adducts. . .	18
2.1	Substituent effects on the overall rate-limiting step of the hydroxylation reaction.	37
4.1	Crystal data and structure refinement for [Cu ₂ (PPN) ₂ (OH) ₂](CF ₃ SO ₃) ₂	105
4.2	Selected bond lengths and angles for [Cu ₂ (PPN) ₂ (OH) ₂](CF ₃ SO ₃) ₂	106
4.3	Crystal data and structure refinement for [Cu(BDED) ₂]CF ₃ SO ₃	107
4.4	Selected bond lengths and angles for [Cu(BDED) ₂]CF ₃ SO ₃ .	108
4.5	Crystal data and structure refinement for [Cu(BDED) ₂]SbF ₆ . . .	109
4.6	Selected bond lengths and angles for [Cu(BDED) ₂]SbF ₆ . . .	110
4.7	Crystal data and structure refinement for [Cu(H ₂ BDED)Cl ₂]·acetone.	111
4.8	Selected bond lengths and angles for [Cu(H ₂ BDED)Cl ₂]·acetone	112
4.9	Crystal data and structure refinement for [Cu ₂ (Et ₂ en)OH ₂](CF ₃ SO ₃) ₂	113
4.10	Selected bond lengths and angles for [Cu ₂ (Et ₂ en)OH ₂](CF ₃ SO ₃) ₂	114
4.11	Crystal data and structure refinement for [Cu(m-Me-BDED) ₂]CF ₃ SO ₃	115
4.12	Selected bond lengths and angles for [Cu(m-Me-BDED) ₂]CF ₃ SO ₃	116
4.13	Total electronic energies and Gibbs free energies (203 K) of the molecules present in Figure 2.5	117
4.14	Total electronic energies and Gibbs free energies (203 K) of the molecules present in Table 2.1	118
4.15	Total electronic energies and Gibbs free energies (203 K) of the molecules present in Figure 2.10	118
4.16	Cartesian coordinates of 1	119
4.17	Cartesian coordinates of TS12	121

4.18	Cartesian coordinates of 2	123
4.19	Cartesian coordinates of TS23	125
4.20	Cartesian coordinates of 3	127
4.21	Cartesian coordinates of TS34 (broken-symmetry singlet geometry)	129
4.22	Cartesian coordinates of 4	131
4.23	Cartesian coordinates of TS35	133
4.24	Cartesian coordinates of 5	135
4.25	Cartesian coordinates of TS56	137
4.26	Cartesian coordinates of 6	139
4.27	Cartesian coordinates of 2-OCH₃	141
4.28	Cartesian coordinates of TS35-OCH₃	143
4.29	Cartesian coordinates of 2-OH	146
4.30	Cartesian coordinates of TS35-OH	148
4.31	Cartesian coordinates of 2-CH₃	150
4.32	Cartesian coordinates of TS35-CH₃	152
4.33	Cartesian coordinates of 2-CH=CH₂	154
4.34	Cartesian coordinates of TS35-CH=CH₂	156
4.35	Cartesian coordinates of 2-F	158
4.36	Cartesian coordinates of TS35-F	160
4.37	Cartesian coordinates of 2-CHO	162
4.38	Cartesian coordinates of TS35-CHO	164
4.39	Cartesian coordinates of 2-CF₃	166
4.40	Cartesian coordinates of TS35-CF₃	168
4.41	Cartesian coordinates of 2-NO₂	170
4.42	Cartesian coordinates of TS35-NO₂	172
4.43	Cartesian coordinates of 1'	174
4.44	Cartesian coordinates of 2'	176
4.45	Cartesian coordinates of 3'	178
4.46	Cartesian coordinates of TS34' (open-shell broken-symmetry singlet)	180
4.47	Cartesian coordinates of TS35'	182
4.48	Crystal data and structure refinement for adamantane-1-carboxylic acid methylester	206
4.49	Bond lengths and angles for adamantane-1-carboxylic acid methylester	207
4.50	Crystal data and structure refinement for 1-hydroxymethyladamantane	208
4.51	Bond lengths and angles for 1-hydroxymethyladamantane	209
4.52	Crystal data and structure refinement for 3-hydroxy-2,2-dimethyl-propionic acid	211

4.53	Bond lengths and angles for 3-hydroxy-2,2-dimethyl-propionic acid	212
4.54	Crystal data and structure refinement for pentafluorophenyl-hydrazin-1-ylidenemethyladamantan-2-ol	213
4.55	Bond lengths and angles for pentafluorophenylhydrazin-1-yl-idenemethyladamantan-2-ol	214
4.56	Crystal data and structure refinement for 2-diethylamino-ethyl-ammonium adamantancarboxylate	215
4.57	Bond lengths and angles for 2-diethylamino-ethyl-ammonium adamantancarboxylate	216
4.58	Crystal data and structure refinement for 2- <i>tert</i> -butyl-5,5-dimethyl-[1,3]dioxan-4-ol	218
4.59	Bond lengths and angles for 2- <i>tert</i> -butyl-5,5-dimethyl-[1,3]dioxan-4-ol	219

9 Publications

9.1 Full Papers

- Characterization of a macrocyclic end-on peroxido copper complex. T. Hoppe, S. Schaub, J. Becker, C. Würtele, S. Schindler, (2013). *Angewandte Chemie - International Edition*, 52(1), 870–873. doi:10.1002/anie.201205663
- Reactions of copper(II) chloride in solution: Facile formation of tetranuclear copper clusters and other complexes that are relevant in catalytic redox processes. S. Löw, J. Becker, C. Würtele, A. Miska, C. Kleeberg, U. Behrens, O. Walter, S. Schindler, (2013). *Chemistry - A European Journal*, 19(17), 5342–5351. doi:10.1002/chem.201203848
- Investigation of Chromium Complexes with a Series of Tripodal Ligands. S. Schäfer, J. Becker, A. Beitat, C. Würtele, (2013). *Zeitschrift Für Anorganische Und Allgemeine Chemie*, 369, 2269–2275. doi:10.1002/zaac.201300170
- Efficient Preparation of Apically Substituted Diamondoid Derivatives. P. Kahl, B. A. Tkachenko, A. Novikovskiy, J. Becker, J. E. P. Dahl, R. M. K. Carlson, A. A. Fokin, P. R. Schreiner, (2014). *Synthesis*, 46(06), 787–798. doi:10.1055/s-0033-1338583
- Selective aromatic hydroxylation with dioxygen and simple copper imine complexes. J. Becker, P. Gupta, F. Angersbach, F. Tuzek, C. Näther, M. C. Holthausen, S. Schindler, (2015). Accepted for publication in *Chemistry - A European Journal*.
- Intramolecular C-H amination provides direct access to 1,2-disubstituted diamondoids. R. Hrdina, F. M. Metz, M. Larrosa, J.-P. Berndt, Y. Y. Zhygadlo, S. Becker, J. Becker, (2015). Manuscript in preparation for *Organic Letters*.
- Functionalized Adamantyl and Diamantyl Phosphines. M. A. Gunawan, D. Poinso, H. Cattey, J. Becker, R. I. Yurchenko, E. D. Butova, H. Hausmann, A. A. Fokin, P. R. Schreiner, J.-C. Hierso, (2015). Manuscript in preparation for *Journal of Organic Chemistry*.

9.2 Oral Presentations

- "Synthetic and Mechanistic Investigations on Substrate Oxidations with Dioxygen using simple Copper(I) Complexes" Cooperation workshop Gießen-Kiev (*with financial support of the DFG*), February 2011 (Kyiv Polytechnic Institute, Ukraine)
- "Copper-Dioxygen-Complexes - From An Enzymatic Model System To A Synthetic Application" Bioinorganic Chemistry Meeting 2013, February 2013 (Costa Teguse, Lanzarote - Spain)

9.3 Poster Presentations

- "Substratoxidationen mit Disauerstoff durch einfache Kupfer(I)-Komplexe" ("*Substrate oxidations with molecular oxygen and simple copper(I) complexes*") Koordinationschemikertreffen 2012, February 2012 (Dortmund, Germany)
- "Copper-Dioxygen-Complexes - From An Enzymatic Model System To A Synthetic Application" Bioinorganic Chemistry Meeting 2013, February 2013 (Costa Teguse, Lanzarote - Spain)

**Der Lebenslauf wurde aus der elektronischen
Version der Arbeit entfernt.**

**The curriculum vitae was removed from the
electronic version of the paper.**

